AD-777 320

OCTAVE-BANDWIDTH, HIGH-DIRECTIVITY MICROSTRIP COUPLERS

Charles Buntschuh

Microwave Associates, Incorporated

Prepared for:

Rome Air Development Center

January 1974

AD 777320

UNCLASSIFIED

SECURITY CLASSIFICATION OF THIS PAGE (When Data Entered)

REPORT DOCUMENTATION PAGE		READ INSTRUCTIONS BEFORE COMPLETING FORM
1. REPORT NUMBER RADC-TR-73-396	2. GOVT ACCESSION NO.	3. RECIPIENT'S CATALOG NUMBER
4. TITLE (and Subtitle) OCTAVE-BANDWIDTH, HIGH-DIRECTIVITY MICROSTRIP COUPLERS		5. TYPE OF REPORT & PERIOD COVERED Final Technical Report 17 Mar 1972 to 30 Jun 1973 6. PERFORMING ORG. REPORT NUMBER N/A
7. AUTHOR(s) Charles Buntschuh		8. CONTRACT OR GRANT NUMBER(s) F30602-72-C-0282
9. PERFORMING ORGANIZATION NAME AND ADDRESS Microwave Associates, Inc. Burlington, MA 01803		10. PROGRAM ELEMENT, PROJECT, TASK AREA & WORK UNIT NUMBERS Job Order No. 45060252
11. CONTROLLING OFFICE NAME AND ADDRESS Rome Air Development Center (OCTE) Griffiss Air Force Base, New York 13441		12. REPORT DATE January 1974 13. NUMBER OF PAGES 206
14. MONITORING AGENCY NAME & ADDRESS(if different from Controlling Office) Same		15. SECURITY CLASS. (of this report) Unclassified 15a. DECLASSIFICATION/DOWNGRADING SCHEDULE N/A

16. DISTRIBUTION STATEMENT (of this Report)

Approved for public release; distribution unlimited.

17. DISTRIBUTION STATEMENT (of the abstract entered in Block 20, if different from Report)

Same

18. SUPPLEMENTARY NOTES

RADC Project Engineer:
P. A. Romanelli (OCTE)

19. KEY WORDS (Continue on reverse side if necessary and identify by block number)

Couplers
Microstrip
Octave-Bandwidth, High-Directivity

20. ABSTRACT (Continue on reverse side if necessary and identify by block number)

Coupled strip directional couplers in microstrip suffer from low directivity due to the inequality of the even and odd mode wave velocities. The coupling bandwidth of single quarter-wave length couplers is limited to about an octave within a 1 dB tolerance. The practical maximum coupling limit for edge coupled lines on microstrip is about 5 dB, using conventional photo etching technology.

The purpose of this study was to examine techniques of velocity compensation, broadbanding, and tight coupling, and combine them to produce high-directivity,

DD FORM 1 JAN 73 1473 EDITION OF 1 NOV 65 IS OBSOLETE

UNCLASSIFIED

SECURITY CLASSIFICATION OF THIS PAGE (When Data Entered)

20. Cont'd

broadband microstrip couplers from 3 to 20 dB. A further objective was to develop a design procedure, with supporting tables and charts, to facilitate the rapid design of microstrip couplers and to verify the procedure experimentally.

We concluded that the most effective and simple velocity compensation technique was by means of dielectric overlays over the coupling gaps. The design procedure developed applies to this method.

The experimental broadband dielectric overlay couplers were 3-section cascaded couplers. Most 3 dB couplers were tandem connections of 3-section 8.34 dB units; we also examined the interdigitated coupler technique.

Bandwidths (1dB) up to 120% were obtained with minimum directivities of 21, 18, and 13 dB in 3, 10 and 20 dB couplers. Also the experimental results on multi-element overlay couplers corroborated the design theory very closely for couplers down to about 25 dB.

OCTAVE-BANDWIDTH, HIGH-DIRECTIVITY MICROSTRIP COUPLERS

Charles Buntschuh

Microwave Associates, Inc.

FOREWORD

This report has been prepared by Microwave Associates, Inc., Burlington, Massachusetts, under Contract F30602-72-C-0282, Job Order No. 45060252. Mr. P. A. Romanelli (OCTE) was the RADC project engineer.

The report has been reviewed by the Office of Information, RADC, and approved for release to the National Technical Information Service (NTIS).

This report has been reviewed and is approved.

APPROVED: P. A. Romanelli

P. A. ROMANELLI
Project Engineer

APPROVED: William T. Pope

WILLIAM T. POPE
Assistant Chief
Surveillance and Control Division

FOR THE COMMANDER: Carlo P. Crocetti

CARLO P. CROCETTI
Chief, Plans Office

ABSTRACT

Coupled strip directional couplers in microstrip suffer from low directivity due to the inequality of the even and odd mode wave velocities. The coupling bandwidth of single quarter-wave length couplers is limited to about an octave within a 1 dB tolerance. The practical maximum coupling limit for edge-coupled lines on microstrip is about 5 dB, using conventional photo etching technology.

The purpose of this study was to examine techniques of velocity compensation, broadbanding, and tight coupling, and combine them to produce high-directivity, broad band microstrip couplers from 3 to 20 dB. A further objective was to develop a design procedure, with supporting tables and charts, to facilitate the rapid design of microstrip couplers and to verify the procedure experimentally.

We concluded that the most effective and simple velocity compensation technique was by means of dielectric overlays over the coupling gaps. The design procedure developed applies to this method.

The experimental broadband dielectric overlay couplers were 3-section cascaded couplers. Most 3-dB couplers were tandem connections of 3-section 8.34 dB units; we also examined the interdigitated coupler technique.

Bandwidths (1dB) up to 120% were obtained with minimum directivities of 21, 18, and 13 dB in 3, 10 and 20 dB couplers. Also the experimental results on multi-element overlay couplers corroborated the design theory very closely for couplers down to about 25 dB.

TABLE OF CONTENTS

TABLE OF CONTENTS

LIST OF ILLUSTRATIONS

EVALUATION

Project No.: 4506
Contract No.: F30602-72-C-0282
Effort Title: Octave-Bandwidth High Directivity Microstrip Couplers
Contractor: Microwave Associates, Burlington, MA 01803

1. The purpose of this study was to examine techniques of velocity compensation, broadbanding, and tight couplings and combine them to produce high-directivity, broadband microstrip couplers from 3 to 20 db in the 1 to 10 GHz range. Extensive material from a number of references has been collected and is set forth as a tutorial review of coupled line theory. Design curves for both uncompensated and compensated couplers are presented. The velocity compensation is achieved by dielectric overlay. Various broadbanding techniques, the approaches to velocity compensation, and the means of achieving tight coupling, considered during this investigation are discussed. Included is a computer program, developed during the course of this work, that can be used for analysis of coupler circuitry.

2. A microstrip broadband coupler design can be expeditiously executed with the aid of the curves and the computer program in this report, thus eliminating the extensive mathematical analysis necessary for arriving at a proper design.

P. A. Romanelli

P. A. ROMANELLI
Project Engineer

OCTAVE-BANDWIDTH, HIGH-DIRECTIVITY MICROSTRIP COUPLERS

I. INTRODUCTION

The transmission line properties and the practical circuit applications of parallel-coupled-line couplers in balanced stripline have been the subjects of active investigation since the middle Fifties. Today, design techniques and data for coupled pairs in stripline and other homogeneous dielectric transmission line media are well-established and readily available for a wide variety of applications. The reprint volumes, references 1 and 2, provide a valuable and convenient collection of significant papers on coupled line theory and techniques through 1970.

The situation with respect to microstrip coupled lines is not so satisfactory. In microstrip, because of its mixed dielectric, the phase velocities of the so-called even and odd mode waves on coupled lines are not equal. This property alters the coupling characteristics of the lines, in particular by decreasing their directivity. Also, the inhomogeneous dielectric makes microstrip dispersive, so that the wave phase velocities are frequency dependent. Moreover, the dispersion characteristics of the even and odd modes on coupled lines are not the same, thereby aggravating the directivity problem in very broad band applications.

The parameters of microstrip in the low frequency limit have been calculated by numerous authors by a variety of mathematical techniques. The most frequently cited treatment is perhaps that of Bryant and Weiss[3].

Similarly, the frequency dispersion characteristics have also been treated by several workers[4 - 7]. Thus the theory relating the electrical to the physical parameters of the microstrip coupled pair is in good shape. On the other hand, very little has been published concerning the effect of unequal velocities on coupler performance, particularly in a form suitable for practical design work. Several techniques for equalizing the velocities or reducing their difference, and improving coupler directivities have been reported,[8 - 11] but general design data and procedures employing these techniques have not been published.

The broad objective of the program reported here was to develop design data and procedures for octave-band, high-directivity couplers in microstrip, and to verify the procedures experimentally. In particular, we wished to:

1. Study theoretically the effects of unequal mode velocities on the characteristics of practical microstrip couplers.

2. Explore several velocity compensation techniques and select one for the detailed design analysis.

3. Develop a design procedure, with supporting tables and charts, to facilitate the rapid design of broadband (>one octave), high directivity ($\gtrsim$ 20 dB) couplers. It was desired that the method be applicable over at least the 2-20 dB and 1-10 GHz ranges.

In order to make this report a practical handbook for the design of microstrip coupler networks, we have collected pertinent information from several sources and woven it into a tutorial review of coupled-line coupler theory. Section II, which is fairly analytical, develops the basic circuit properties of couplers. It starts with the simple homogeneous symmetrical coupler; we then add asymmetry and finally consider unequal

phase velocities. In Section III we present the coupler design data. First we cover the uncompensated coupler based on the microstrip parameter data of Bryant and Weiss. Second, we discuss velocity compensation by means of dielectric overlays and provide design curves for compensated couplers. Finally, Getsinger's dispersion formula is discussed.

In the first part of Section IV, we consider the various broadbanding techniques, and provide some useful design charts for two- and three-element couplers. In the second part we discuss the problem of achieving tight coupling, i.e. greater than about 5 dB, in microstrip couplers.

Section V covers the experimental work, which, after some introductory material, breaks down into five topics. The first concerns the results on loosely coupled couplers, 8 to 20 dB, and the verification of the design theory. The second and third treat tight coupling by means of tandem connections of weakly coupled elements and by interdigitated structures. The fourth briefly covers our experiments on sawtooth couplers, and the fifth presents the results on band pass filters.

A significant portion of the analytical work included writing a computer program, CASCADE, to analyse the circuit properties of cascaded directional couplers. The program coding and user manual are included here as Appendix D.

II. PARALLEL COUPLED LINE THEORY

A. The Ideal Symmetrical Coupler

Consider first the coupled line transmission line diagrammed in Fig. 1, consisting of two identical, uniform parallel conducting strips above a ground plane and immersed in an homogeneous dielectric. The line is lossless and it is symmetrical about the central plane between the strips. This three-conductor system supports the propagation of two linearly independent TEM waves, the even, or unbalanced, mode and the odd, or balanced mode. In the even mode the voltages along the two strips are in phase while in odd mode they are 180° out of phase, as indicated by the electric field patterns sketched in Fig. 1 b, c. Any TEM wave propagating on the structure can be uniquely decomposed into its even and odd mode components. Also it can propagate down to zero frequency and it is non-dispersive. Of course, higher order, non-TEM waves can also propagate above their cutoff frequencies, however, we shall not consider these modes at all throughout our discussion.

When the strips are of finite length, the structure is a microwave four-port network, with the terminals across each strip end and the ground plane corresponding to a port. The network properties of the coupler have been analyzed by Jones and Bolljahn [13] who derived the impedance matrix of the coupled pair (c f. Fig. 2)

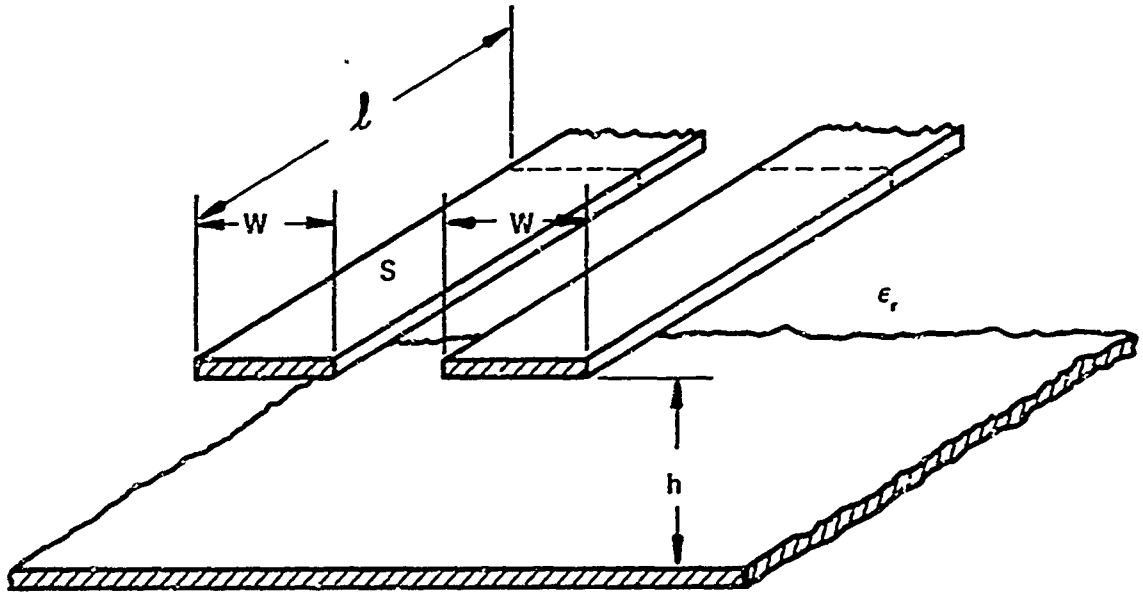

a) COUPLED STRIP GEOMETRY

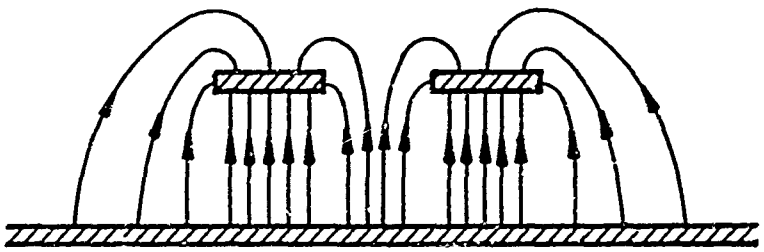

b) EVEN MODE ELECTRIC FIELD PATTERN (SCHEMATIC)

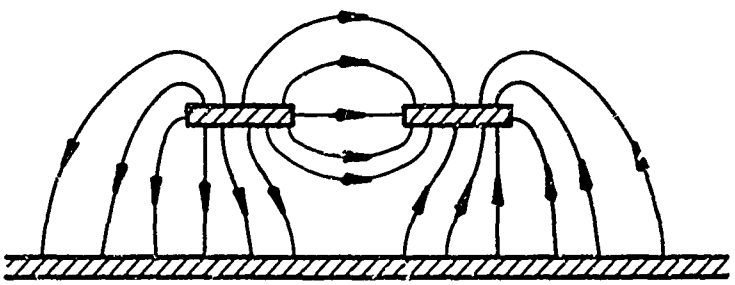

c) ODD MODE ELECTRIC FIELD PATTERN (SCHEMATIC)

FIGURE 1 THE COUPLED STRIP TRANSMISSION LINE

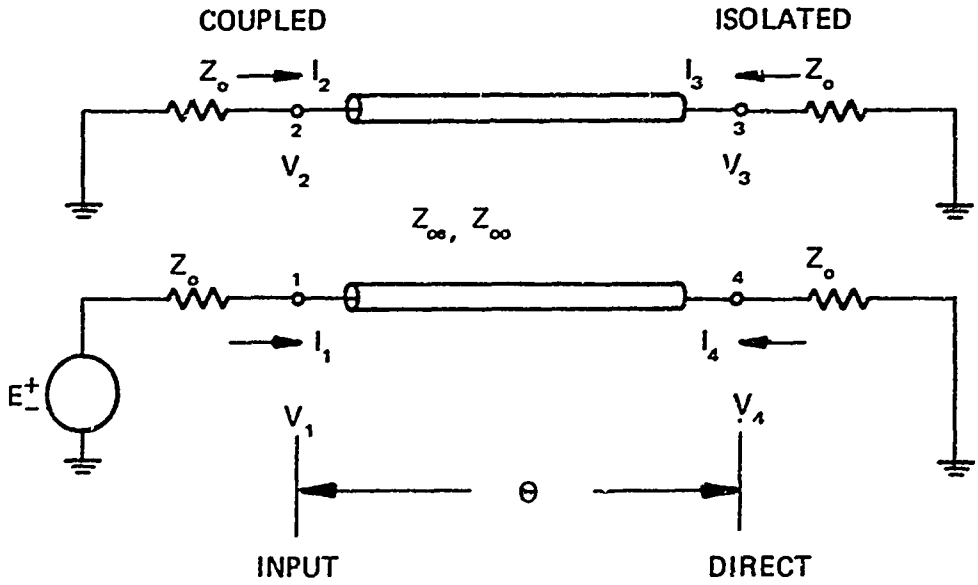

FIGURE 2 COUPLED STRIP COUPLER NOTATION

D-12034

$$\bar{\bar{Z}} = -j \begin{bmatrix} Z_+ \operatorname{ctn}\theta & Z_- \operatorname{ctn}\theta & Z_- \operatorname{csc}\theta & Z_+ \operatorname{csc}\theta \\ Z_- \operatorname{ctn}\theta & Z_+ \operatorname{ctn}\theta & Z_+ \operatorname{csc}\theta & Z_- \operatorname{csc}\theta \\ Z_- \operatorname{csc}\theta & Z_+ \operatorname{csc}\theta & Z_+ \operatorname{ctn}\theta & Z_- \operatorname{ctn}\theta \\ Z_+ \operatorname{csc}\theta & Z_- \operatorname{csc}\theta & Z_- \operatorname{ctn}\theta & Z_+ \operatorname{ctn}\theta \end{bmatrix} \qquad (2)$$

Where $Z_+ = (Z_{oe} + Z_{oo})/2$

$Z_- = (Z_{oe} - Z_{oo})/2$

and Z_{oe} = the even mode impedance, i.e. the characteristic impedance of one strip to ground with equal currents flowing in the same direction on both strips;

Z_{oo} = the odd mode impedance, i.e. the characteristic impedance of one strip to ground with equal currents flowing in opposite directions on both strip and

θ = the electrical length of the coupled lines.

These three parameters completely specify the coupler, and, of course, the impedance matrix completely describes its electrical properties. However, the impedance matrix formation is not a very illuminating description as far as the coupling properties are concerned. The scattering matrix formulation is far better suited to this purpose.

Jones and Bolljahn have also derived the scattering matrix for the special case when

$$Z_k = \sqrt{Z_{oe} Z_{oo}} = Z_o, \qquad (3)$$

where Z_k is the characteristic impedance of the coupler. Under this conditon, the coupler is completely matched and has perfect isolation at all frequencies; it is an ideal four-port coupler with the scattering matrix

$$\bar{\bar{S}} = \begin{bmatrix} 0 & S_{12} & 0 & S_{14} \\ S_{12} & 0 & S_{14} & 0 \\ 0 & S_{14} & 0 & S_{12} \\ S_{14} & 0 & S_{12} & 0 \end{bmatrix} \qquad (4)$$

where $S_{12} = \dfrac{jk \sin \theta}{\sqrt{1-k^2} \cos \theta + j \sin \theta}$ (5)

$$S_{14} = \frac{\sqrt{1-k^2}}{\sqrt{1-k^2} \cos \theta + j \sin \theta} \quad (6)$$

and $$k = \frac{Z_{oe} - Z_{oo}}{Z_{oe} + Z_{oo}} \quad . \quad (7)$$

The coupler characteristics are quite readily deduced from Eqs. (4-7). S_{12} and S_{14} are the complex voltage coupling and direct transmission coefficients repsectively. The coupling coefficient has the maximum magnitude of k at the center frequency, fo, when the coupler is a quarter wavelength long ($\theta = 90^{o}$), and at all odd multiples of f_o. The coupling drops to zero at dc and all even multiples of f_o, and the coupling characteristic repeats every $2f_o$ as the frequency increases. The frequency dependence of the coupling of the ideal coupler is shown in Fig. 3 for several values of mid band coupling, $k_p = -20 \log k$ dB in which the deviation in coupling from the midband value--the relative coupling is plotted against the normalized frequency f/f_o. Note that for a given deviation the bandwidth decreases as the coupling becomes looser.

Frequently coupler requirements are specified in terms of a mean coupling and maximum deviation over a given frequency band Fig.4 shows the bandwidth of an ideal coupler as a function of the midband coupling for several values of band-edge deviation (recall that this is one-sided deviation, one-half of the usual plus-or-minus tolerance), from which one can readily ascertain whether a simple coupler will suffice or whether one must resort to broadbanding techniques (cf. Chap IV.)

The ratio of coupled to direct wave amplitudes, as given by

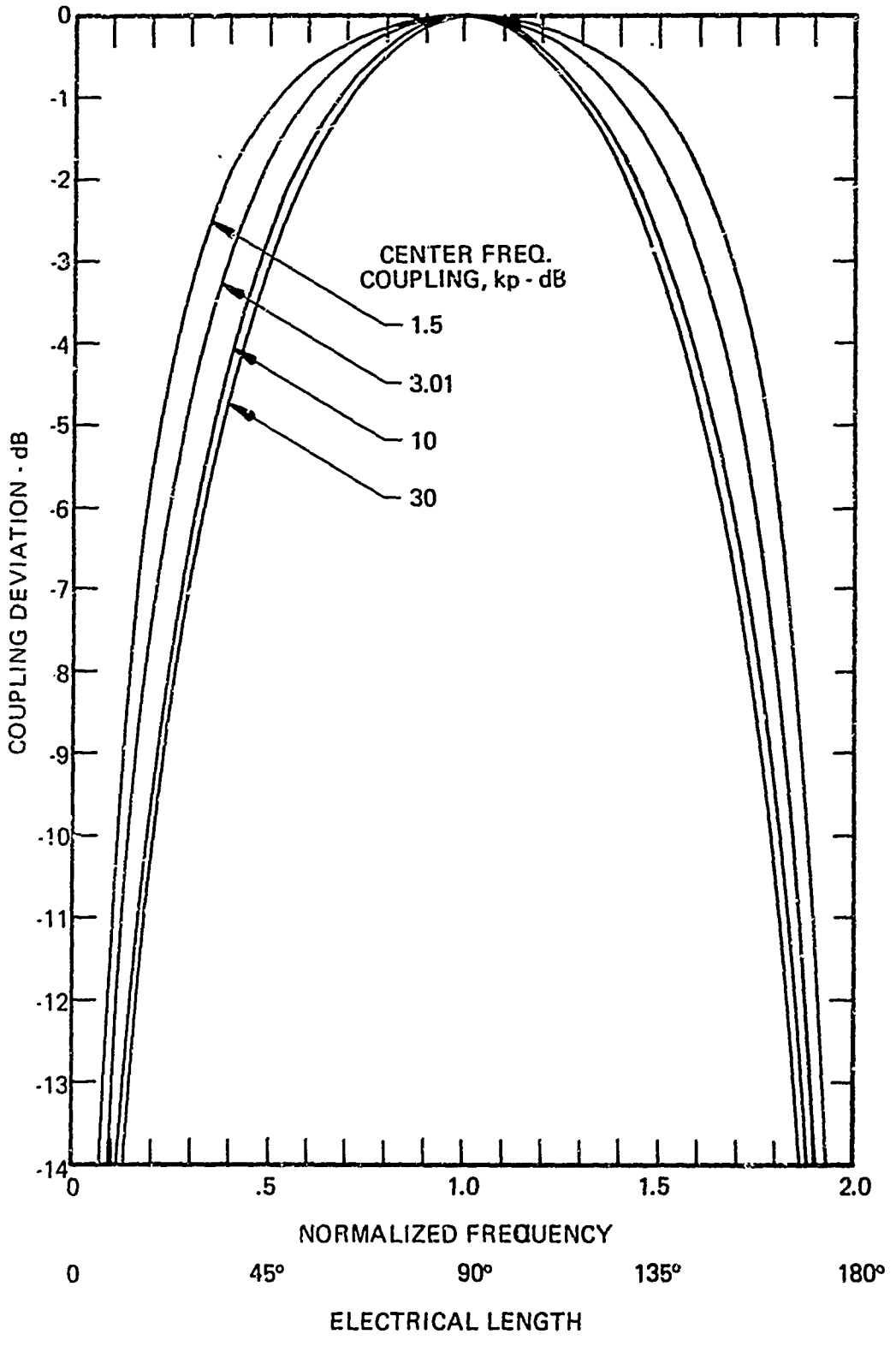

FIGURE 3 NORMALIZED COUPLING CHARACTERISTICS OF IDEAL QUARTER WAVELENGTH COUPLED LINE COUPLERS.

D-12052

$$\frac{S_{12}}{S_{14}} = \frac{j\,k\,\sin\theta}{\sqrt{1-k^2}} \quad , \tag{8}$$

is pure imaginary for all values of k and θ. This means that the phase of the two waves differ by 90^{o} for all frequencies regardless of the coupling value.

In Appendix A we have derived the coupler scattering matrix for the general case, when $Z_k \neq Z_o$, that is for the mismatched coupler. The exact expressions for the scattering coefficients, given by Eqs. A-12, 13, and 14, are quite complex and perhaps of little practical utility as they stand. It is, however, informative to consider the case of the slightly mismatched coupler, $Z_k \approx Z_o$, since variations of coupler impedance from the line impedance of a few percent are quite common in practice.

If we substitute

$$\mathcal{Z}_k = \frac{Z_k}{Z_o} = 1 + \zeta \tag{9}$$

where $\zeta << 1$, into Eqs. A-13, 14, and expand to first order in ζ, we find first that the coupling and direct transmission are unchanged. Second, the reflection and isolation coefficient become

$$S_{11} \approx \frac{jk_1 \sin\theta(\cos\theta + jk_1 \sin\theta)}{(k_1 \cos\theta + j \sin\theta)}\ \zeta \ , \tag{10}$$

and

$$S_{13} = \frac{jk\,k_1 \sin\theta}{(k_1 \cos\theta + j \sin\theta)^2}\ \zeta \ , \tag{11}$$

where $k_1 = \sqrt{1-k^2}$.

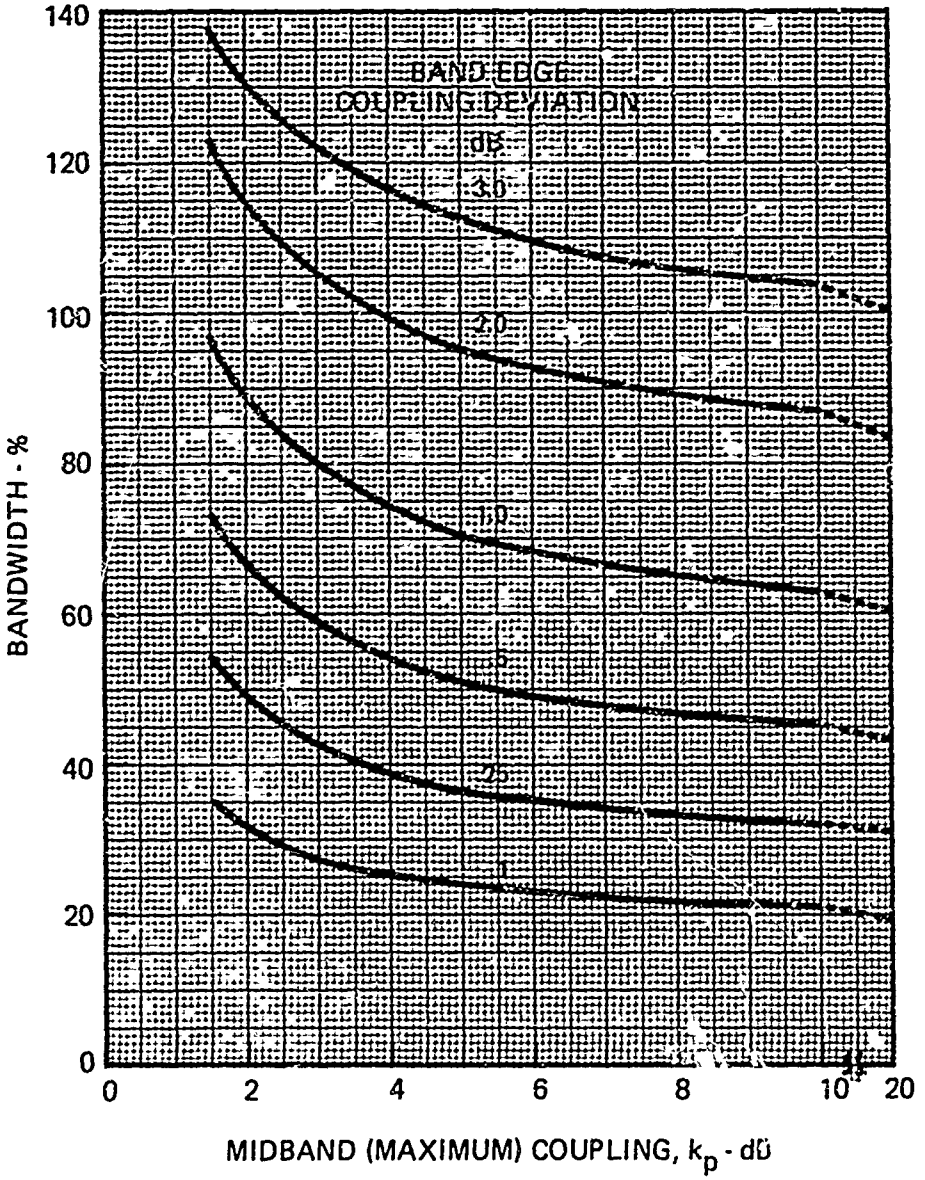

FIGURE 4 COUPLING BANDWIDTH VS. COUPLING FOR IDEAL QUARTER WAVELENGTH COUPLERS.

The mismatch and isolation are worst at midband, and drop to zero (to all orders) at dc and even multiples of f_o. At mid band. we have

$$S_{11} = k_1^2 \zeta = (1-k^2)\zeta \tag{12}$$

and

$$S_{13} = j k k_1 \zeta = jk\sqrt{1-k^2}\,\zeta . \tag{13}$$

The mid band voltage coefficient of directivity is

$$d = \frac{S_{13}}{k} = jk_1\zeta = j\sqrt{1-k^2}\,\zeta . \tag{14}$$

From these expressions we see that for a given coupler impedance error, the mismatch and directivity will decrease as the coupling is increased. Thus for loosely coupled couplers, close control on the coupler impedance is required to achieve high directivity; in fact when $k << 1$ the directivity equals the return loss. As an aside, we might also note, from Eqs (12 and (13), that for a 3 dB coupler ($k^2 = 1/2$), the isolation is equal to the return loss.

As we have mentioned earlier, a coupler is completely specified by three parameters, Z_{oe}, Z_{oo}, and θ. While the even and odd mode impedances have fundamental significance in terms of coupler theory and analysis, we have seen in the preceding discussion that from the circuit analysis standpoint it is much more convenient and meaningful to think in terms of the coupler impedance Z_k and the coupling parameter k (or k_p). Since virtually all coupler design data in the literature relate Z_{oe} and Z_{oo} to the dimensions of the coupled lines, the designer

must always determine the required even and odd mode impedances from the desired Z_k and k_p, by converting k_p to $k = 10^{-k_p/20}$, and then using Eqs (3) and (7): This conversion is facilitated by the chart in Fig. 5. In this report, wherever possible, we provide the design data directly in terms of Z_k and k_p and relegate Z_{oe} and Z_{co} to the status of implicit variables, thereby saving a step in the design process.

The symmetrical coupled-strip coupler with homogeneous dielectric and infinitely thin strips in Fig. 1a, is specified by five parameters, the strip with w, their spacing s, their height above the ground plane h, the coupler length ℓ, and the relative dielectric constant of the medium ε_r. These five parameters must be related to the three electrical parameters Z_{oe}, Z_{oo}, and θ or Z_k, k_p, and θ.

The impedances and coupling depend only on the ratios of the cross-sectional dimensions and the dielectric constant, such that we can write

$$Z_{oe} = \frac{Z_{e,air}\ (w/h,\ s/h)}{\sqrt{\varepsilon_r}} \qquad (15)$$

and

$$Z_{oo} = \frac{Z_{o,air}\ (w/h,\ s/h)}{\sqrt{\varepsilon_r}}\ , \qquad (16)$$

where the functions $Z_{e,air}$ and $Z_{o,air}$ are the even and odd mode impedances of the strips in air, $\varepsilon_r = 1$, as functions of the width and spacing relative to the height. Introducing Eqs.(15) and(16) into Eqs.(3)

and (7), we obtain

$$Z_k = \sqrt{\frac{Z_{e,air}\, Z_{o,air}}{\epsilon_r}}$$

and

$$k = \frac{Z_{e,air} - Z_{o,air}}{Z_{e,air} + Z_{o,air}}$$

Thus we see that it is necessary to determine the impedance functions for air dielectric only; then the impedances for any other dielectric are proportional to $1/\sqrt{\epsilon_r}$, while the coupling is independent of the dielectric constant. This last, rather interesting, property does not hold for microstrip, with its inhomogeneous dielectric, as we shall see in Section C below.

The coupler length ℓ is related to the desired center frequency f_o by

$$\ell = \frac{c}{4f_o\sqrt{\epsilon_r}} ,$$

where $c = 3 \times 10^{10}$ cm/sec is the velocity of light in vacuum.

The foregoing analysis of symmetrical couplers is quite general and it applies to any coupler as long as it is immersed in a uniform dielectric, the two conductors have the same size and shape, and there

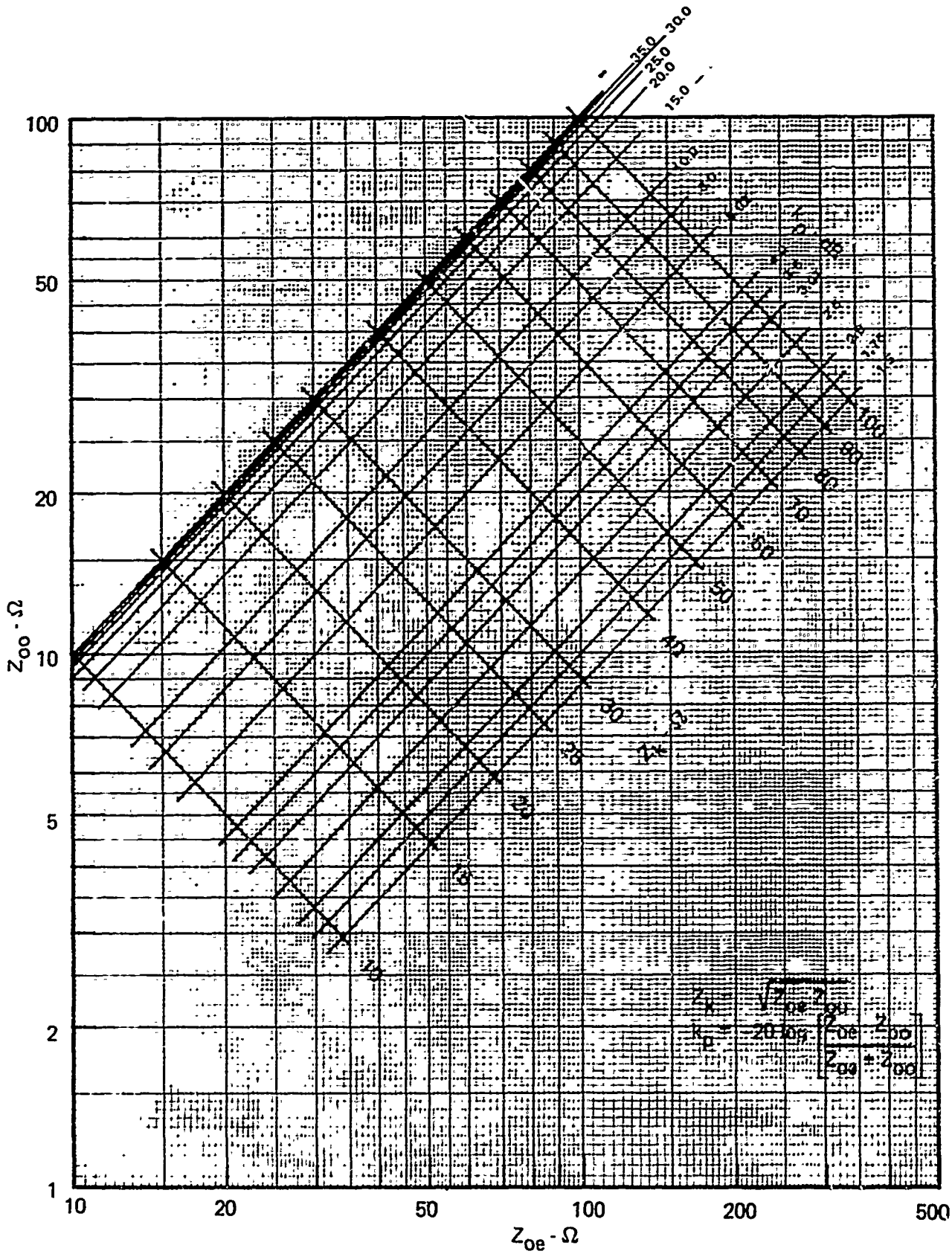

FIGURE 5 COUPLER IMPEDANCE AND COUPLING AS FUNCTIONS OF EVEN AND ODD MODE IMPEDANCES

D-12050

is a plane of symmetry between the conductors. The only distinction among all such couplers, such as those with round wire, rectangular bars, thick or thin straps, edge or broadside coupling, or one or two ground planes, is in the details of the geometric function $Z_{e,air}$ and $Z_{o,air}$. Design equations and graphs for most common coupled-line geometries located midway between two ground planes--strip or slab line geometries--are available in Ref. 1. Although considerable design time and effort could be saved by condensing the essential data into a few simple charts, we shall not pursue that course here since it does not apply to microstrip.

B. The Nonsymmetrical Coupler

In the preceding section we required that both conductors of a coupler be identical and symmetrically located about some plane between them. The "non-symmetrical"* coupler lacks this symmetry such that the two conductors may have different cross-sectional shapes or sizes; in stripline and microstrip this would typically mean unequal strip widths as sketched in Fig. 6.

The non-symmetrical coupler with homogeneous dielectric has been analyzed in some detail by Cristal who has shown that it has two interesting properties not shared by the symmetrical coupler.

* We have adopted the terminology proposed by Cristal[14], who suggests that "non-symmetrical" describe side-by-side asymmetry and "asymmetrical" the end-to-end asymmetry of cascaded couplers.

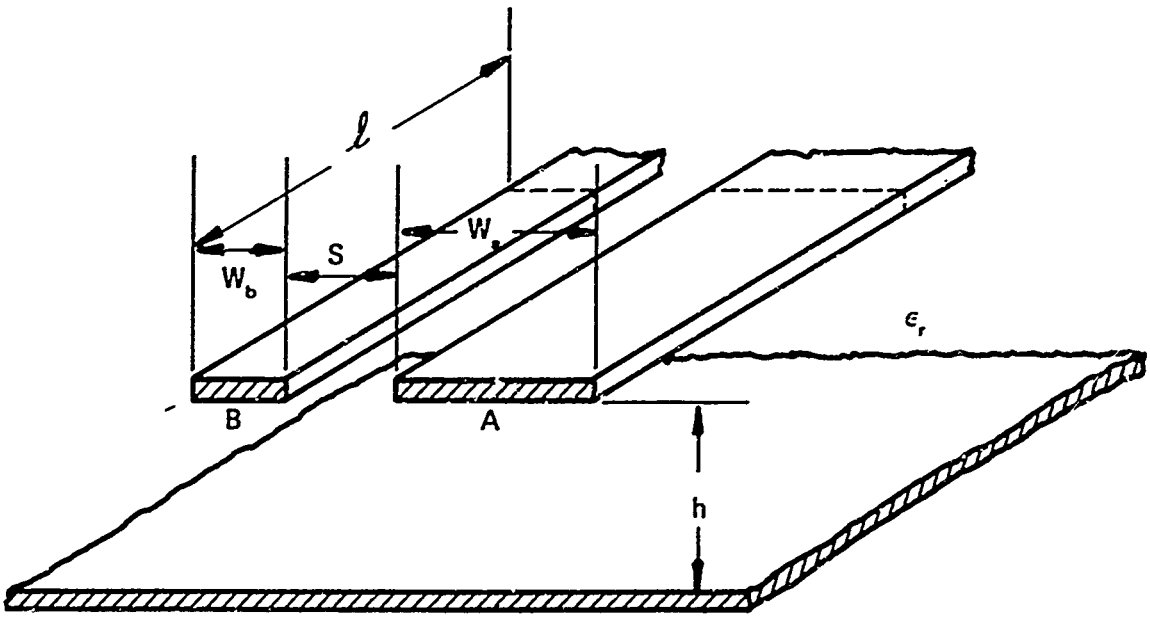

FIGURE 6 NON-SYMMETRICAL COUPLED LINE GEOMETRY

The first, which is fairly obvious, is that the impedance levels of the coupled and direct waves are different, so that the coupler has impedance transforming properties. The second is that the coupler can, within limits, be mismatched and still have infinite directivity.

Although these special properties are quite useful and offer the circuit designer an additional degree of freedom and flexibility, the non-symmetrical coupler does not appear to have received much attention as yet. An impedance transforming coupler could be handy as a directional detector, as suggested by Cristal, to match into the detector without a separate transformer. It could also be quite useful in coupled-line filters. This was suggested by Ozaki and Ishii back in 1958, but not much has come of it, principally for the want of filter synthesis procedures exploiting the impedance transformation property. Infinite directivity of a mismatched coupler can be used to stretch the coupling bandwidth and impedance transformation ratio beyond the limits of the matched coupler. The impedance transforming property will apply to microstrip couplers as it does to homogeneous dielectric couplers, and the infinite directivity of mismatched couplers will apply, at least in principle, to compensated microstrip couplers.

Because of the added design flexibility afforded by non-symmetrical couplers, we wish to promote and encourage the development of synthesis and design techniques for couplers and filters employing this element, particularly in stripline and microstrip. To this end, in this Section we review the principle results of Cristal's analysis; for the detailed analysis the reader is referred to Cristal's paper,Ref. 14.

In Appendix B we discuss the relationships among the various impedance and admittance parameters which sometimes tend to be confusing.

The notation for the non-symmetrical coupler is shown in Fig. 7. Note that the lines are specified in terms of admittances. The even and odd modes on a non-symmetrical pair are not exactly the same on an admittance basis as they are on an impedance basis, and we find the admittance formation conceptually simpler, since the modes are then defined in terms of equal and opposite line <u>voltages</u>. (cf.Appendix B). Since we prefer to think quantitatively in terms of impedance and ohms, we shall, for the most part, refer to impedances. However, since the even and odd mode impedances do not equal the reciprocals of the even and odd mode admittances, e.g. $Z_{oe}^{a} \neq 1/Y_{oe}^{a}$, when the lines are unequal, we shall refer to $1/Y_{oe}^{a}$, etc. as reciprocal admittances. Although there are four characteristic admittances, Y_{oe}^{a}, Y_{oo}^{a}, Y_{oe}^{b}, Y_{oo}^{b}, only three are independent since,by reciprocity, the transfer admittance Y_t is the same when viewed from either line.

The admittances $Y_{oa} = \frac{1}{2}(Y_{oe}^{a} + Y_{oo}^{a})$

and $Y_{ob} = \frac{1}{2}(Y_{oe}^{b} + Y_{oo}^{b})$

are the characteristic admittances of each line when the input to the other is grounded.

End-to-end symmetry is maintained by terminating both ends of the A and B lines in loads $Z_a = 1/Y_a$ and $Z_b = 1/Y_b$, respectively.

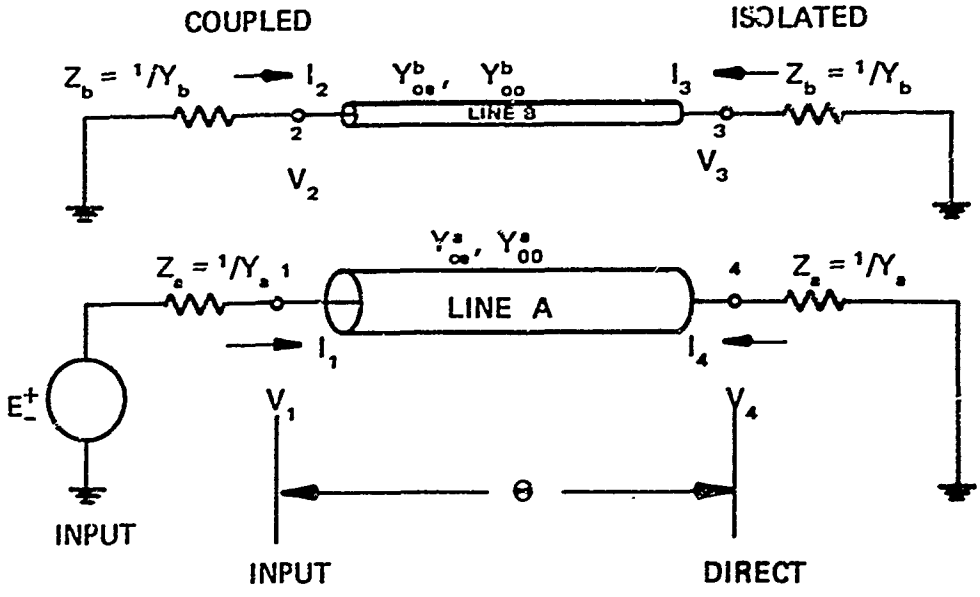

$$Y_{oe} = \tfrac{1}{2}(Y^a_{oo} + Y^a_{oe})$$
$$Y_{ob} = \tfrac{1}{2}(Y^b_{oo} + Y^b_{oe})$$
$$Y_t = \tfrac{1}{2}(Y^a_{oo} - Y^a_{oe}) = \tfrac{1}{2}(Y^b_{oo} - Y^b_{oe})$$

FIGURE 7 NON-SYMMETRICAL COUPLER NOTATION

The conditions for impedance matching are that

$$\frac{Z_b}{Z_a} = \frac{Y_{oa}}{Y_{ob}} , \tag{17}$$

and

$$\frac{1}{Z_a Z_b} = Y_{oa} Y_{ob} - Y_t^2 = \frac{1}{2} \left(Y_{oe}^{\ a} Y_{oo}^{\ b} + Y_{oe}^{\ b} Y_{oo}^{\ a} \right) \tag{18}$$

be satisfield simultaneously. When the lines are equal, Eq. (17) reduces to an identity and Eq. (18) reduces to Eq. (3). The voltage coupling at midband is given by

$$k = \frac{Y_t}{\sqrt{Y_{oa} Y_{ob}}}$$

$$= \frac{Y_{oo}^{\ a} - Y_{oe}^{\ a}}{\sqrt{\left(Y_{oe}^{\ a} + Y_{oo}^{\ a}\right) \left(Y_{oe}^{\ b} + Y_{oo}^{\ b}\right)}}$$

which reduces to Eq. (7) for equal lines. The condition for infinite directivity is Eq. (18) alone, so that it is possible to satisfy Eq. (18) but not Eq. (17) and have a mismatched coupler with infinite directivity.

The circuit parameters of interest for the matched coupler are its length, θ, the midband coupling, $k_p = -20 \log k$, and the impedance levels of the two sides, Z_a and Z_b, or the impedance level of one side and the impedance ratio $R_T = Z_b / Z_a$.

The even and odd mode reciprocal admittances are related to the circuit parameters as follows:

$$\frac{1}{Y_{oe}^{a}} = \frac{Z_a\sqrt{1-k^2}}{1-k/\sqrt{R_T}} \tag{19}$$

$$\frac{1}{Y_{oo}^{a}} = \frac{Z_a\sqrt{1-k^2}}{1+k/\sqrt{R_T}} \tag{20}$$

$$\frac{1}{Y_{oe}^{b}} = \frac{Z_b\sqrt{1-k^2}}{1-k\sqrt{R_T}} \tag{21}$$

$$\frac{1}{Y_{oo}^{b}} = \frac{Z_b\sqrt{1-k^2}}{1+k\sqrt{R_T}} \tag{22}$$

By dividing and multiplying Eq. (20) by Eq. (19) and Eq. (22) by Eq. (21), we obtain

$$\frac{1}{Y_{oo}^{a}} = \frac{1}{Y_{oe}^{a}}\left[\frac{1-k/\sqrt{R_T}}{1+k/\sqrt{R_T}}\right] \tag{23}$$

$$\frac{1}{Y_{oo}^{b}} = \frac{1}{Y_{oe}^{b}}\left[\frac{1-k\sqrt{R_T}}{1+k\sqrt{R_T}}\right] \tag{24}$$

$$\frac{1}{Y_{oo}^{a}} = \frac{Z_a^2}{(1/Y_{oe}^{a})} \left[\frac{1 - k^2}{1 - k^2/R_T} \right] \tag{25}$$

$$\frac{1}{Y_{oo}^{b}} = \frac{Z_b^2}{(1/Y_{oe}^{b})} \left[\frac{1 - k^2}{1 - k^2 R_T} \right] . \tag{26}$$

If we now define coupling parameters

$$k_a = k/\sqrt{R_T}$$

and

$$k_b = k\sqrt{R_T},$$

Eqs. (23) and (24) relate the A and B even and odd mode reciprocal admittances in the same way they would for symmetrical couplers of coupling k_a or k_b. Similarly, by defining impedance parameters

$$\mathcal{Z}_a = Z_a \sqrt{\frac{1 - k^2}{1 - k^2/R_T}}$$

$$\mathcal{Z}_b = Z_b \sqrt{\frac{1 - k^2}{1 - k^2 R_T}}$$

Eqs. (25) and (26) relate the the A and B reciprocal admittances in the same way as for symmetrical couplers of impedance $\mathcal{Z}_a$ or $\mathcal{Z}_b$.

Thus, we may use Fig. 5 to read off the reciprocal admittances for given k_p, Z_a, Z_b and $R_T = Z_b / Z_a$. First compute the coupling and impedance parameters for each line, k_{pa}, k_{pb}, z_a, z_b, or determine them from Figs. 8 and 9. Then, on Fig. 5, simply interpret Z_{oo} as $1/Y_{oo}^a$, Z_{oe} as $1/Y_{oe}^a$ for coupling k_{pa} and impedance z_a, and similarly for line B.

Since $1/Y_{oe}^a$ and $1/Y_{oe}^b$ must remain finite and positive, Eqs. (19) and (21) require that $k/\sqrt{R_T}$ and $k\sqrt{R_T}$ both be less than one, or that, $k^2 < R_T$ or $1/R_T$, whichever is less than one. This means there is a theoretical limit to the amount of impedance transformation and coupling that can be attained simultaneously. This limit is shown in Figs. 8 and 10. Clearly it is impossible to reach this limit, since it would require $1/Y_{oe}^a$ or $1/Y_{oe}^b$ be infinite. The dotted line in Fig. 10 indicates the area of a practical limit for microstrip based on a maximum $1/Y_{oe}^a$ of 200 Ω in a 50 Ω system.

Except for the impedance transforming properly, the matched non-symmetrical coupler behaves in every respect just like a matched symmetrical coupler. In particular, the coupling curves and bandwidth characteristics in Figs. 3 and 4 still apply. Also, the coupled and direct waves are always in phase quadrature, and the coupling is independent of the dielectric constant of the medium.

The mismatched, infinite-directivity coupler will have its maximum VSWR, σ, at its center frequency, and it will be matched at $f = 0$ and $2f_o$. It is also a quadrature coupler at all frequencies. The power split, i.e. the ratio of coupled to direct output powers, is

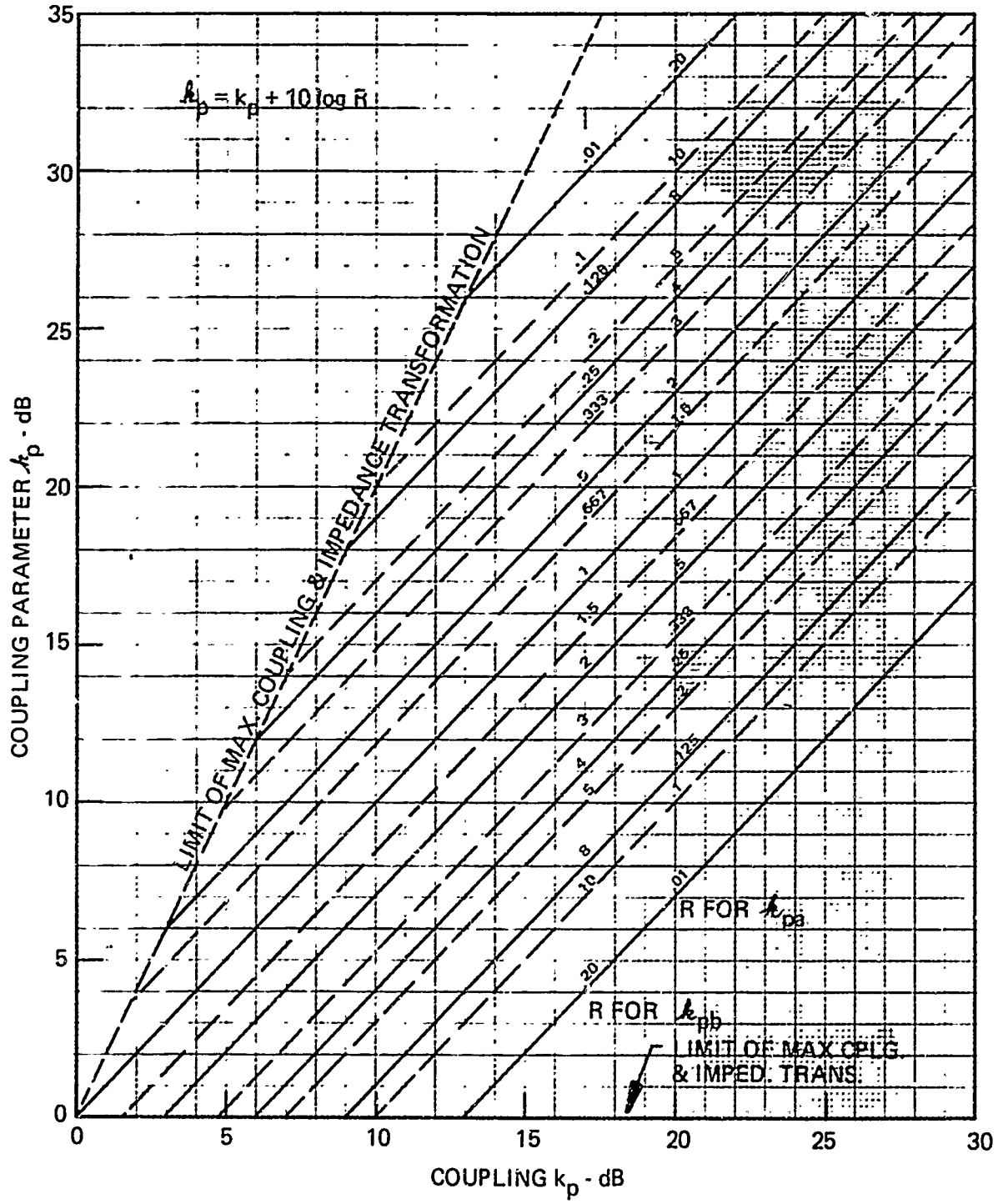

FIGURE 8 NON-SYMMETRICAL COUPLER COUPLING PARAMETER VS. COUPLING AND IMPEDANCE TRANSFORMATION RATIO.

D 12025

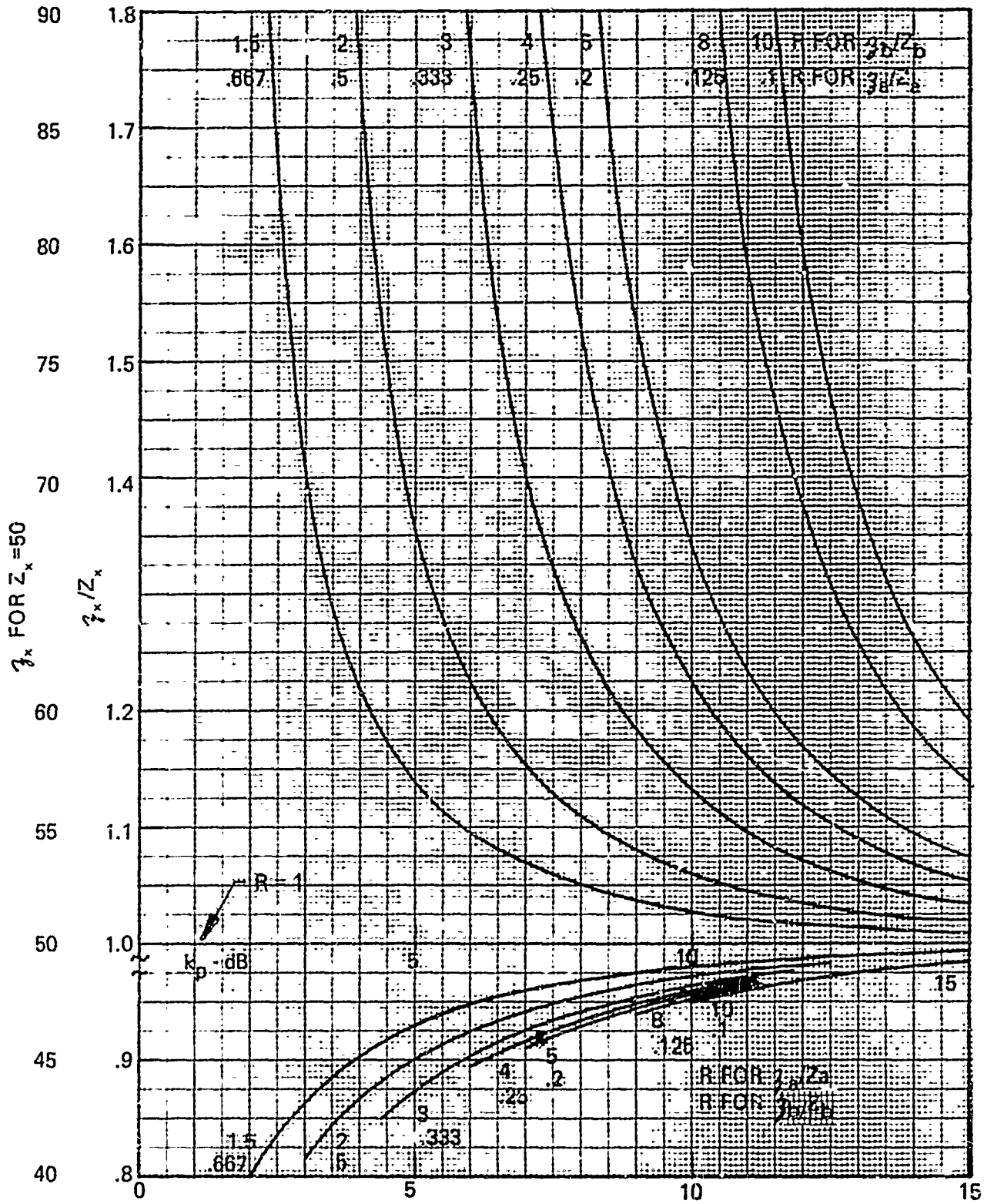

FIGURE 9 NON-SYMMETRICAL COUPLER IMPEDANCE PARAMETER VS. COUPLING AND IMPEDANCE TRANSFORMATION RATIO.

D-12054

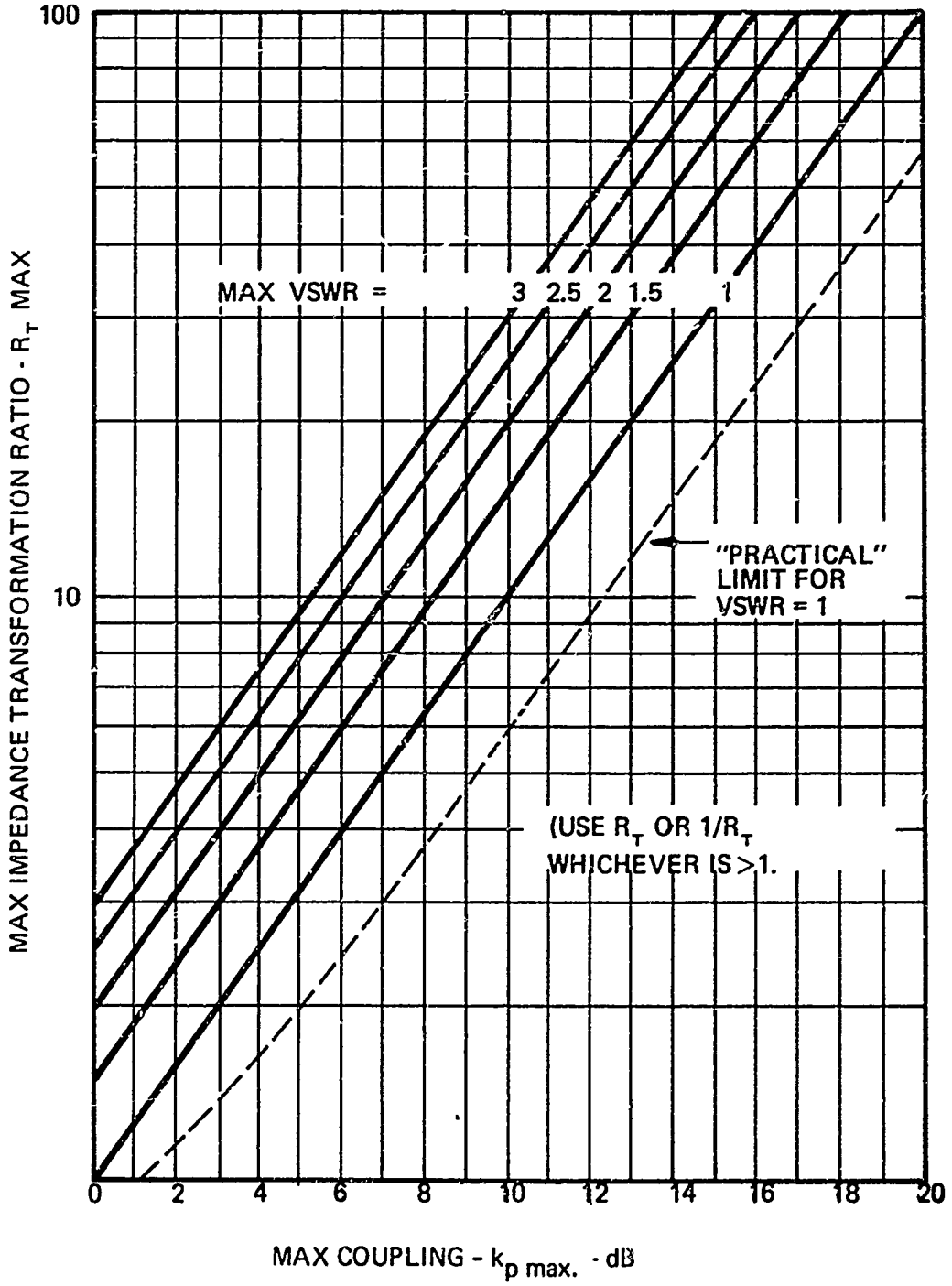

FIGURE 10 THEORETICAL LIMIT OF IMPEDANCE TRANSFORMATION AS FUNCTIONS OF NOMINAL MIDBAND COUPLING AND MISMATCH.

D-12051

independent of the mismatch. The coupling relative to the incident power is, of course, reduced from its nominal value k_p i.e. the coupling when matched, by the reflection loss.

The putative advantages of the mismatched coupler are an increase in the coupling-impedance transformation limit and an increase in the coupling bandwidth. Fig. 10 shows the theoretical coupling-transformation limit for several values of midband VSWR; the relationship is simply $R_T = \sigma k^2$, when R_T is taken as greater than one. Fig.11, which is an extension of Fig. 4, shows the coupling bandwidths for matched and 2:1 and 3:1 mismatched couplers. Note that the coupling bandwidth increase is modest even for substantial mismatches. Just how modest can perhaps be better appreciated from Fig. 12 in which the coupling curves are plotted for matched and 2:1 mismatched 3 and 10 dB couplers. Also plotted are mismatched 2.50 and 9.49 dB couplers, which have 3 and 10 dB coupling with respect to the incident power. It would seem that a mismatched non-symmetrical coupler could be used to advantage to increase the attainable coupling or impedance transformation, but it is of dubious value in stretching the useable bandwidth.

The even and odd mode reciprocal admittances for the mismatched coupler may be obtained from Figs. 8 , 9 and 5 by replacing Z_a and Z_b by $Z_a\sqrt{\sigma}$ and $Z_b/\sqrt{\sigma}$, or $Z_a/\sqrt{\sigma}$ and $Z_b\sqrt{\sigma}$ and following the procedure for a matched coupler. For instance, to design a coupler for a 2:1 mismatch and 50 Ω lines at all ports, use the design for a matched coupler transforming from 70.7 Ω to 35.4 Ω.

Cristal provides several references to design data, relating line dimensions to the even and odd mode admittances for homogeneous dielectric transmission line media. Unfortunately, similar data is not

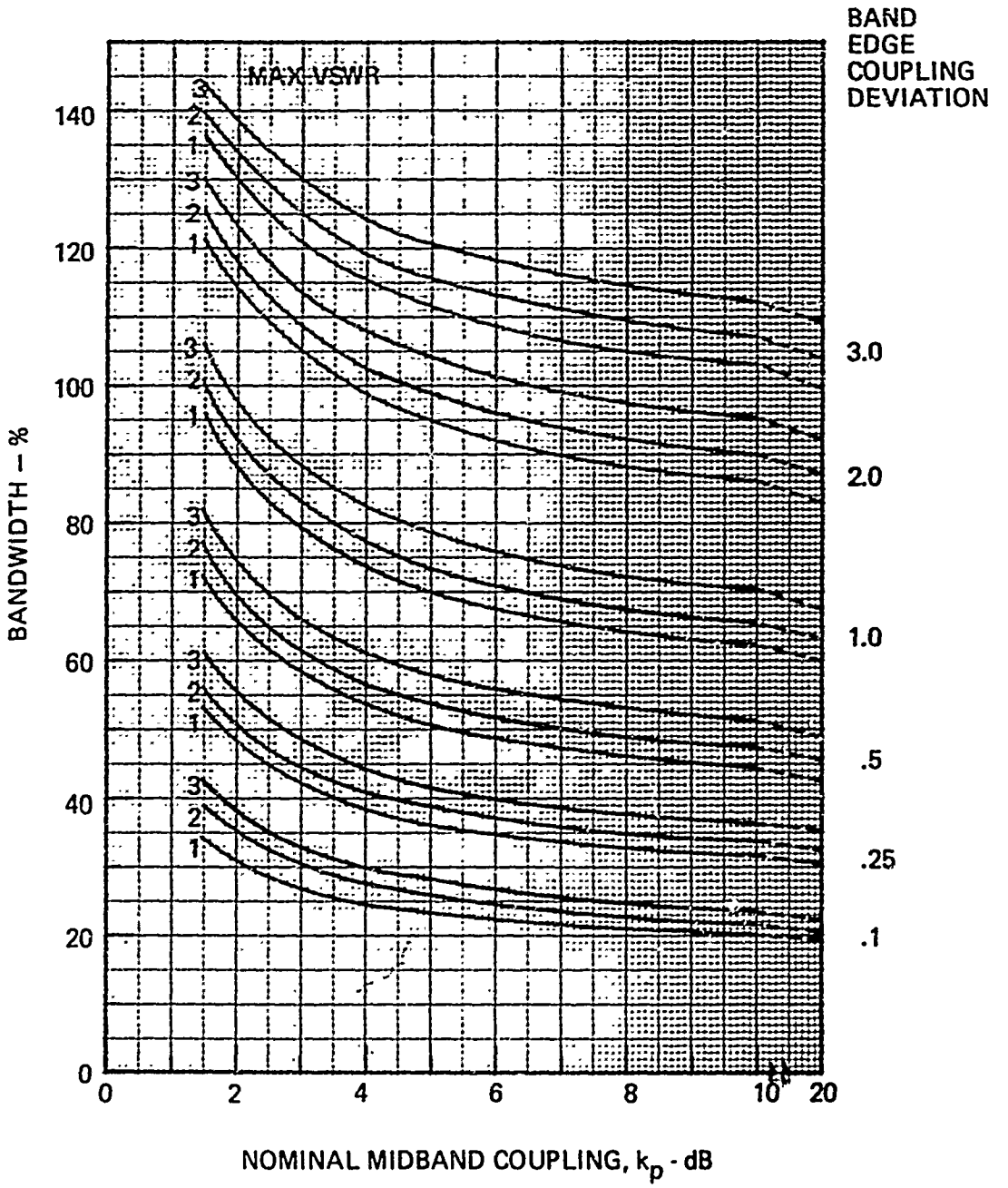

FIGURE 11 COUPLING BANDWIDTH VS. NOMINAL COUPLING AND MIDBAND VSWR FOR NON-SYMMETRICAL COUPLERS.

D-12055

yet available for non-symmetrical microstrip lines. We will, however, in the next Section suggest an approximate method for deriving the design data from the symmetrical coupler data.

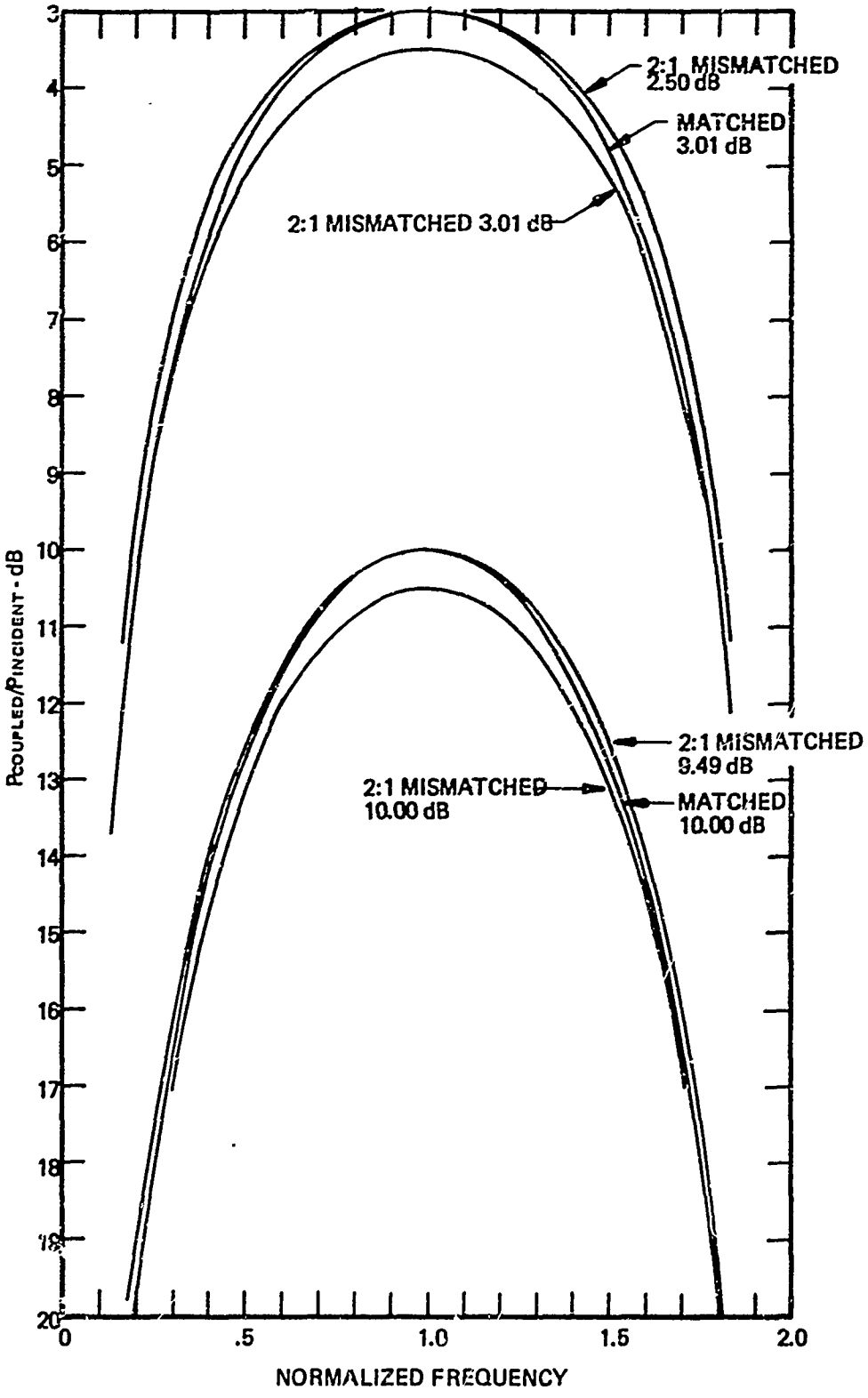

FIGURE 12 COUPLING CHARACTERISTICS OF MATCHED AND MISMATCHED NON-SYMMETRICAL COUPLERS.

D-12052

C. The Symmetrical Microstrip Coupler

Microstrip coupled lines, Fig. 13, with mixed dielectric does not support pure TEM modes of propagation. However, it is well known that two modes do propagate down to dc, where they reduce to the TEM even and odd modes of the homogeneous dielectric line. These modes are almost TEM and, aside from their frequency dispersion, they are quite adequately approximated by the TEM modes in an homogeneous dielectric with an appropriately chosen effective dielectric constant.

The effective relative dielectric constant, ϵ_{eff}, of a microstrip line depends on the width-to-height ratio of the strip and the frequency. One definition of the effective dielectric constant is the ratio of static capacitances per unit length of the line with and without the dielectric in place. Another is $\epsilon_{eff} = c^2/v_p^2$, where c is the free space velocity of light and v_p is the phase velocity of a wave on the line. These two definitions are equivalent at dc and low frequencies, but the second is valid at all frequencies since it includes the effect of dispersion, i.e. the variation of the effective dielectric constant with frequency. Normally, ϵ_{eff} is calculated from the static capacitances and the dispersion is handled as a separate problem. Dispersion, over the useful frequency range of a microstrip line--up to the cutoff of the first higher order mode--usually amounts to just a slight correction to the static dielectric constant. An alternative form of the phase velocity definition is: $\epsilon_{eff} = (\lambda_o / \lambda_g)^2$, where λ_o is the free-space wavelength and λ_g is the guide wavelength.

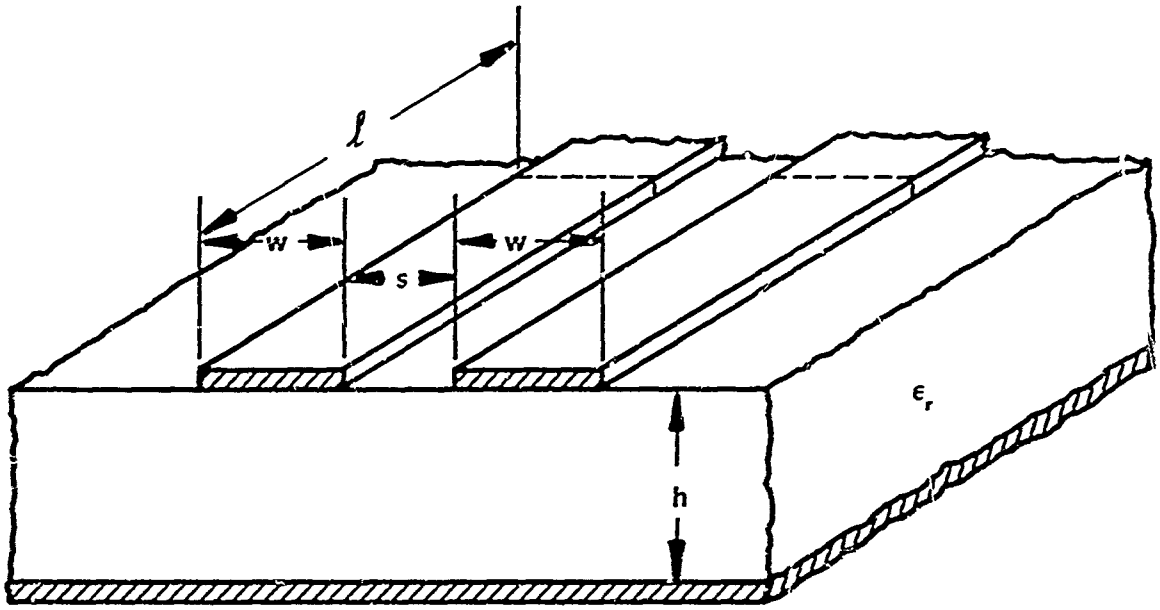

a) MICROSTRIP COUPLED LINE GEOMETRY

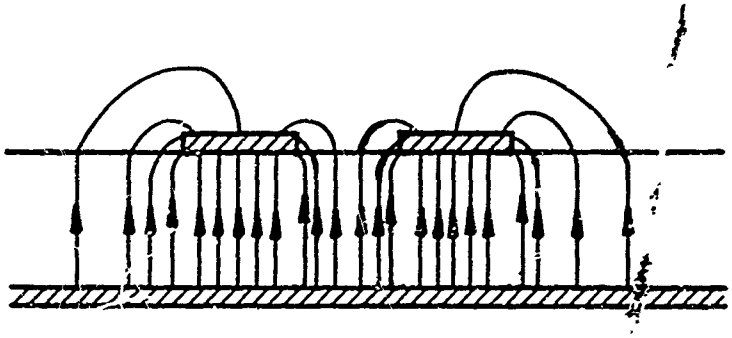

b) EVEN MODE ELECTRIC FIELD PATTERN (SCHEMATIC)

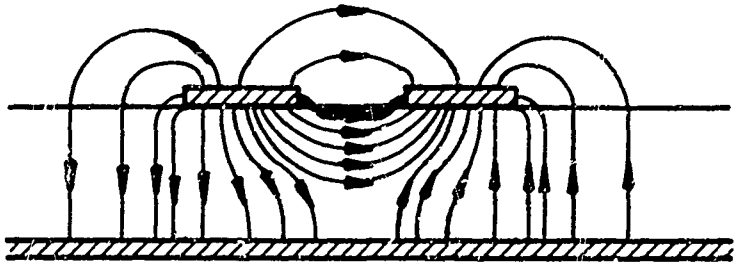

c) ODD MODE ELECTRIC FIELD PATTERN (SCHEMATIC)

FIGURE 13 THE MICROSTRIP COUPLED STRIP TRANSMISSION LINE.

Since λ_g is easily measured, this definition is commonly used in empirical determinations of ε_{eff}.

In general, the more the electrical energy is confined to the dielectric substrate, the closer these effective dielectric constants will be to the constant of the substrate material itself. It can be readily appreciated from Fig. 13 that the even mode electric fields on coupled lines will be more concentrated in the dielectric than those of the odd mode. Thus, the even mode will have a higher effective dielectric constant, lower phase velocity and shorter wavelength than the odd mode. In microstrip couplers on ceramic substrates the even mode wave velocity will run up to 15%, typically 8 - 12%, below the odd mode velocity.

In this section we shall examine the effect of the unequal velocities of the even and odd modes on the RF characteristics of the symmetrical coupled pair. We shall consider the low frequency, non-dispersive case here, and defer a discussion of dispersion until after looking at the design relationships in the next section.

Zysman and Johnson[15] have deduced the impedance matrix for the microstrip coupler:

$$Z = \begin{bmatrix} Z_{11} & Z_{12} & Z_{13} & Z_{14} \\ Z_{12} & Z_{11} & Z_{14} & Z_{13} \\ Z_{13} & Z_{14} & Z_{11} & Z_{12} \\ Z_{14} & Z_{13} & Z_{12} & Z_{11} \end{bmatrix} \tag{27}$$

where $Z_{11} = -\frac{j}{2}(Z_{oe} \operatorname{ctn} \theta_e + Z_{oo} \operatorname{ctn} \theta_o)$

$$Z_{12} = -\frac{j}{2}(Z_{oe} \operatorname{ctn} \theta_e - Z_{oo} \operatorname{ctn} \theta_o)$$

$$Z_{13} = -\frac{j}{2}(Z_{oe} \csc \theta_e - Z_{oo} \csc \theta_o)$$

$$Z_{14} = -\frac{j}{2}(Z_{oe} \csc \theta_e + Z_{oo} \csc \theta_o) \quad ,$$

and θ_e and θ_o are the electric length of the coupler for the even and odd mode waves respectively. As in the case of the ideal coupler, the impedance matrix completely specifies the coupler's electrical properties, but not in a very transparent fashion. Again we need the scattering matrix. However, the similarity of Eq. (27) with the matrix for the ideal coupler, Eq. (2) should be noted. The coupler is still described by just two impedance parameters, Z_{oe} and Z_{oo}, but requires two length parameters, θ_e and θ_o. (We will sometimes use θ_e and the velocity ratio $\rho_v = v_o / v_e = \theta_e / \theta_o$.) Note also that in Eq. (27) the trigonometric functions of θ_e and θ_o multiply the corresponding impedances and the even and odd mode terms add with the same signs as in Eq. (2).

The scattering matrix for the microstrip coupler has been in fact derived by Krage and Haddad,[16] using coupled-mode analysis. Their analysis, although very thorough and elegant, is based on coupling of the modes on each line rather than the even and odd modes. As a

consequence, their final formulation of the scattering coefficients (Eqs. (36), Ref. 16) employs so many subsidiary variables as to make it intractable. The similarity of impedance matrices suggested to us that a much simpler formulation of the scattering matrix using just four parameters should be possible. The derivation and the general scattering coefficients are given in Appendix C. We see that the scattering matrix is the same as that of the ideal coupler, with the addition of the appropriate subscripts to the electrical length.

Of particular importance is the fact that the coupler impedance level $Z_k = \sqrt{Z_{oe} Z_{oo}}$ and voltage coupling coefficient $k = (Z_{oe} - Z_{oo}) / (Z_{oe} + Z_{oo})$ defined for the ideal coupler are still useful parameters to describe the microstrip coupler, although the former can no longer be interpreted as the matching impedance.

Consider the scattering matrix for the special case when $\mathcal{Z}_k = Z_k / Z_o = 1$. From Eqs. (C-17) and (C-18), Appendix C, we obtain

$$S_{11} = \frac{jk}{2}\left[\frac{\sin\theta_e}{\sqrt{1-k^2}\cos\theta_e + j\sin\theta_e} - \frac{\sin\theta_o}{\sqrt{1-k^2}\cos\theta_o + j\sin\theta_o}\right] \quad (28)$$

$$S_{12} = \frac{jk}{2}\left[\frac{\sin\theta_e}{\sqrt{1-k^2}\cos\theta_e + j\sin\theta_e} + \frac{\sin\theta_o}{\sqrt{1-k^2}\cos\theta_o + j\sin\theta_o}\right] \quad (29)$$

$$S_{13} = \frac{\sqrt{1-k^2}}{2}\left[\frac{1}{\sqrt{1-k^2}\cos\theta_e + j\sin\theta_e} - \frac{1}{\sqrt{1-k^2}\cos\theta_o + j\sin\theta_o}\right] \tag{30}$$

$$S_{14} = \frac{\sqrt{1-k^2}}{2}\left[\frac{1}{\sqrt{1-k^2}\cos\theta_e + j\sin\theta_e} + \frac{1}{\sqrt{1-k^2}\cos\theta_o + j\sin\theta_o}\right] \tag{31}$$

Compare these scattering coefficients with Eqs. (4) - (6) for the ideal coupler. In particular note that when $\theta_e \neq \theta_o$ the coupler is not matched and the isolation is finite.

Since θ_e and θ_o normally differ by only about 10% in microstrip, near midband where the coupler is approximately 90^o long we can make the following approximations:

$$\sin\theta_e \approx \sin\theta_o \approx 1$$

$$\cos\theta_e \approx \frac{\pi}{2} - \theta_e = -\delta\theta_e$$

$$\cos\theta_o \approx \frac{\pi}{2} - \theta_e = -\delta\theta_e .$$

Thus, near midband, the scattering coefficients are approximately:

$$S_{11} = \frac{jk\sqrt{1-k^2}}{2}\left(\delta\theta_o - \delta\theta_e\right) \tag{32}$$

$$S_{12} = k\left[1 - j\frac{\sqrt{1-k^2}}{2}(\delta\theta_o + \delta\theta_e)\right] \tag{33}$$

$$S_{13} = \frac{(1-k^2)}{2}(\delta\theta_o - \delta\theta_e) \tag{34}$$

$$S_{14} = -j\sqrt{1-k^2}\left[1 - j\frac{\sqrt{1-k^2}}{2}(\delta\theta_o + \delta\theta_e)\right] \tag{35}$$

From Eq. (33) it is clear that k is still the voltage coupling coefficient at midband, where midband occurs when the average of the even and odd mode lengths of the coupler is one-quarter wavelength. From Eqs. (32) and (34), and the fact that $\delta\theta_o - \delta\theta_e = \theta_e\left(\frac{v_e}{v_o} - 1\right)$, we see that the VSWR increases and the isolation decreases with increasing frequency. Furthermore, the looser the coupling, i.e. the smaller k becomes, the lower the isolation; consequently the directivity problem becomes rapidly worse as the coupling is decreased. Finally, the ratio of Eq. (35) to (33) shows that it is still a quadrature coupler in the neighborhood of the band center. The exact coefficients, Eqs. (29) and (31) show that it will deviate slightly from phase quadrature as $\sin\theta_e = \sin\theta_o$ ceases to be a good approximation.

To illustrate the basic behavior of the microstrip coupler, the computed transmission characteristics of 3, 10, and 20 dB couplers are shown in Figs. 14, 15 and 16. The velocity ratios are typical for microstrip couplers with a substrate dielectric constant $\varepsilon_r = 10.0$.

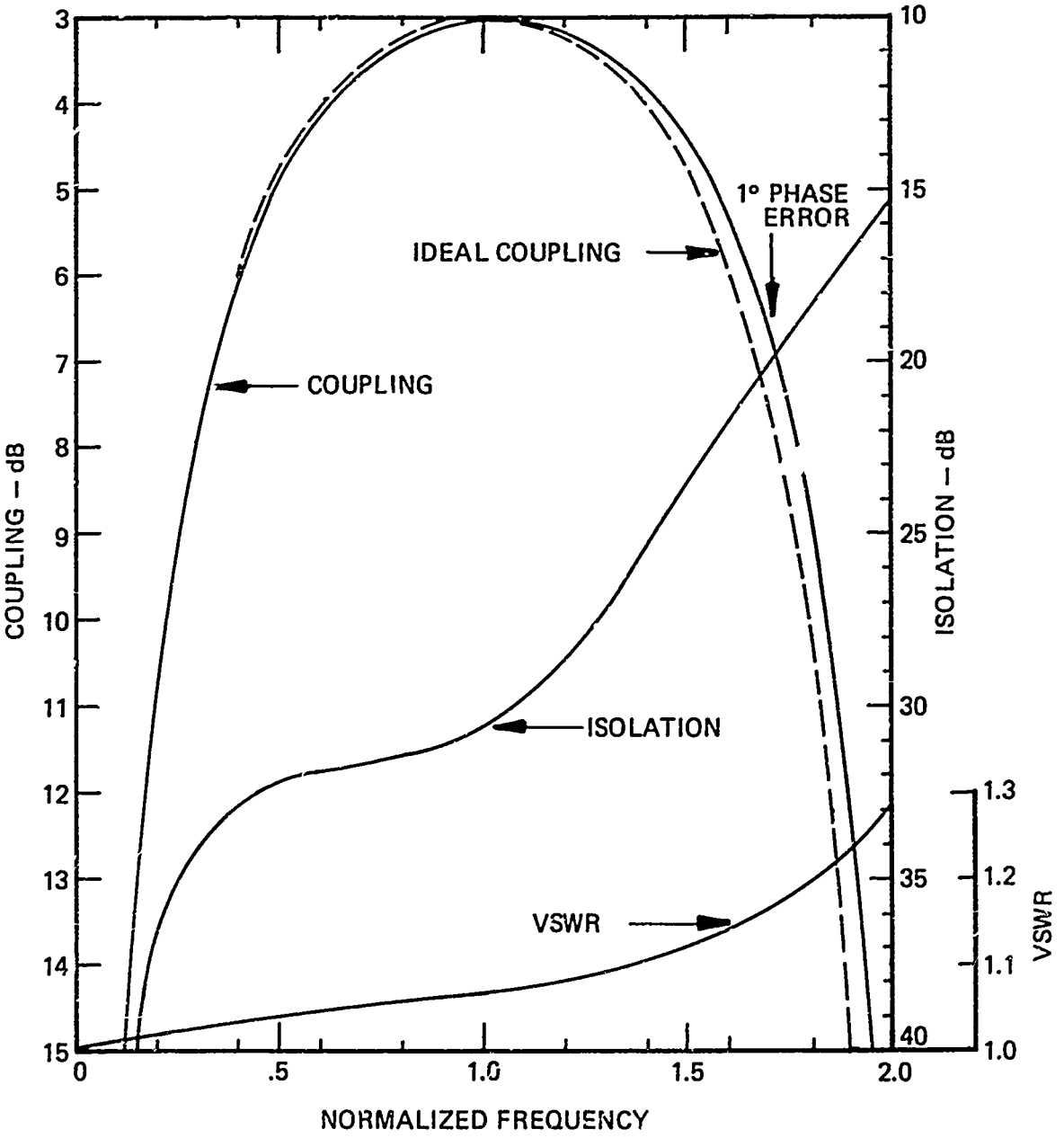

FIGURE 14 CHARACTERISTICS OF A 3 dB COUPLER WITH UNEQUAL MODE VELOCITIES. $V_o/V_e = 1.08$. $\Theta_e = 90°$ @ f = 1.0

D-12057

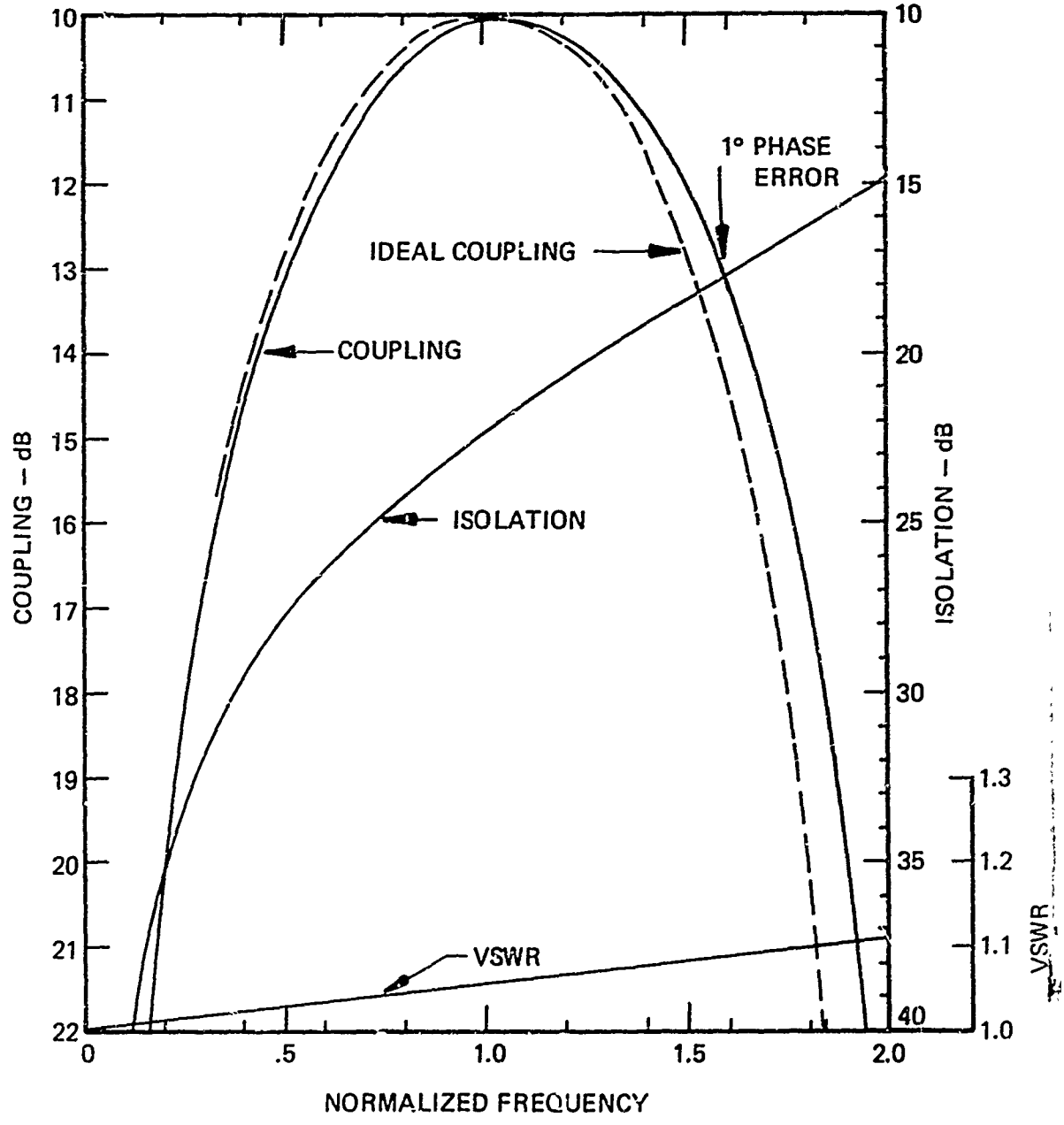

FIGURE 15 CHARACTERISTICS OF A 10 - dB COUPLER WITH UNEQUAL MODE VELOCITIES. $V_o/V_e = 1.12$. $\Theta_e = 90^o$ @ f = 1.0

D-12058

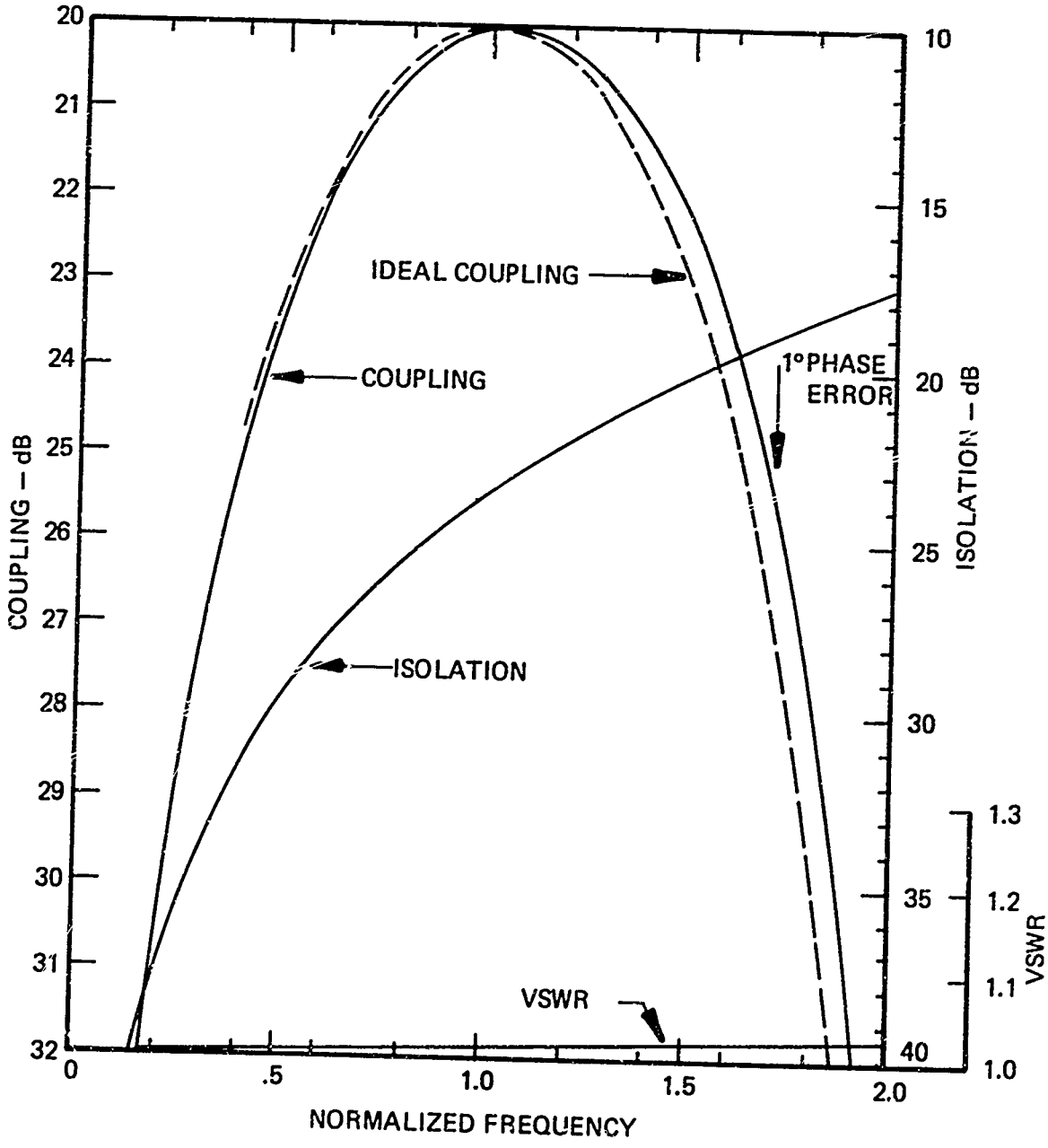

FIGURE 16 CHARACTERISTICS OF A 20 - dB COUPLER WITH UNEQUAL MODE VELOCITIES. $V_o/V_e = 1.09$ $\Theta_e = 90°$ @ f = 1.0.

D-12059

In these Figures, we have chosen the "center" frequency when the coupler is 90^{o} long to the even mode, and the ideal coupling characteristic is shown by dashed lines. In this way we see the effect of "switching on" the velocity inequality of the odd mode. Note that the coupling maximum shifts to a higher frequency, and the maximum is just a little less than the nominal coupling. The frequencies at which the departure from phase quadrature reaches 1^{o} is indicated - the couplers clearly maintain excellent quadrature properties over any useful bandwidth.

All in all, except for its low directivity, the microstrip coupler behaves very nearly like the ideal coupler. The coupling curves differ by a fraction of a dB over the useful bandwidth, the mismatch is not serious, and phase quadrature is well maintained. In many non-critical applications, such as signal sampling, high directivity may not be required, or the bandwidth may be narrow enough that the very low directivity at the high frequency end is not of concern. In such cases one need not velocity-compensate the coupler. To help decide this question, Fig. 17 shows the directivity of microstrip couplers as a function of the nominal coupling. The directivity is given at midband, defined here as $\theta_e = 90^{o}$, and at $1.5\ f_o$. The velocity ratio and the coupling deviation at $1.5\ f_o$ are also shown. The velocity ratio was computed for a substrate dielectric constant $\varepsilon_r = 10.$ and for coupler impedances of 50 Ω.

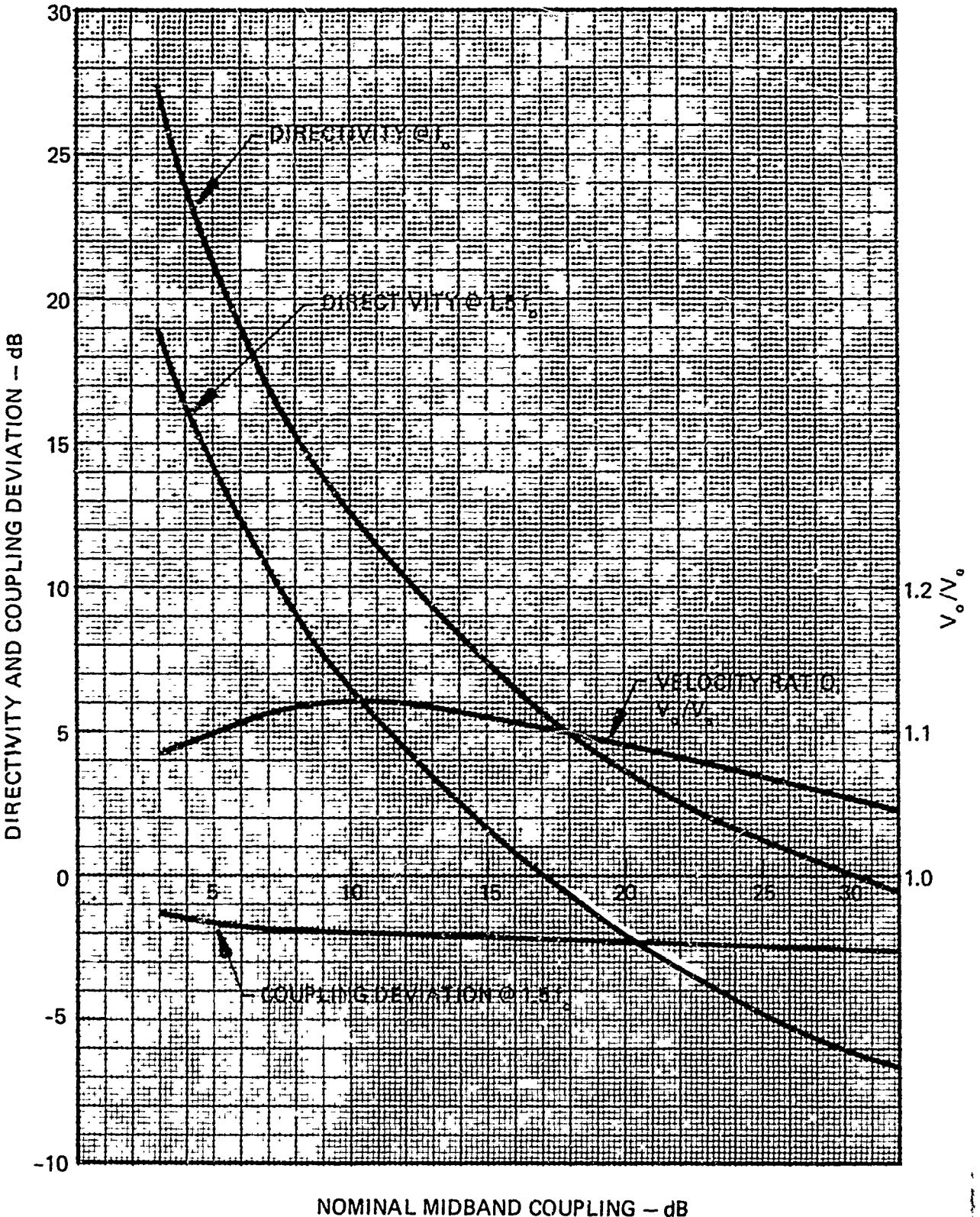

FIGURE 17 DIRECTIVITY OF TYPICAL MICROSTRIP COUPLIERS.

D-12060

III. MICROSTRIP COUPLER DESIGN DATA

A. The Parameters of Microstrip Coupled Lines

We have now completed the discussion of the transmission line properties of coupled-line couplers in terms of the basic electrical parameters Z_{oe}, Z_{oo}, θ_e and θ_o, or Z_k, k_p, θ_e, and v_o/v_e. We now turn to the design problem of relating these electrical parameters to the geometric parameters w/h and s/h and the substrate dielectric constant. Several solutions to the microstrip coupled-line problem have been published. Most frequently cited are the calculations of Bryant and Weiss[3] for symmetrical coupled strips of zero thickness. Graphs of the even and odd mode impedances for several dielectric constants for a size of strip widths and several strip spacings are given in their papers, Ref. 3, and in the Microwave Engineers Handbook, Vol I.[17]

In this section we shall present the Bryant and Weiss impedance data in such a form to make interpolation and extrapolation somewhat easier and more accurate than is possible from Refs. 3 and 17. We shall also provide the even and odd mode effective dielectric constants which were not included in those references. And, finally, we provide a design chart which relates the line widths and spacing directly to the coupling and coupler impedance. All the curves are for a substrate dielectric constant $\varepsilon_r = 10.0$; the data can be readily adjusted for other dielectric constants in that vicinity, as will be discussed later.

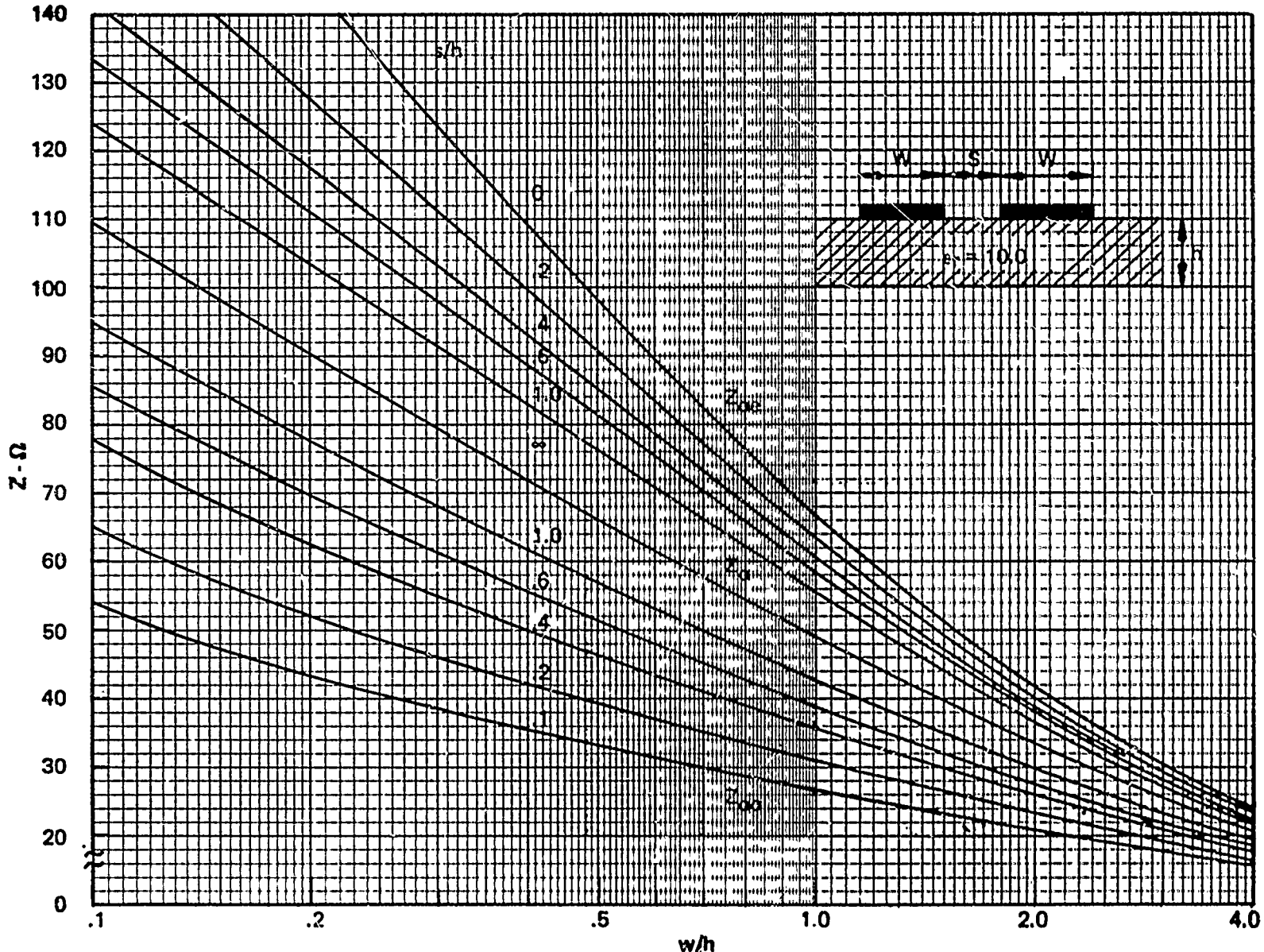

FIGURE 18 EVEN AND ODD MODE IMPEDANCES VS. LINE WIDTH WITH SPACING AS PARAMETER, FOR ϵ_r = 10

D-12061

Figure 18 gives the even and odd mode impedances as functions of normalized line width w/h with the normalized spacing or gap width s/h as a parameter. This graph is in the same form as those in Refs. 3 and and 17 with the important difference that the log and linear scales are interchanged. By plotting Z versus the logarithm of w/h the curves are more nearly straight, especially as w/h becomes small. As w/h goes to zero we would expect the coupled pair to be reasonably well approximated by a pair of small diameter, widely spaced wires, for which the impedances are known to go as the logarithm of the wire diameters. Consequently we expect that straight-line extrapolations of Fig. 18 to smaller w/h will be quite accurate, while the Bryant and Weiss computer program begins to lose accuracy as the strips become very narrow.

As the gap width goes to zero the even mode impedance approaches the limit

$$Z_{oe}(w, s) \xrightarrow[s \to 0]{} 2 Z_o (2w)$$

where Z_o is the impedance of a single strip. Thus the curve for $Z_{oe}(s = 0)$ can be readily determined from the curve for $s = \infty$. The odd mode impedance goes to zero as $s \to 0$. Consequently Fig. 18 is not too useful for determining Z_{oo} for narrow gaps. Fig. 19 gives Z_{oo} versus s/h with w/h as the parameter. These curves were computed from the Bryant and Weiss program for s/h down to .025 and then extrapolated down to .01. The accuracy of the calculations begins to suffer as the gap and/or line width decrease much below 0.1, however no estimate of the magnitude of the error has been made. We expect that the error at s = .01 would be no worse than the difference between the

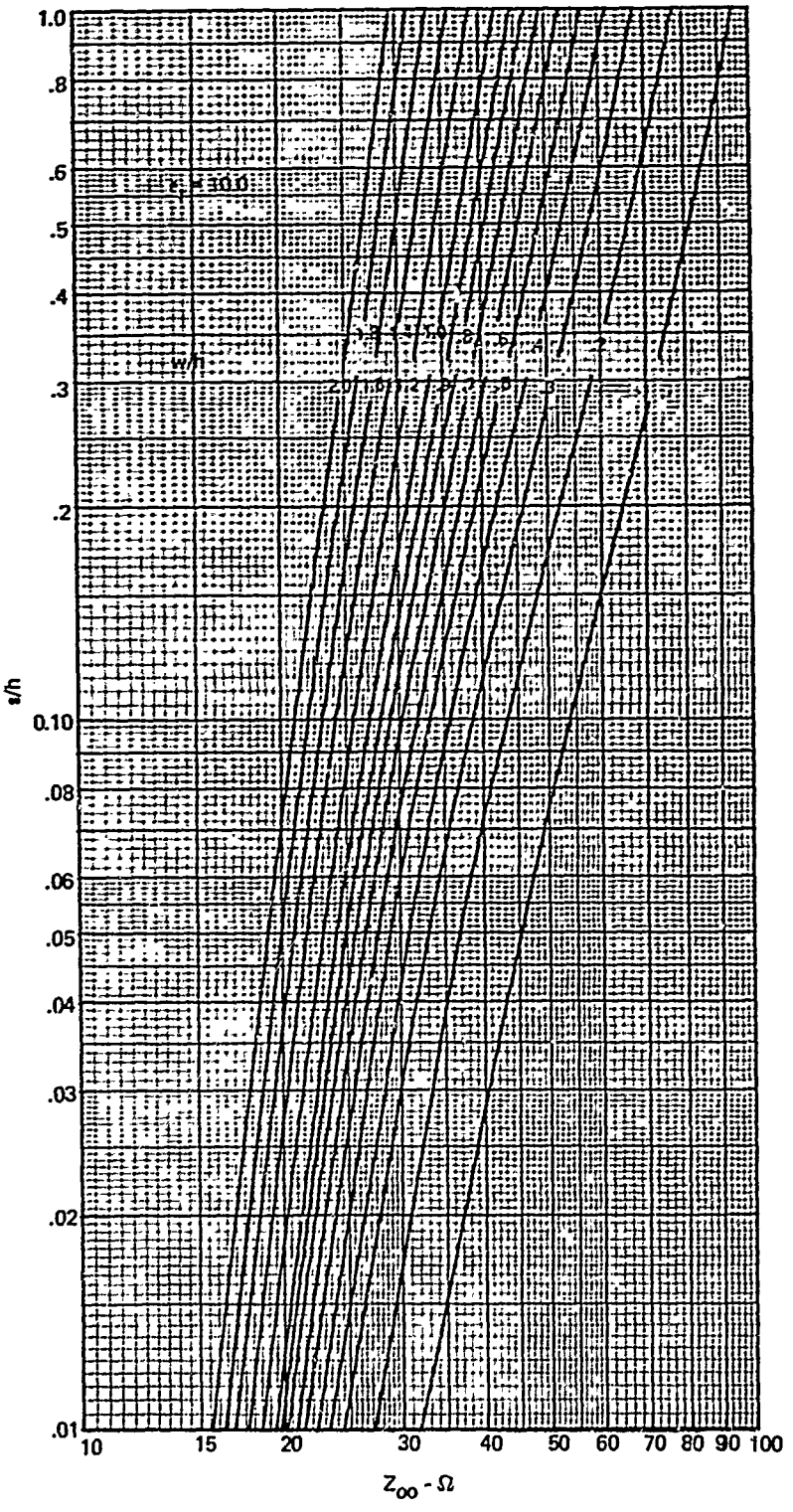

FIGURE 19 ODD MODE IMPEDANCE VS. SPACING WITH LINE WIDTH AS PARAMETER

D-12082

plotted values and the values obtained by a straight line extrapolation from the s = 0.1 - 0.2 range, which runs 5 to 15%.

In this regard, it should be borne in mind that the calculations are all for zero thickness lines. This is normally an excellent approximation for microstrip lines, since the printed lines are indeed quite thin compared to the substrate thickness. For single strips one can correct for the line thickness by making the lines narrower by about one thickness,[18] which is typically of the order of 10^{-4} in. wide on lines 10^{-2} inches. In most practical instances this correction may be neglected since it falls within the normal tolerances of etching the lines and maintaining the dielectric constant of the material. Clearly, in the case of narrow gaps between coupled lines, the line thickness will begin to become important in the determination of the odd mode impedance when the gap becomes smaller than the thickness. An evaluation of the thickness correction to Z_{oo} for narrow gaps has apparently never been published, and it is certainly not a trivial problem. Thus Fig. 19, and its extrapolation to still smaller gaps must be treated as an approximation suitable as an adequate starting point for the design of extremely narrow gap devices.

Fig. 20 gives the impedances versus gap width with line width as the parameter. Here we have made the scale linear in the parameter $e^{-s/h}$. This conveniently compresses the entire 0 to ∞ range of s into the 0 to 1 interval, and does so in such a way that Z_{oe} and Z_{oo} for large s/h are quite well represented by straight lines. Although the impedances are not precisely linear in $e^{-s/h}$ for large s/h, the extrapolation--or interpolation as plotted here--is accurate to better than 1 Ω for $s \gtrsim 2$; the interpolations were done from s/h = 1 or 2 on each side through the single strip Z_o, so that the maximum errors will occur in the s/h = 3 to 4 range.

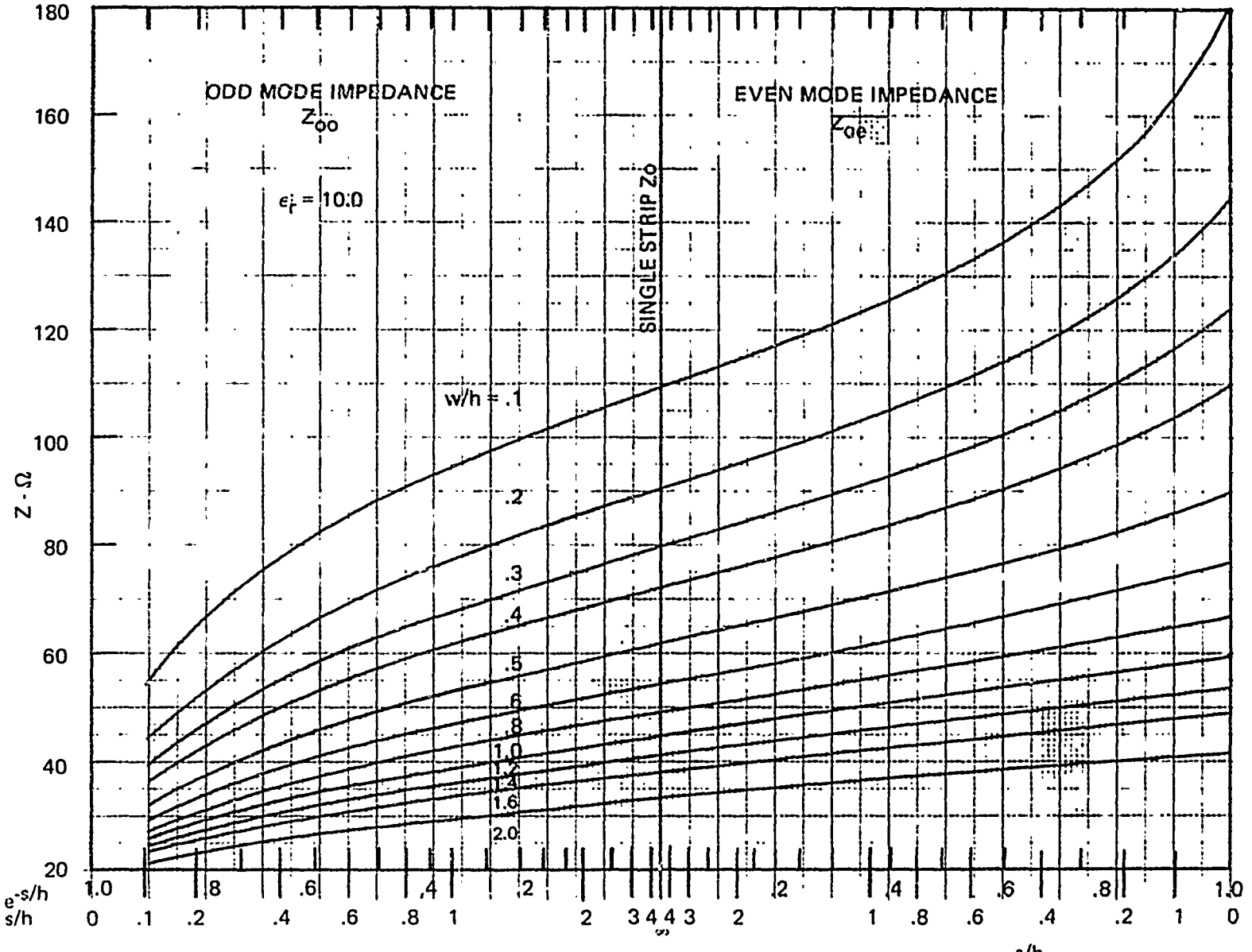

FIGURE 20 MICROSTRIP EVEN AND ODD MODE IMPEDANCES VS. $e^{-s/h}$

The effective dielectric constants for each mode are plotted in Fig. 21, using the exponential scale of Fig. 20 in order to cover the entire range of gap widths. The odd mode ε_{eff} plotted for small gaps are simple extrapolations from the wider gap ($s/h \geq .025$) data. The curves are least accurate in the $s/h = 2$ to 4 range where the slopes are changing rapidly. Nevertheless, the maximum error in that range is about .05 units or < 1% of ε_{eff}.

The log - log plot of Z_{oo} versus s/h in Fig. 19 suggests a small gap extrapolation formula--bearing in mind the reservations with respect to accuracy pointed out earlier--of the form

$$Z_{oo} = Z_{os} \, (w/h) \, (s/h)^{n\,(w/h)} \quad , \quad s/h \longrightarrow 0 \tag{36}$$

Figure 22 gives the coefficient Z_{os} and the exponent n, derived from the small gap end of Fig. 19, as functions of w/h.

Similarly, for large gaps, Fig. 20 suggest the approximations

$$\begin{aligned} Z_{oe} &= Z_o \, (w) \, (1 + \Delta \, e^{-s/h}) \\ Z_{oo} &= Z_o \, (w) \, (1 - \Delta \, e^{-s/h}) \end{aligned} \quad , \quad s/h \longrightarrow \infty \tag{37}$$

where $Z_o(w)$ is the single strip impedance from Fig. 18. The slope parameter Δ is given in Fig. 23 as a function of w/h.

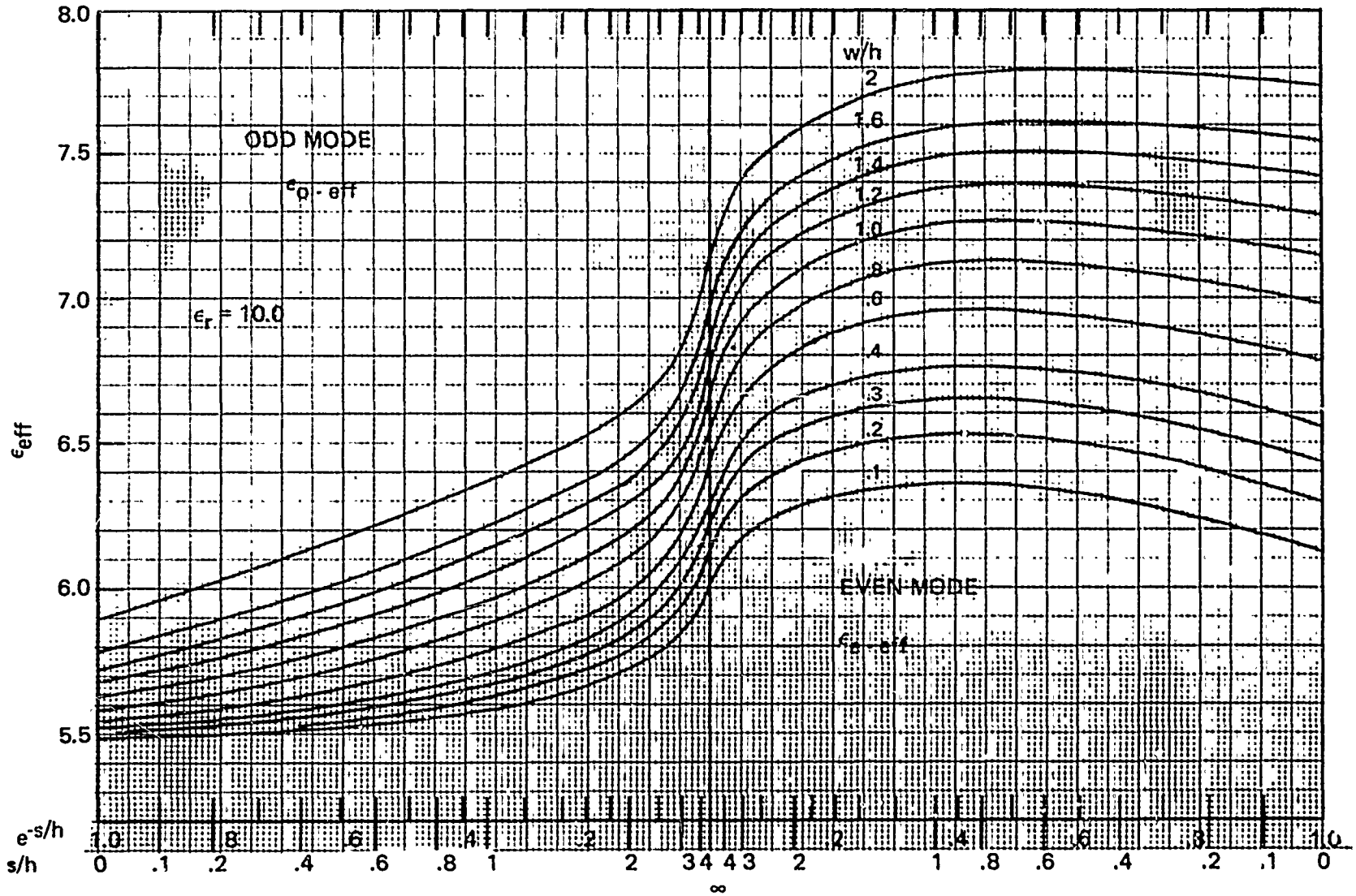

FIGURE 21 MICROSTRIP EVEN AND ODD MODE EFFECTIVE DIELECTRIC CONSTANT FOR ϵ_r = 10.0.

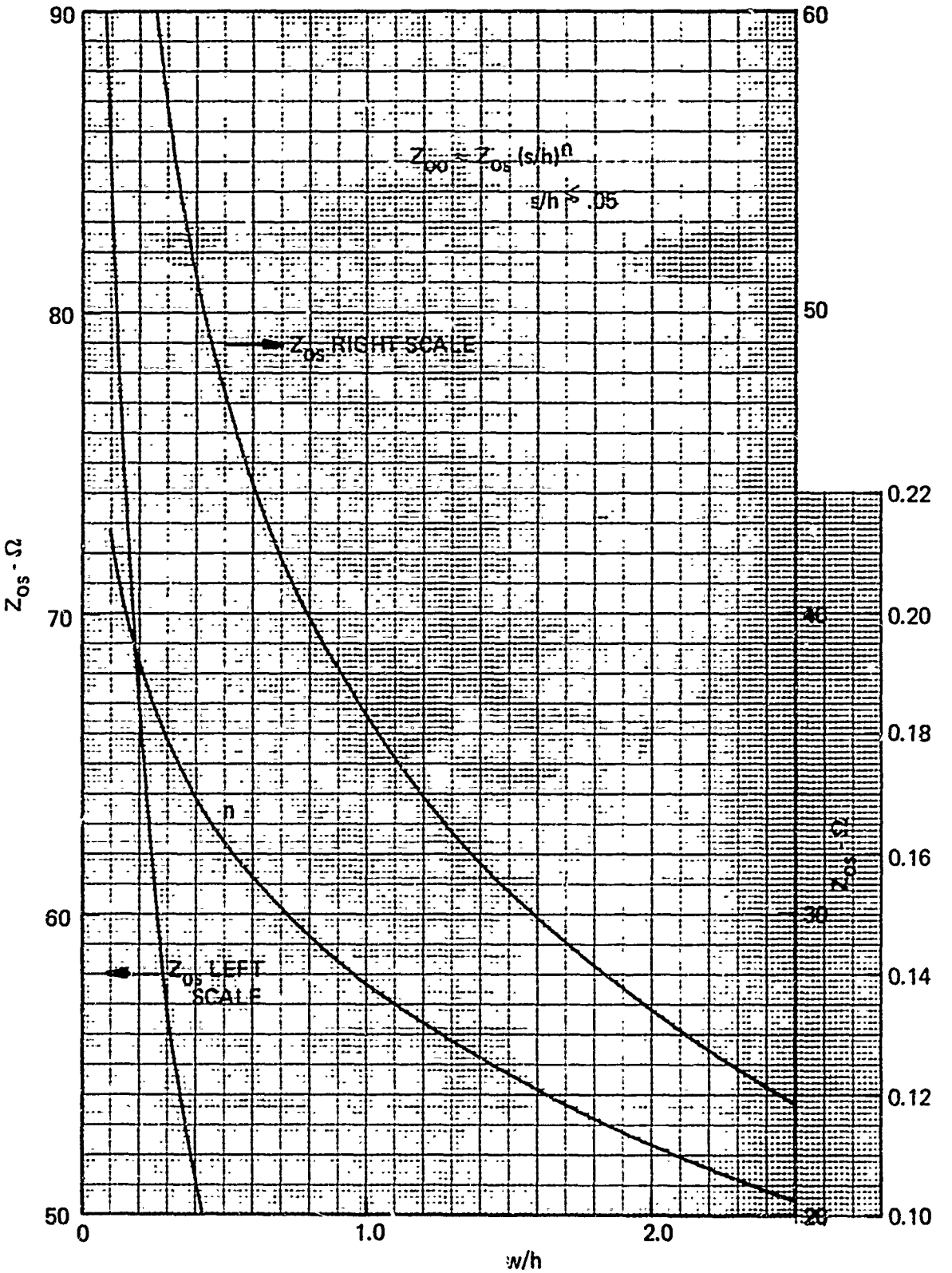

FIGURE 22 COEFFICIENT AND EXPONENT FOR ODD-MODE SMALL GAP APPROXIMATI FOR ϵ_r = 10.0.

D-12084

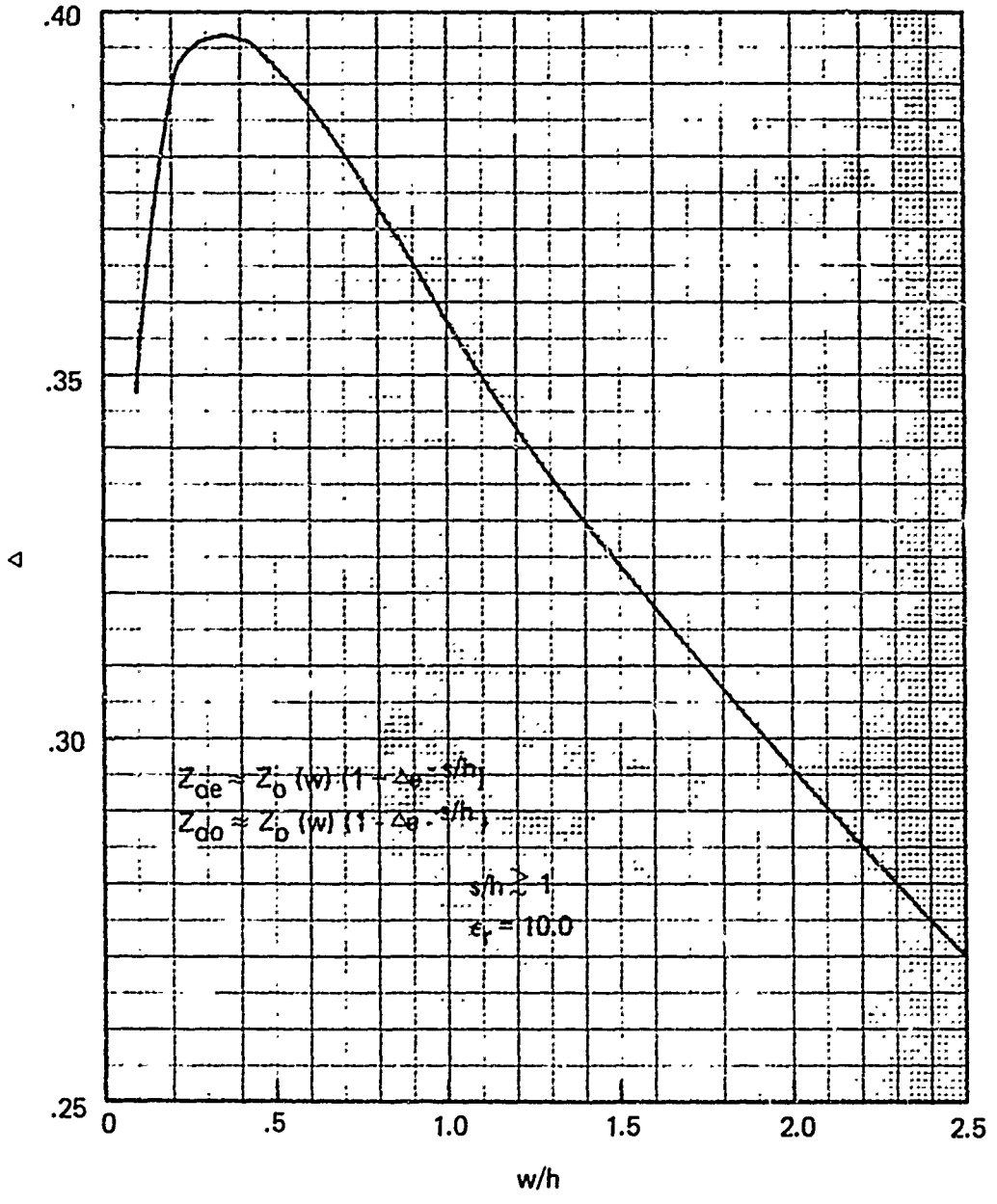

FIGURE 23 LARGE GAP APPROXIMATION PARAMETER.

The data in Figs. 18 - 23, which all apply for $\varepsilon_r = 10.0$ may be readily and accurately adjusted for other substrate dielectric constants over a fairly wide range about 10. From the Bryant and Weiss data on effective dielectric constants, we find that ε_{eff} is proportional to ε_r within a few percent for ε_r up to at least 16, but the proportionality constant depends on w, s and the mode. For substrate dielectric constants near 10, we can relate the effective dielectric constant for either mode and a given w and s, to the corresponding ε_{eff} when $\varepsilon_r = 10$ by

$$\varepsilon_{eff}(\varepsilon_r) = \varepsilon_{eff}(10)\left[\frac{\varepsilon_r}{10}\right] \cdot f(w,s,\varepsilon_r) \qquad (28)$$

where $f(w,s,\varepsilon_r)$ is a second order correction to adjust for the non-linearity of ε_{eff} with ε_r. The correction factor f is plotted versus ε_r in Fig. 24 for several values of w/h for the case of widely spaced lines, $s \to \infty$ For closely spaced lines, $s/h \sim 0.1$, f for the even mode is a fraction of a percent higher, and for the odd mode lower, than the $s \to \infty$ curve for $\varepsilon_r > 10$, and conversely for $\varepsilon_r < 10$. This is generally a negligible correction.

Thus, when $\varepsilon_r \neq 10$, Eq. (38), with f from Fig. 24, may be used to determine $\varepsilon_{e\text{-}eff}$ and $\varepsilon_{o\text{-}eff}$ from Fig. 21. Z_{oe} and Z_{oo} are determined from Figs. 18, 19, and 20 by dividing $\sqrt{\varepsilon_r \; f/10}$.

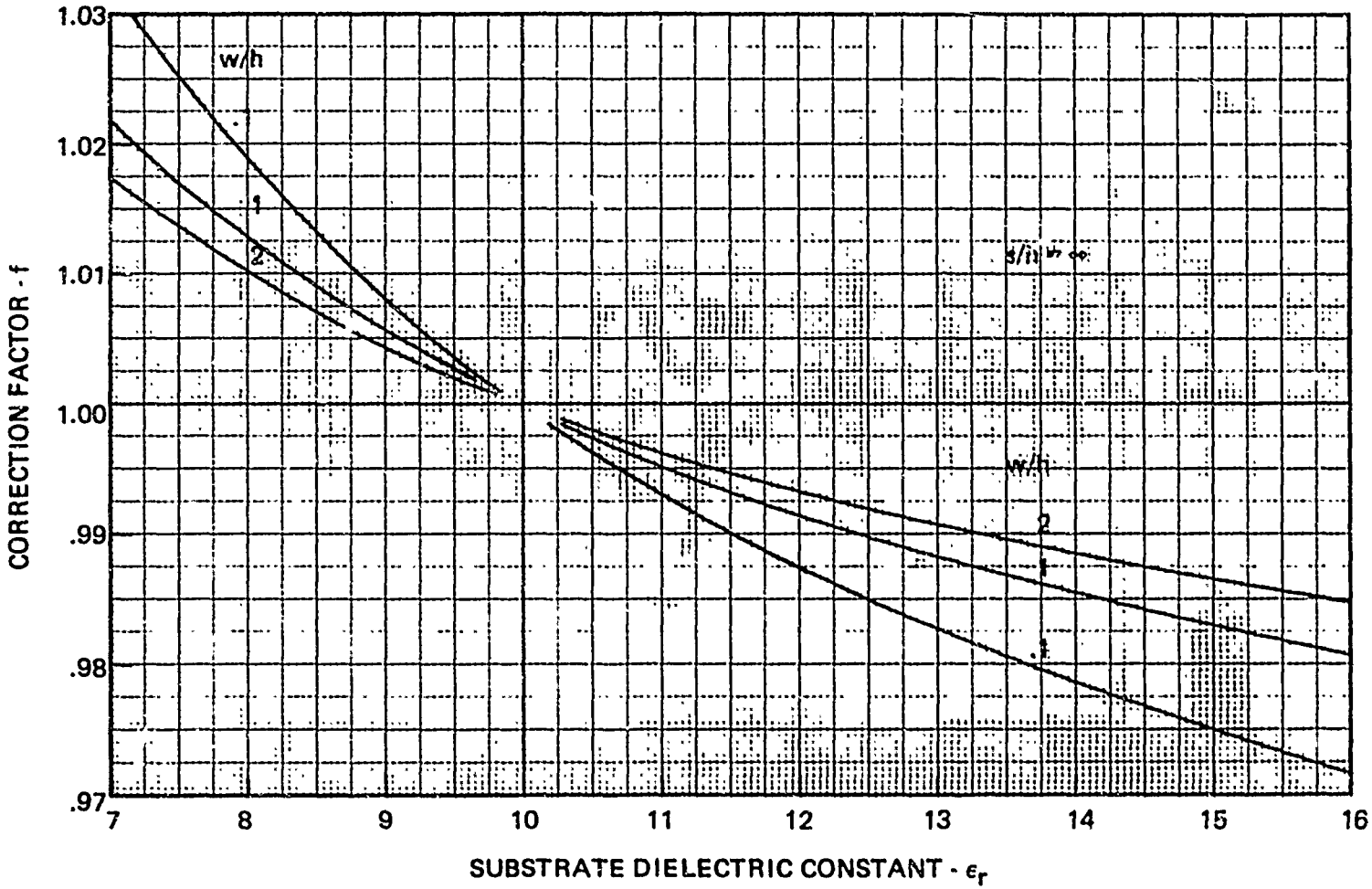

FIGURE 24 EFFECTIVE DIELECTRIC CONSTANT CORRECTION FACTOR.

The normal design procedure in designing a coupler of specified coupling k_p, impedance level Z_k, and center frequency fo is as follows: First determine the required Z_{oe} and Z_{oo} from

$$k = 10^{-\frac{kp}{20}} ,$$

$$Z_{oe} = Z_k \frac{1+k}{1-k} ,$$

and

$$Z_{oo} = Z_k \frac{1-k}{1+k} . \tag{39}$$

Second, from Figs. 18-20 determine those values of w/h and s/h which simultaneously yield the desired Z_{oe} and Z_{oo}. Third, from the width and gap just determined, find $\varepsilon_{e\text{-}eff}$ and $\varepsilon_{o\text{-}eff}$ from Fig. 21. And, fourth, determine the coupler length from

$$\ell = \frac{c}{4 \text{ fo } \sqrt{(\varepsilon_{e\text{-}eff} + \varepsilon_{o\text{-}eff})/2}} , \tag{40}$$

where $c = 3 \times 10^{10}$ cm/sec.

The second step is a tedious process requiring cross-plots and interpolations to find the solution. This tedium can be greatly relieved by doing the job once and for all. In Fig. 25 we have plotted lines of constant coupler impedance and constant coupling in the w/h - s/h plane. for the case of $\varepsilon_r = 10$. It might be pointed out that not only does this chart greatly simplify the design process, it also provides a very quick and simple evaluation of the coupling and impedance variations with respect to changes in the line parameters.

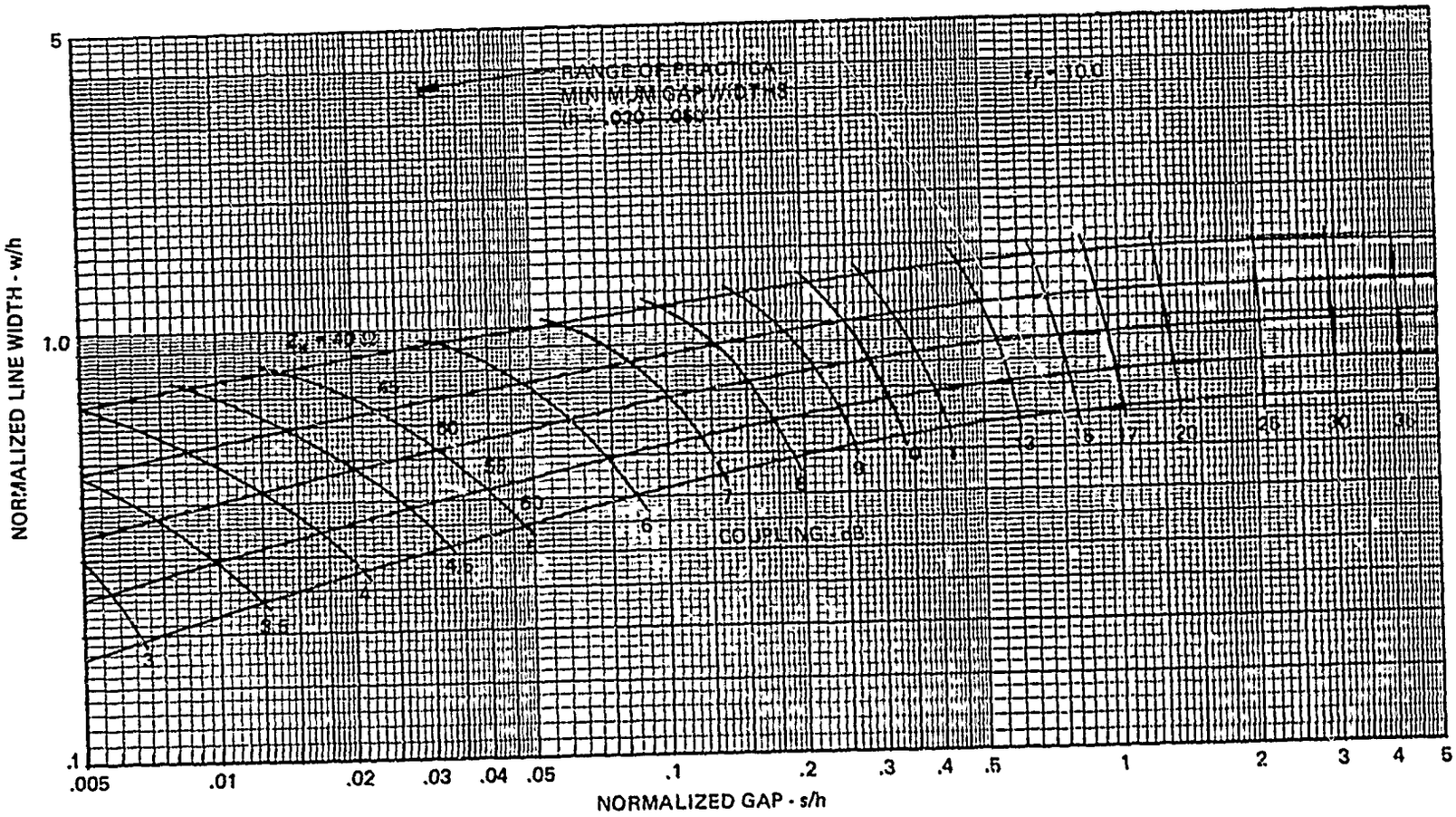

FIGURE 25 MICROSTRIP COUPLED PAIR COUPLER DESIGN CHART FOR SUBSTRATE DIELECTRIC CONSTANT ϵ_r = 10.0

D-12087

In particular we see that as the gap becomes very wide, the spacing controls the coupling and the line width controls the impedance level, as we might expect. However, for moderate to narrow gaps this is no longer true, and a change in either parameter will have a significant effect on both impedance and coupling.

Figs. 26 and 27 are plots of coupling versus w/h and s/h, intended to make interpolation on Fig. 25 easier and more accurate.

Figs. 25 - 27 may also be quickly adapted to other substrate dielectric constants. To the extent that the even and odd mode effective dielectric constants change by the same factor with a change in substrate dielectric constant, the coupling of a line pair is independent of the dielectric constant. We have pointed out that this is true to within a percent for ϵ_r from 7 to 16 at least. Consequently, we need only relabel the impedances by $Z_k' = Z_k \sqrt{10/\epsilon_r}$ to make Figs 25 - 27 applicable to substrates of dielectric constant ϵ_r.

Design data for non-symmetrical microstrip couplers have not yet been calculated to our knowledge. In lieu thereof, we suggest the following approximate design procedure for impedance transforming microstrip couplers. First determine the reciprocal admittances for each mode and each line from the desired coupling and input and coupled line impedance levels as prescribed in Section IIB. Second, average the even and odd mode admittances:

$$\bar{Y}_{oe} = \frac{1}{2} \left(Y_{oe}{}^{a} + Y_{oe}{}^{b}\right) = 1/\bar{Z}_{oe}$$

$$\bar{Y}_{oo} = \frac{1}{2} \left(Y_{oo}{}^{a} + Y_{oo}{}^{b}\right) = 1/\bar{Z}_{oo} \ .$$

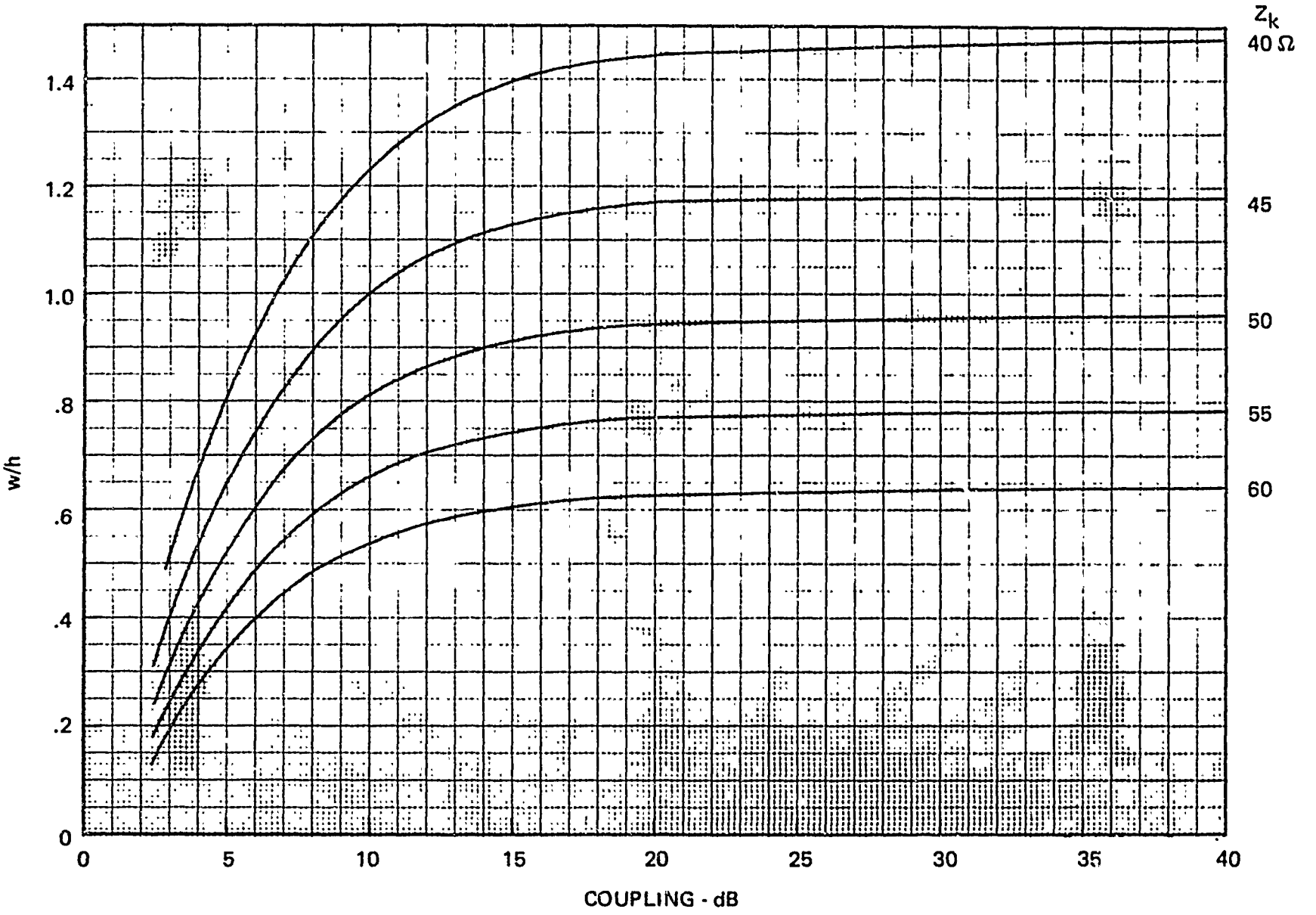

FIGURE 26 LINE WIDTH VS. COUPLING FOR VARIOUS COUPLER IMPEDANCES

D-12088

Third, determine the line width and gap for this "averaged" symmetrical coupler from the charts in this Section. (The total currents for the even and odd modes in this coupler will be the same as in the desired non-symmetrical coupler, but they will not be properly divided.) Fourth, keeping the gap fixed, use Fig. 18 to find the new widths for each line from the A and B line even mode reciprocal admittances.

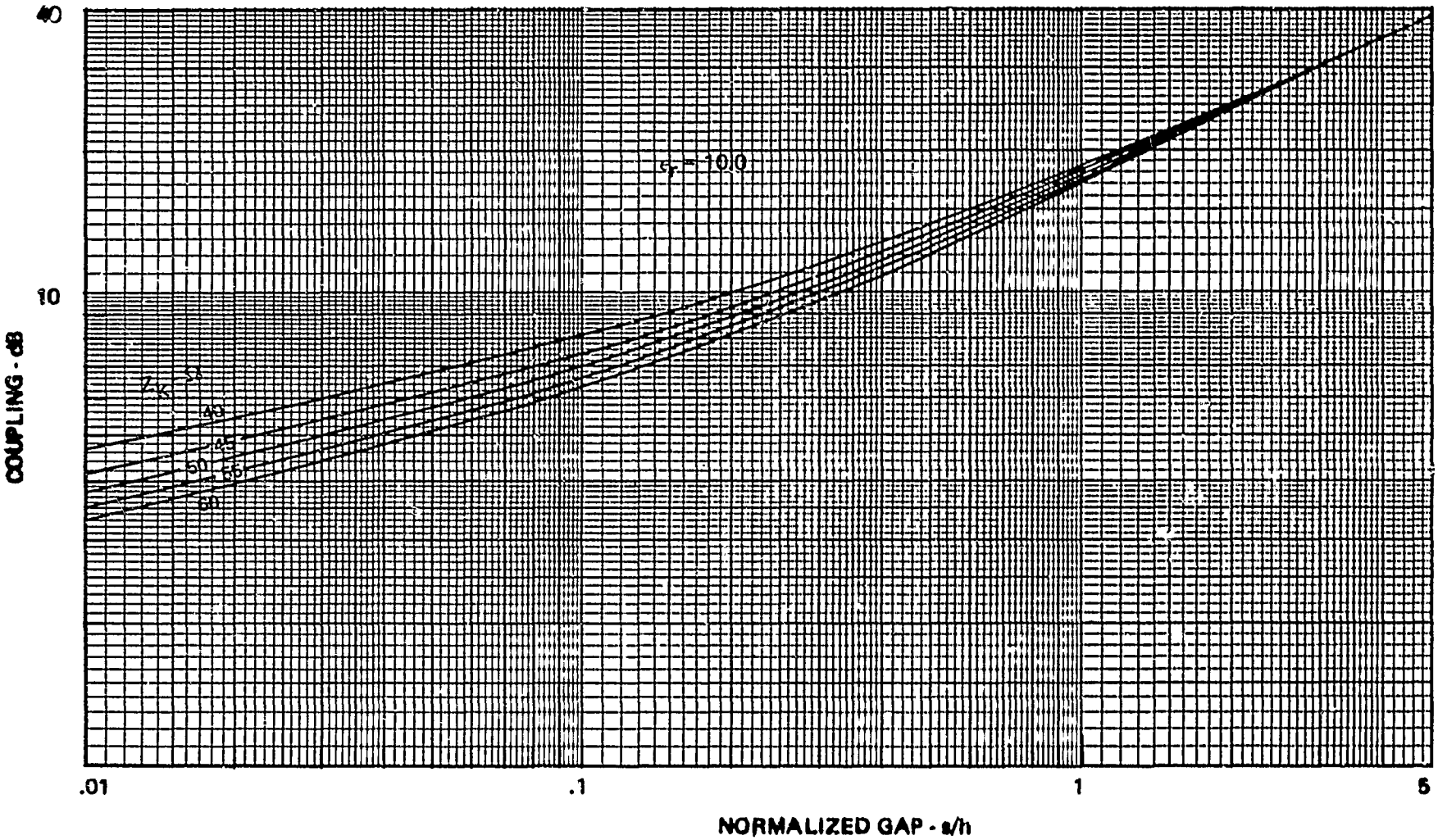

FIGURE 27 COUPLING VS. GAP WIDTH FOR VARIOUS COUPLER IMPEDANCES

D-12088

B. Velocity-Compensated Microstrip Coupler Design

The most successful method we have found for equalizing the even and odd mode velocities to improve coupler directivity, is by means of a dielectric rod or block over the coupling gap which increases the odd mode dielectric constant by more than the even. In this section we cover the design priciples and present design curves for such dielectric-overlay,velocity-compensated couplers.

The basic design idea is simple and straightforward. A dielectric block covering the coupling gap and a portion of the lines will increase $\varepsilon_{o\text{-}eff}$ relativity more than it will $\varepsilon_{e\text{-}eff}$ because of the odd mode's greater fringing fields above the dielectric. With the right amount of dielectric, both effective dielectric constants will be almost equal at a new value slightly higher than the original $\varepsilon_{e\text{-}eff}$. The overlay will increase the coupling and decrease the coupler impedance, besides (almost) equalizing the velocities. The task, then, is to estimate the amount of coupling and impedance change caused by the overlay, and determine the parameters of an uncompensated coupler of correspondingly higher impedance and looser coupling.

We should point out that the dielectric constants cannot be exactly equalized without completely covering the lines with a thick overlay, of the same constant as the substrate. This is undesirable on several counts. One, it increases the effective dielectric constant fo ε_r, which is usually so high that the lines must be made quite narrow for 50 Ω systems and are consequently too lossy. Two, the electric fields are no longer well-constrained under the strips, which

can lead to radiation and higher-order mode problems. And, three, we have found experimentally that better directivity could be obtained with narrow blocks, i.e. no wider than $2(w + s)$.

It is probable that exact equalization could be achieved with a narrow block of a higher dielectric constant or a thin layer of material of the same constant entirely cover the coupler[19]. These are added refinements which we have not considered. However, the general procedure and design curves given here will still apply reasonably accurately to these kinds of overlay.

The amount of coupling change caused by the overlay can be determined quite accurately, as follows. Recall that the even and odd mode impedances for a pair of lines at given width and spacing are

$$Z_{oe} = Z_{oe,air} / \sqrt{\epsilon_{e\text{-}eff}}$$

$$Z_{oo} = Z_{oo,air} / \sqrt{\epsilon_{o\text{-}eff}},$$

where $Z_{oe,air}$, $Z_{oo,air}$ are the impedances of the same lines without the substrate. Now, with the dielectric overlay in place, let ϵ'_{eff} be the effective dielectric constant of both modes. Then

$$Z'_{oe} = Z_{oe,air} / \sqrt{\epsilon'_{eff}} = Z_{oe} \sqrt{\epsilon_{e\text{-}eff} / \epsilon'_{eff}}$$

$$Z'_{oo} = Z_{oo,air} / \sqrt{\epsilon'_{eff}} = Z_{oo} \sqrt{\epsilon_{o\text{-}eff} / \epsilon'_{eff}}$$

The voltage coupling without the overlay is

$$k = \frac{Z_{oe} - Z_{oo}}{Z_{oe} + Z_{oo}}$$

and with the overlay

$$k' = \frac{Z'_{oe} - Z'_{oo}}{Z'_{oe} + Z'_{oo}}$$

$$= \frac{Z_{oe} - Z_{oo}\, g}{Z_{oe} + Z_{oo}\, g}$$

$$= \frac{(1+k) - (1-k)\, g}{(1+k) + (1-k)\, g} \qquad (41)$$

where $g = \sqrt{\epsilon_{o\text{-}eff} / \epsilon_{e\text{-}eff}}$

The new coupling depends only on the ratio of odd and even mode dielectric constants and the coupling of the uncompensated coupler. It does <u>not</u> depend upon the final, equalized value of ϵ'_{eff} nor on Z_k. Also, since for most practical purposes the ratio of dielectric constants is sensibly independent of the substrate dielectric constant, the change in coupling with the overlay depends only on the initial coupling. The coupling change is plotted in Fig. 28, based on the data in the previous section for couplers near 50 Ω.

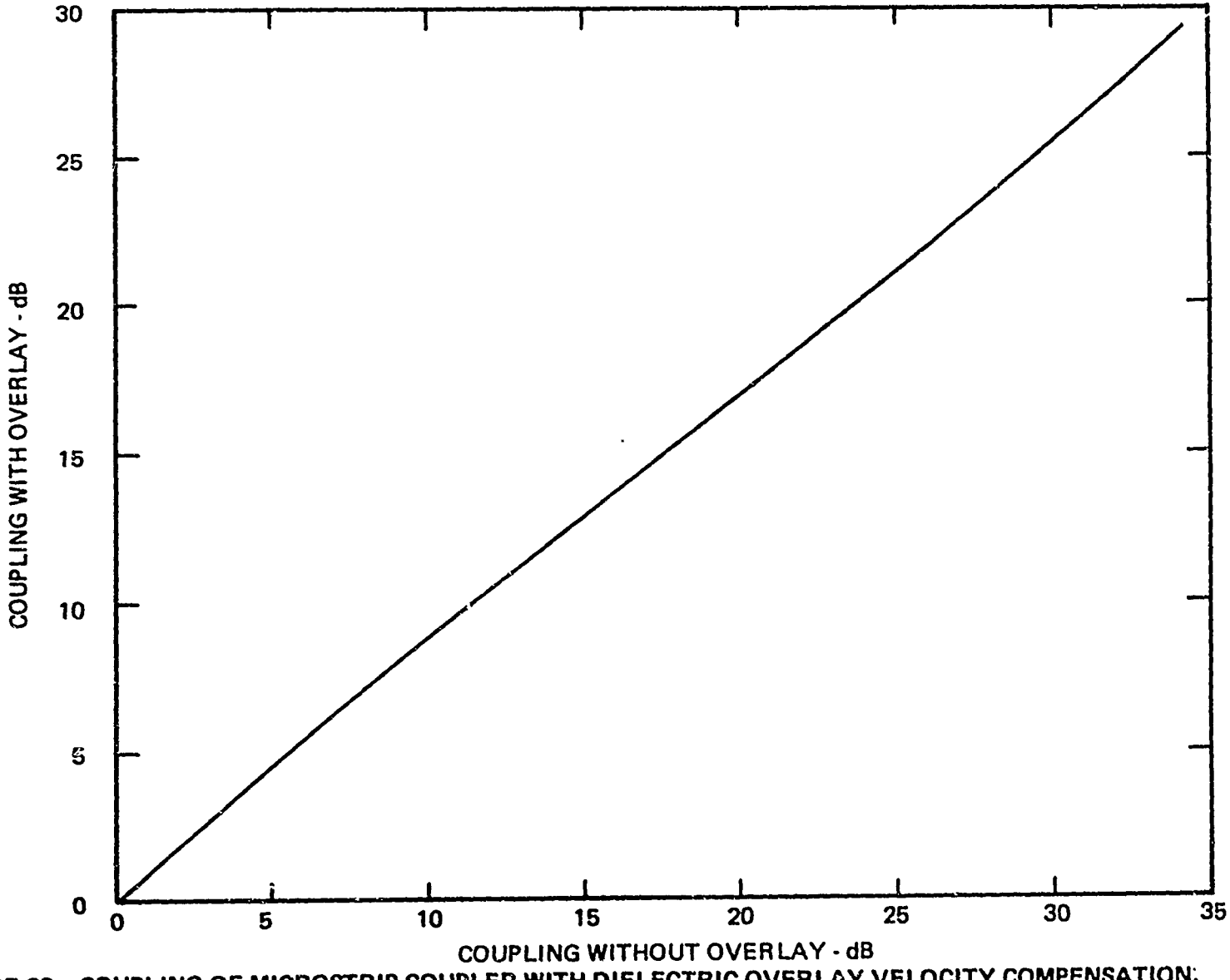

FIGURE 28 COUPLING OF MICROSTRIP COUPLER WITH DIELECTRIC OVERLAY VELOCITY COMPENSATION.

The impedance of the overlay coupler will, of course, depend on the final value of ε'_{eff}:

$$Z_k = Z_k \sqrt{\frac{\varepsilon_{e\text{-}eff} \cdot \varepsilon_{o\text{-}eff}}{\varepsilon'^{2}_{eff}}} \tag{42}$$

Now, our design theory says nothing about how much dielectric to use other than "enough"--presumably a minimum amount to achieve the best directivity response. Determining the right amount is left as an empirical task.

Nevertheless, we need a simple prescription to estimate the likely value of ε'_{eff}. To this end, we make the following argument: In the limit as the gap goes to zero, there are virtually no even mode fields above the gap. Only a very small overlay will be required, and it will change only $\varepsilon_{o\text{-}eff}$. So, for $s = 0$, $\varepsilon'_{eff} = \varepsilon_{e\text{-}eff}$. As the gap becomes very wide, the fields of the even and odd modes become more and more alike. A very thick overlay will be required--even though the two dielectric constants are not very different--increasing both effective dielectric constants substantially. A reasonable guess is that they reach the average of $\varepsilon_{e\text{-}eff}$ and ε_r (assuming that the overlay and substrate are both ε_r). Thus, as $s \to \infty$, $\varepsilon'_{eff} \to (\varepsilon_{e\text{-}eff} + \varepsilon_r)/2$. Finally, for arbitrary spacing, we have adopted the following simple formula to derive the design curves.

$$\varepsilon'_{eff} = \varepsilon_{e\text{-}eff} + \frac{\varepsilon_r - \varepsilon_{e\text{-}eff}}{2} \left(1 - e^{-s/h}\right), \tag{43}$$

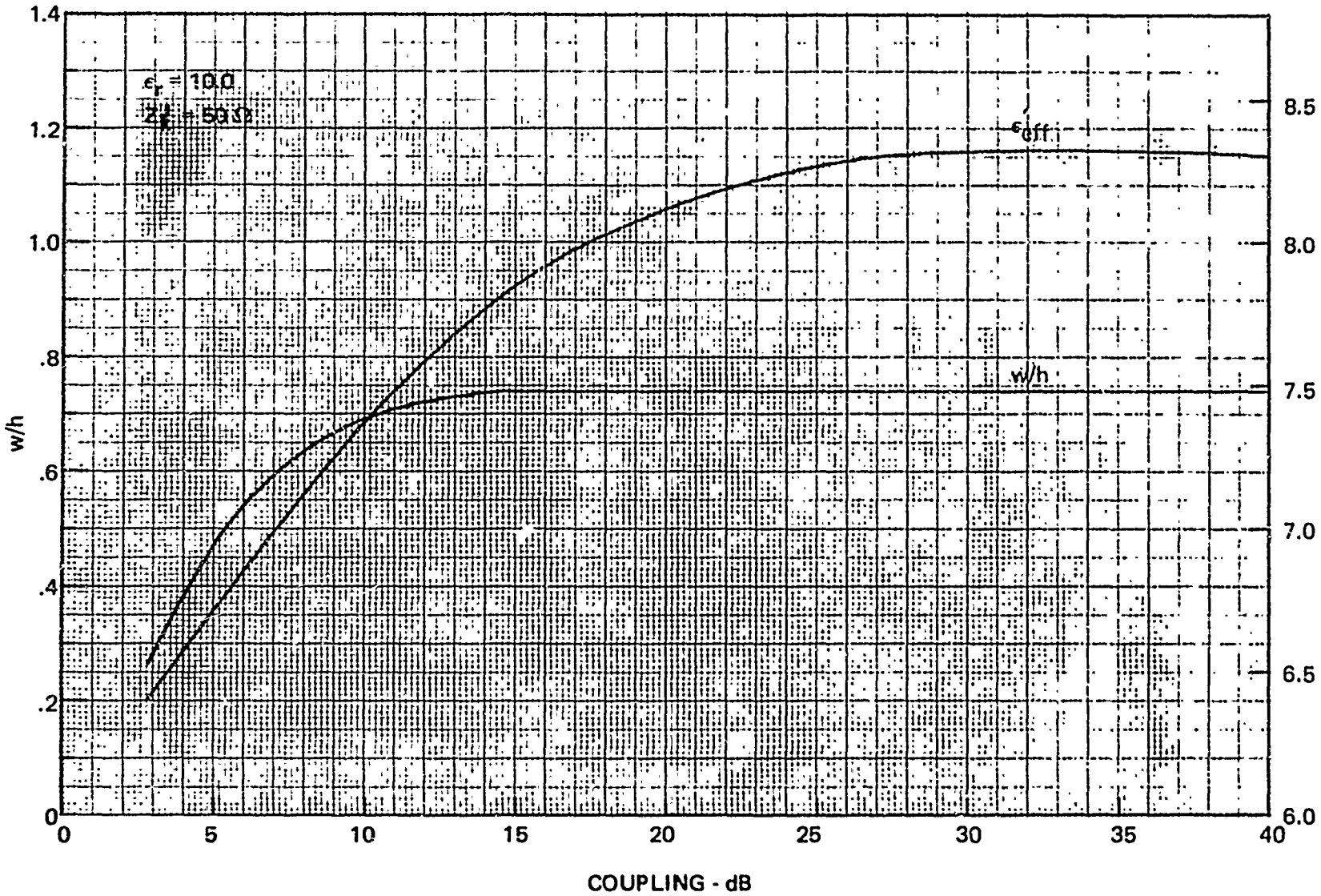

FIGURE 29 OVERLAY COUPLER DESIGN CHART: LINE WIDTH AND EFFECTIVE DIELECTRIC CONSTANT VS. COUPLING FOR 50 Ω COUPLER.

D-12091

Using Eqs. (42) and (43) and the data in Section IIIA we have determined the line width and spacing and ε'_{eff} as functions of the coupling (with overlay) for couplers of 50 Ω with overlay on $\varepsilon_r = 10.0$ substrates as shown in Figs. 29 and 30. For other impedances near 50 Ω, proportion w/h and s/h according to Fig. 25, along a line of constant coupling. For other substrates near $\varepsilon_r = 10$, multiply ε'_{eff} for the desired coupling by $\varepsilon_r/10$ to get ε''_{eff} and determine the design for a coupler of $Z'_k = 50\sqrt{\varepsilon'_{eff} / \varepsilon''_{eff}}$.

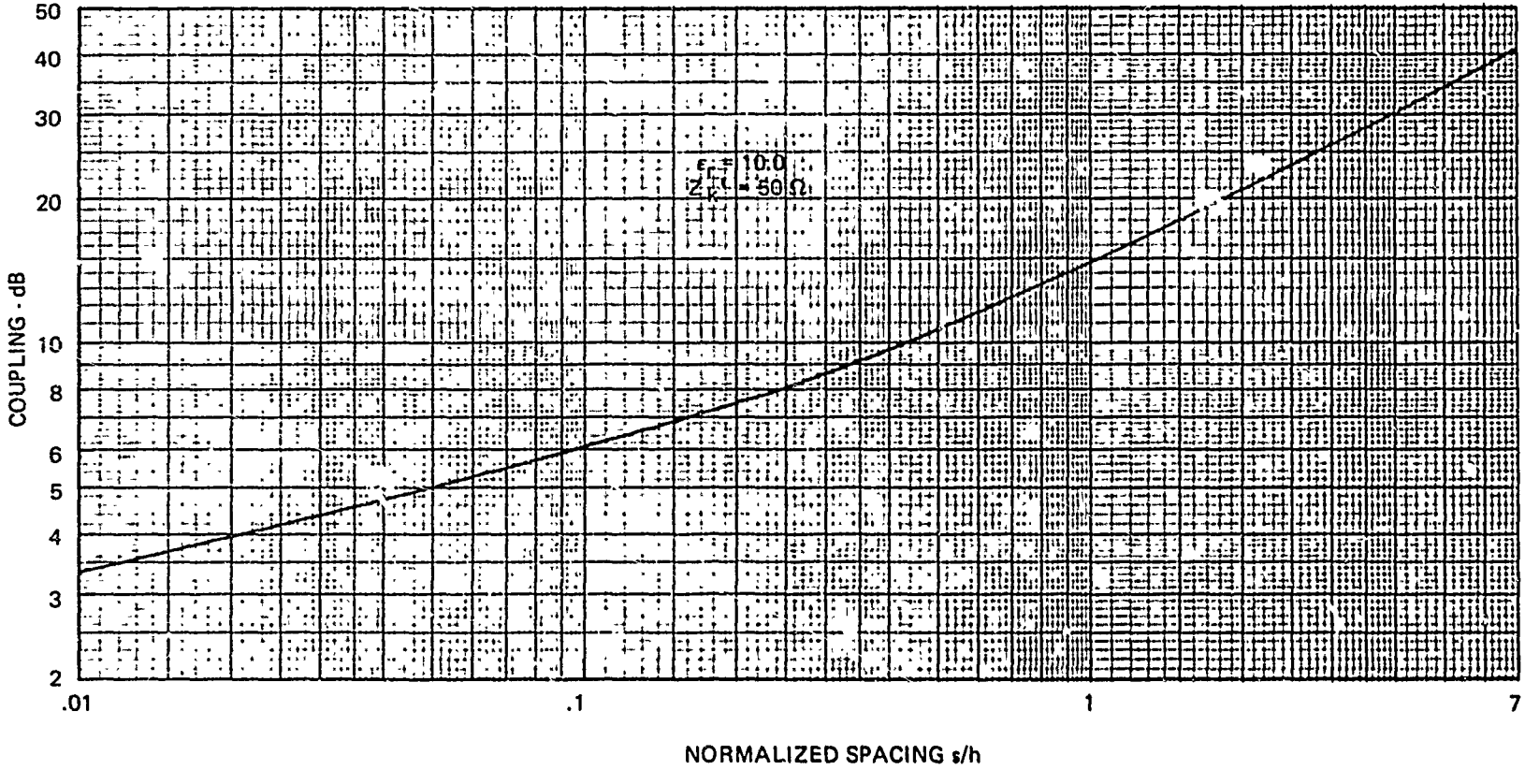

FIGURE 30 OVERLAY COUPLER DESIGN CHART: LINE SPACING VS. COUPLING FOR 50 Ω COUPLERS

D-12092

C. Dispersion

The frequency variation of the effective dielectric constants of single and coupled microstrips has been studied by several authors. Getsinger [4] has deduced especially simple analytical approximations which agree excellently with experiment and which have the distinct advantage of being calculable by human beings , unaided by a gigantic computer.

The reader interested in the model and derivation is referred to Getsinger's papers. Here we shall simply provide the formula and some graphs for the coupled line case.

From Ref. 4, the dispersion formula is

$$\epsilon_x = \epsilon_r - \frac{\epsilon_r - \epsilon_{x=o}}{1 + G_x (f/f_{px})^2} \tag{44}$$

$$G_x = 0.6 + .009\, Z_x$$

$$f_{px} = Z_x / 2\mu_o h,$$

where

x = e or o for the even and odd modes;

ϵ_x = effective dielectric constant, $f \neq 0$;

ϵ_{xo} = effective dielectric constant, $f = 0$;

ϵ_r = substrate dielectric constant;

$Z_x = Z_{oe}/2$ or $2 Z_{oo}$ for x = e or o.

h = substrate thickness

μ_o = 31.92 nH/in.

As the effective dielectric constants vary with frequency, the even and odd mode impedance will change as well as the electrical length, relative to the dc-derived length. As usual, our interest is less in the variations of Z_{oe} and Z_{oo} with frequency, but more in how the coupler's circuit performance will be affected. In particular, we would like to know how a coupler, designed with the dc design data, will behave at microwave frequencies. We have computed, from Eqs. (44), the frequency variations of midband impedance, coupling, and directivity for uncompensated 50 Ω couplers on ε_r = substrates: These results, as well as a midband length correction, are plotted in Figs. 31 and 32.

In general, over the useful frequency range of a coupler, dispersion is a relatively small effect. Also, we would expect the effects to be even smaller in the case of dielectric-overlay couplers. Figs. 31 and 32 may be used to estimate corrections to a dc-based design. One must bear in mind, though, that the impedances of the interconnecting lines will also change by about the same amount, so that one should not correct for Z_k. The only practical corrections might be for the coupling of loose couplers and the length needed for 90^o.

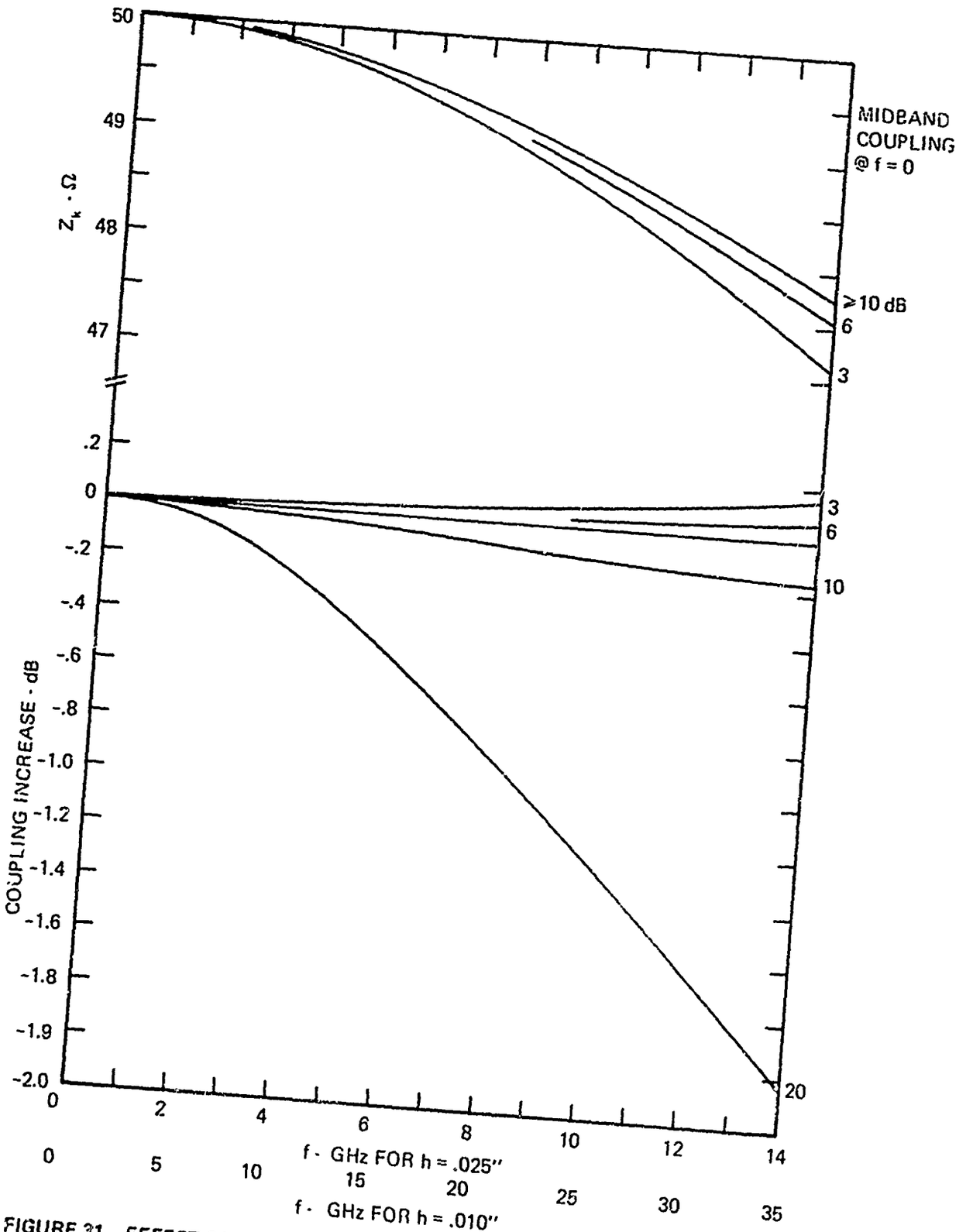

FIGURE 31 EFFECT OF DISPERSION ON IMPEDANCE AND MIDBAND COUPLING OF 50 Ω COUPLERS.

D-12093

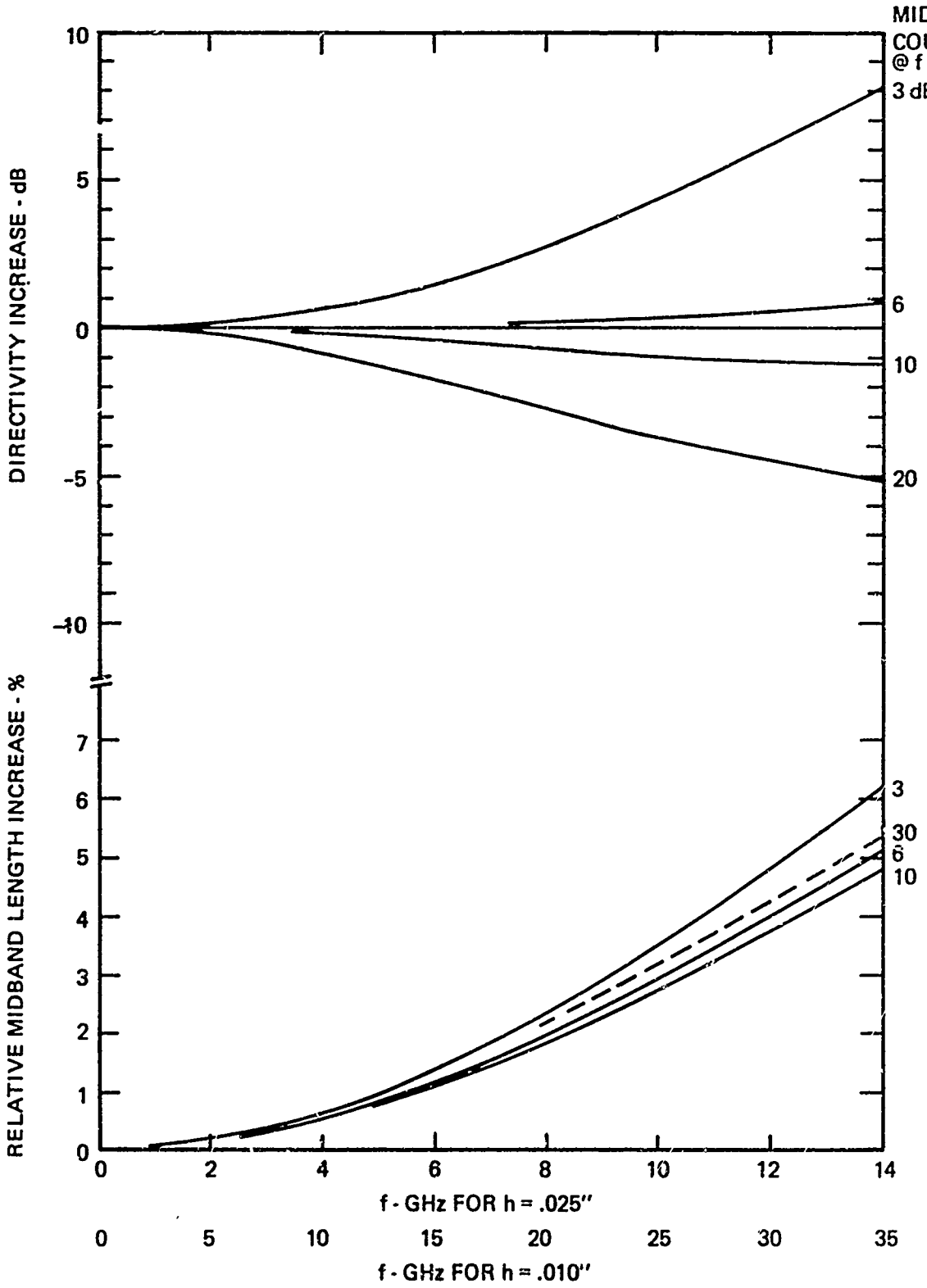

FIGURE 32 EFFECT OF DISPERSION ON DIRECTIVITY AND ELECTRICAL LENGTH OF 50 Ω COUPLERS

D-12094

IV. BROADBANDING AND TIGHT COUPLING TECHNIQUES

A. Broadband Couplers

In Section II we discussed at length the coupling bandwidth of ideal and microstrip couplers, consisting of a uniform, single quarter wavelength coupled-line sections; see Figs. 3, 4, 14, 15 and 16. Broadly speaking, a single section coupler has about an octave bandwidth for about 1/2 to 1 dB coupling variation, but, in microstrip, the directivity in the upper range is low, especially for loose coupling. The specific goal in this work was the design of octave bandwidth couplers with less than 0.2 dB deviation and at least 20 dB of directivity. This is just beyond the reach of single-section couplers and a method of increasing the bandwidth was required. In this Section we shall briefly review the principle coupler broadbanding techniques which have been proposed, and discuss in more detail the method adopted for our experimental couplers.

There are basically two ways of broadbanding the coupling characteristic--either by cascading* a number of quarter wavelength sections of appropriately chosen coupling, or by continuously varying the coupling along the coupler length. In each of these methods, the

---

* We use the term cascade to deonote direct end-to-end connection, i.e. ports 3 and 4 to ports 2 and 1 of the following coupler; this connection has no crossover. Tandem connection will refer to ports 2 and 4 connected to 3 and 1; this does require a crossover.

Coupling variation along the coupler's length may be symmetrical*, or asymmetrical, as illustrated in Fig. 33. An asymmetrical coupler need not have a monotonic coupling variation from one end to the other, but this is the only case ever considered.

All of these broadbanding methods rely on the property that two cascaded $\lambda/4$ couplers, of the same impedance but different coupling, will have a net coupling intermediate between the two near midband and tighter than both towards the band edges. As an example, Fig. 34 compares the coupling curve of a cascade connection of a 3.01 dB and a 10 dB coupler with the curves for each by itself. With a little reflection, one can readily appreciate that, as the coupling of the 10 dB coupler is increased to 3 dB the net coupling curve will devlop into the curve for a single 3 dB coupler of twice the original length.

By cascading two or more couplers, the couplings can be chosen to control the mean coupling and ripple amplitude. In particular, the ripple amplitude can be set equal to zero, a maximally flat design, or the ripples may all be made the same, an equal ripple design. As more sections are added the maximally flat or equal ripple bandwidth becomes wider, approaching the 0- to -2 normalized frequency band as the number of sections goes to infinity. The coupling will always go to zero at the ends of this band, however.

---

* Asymmetrical refers to end-to-end asymmetry, non-symmetrical refers to side-by-side asymmetry. c f. footnote p. 16

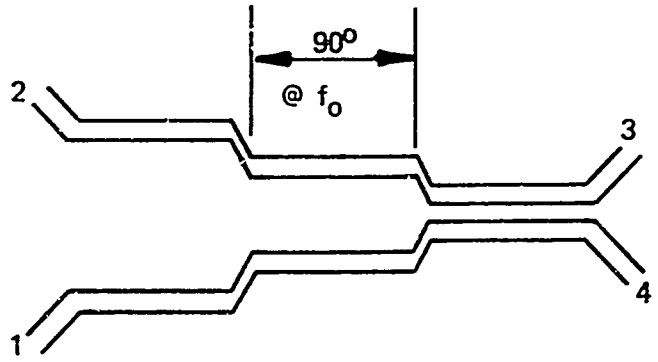

a) STEPPED ASYMMETRICAL COUPLER

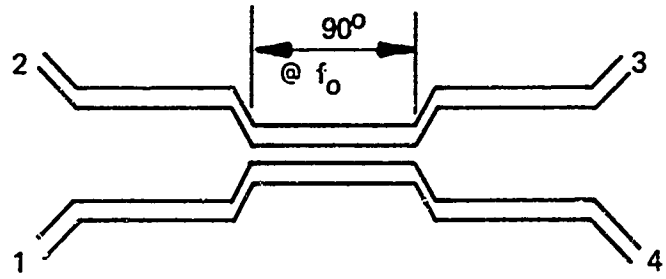

b) STEPPED SYMMETRICAL COUPLER

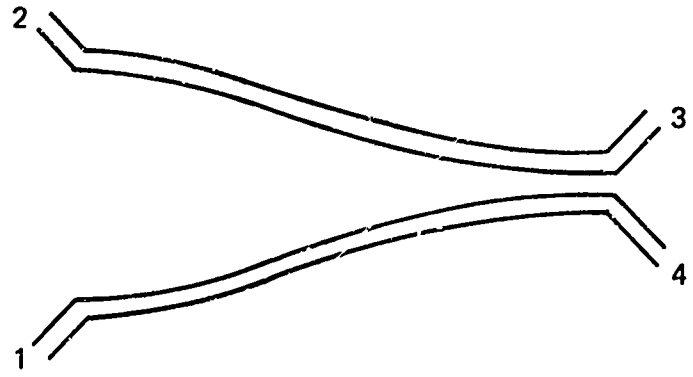

c) TAPERED ASYMMETRICAL COUPLER

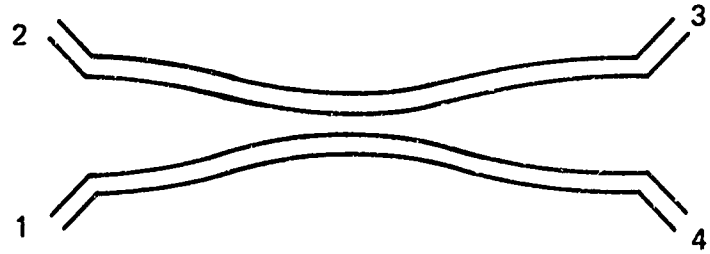

d) TAPERED SYMMETRICAL COUPLER

FIGURE 33 SCHEMATIC ILLUSTRATION OF BROADBAND COUPLED-STRIP COUPLER TYPES.

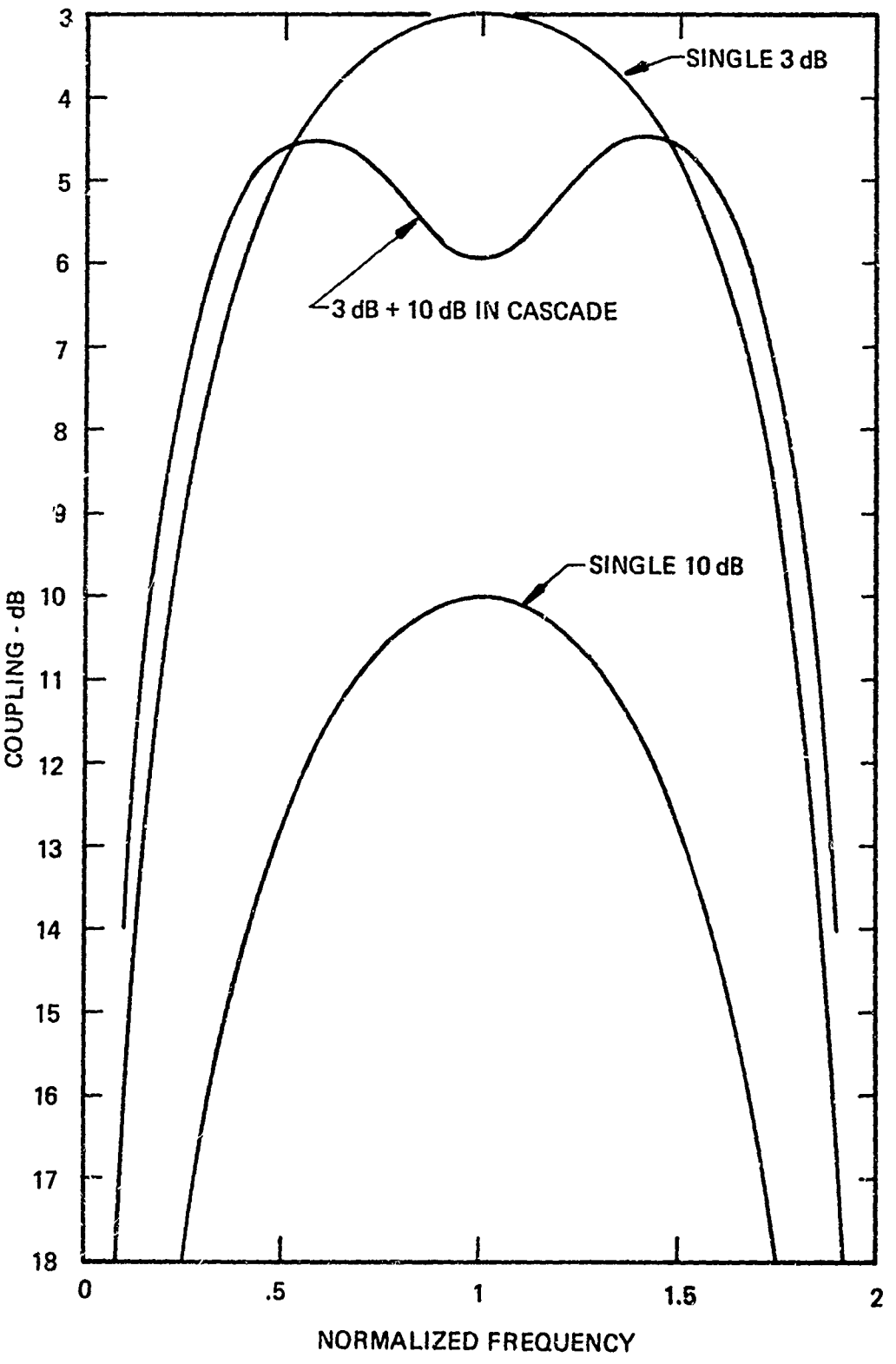

FIGURE 34 EFFECT ON COUPLING CHARACTERISTIC OF CASCADING TWO UNEQUAL COUPLERS.

The tapered line couplers may be thought of as a cascade of stepped quarterwave length couplers in the limit that the quarterwave length frequency and the number of sections go to infinity. Theoretically then the half-wavelength frequency is also infinite and there is no upper limit to the flat or equal ripple band. The lower band edge will still occur where the entire coupler is approximately a quarter wave length long, just as in the stepped coupler cases. The broadbanding design problem is then to determine the couplings required for each section--or the coupling as a function of distance for the continuously tapered couplers--in order to obtain a given overall mean coupling and ripple amplitude. We also need to know what the bandwidth will be as a function of the number of sections and coupling tolerance (ripple).

Levy has treated the synthesis of stepped asymmetrical couplers,[20] and has provided convenient tables for couplers of two to six sections and 3 to 20 dB of coupling.[21] As usual, these tables give the even mode impedances of each section (the odd mode impedances are implicit since the couplers all have unit impedance) rather than the couplings. For two-section couplers, two quantities, the mean coupling and the ripple, are related to just two others, the coupling of each section. Thus it is quite simple to relate these quantities on a chart, Fig. 35. For three or more sections turn to the tables in Ref. 21. For two-section coupler combinations lying to the right of the maximally flat locus, the bandwidth will still be greater and the mean coupling less than for the single coupler #1, but the characteristic will peak at midband. "Mean coupling" must be interpreted as "Peak coupling" in this region, and it asymptotically approaches coupling #1 as coupling #2 goes to infinity.

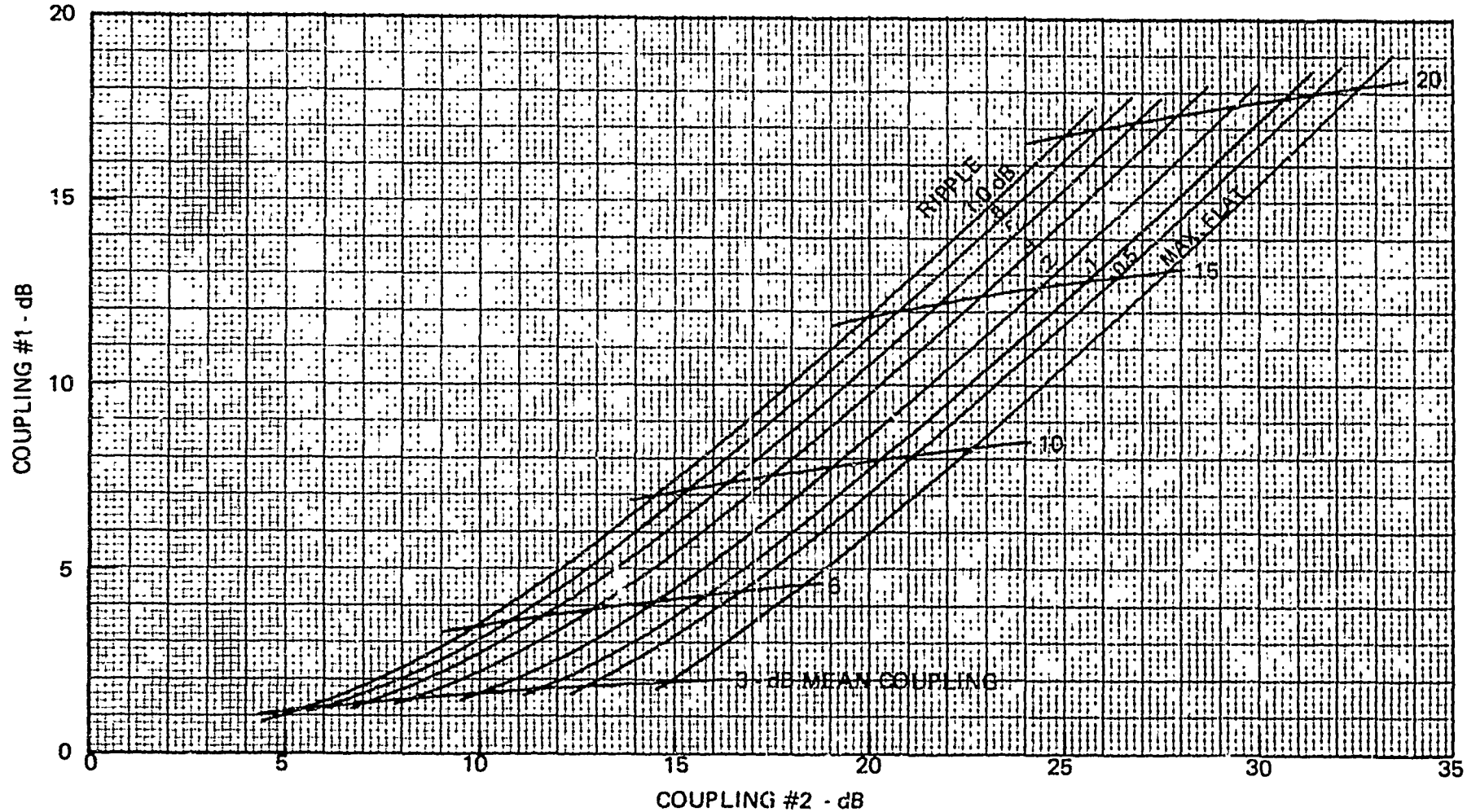

FIGURE 35 MEAN COUPLING AND RIPPLE FOR TWO SECTION ASYMMETRICAL COUPLERS.

The equal ripple bandwidths of 0.1, 0.25 and 0.5 dB ripple 2- and 3- section couplers are compared with the bandwidths of single sections in Fig. 36. In the Figure, the "ripple" of the single section is simply half the coupling deviation from the center frequency. We see that adding one section roughly doubles the bandwidth of the single section for these relatively small coupling tolerances.

Asymmetrical multi-section couplers are no longer quadrature couplers, although by adding a piece of line to the direct output they can be made approximately so. Figs. 37 and 38 show the coupling and phase difference characteristics of a 2- and a 3-section 3 dB coupler. The two section coupler with an extra 90° line will have a $90^{\circ} \pm 10^{\circ}$ phase difference, which may suffice for many quad coupler applications. However, as we shall see, symmetrical couplers are exactly quad couplers, so one may as well use a 3-section symmetrical coupler as to use a compensated 2-section asymmetrical coupler. The 3-section coupler needs a 180° (@ f_o) for compensation, but the error from 90° reaches almost 30°.

The synthesis of equal ripple symmetrical couplers has been given by Cristal and Young,[22] including design tables. Since the three-section symmetrical coupler has just two coupling values, we can derive a design chart, similar to Fig. 35, relating the mean coupling and ripple to the center and end coupler couplings, Fig. 39. Interestingly, Fig. 39 is almost the same as Fig. 35 with 6.5 dB added to the horizontal axis.

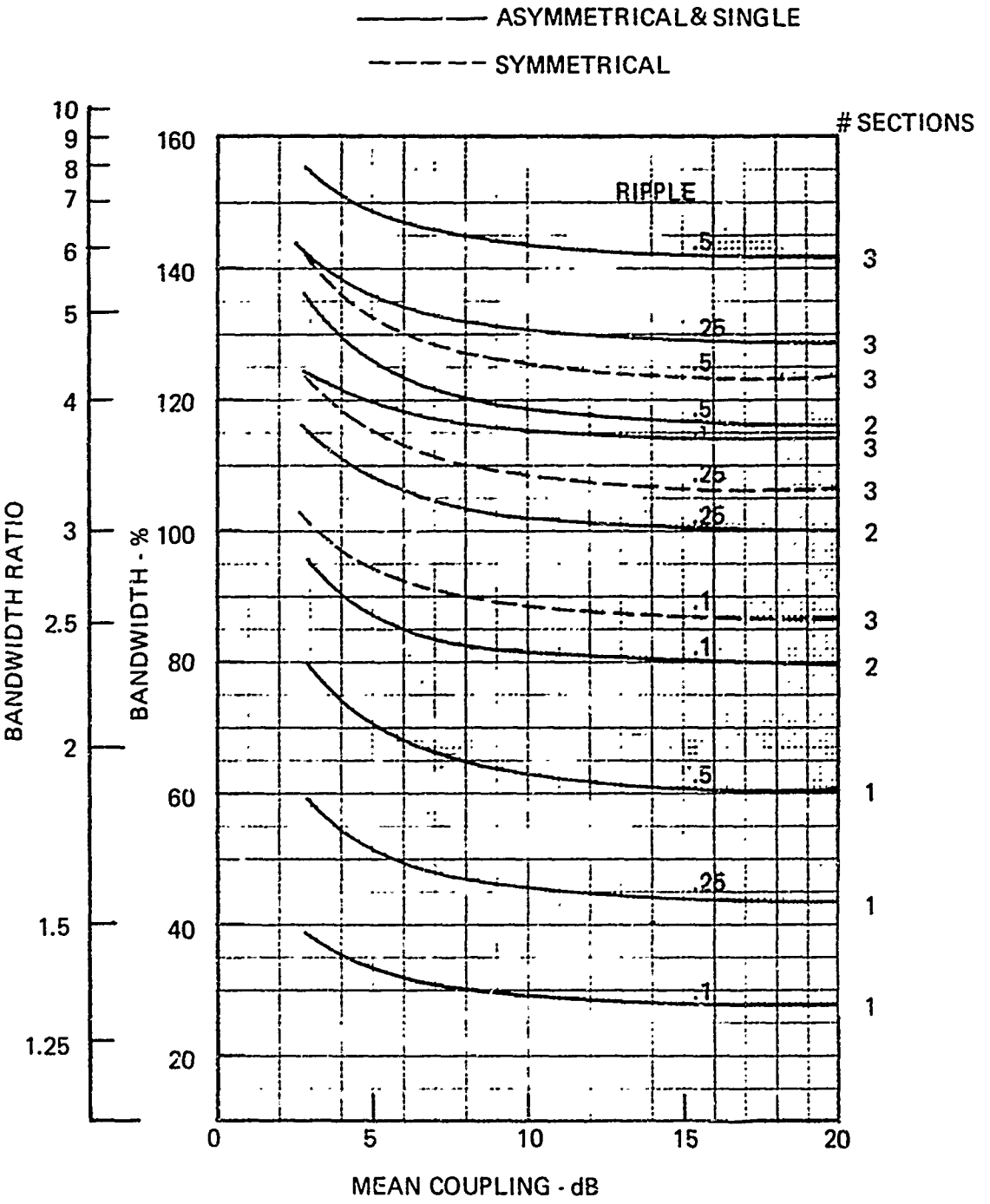

FIGURE 36 COUPLING BANDWIDTH FOR 1, 2 & 3 SECTION ASYMMETRICAL COUPLERS & 3-SECTION SYMMETRICAL COUPLERS.

D-12098

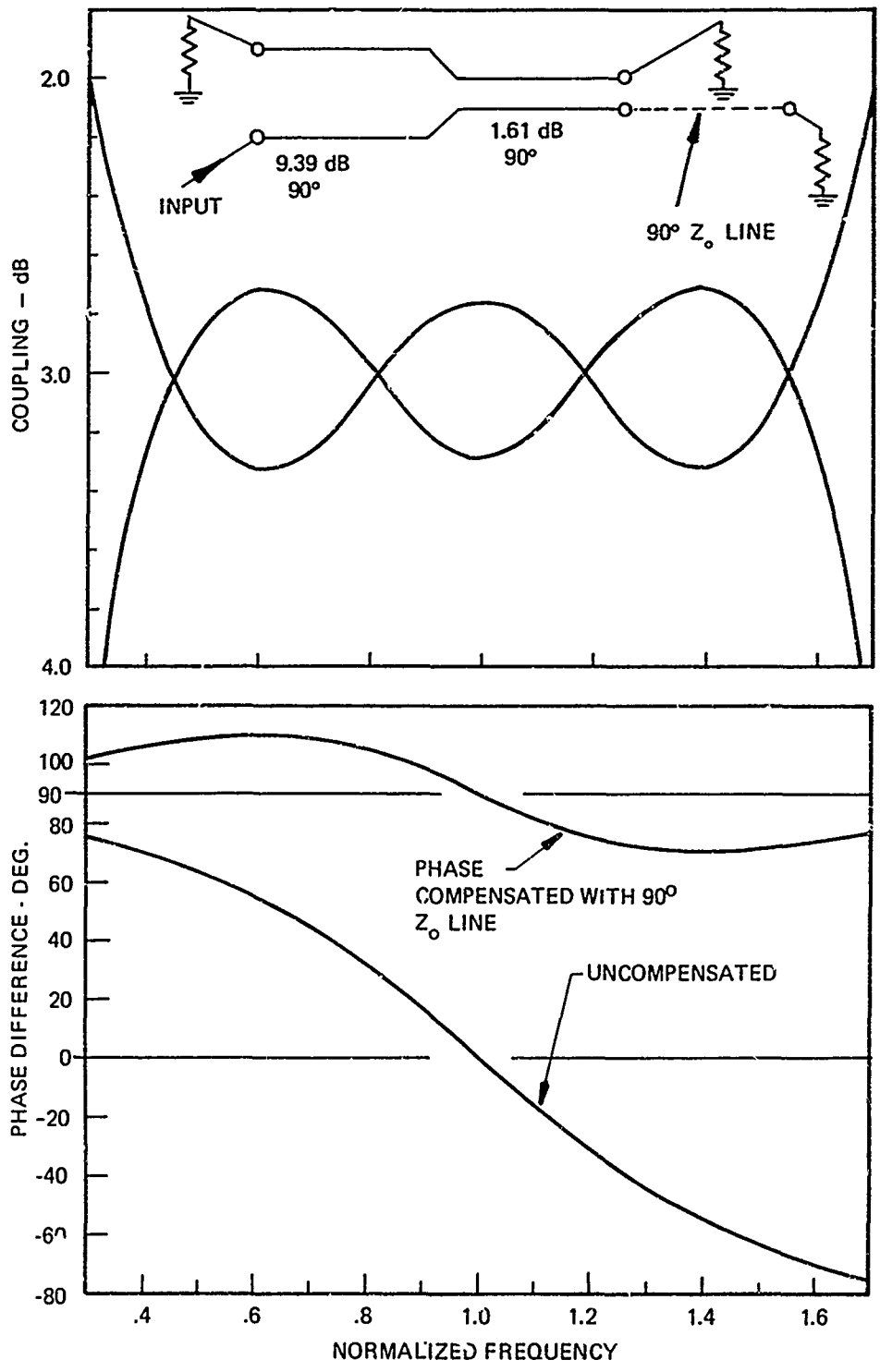

FIGURE 37 AMPLITUDE AND PHASE RESPONSE OF 2-SECTION ASYMMETRICAL 3 dB, .3 dB RIPPLE COUPLER

D-11665

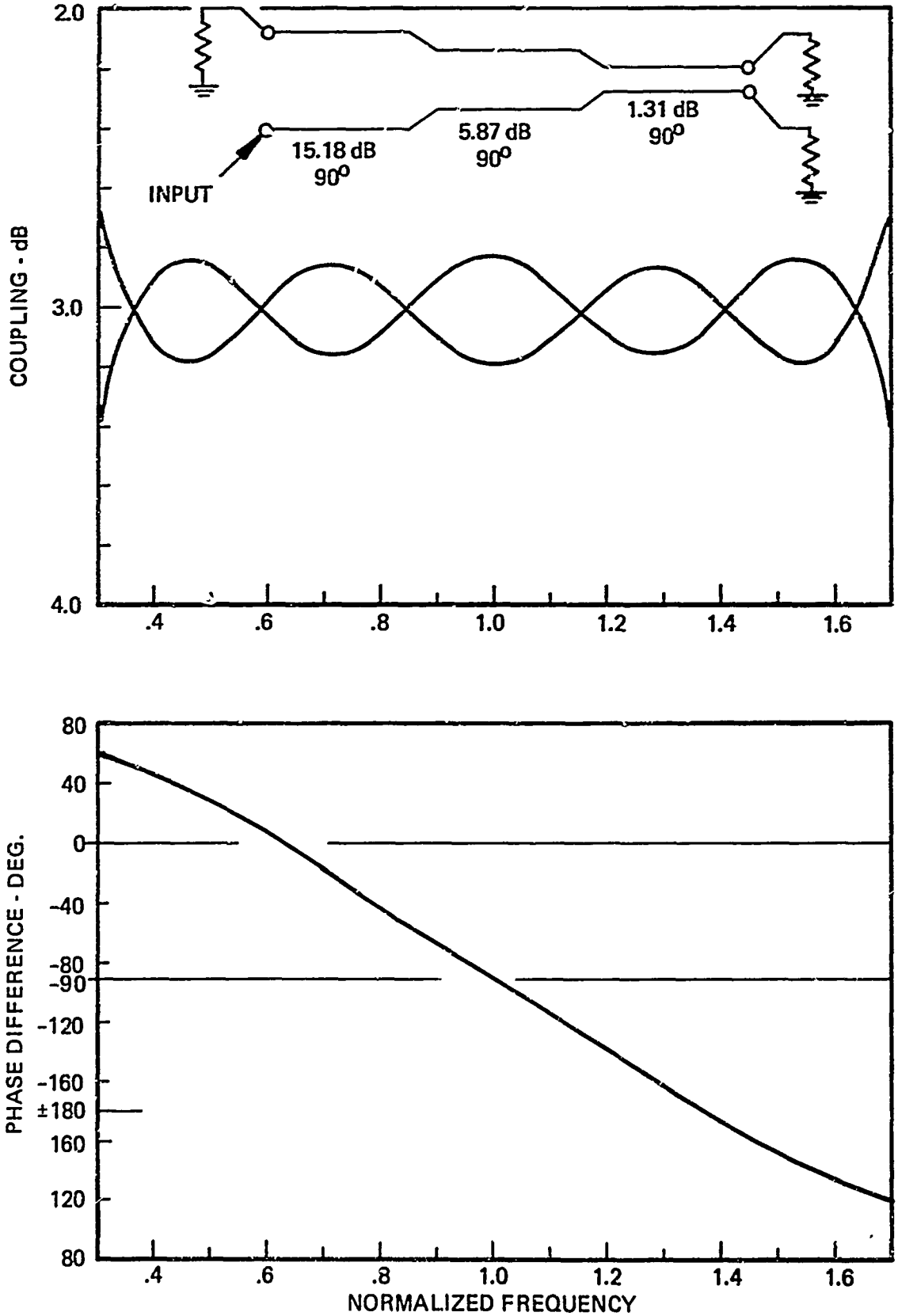

FIGURE 38 AMPLITUDE & PHASE RESPONSE OF 3-SECTION ASYMMETRICAL 3-dB, .16 dB RIPPLE COUPLER.

D-12100

The equal ripple bandwidths of 3-section symmetrical couplers of .1, .25, and .5 dB ripple are shown in Fig. 36, for comparison with single section and asymmetrical couplers. Note that the 3-section symmetrical coupler has just a shade more bandwidth than does the 2-section asymmetrical coupler. This circumstance can best be appreciated by comparing the coupling characteristics of the 3-section symmetrical couplers in Fig. 40 with that of the asymmetrical coupler in Fig. 38--the coupling curve ripples downward just once, as in a 2-section coupler, and not twice. Thus the symmetrical coupler uses 3-sections to get the same ripple as a 2-section coupler, with only a slight gain in bandwidth. But the symmetrical coupler is a true quadrature coupler; hence our earlier statement that it rarely pays to compensate a 2-section coupler with an extra line in one output, when the 3-section symmetrical coupler will have exactly 90° phase difference, take up the same area, and provide some margin of bandwidth.

It is interesting to note that the 2-section couplers obtained by deleting one end of the couplers in Fig. 40 would be 2.4 - 2.5 dB, approximately maximally flat. It is the second end coupler which produces the first ripple, rather than generating another. In general, asymmetrical couplers of n sections have n-1 ripples (counting dips in coupling) while symmetrical couplers have half as many. Symmetrical couplers are not optimum in the sense of yielding the most bandwidth for a given ripple and total length; however under the constraints of symmetry and phase quadrature the equal ripple design is optimum.

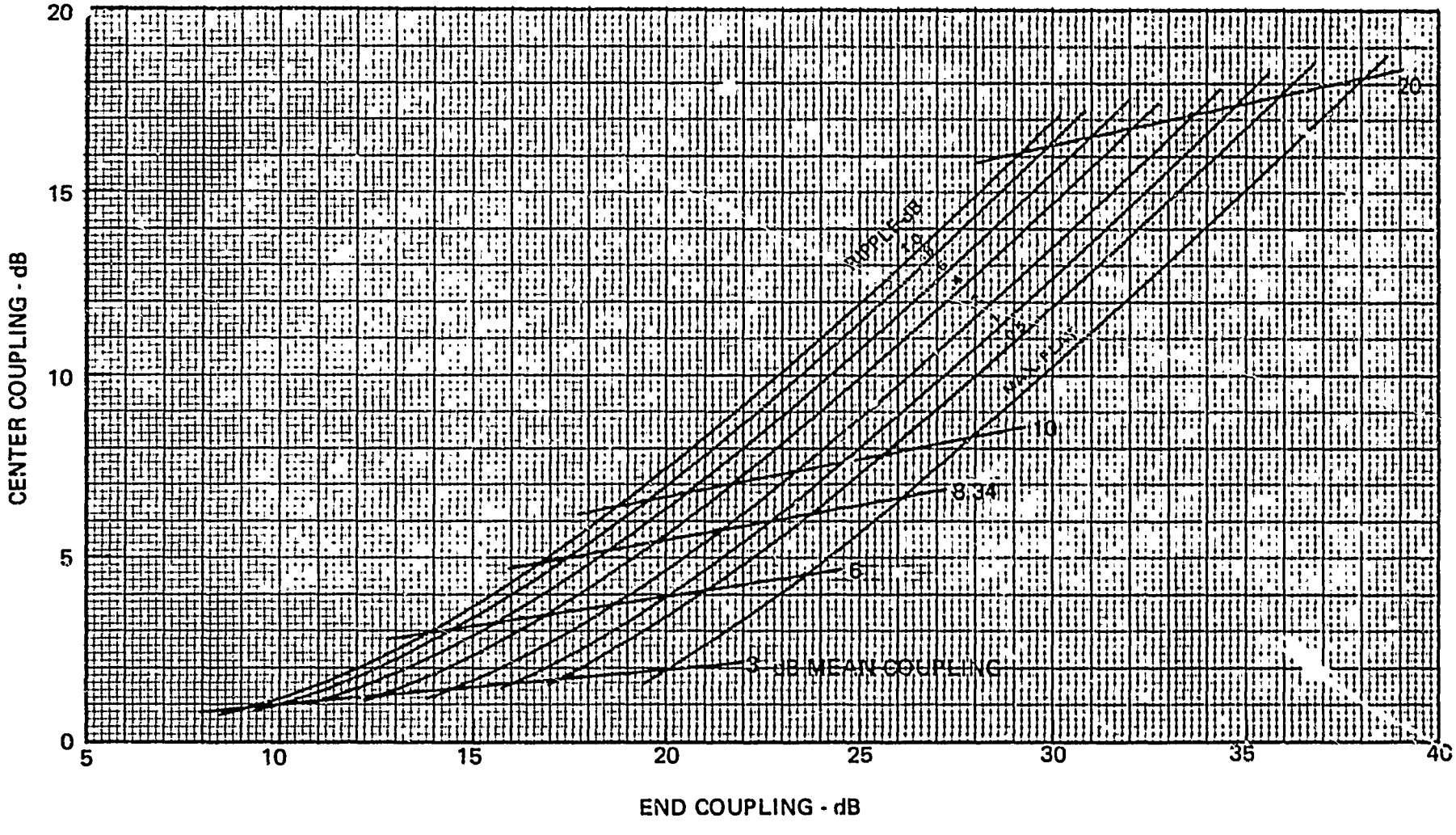

FIGURE 39 MEAN COUPLING AND RIPPLE FOR 3-SECTION SYMMETRICAL COUPLERS

D-12101

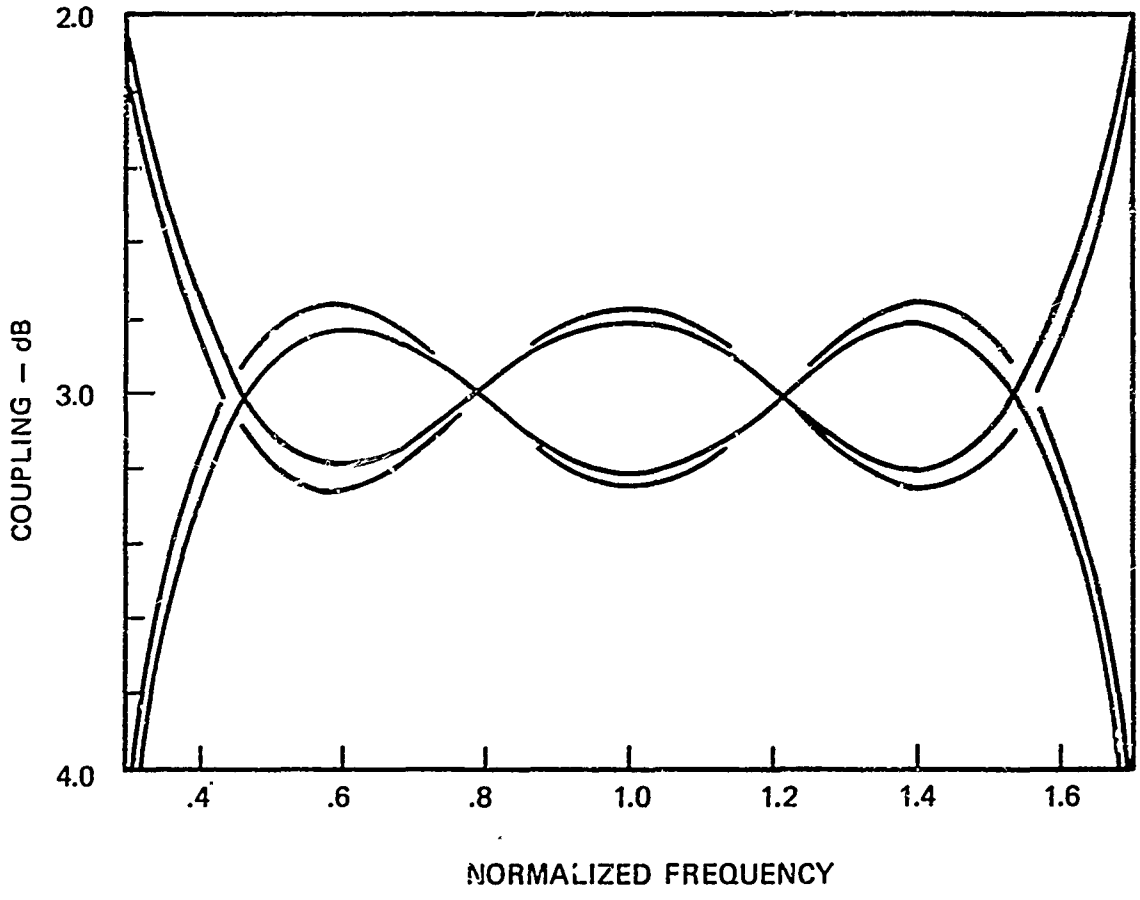

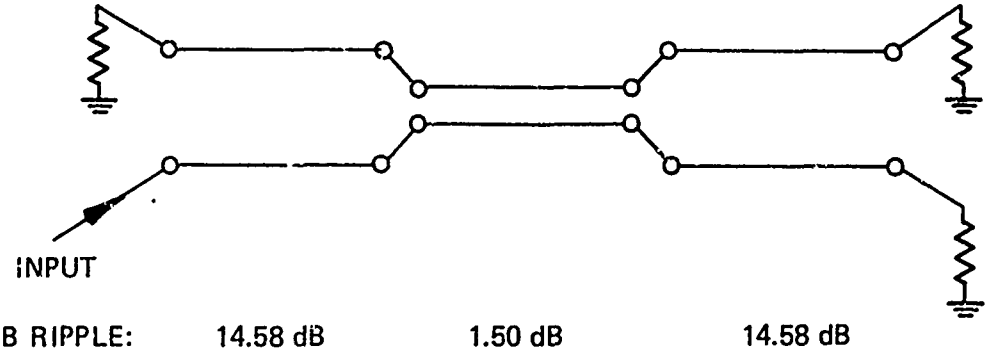

.2 dB RIPPLE:	14.58 dB	1.50 dB	14.58 dB
.25 dB RIPPLE:	14.00 dB	1.438 dB	14.00 dB

FIGURE 40 AMPLITUDE RESPONSES OF 3-SECTION SYMMETRICAL 3dB (QUADRATURE) COUPLERS OF 0.2 dB AND 0.25 dB RIPPLE

D-11666

A practical problem in multi-element couplers is the treatment of the transition zones where the ends of one coupler are joined to the next. The junction discontinuities must be tuned out over the coupling bandwidth to achieve low VSWR and high directivity performance. Also, the transitions inevitably take up space and contribute to the length of the coupler.

In our early experimental couplers we included the lengths of the transitions in the lengths of the end couplers. That is, the center coupler was made 90^{o} long at f_o and the end couplers plus an estimate for the transitions were also 90^{o} long. The reasoning was that the transition regions were still coupling zones, with the coupling changing rapidly from the center to the end value, and although the coupling was not the correct value, it dropped very rapidly such that it could be considered a small perturbation on the weak end couplers. Our object was to keep the entire coupler 270^{o} long at f_o.

The coupling characteristics of those couplers always exhibited a pronounced coupling roll off with increasing frequency. This effect was attributed, with the help of computer modeling experiments, to the foreshortening of the end couplers. Fig. 41 shows the results of the computer experiments on a 3-section 10 dB coupler. All curves are for equal mode velocities, and junction discontinuities are ignored in order to demonstrate only the effect of the lengths of the couplers and transitions.

Curve #1 is the response of the ideal coupler---without transitions--- which, with the rounded off coupling values, is a $9.95 \pm .05$ dB coupler. Curve #3 illustrates what happens when we approximate the transitions by 15^{o} of 17 dB coupling and shorten the ends by 15^{o} to maintain a

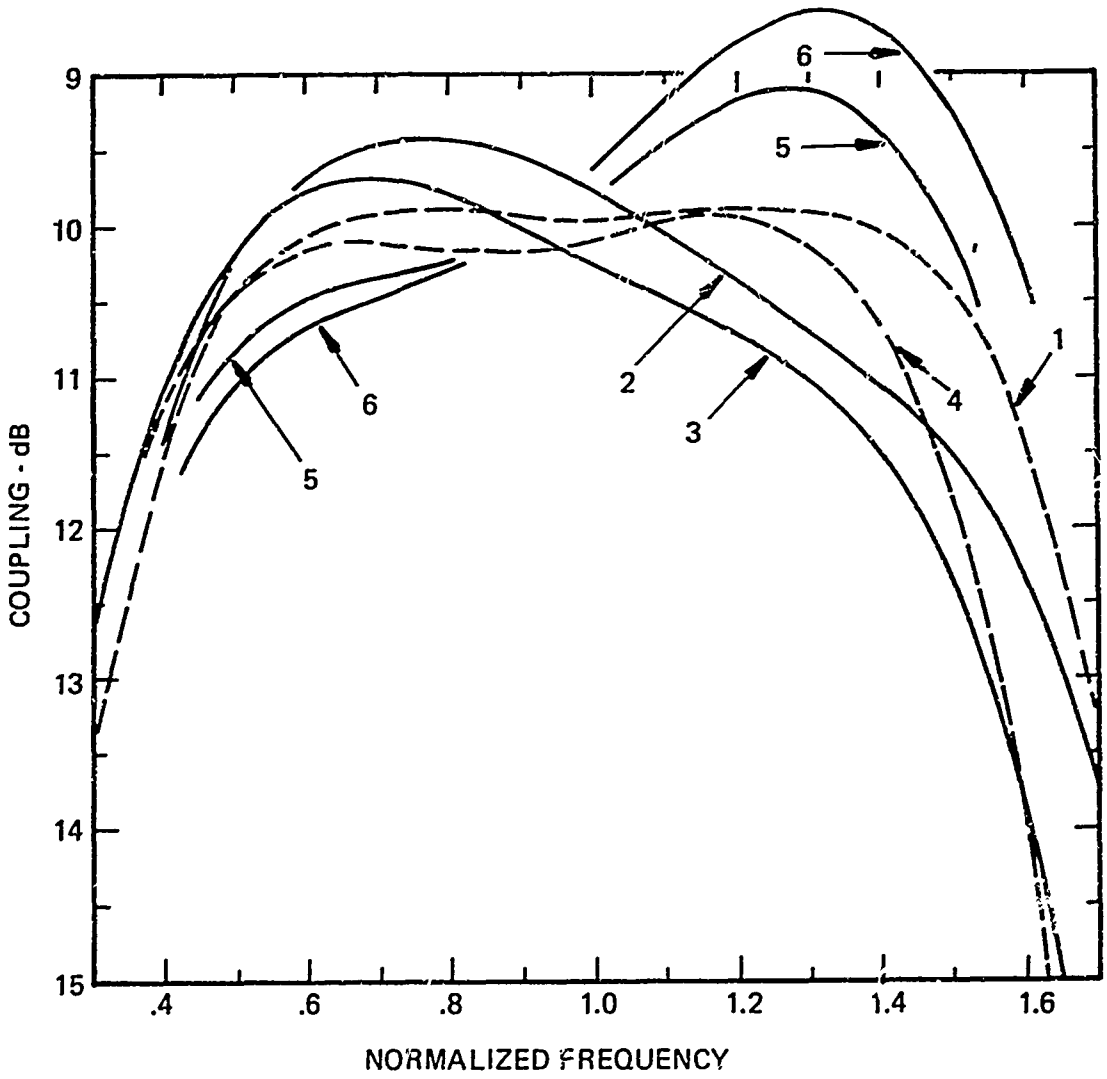

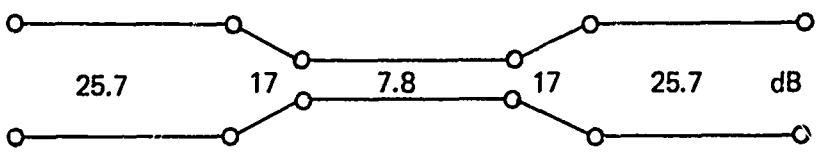

1.	90°	0°	90°	0°	90°
2.	75°	0°	90°	0°	75°
3.	75°	15°	90°	15°	75°
4.	90°	15°	90°	15°	90°
5.	105°	0°	90°	0°	105°
6.	90°	15° (120 dB)	90°	15° (120 dB)	90°

FIGURE 41 EFFECT OF END COUPLER AND TRANSITION LENGTHS ON 3-SECTION COUPLER CHARACTERISTICS.

D 12102

270° overall length. The tilting of the characteristic corresponds to the experimentally observed roll off. Curve #2, in which the transition is removed but the ends are kept short has the same general shape. This indicates that the length of the 25.7 dB couplers and not the overall length which is important. This is confirmed by curve #4, where the ends are 90° long and the 15° long transitions are inserted; the coupling curve is quite flat, although the bandwidth is narrower and the center frequency has shifted downward from the ideal coupler.

Finally, curve #5 illustrates that the coupling increases with frequency if the ends are too long, as we might now expect. Curve #6 shows what happens if we have three 90° long couplers joined by transitions 15° long but completely decoupled.

Two rules may be drawn from these experiments. First the individual couplers must all be 90° long and the transition zones should have an intermediate coupling value, to maintain coupling flatness. Second, the transitions must be made as short as possible to avoid excessive loss of bandwidth. We might also remark that as long as the symmetry is maintained, the ideal directivity and phase quadrature are not affected by the lengths or coupling of the transition zones.

Tapered line couplers theoretically have a high-pass coupling characteristic and eliminate the problem of intercoupler transitions. In practice, however, there are still junctions where the coupler meets the decoupled feed lines, and these discontinuities will limit the high frequency performance. Nevertheless extremely broad bandwidths are attainable, 40-to-1 or more, in media with equal phase velocities. We are not aware of very broadband tapered-line microstrip couplers having been reported. Certainly the problem of velocity compensation

and attaining high directivity over decade bandwidths in microstrip couplers presents something of a challenge--which we have not undertaken in this work.

We have also not prepared any design charts for tapered line couplers. Arndt[23] has synthesized asymmetrical tapered couplers with Chebyshev characteristics and provides coupling tables for 3,6,8,34, 10 and 20 dB couplers with ripples up to .83 dB. The tables are in the form of coefficients of 6th order polynomials giving the coupling as a function of length. The equal-ripple low frequency band edges are also tabulated. These couplers are not quadrature couplers and, as Arndt points out, are not easily phase compensated.

DuHamel and Armstrong[24] have given a synthesis prescription for tapered line magic-T's, i.e. in-or out-of-phase outputs, based on a Klopfenstein taper. The design procedure appears to be quite tedious.

The design of symmetrical tapered couplers has been treated by Tresselt,[25] and by Kammler[26]. Tresselt determined that, in the loose coupling approximation employed, the high pass characteristic required that the coupling go to 0 dB at the center. He did not prove that this was true in any higher order theory, but turned to the synthesis of equal ripple couplers of finite bandwidth. In the design procedure developed, the coupling versus distance function is much like the staircase of the stepped symmetrical coupler, but with rounded corners and not-quite-flat steps. In fact the stepped coupler impedance values are used as weighing functions in the tapered coupler design. The coupling curves and bandwidths of the tapered coupler and stepped prototype will be very much the same. The tapered coupler turns out to

be a little longer and requires slightly tighter coupling at the center.

The great advantage of this technique is the elimination of the transition regions by incorporating them into the overall coupler design in a rigorous fashion. The design procedure is quite involved, and we have not attempted to reduce it to practically manageable tables or charts. This is, however, a job that definitely should be done.

B. Tight-Coupling Methods

The practical limit for narrow gaps between coupled microstrip lines fabricated by conventional photo etching techniques is about .0008" to .001". Typical substrate thicknesses are .010" to .050", with .020" and .025" generally used for S- through K_u-bands. Thus the minimum practical s/h is in the .02 to .04 range, depending on the substrate thickness. Referring to the basic design chart, Fig. 25, we see that this limits the tightest coupling of 50 Ω couplers to about 5 dB.

To meet the demand for 3 dB couplers we need to explore ways of increasing the coupling of microstrip couplers within the framework of the gap width limitation. Recall also that broadband 3 dB couplers can require coupling even greater than 1 dB; the center of a 9-section symmetrical 3 dB coupler with 1 dB of ripple. for instance, is an 0.3 dB coupler! In this Section we shall discuss three methods for achieving tight coupling using fairly conventional microstrip techniques. These are (1) transformation to high impedance couplers, (2) interdigitated structures, and (3) tandem connections of more loosely coupled couplers.

From Fig. 25 we can see that at the narrow gap end the coupling tightens as the impedance of a coupler is increased by narrowing the lines, keeping the gap fixed. The practical limit here is perhaps 75 to 80 Ω, which will pick up about 1 dB in coupling. The transformation up to and down from the coupler impedance will need a bandwidth at least as great as the coupler to avoid undue loss in directivity. The very narrow coupler strips will also cause higher dissipative loss. Clearly, the marginal gain in coupling by this method is not worth the degradation in directivity and loss.

Lange[27, 28] has designed and constructed interdigitated 3 dB and 1.47 dB (center section of 3-section 3 dB coupler) couplers. In this design, diagrammed in Fig. 42, tight coupling with moderate spacing is achieved by tripling the length of the coupling gap. It requires everal jumpers to connect the ends of the fingers belonging to the same conductor strip. The jumpers are normally several .0005" to .001" gold wires, thermo-compression bonded to the gold fingers; Fig. 43 shows the construction details.

The couplers in Figs. 42 and 43 have the direct and isolated ports interchanged, which is handy for microwave mixer applications. This crossing over of the lines is possible because of the jumpers, which were needed anyway. One can also "reverse" the Lange coupler, bringing the direct and isolated ports out on their usual sides, as diagrammed in Fig. 44. This layout dispenses with the center cross-over wires.

The directivity of 3-dB interdigitated couplers is excellent ($\gtrsim$20dB) even without velocity compensation. Typical performance of a single section C-band coupler used in octave bandwidth mixers is shown in Fig. 45. The isolation curve here is quite close--within about 2 dB of the theoretical curve for a single gap 3-dB coupler, Fig. 14. Thus we expect that the even-odd mode velocity ratio of the interdigitated coupler to be comparable to that of the corresponding single gap structure.

Lange's 1.47 dB coupler required 0.6-mil gaps and 1.9-mil lines on 42-mil alumina, which was pushing the limits of the photo etching technique. As it was, the coupling was low and the directivity was as low as 15 dB.

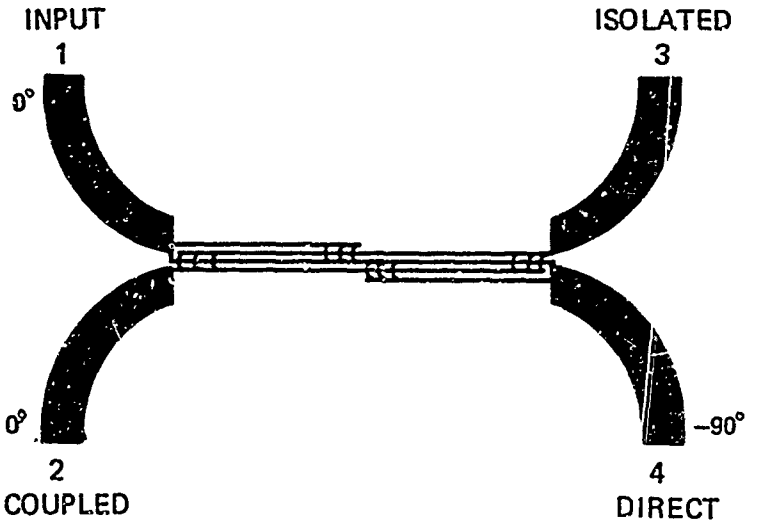

FIGURE 42 INTERDIGITATED 3 dB QUADRATURE MICROSTRIP COUPLER

D-10162

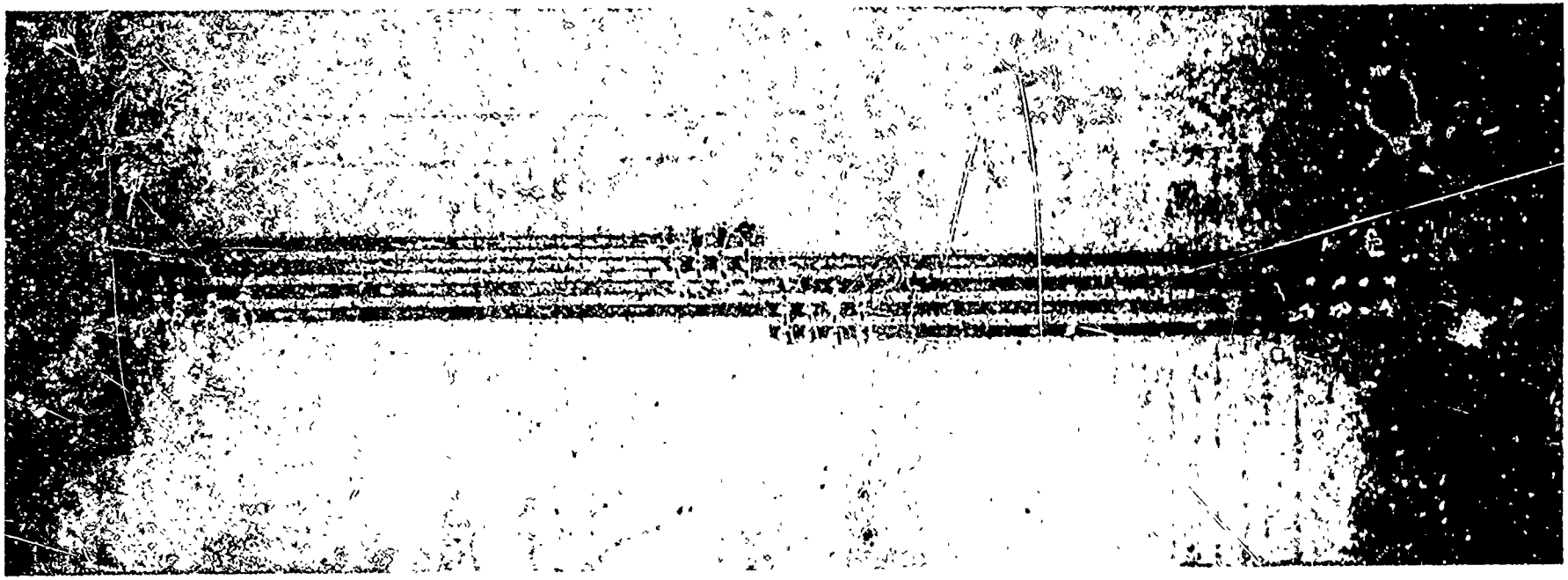

FIGURE 43 DETAILS OF MICROSTRIP INTERDIGITAL QUADRATURE COUPLER FABRICATION

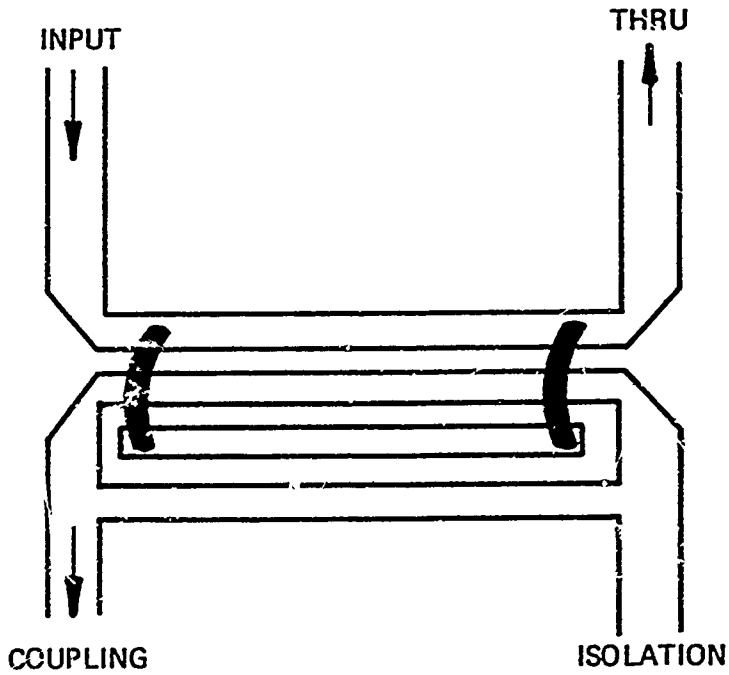

(a) REVERSED LANGE COUPLER

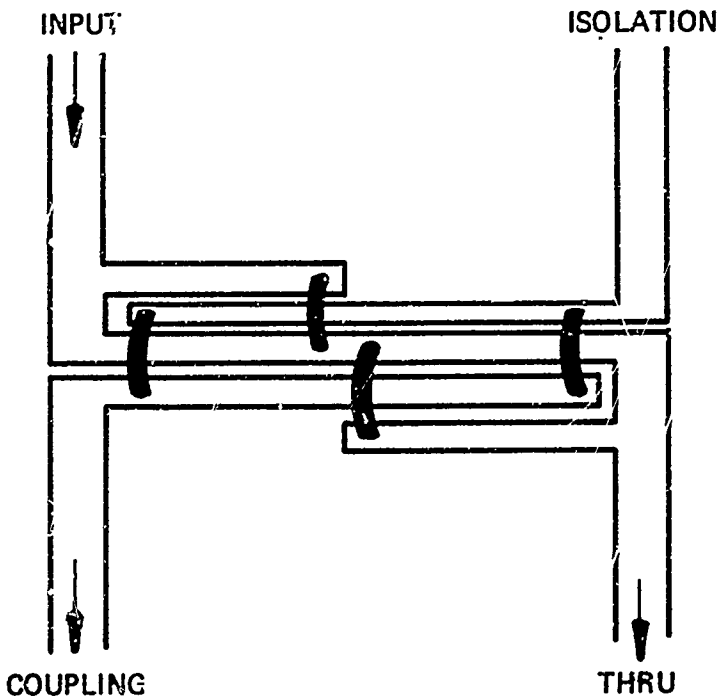

(b) 3 dB LANGE COUPLER

FIGURE 44 COMPARISON OF LANGE AND REVERSED LANGE COUPLERS

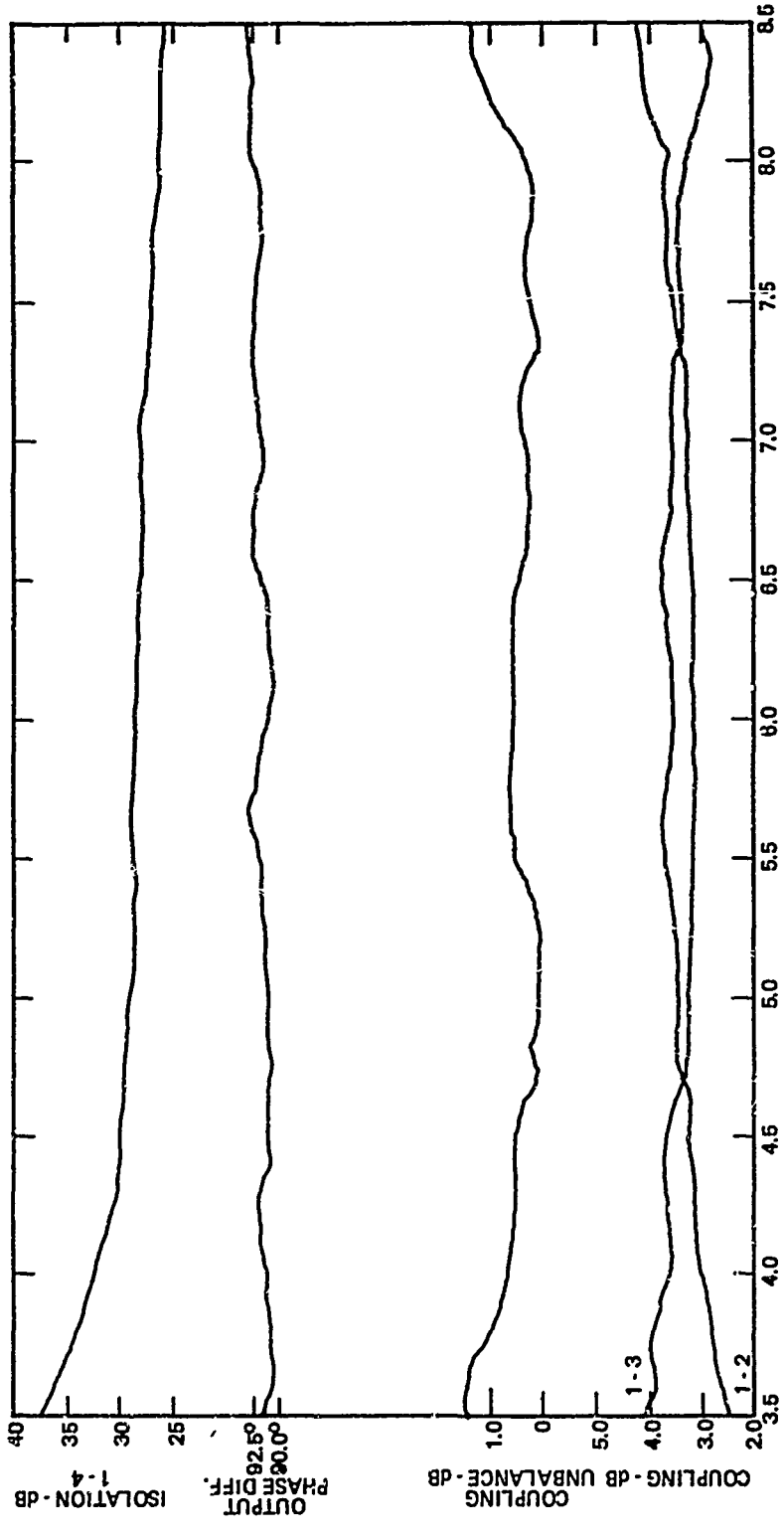

FIGURE 45 RESPONSE OF 4-8 GHz MICROSTRIP INTERDIGITAL QUADRATURE COUPLER

Thus, the interdigitated coupler approach appears to be excellent for couplers up to about 2.5 dB on .020" - .025" substrates and 2 dB on .050" substrates. Reaching 1.5 dB means extraordinary control on tolerances. Consequently, this coupler is almost ruled out of multisection 3-dB coupler applications. One could possibly tighten the coupling still more by using more, narrower, fingers, but they are pretty narrow already and bonding the jumper wires without shorting to adjacent fingers is an exacting task.

Unfortunately, no general design data has been published on the parameters of interdigitated couplers. However, since their widest use will be as single-section, 3 dB couplers, the empirical values $s/h = .072$, $w/h = .11$, $\epsilon_r \approx 10.0$ should suffice for most of the work.

It is well-known that two quadrature couplers connected in tandem will have an overall coupling greater than either and will still be a quad coupler. The tandem connection* of two couplers exists when the coupled and direct ports (ports 2 and 4) of one coupler feed diagonally opposed ports (input, 1, and isolated, 3) of the second, Figure 46.

---

* c f. footnote, p. 74

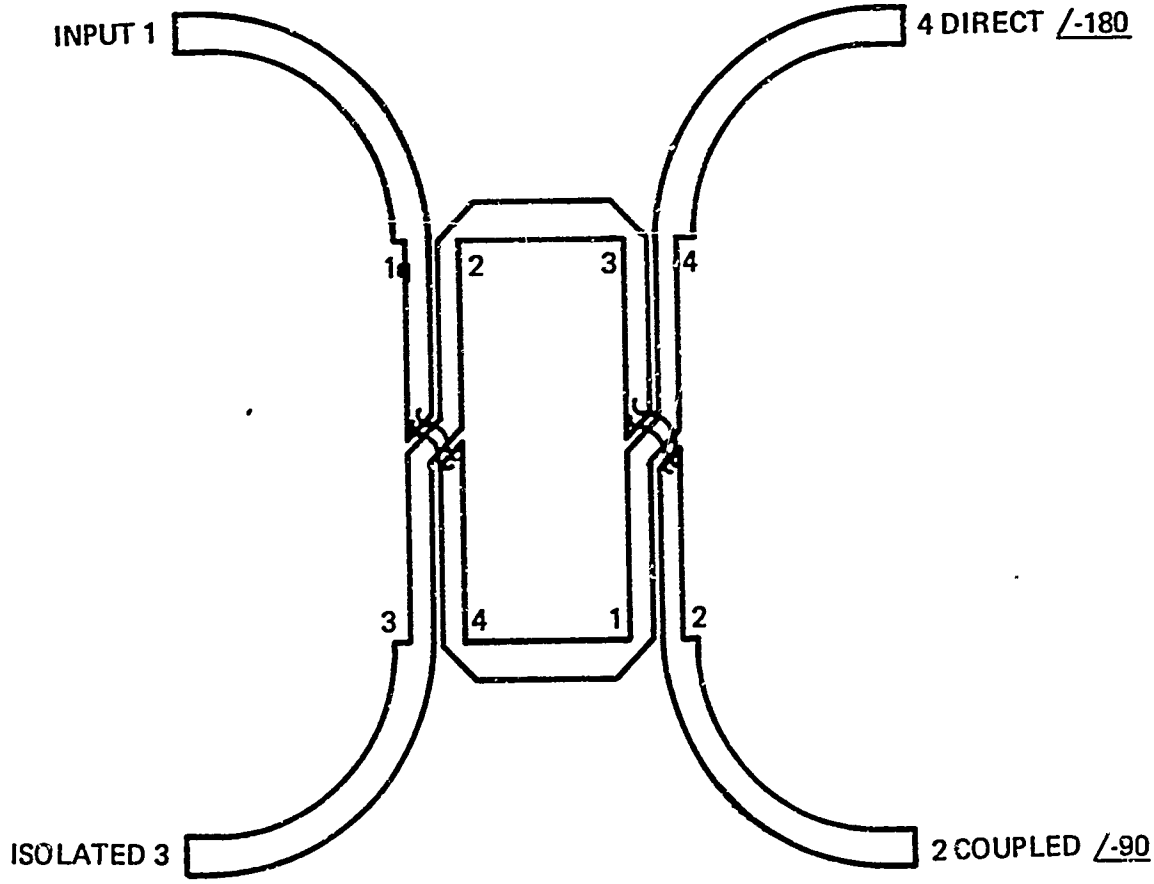

FIGURE 46 MICROSTRIP TANDEM QUADRATURE HYBRID COUPLER SCHEMATIC

D-10954

Note that the isolated port is on the input port side and the coupled port is diagonal to the input. The composite coupler can be treated as a single coupler and connected in tandem with yet another.

Denote the scattering coefficients of the tandem coupler by T_{12} and T_{14}, and those of the individual couplers by S_{12}, S_{14} and $\mathscr{S}_{12}$, $\mathscr{S}_{14}$.
then,

$$T_{12} = \mathscr{S}_{12} S_{14} + \mathscr{S}_{14} S_{12}$$

$$T_{14} = \mathscr{S}_{12} S_{12} + \mathscr{S}_{14} S_{14} \tag{45}$$

For two identical couplers, we have at midband, where $S_{12} = k$, $S_{14} = -j\sqrt{1-k^2}$,

$$|T_{12}|^2 = 4k^2(1-k^2)$$

$$|T_{14}|^2 = (2k^2-1)^2 \tag{46}$$

The net power coupling of two identical couplers is plotted in Fig. 47. Note in particular that two 8.34 dB couplers gives 3 dB and that a pair of 5 dB couplers--the practical tight-coupling limit--yields an 0.63 dB coupler. If still tighter coupling were required a third tandem element could be added, but this would be a rare necessity. As the coupling of the individual couplers becomes weak, $k^2 << 1$, the coupling of the tandem pair approaches 6.02 dB greater than the single coupler. When the individual couplers are tighter than 3 dB, the net coupling goes down again, the direct and coupled ports in a sense interchanging roles.

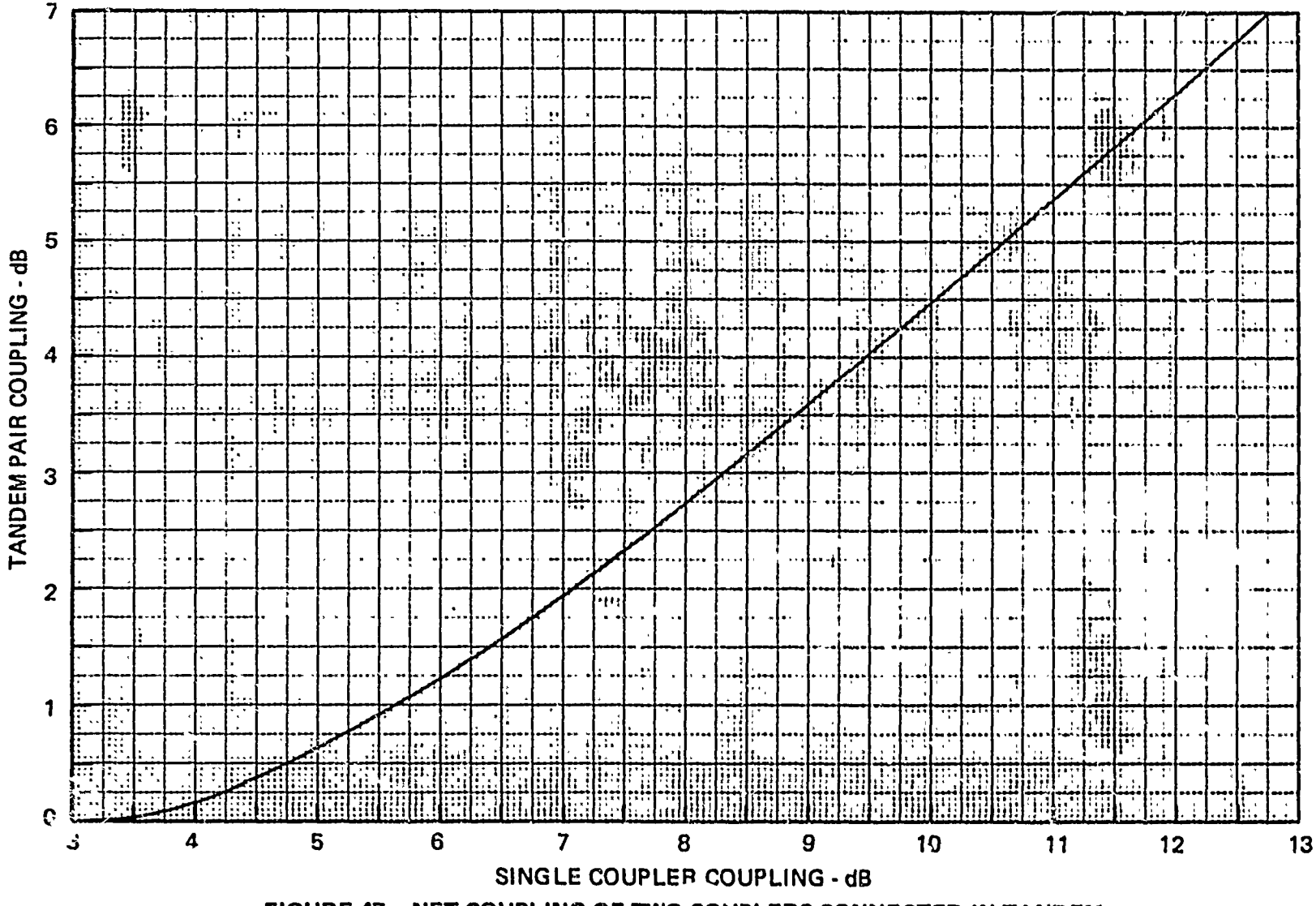

FIGURE 47 NET COUPLING OF TWO COUPLERS CONNECTED IN TANDEM.

The bandwidth of a tandem pair is less than that of a single coupler of the same overall coupling. This is illustrated in Fig. 48 for a 3 dB coupler and a tandem pair of 8.34 dB couplers. The bandwidth of the pair is essentially that of an 8.34 dB coupler; cf Fig 3.

The tandem coupler has the advantages that very tight coupling can be achieved with just two couplers, conventional design procedure is applicable, and velocity compensation is easy. They do, however, require cross-overs, but these are bonded to broad lines and do not present any fabrication or serious matching problems. The couplers also require more than twice the area of a single coupler, and there is no choice, without additional crossovers, on the ordering of the ports.

In principle there are two ways of broadbanding the tandem coupler. These are diagrammed in Fig. 49 for a 3-section 3 dB coupler. The first is a tandem connection of two 3-section, cascaded, 8.34 dB couplers; the second is a 3-section cascade with a 1.5 dB center section composed of tandem 6.4 dB couplers. The latter eliminates two couplers, but adds a cross-over in the interconnecting 50 Ω line is undesirable because cross-coupling here is to be avoided. Conversely, because of the geometry, the inter-stage connecting lines, which should be coupled to some extent, will tend to be two far apart and decoupled. Clearly the tandem 3-section 8.34 dB couplers represent the cleaner, more straightforward design. Fig. 50 shows the computed coupling response of the arrangement in Fig. 49(a). The ripple of the composite coupler is slightly less than the ripple of each 8.34 dB coupler, i.e. ~0.2 dB versus 0.25 dB. The equal ripple bandwidth is 111% (3.5 to 1), which compares quite favorably with the 117% (3.8 to 1) of a single 3-section 3 dB, 0.2 dB ripple coupler.

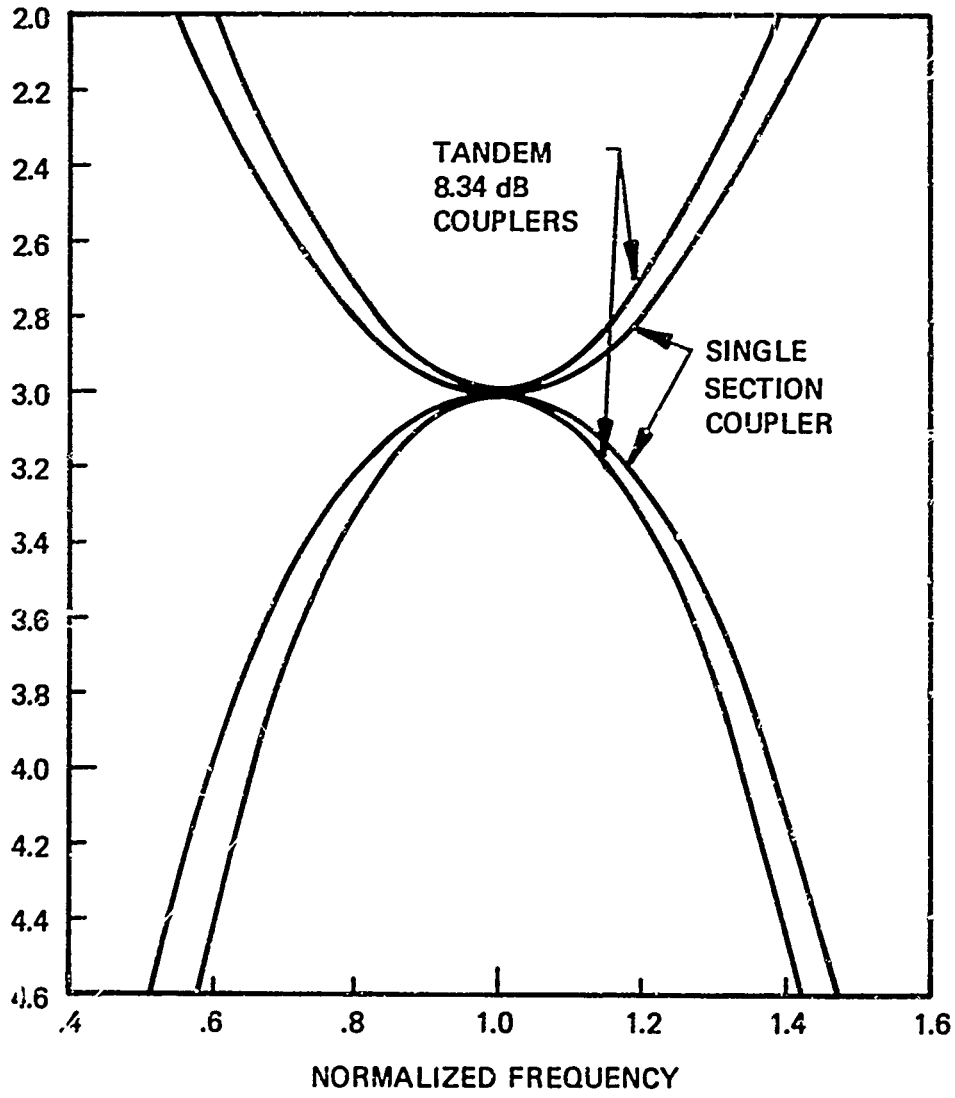

FIGURE 48 COUPLING RESPONSE OF TANDEM 8.34 dB COUPLER COMPARED TO RESPONSE OF SINGLE SECTION 3 dB COUPLER

D-11668

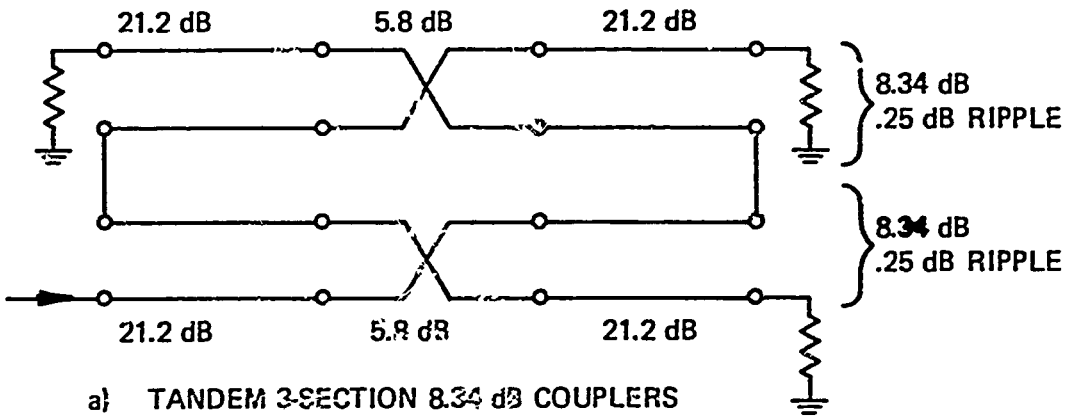

a) TANDEM 3-SECTION 8.34 dB COUPLERS

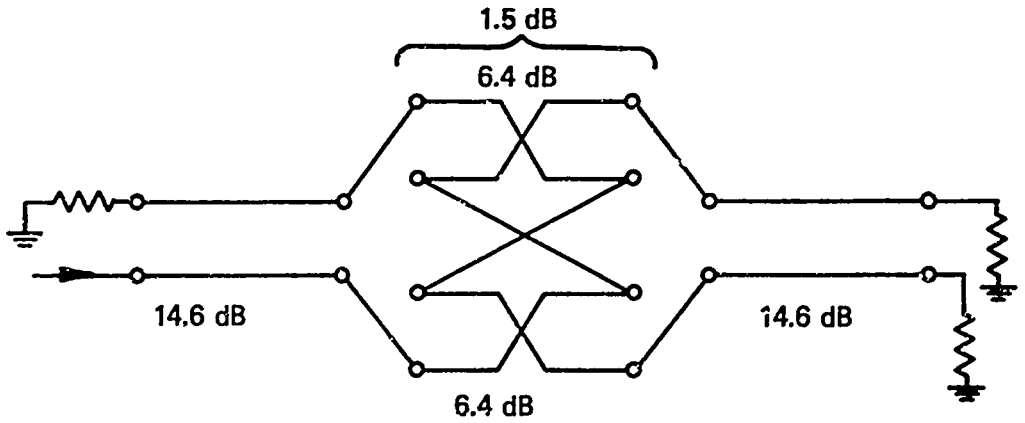

b) TANDEM 6.4 dB CENTER SECTION

FIGURE 49 SCHEMATIC DESIGNS OF BROADBAND 3 dB COUPLERS EMPLOYING TANDEM-CONNECTED LOOSELY-COUPLED COUPLERS

D-11669

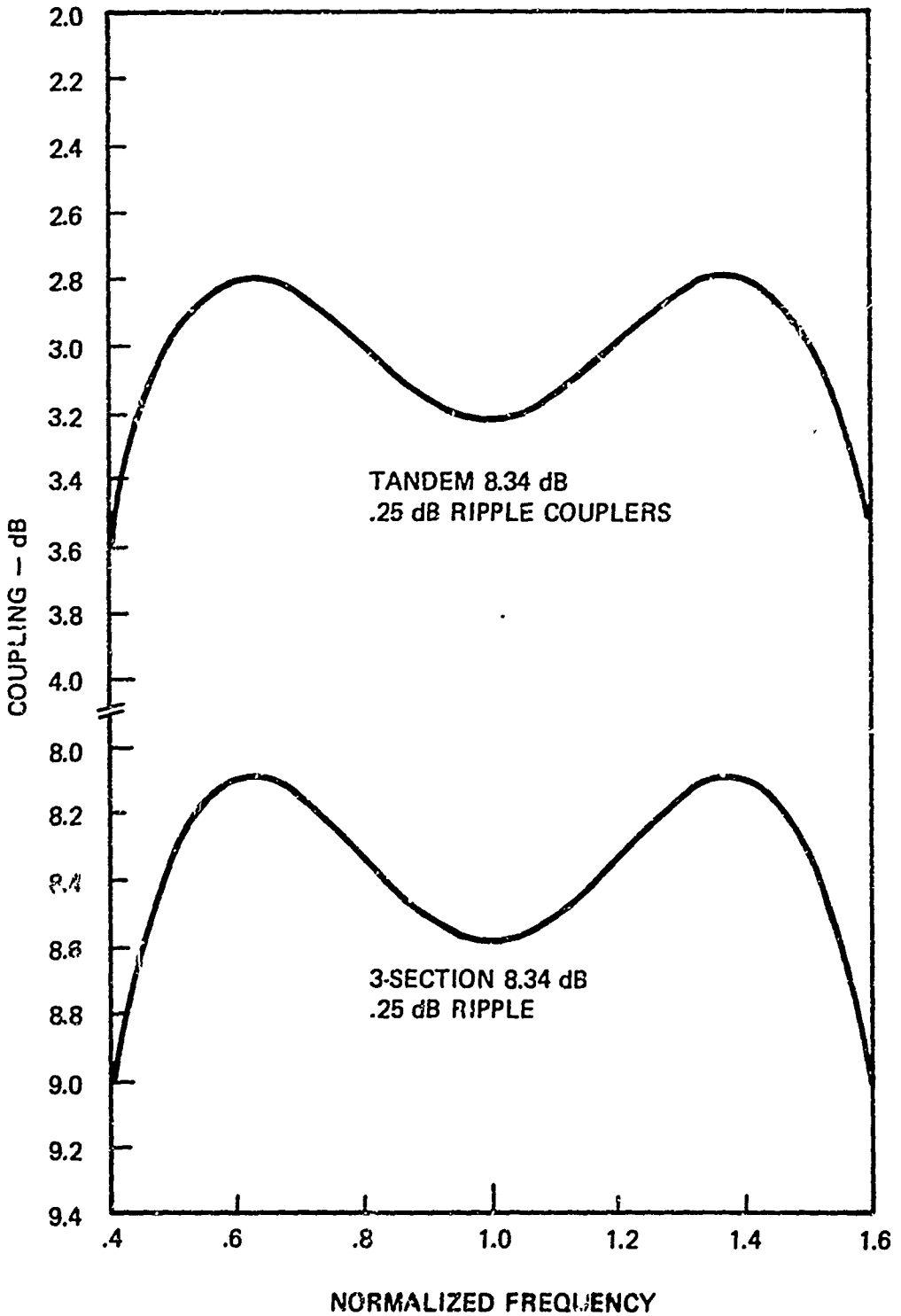

FIGURE 50 COUPLING RESPONSES OF 3-SECTION 8.34 dB COUPLERS SINGLY AND IN TANDEM

D-11670

V. EXPERIMENTAL COUPLERS

A. Introduction

A number of experimental couplers were made with the objectives of obtaining octave bandwidth coupling responses with small coupling tolerance and high directivity, as well as to compare with the design data of the previous chapters. For the sake of uniformity and ease of comparison, all couplers were 3-section symmetrical couplers. Two-section asymmetrical couplers would have provided the bandwidth, but the appeal of phase quadrature and symmetry led us to opt for the symmetrical designs.

Dielectric overlay couplers of 8.34, 10, and 20 dB, centered at 6 GHz are described in Section C; tandem 8.34 dB, 3-dB couplers at 6, 4.5 and 3 GHz are covered in Section D. We experimented with a 3-section 3 dB coupler with an interdigitated center section, Section E. This was not pursued beyond one trial, but it does show promise within the limitations discussed in the last chapter. In our early work, before turning to the dielectric overlay, we experimented with the wiggly-line coupler intoduced by Podel.[8] We were not successful in improving directivity with this technique; however some results of this effort will be covered in Section F. Finally, in Section G we discuss the results on band pass filters made with and without a dielectric overlays. All circuits were on .025" (±.0005") 99.5% alumina (Alsimag 772, American Lava Corp.) except the interdigitals which were on .050" material. The substrates were polished to 1.5 μin finish and coated with a standard 100 μin Cr - Au metalization. The dielectric constant quoted by the manufacturer was 9.8; our measurements, described in Section B indicated that ε_r was near 10.0. The same material was used for the overlays.

The circuits were soldered into gold-plated machined aluminum housings, fitted with OSM-220 -8873A hermetic MIC connectors. The launchers were modified to an air-line entry to the microstrip. (The standard connector has a teflon-loaded line.)

B. Dielectric Constant Measurements

To measure the dielectric constant, ε_r, and the effective microwave dielectric constant, ε_{eff}, of the substrate material, a special test pattern was etched. It consisted of a series of four different-sized circular dots and a capacitively-coupled transmission line resonator.

By plotting the square root of the low-frequency capacitances of the dots, versus their radii, Fig. 51, we find that the effective radius, which accounts for the effect of fringing is .010" greater than the geometrical radius. (The largest dot was in rather close proximity to the transmission line and was perhaps loaded by it slightly; hence this high point was not weighted in drawing the straight lines.) From this data, $\varepsilon_r = 10.7$ clearly represents the best fit to the three lower points, although $\varepsilon_r = 10.0$ appears to be within experimental error.

A time-domain reflectometer measurement of the line impedance of the resonator section which had w/h = .985 was 48 $\pm$ .3 Ω. This implies $\varepsilon_r \approx 10.6$, based on Bryant and Weiss' calculations for zero thickness lines. Allowing for the line thickness would bring ε_r down to about 10.4.

The transmission resonant frequencies of the resonator from S to X band were measured. The effective dielectric constants at each resonant frequency were computed, assuming the line was .020" longer than its physical length, to allow for end fringing. These data are plotted in Fig. 52 with a dispersion curve calculated from Getsingers' formula, Eq. 44; for $\varepsilon_r = 10.0$ and $\varepsilon_{eo} = 6.68$. This value for the low frequency effective dielectric constant is consistent with the resonator data and with Bryant and Weiss' calculated value for $\varepsilon_r = 10.0$, w/h = .985.

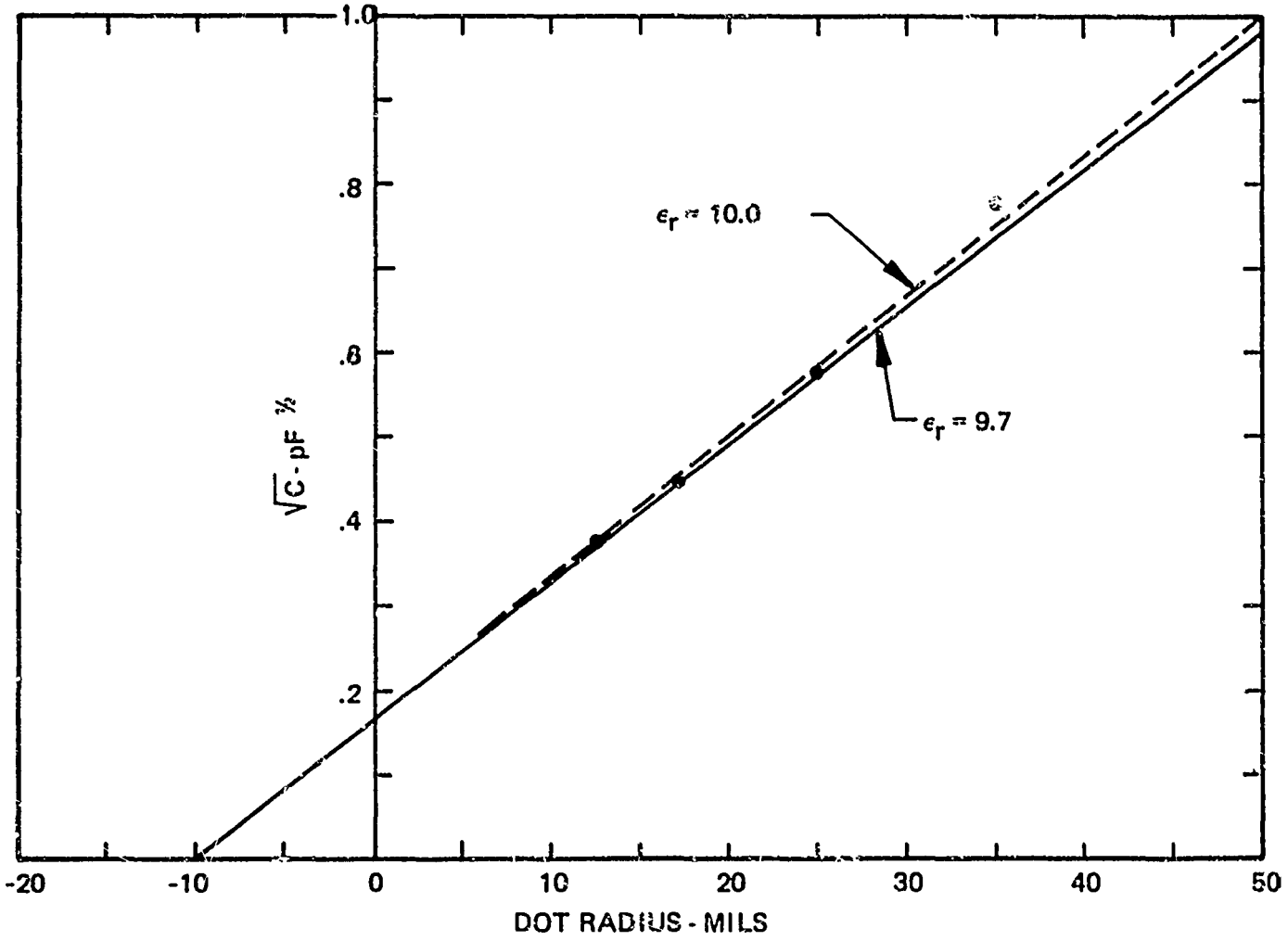

FIGURE 51 DETERMINATION OF FRINGING EFFECT ON .025" ALUMINA SUBSTRATE.

Thus, this microwave-derived value of $\epsilon_r = 10.0$ was chosen since it was within a few percent of the low frequency values, and it was obviously easier to use. A more precise value was not deemed necessary since coupling depends only weakly upon ϵ_r and coupler impedances with dielectric overlays are semi-empirically determined anyway. For the same reasons we did not generally apply dispersion corrections in deriving the coupler designs.

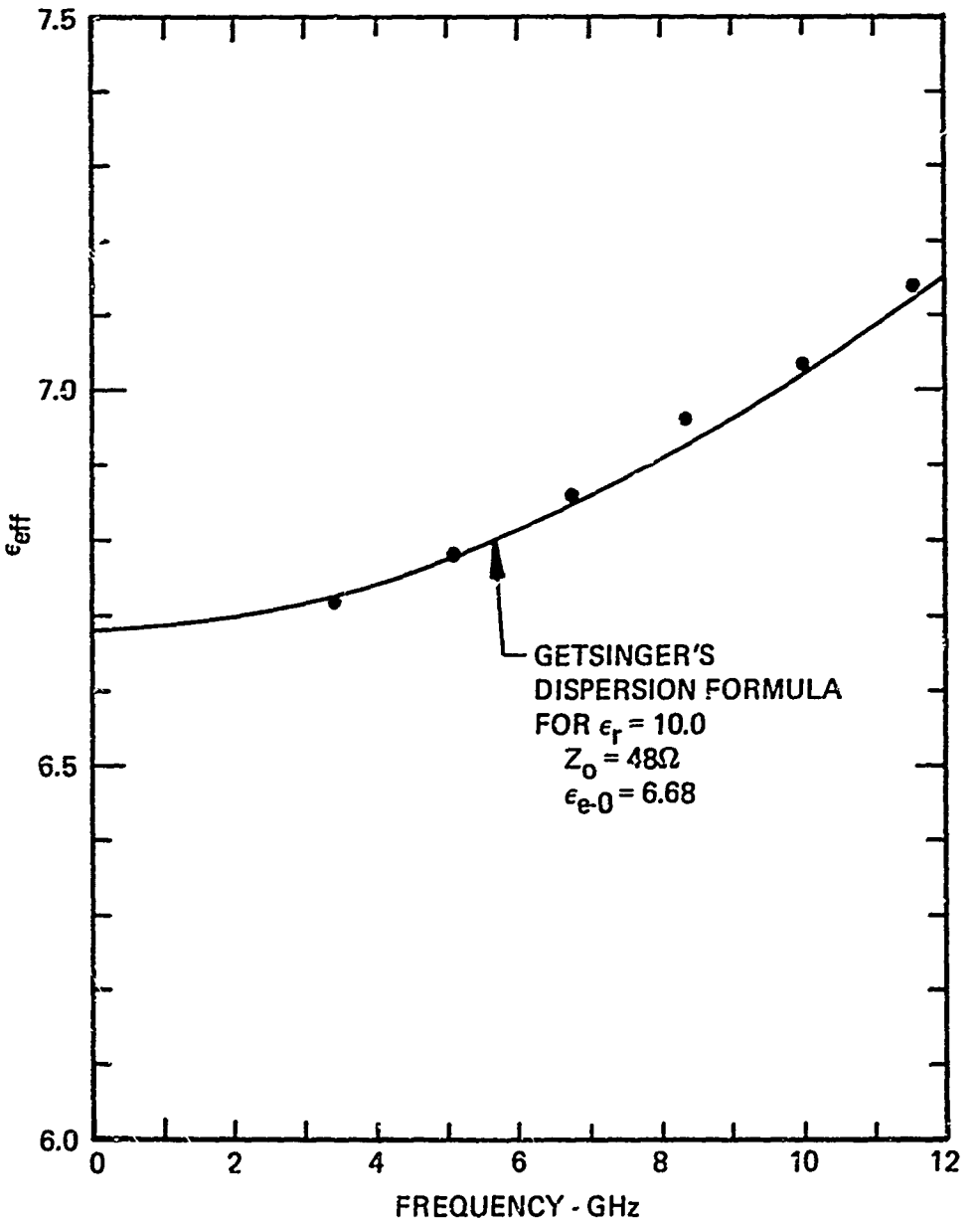

FIGURE 52 EFFECTIVE DIELECTRIC CONSTANT OF ALSIMAG 772 FROM HALF-WAVE RESONATOR MEASUREMENTS.

C. 8.34 dB, 10 dB, and 20 dB Couplers

Our target designs for these three couplers were:

Coupler	Ripple	Center Coupler	End Coupler	
8.34	0.05	6.28	23.8	dB
10.0	0.20	7.44	23.5	dB
20.0	0.20	17.2	33.8	dB

where the individual coupler values were computed from Cristal and Young's data for 3-section symmetrical couplers, cf. Fig. 39. The theoretical responses of these couplers, with and without velocity compensation are shown in Figs. 53, 54, and 55.

Photographs of 8.34, 10, and 20 dB couplers without the dielectric overlays in place are shown in Figs. 56, 57 and 58. The cross-over jumper is visible in the center of the 8.34 dB coupler. It is a 10-mil wide gold strap welded to the lower left and upper right coupler branches. 8.34 dB couplers were also made without the crossed over lines, for comparison. Figs. 59 and 60 show the 10 and 20 dB couplers with the dielectric blocks in place, after being tuned for best performance. They are glued down with Eastman 910 cement. The overlay for the center of the 8.34 dB coupler with crossover is in two short pieces, one each side of the jumper. In all of these couplers, the outermost sections are decoupled ($\sim$50 dB) 50 Ω feed lines to the launchers, and are not part of the coupled zones.

The coupling and isolation responses from 1 to 11 GHz of four couplers designed according to Figures 29 and 30 are shown in Figs. 61, 62 and 63. The VSWR data for these couplers are in Fig. 64.

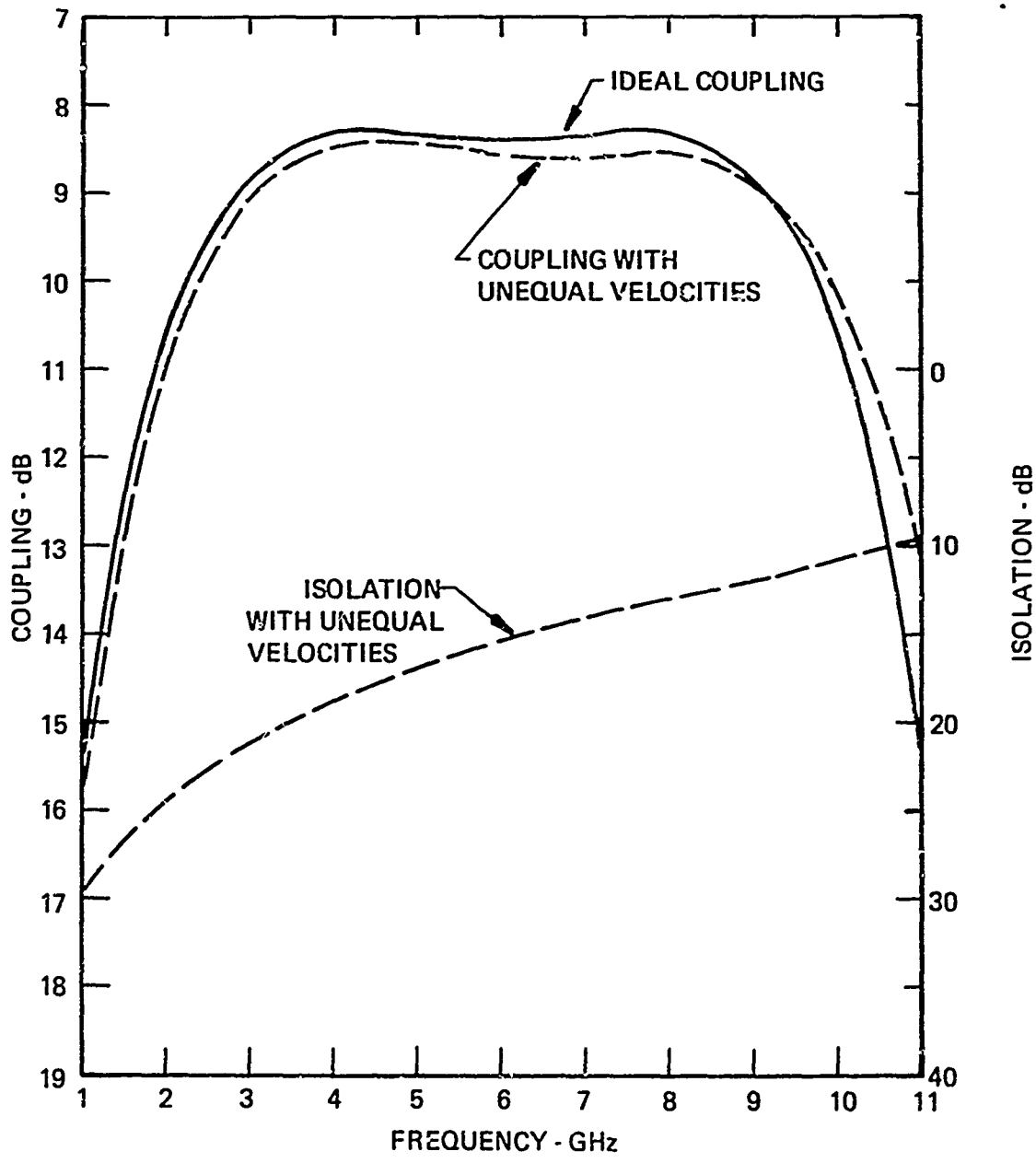

FIGURE 53 COMPUTED FREQUENCY RESPONSES OF 3-SECTION 8.34 dB .05 dB RIPPLE COUPLERS.

D-12106

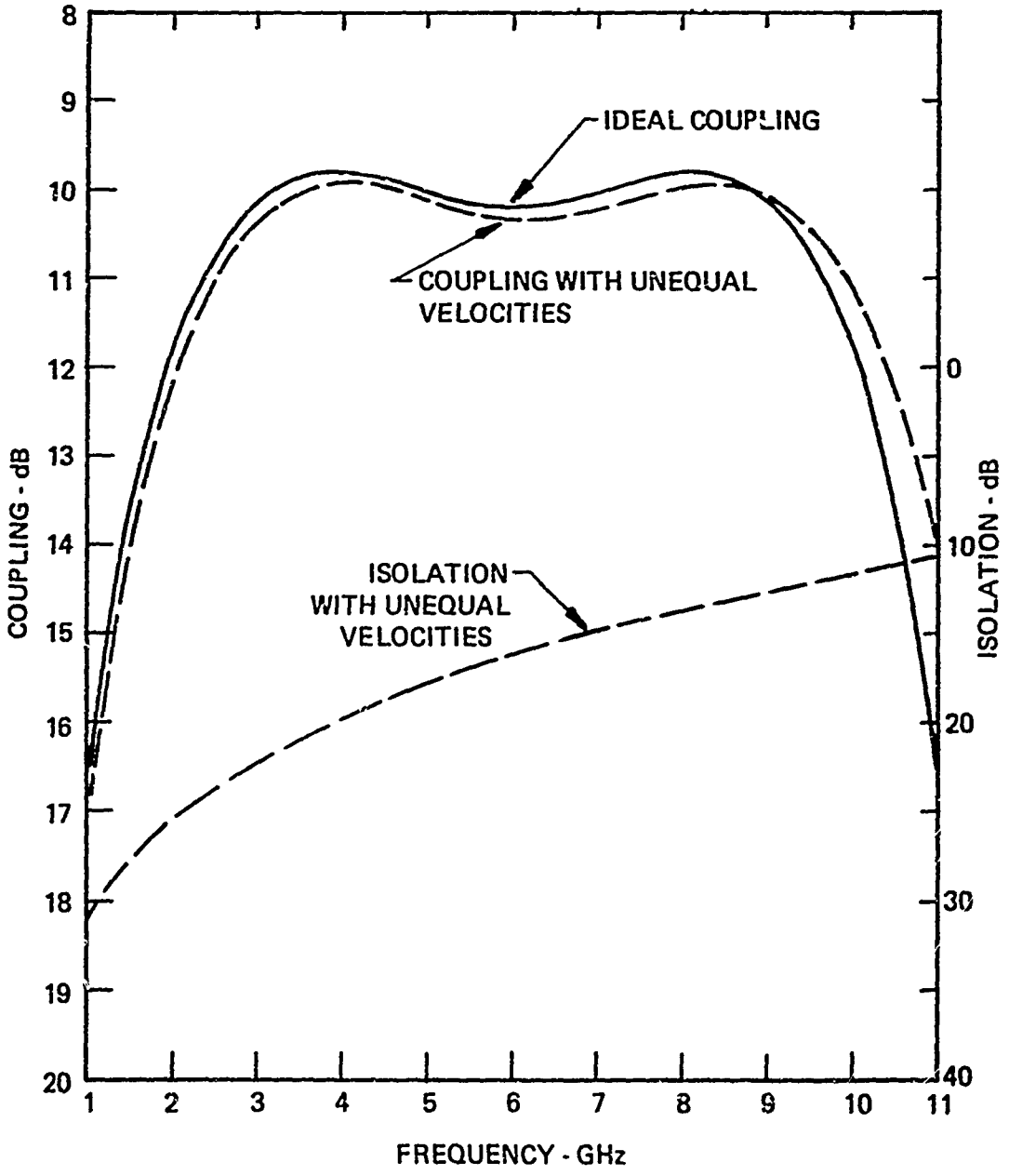

FIGURE 54 COMPUTED RESPONSES OF 3-SECTION 10 dB, 0.2 dB RIPPLE COUPLERS

D-12107

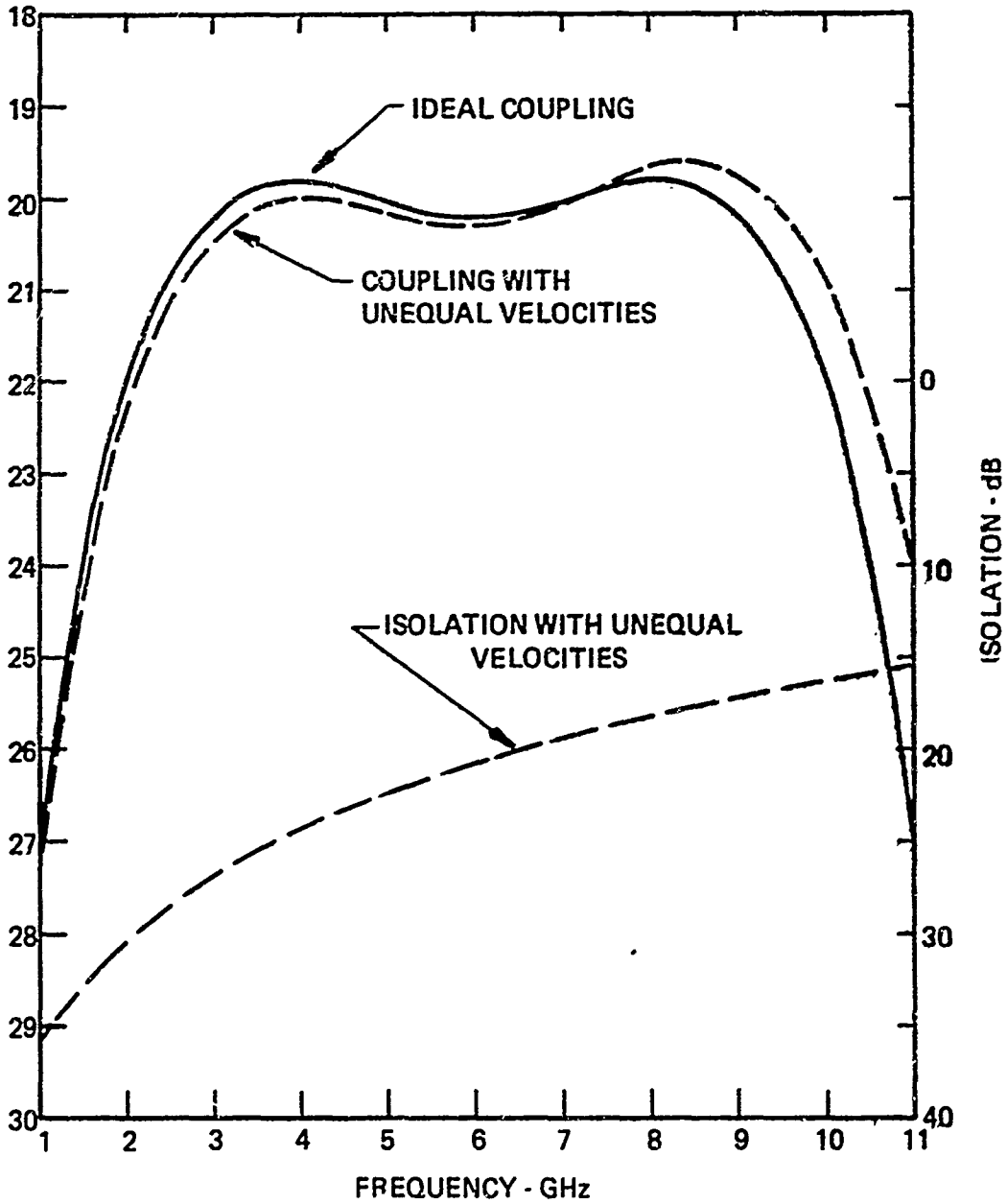

FIGURE 55 COMPUTED RESPONSES OF 20 dB, 0.2 dB RIPPLE COUPLERS

D-12108

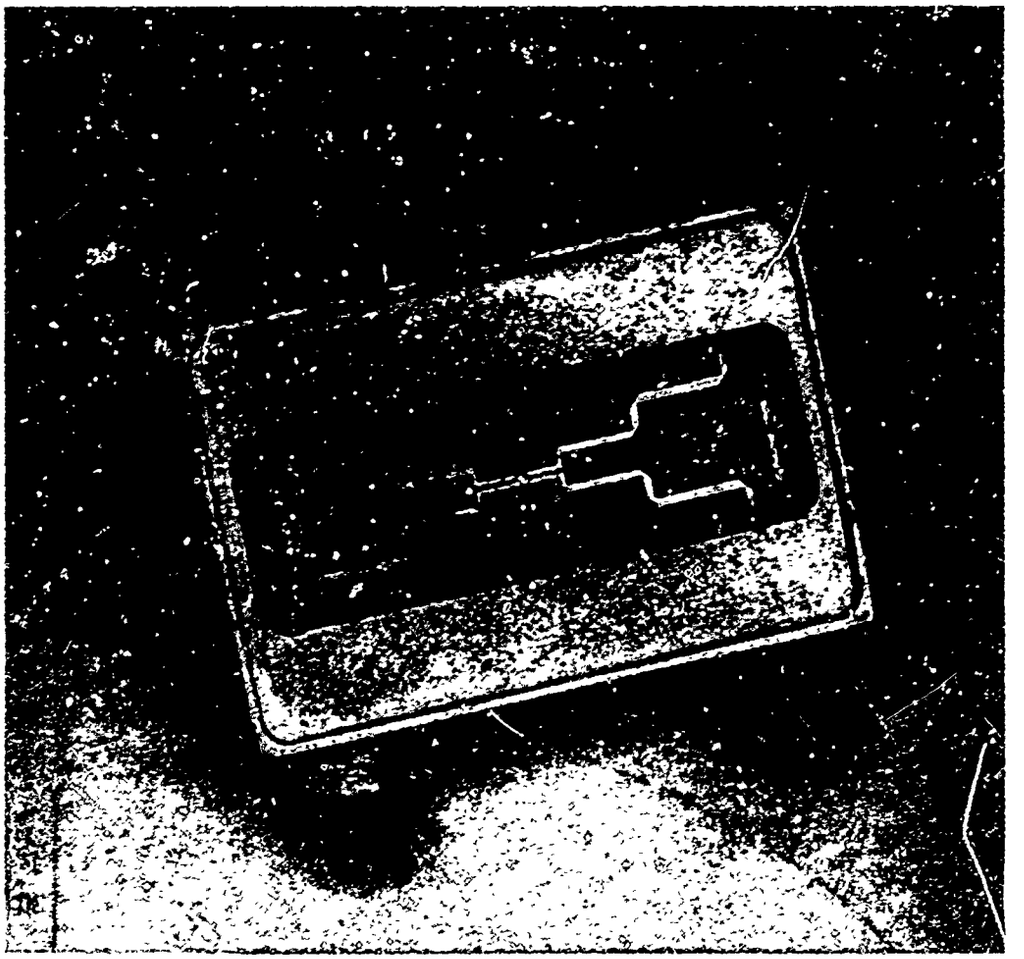

FIGURE 56 3-SECTION 8.34 dB COUPLER WITH CROSS OVER, WITHOUT DIELECTRIC OVERLAY.

D-12126

FIGURE 57 3-SECTION 10 dB COUPLER WITHOUT DIELECTRIC OVERLAY.

D-12127

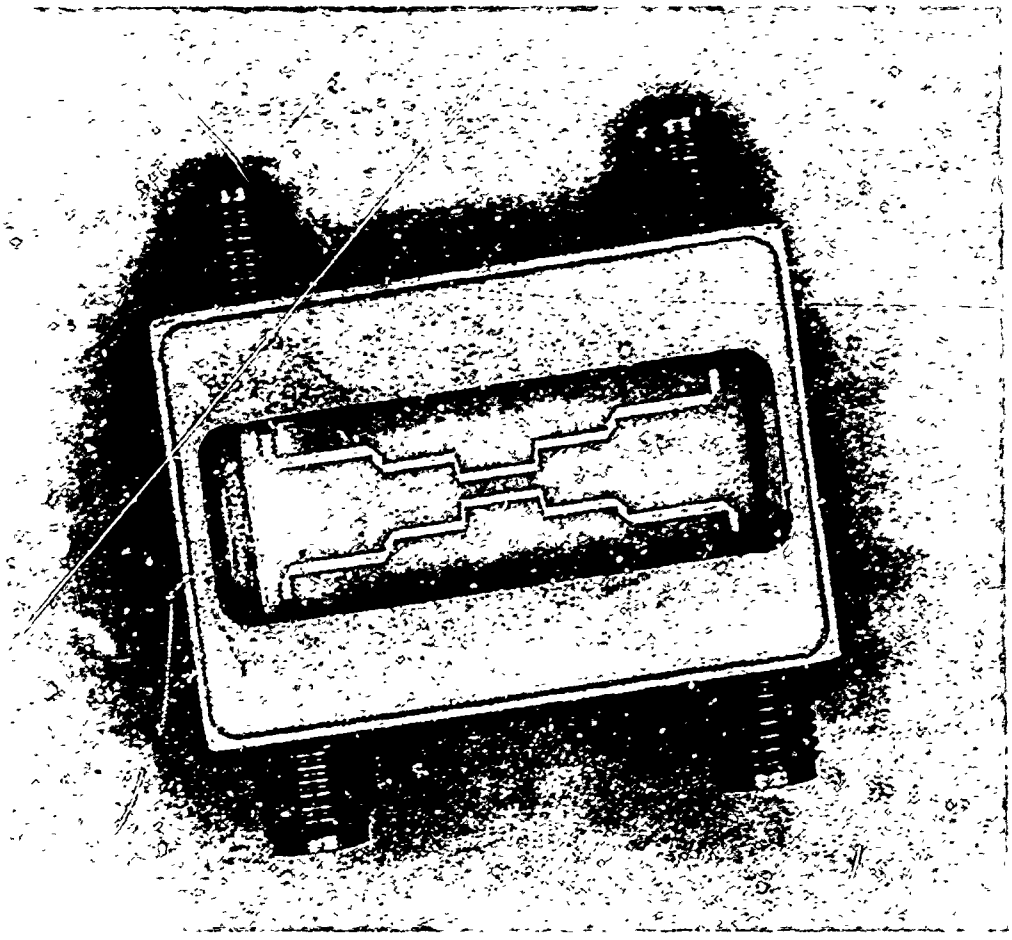

FIGURE 58 3- SECTION 20 dB COUPLER WITHOUT DIELECTRIC OVERLAY.

D-12128

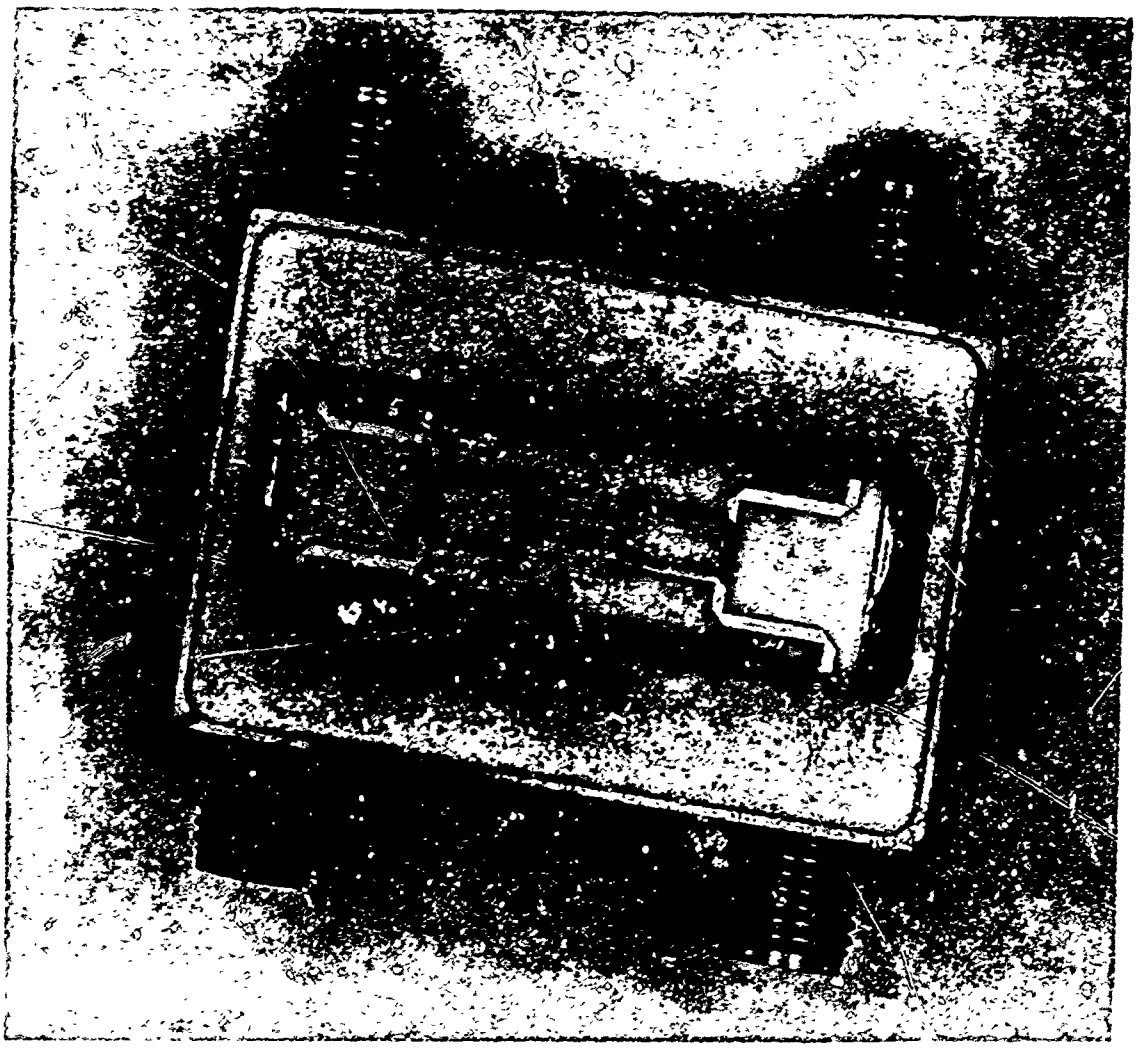

FIGURE 59 10 dB COUPLER WITH DIELECTRIC OVERLAY IN PLACE

D-12129

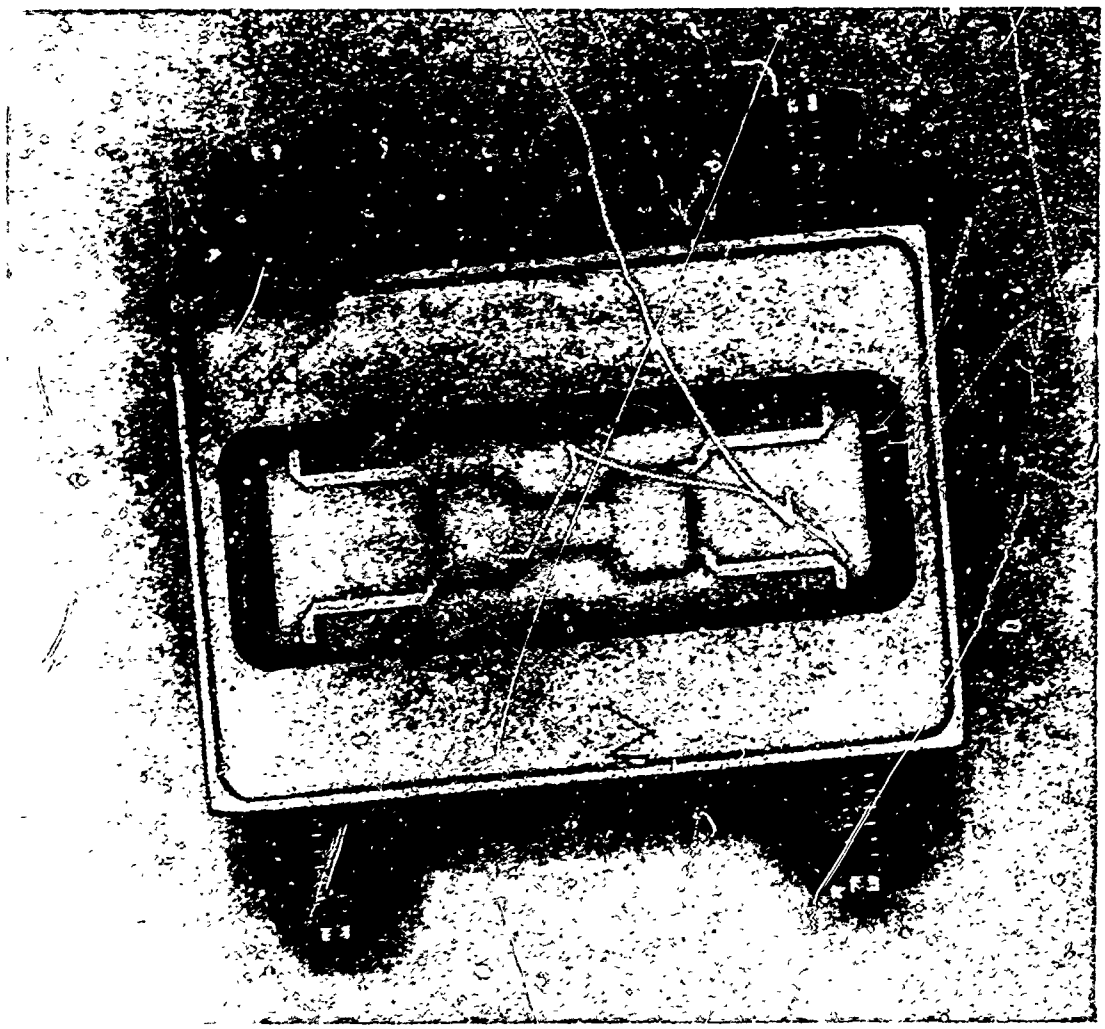

FIGURE 60 20 dB COUPLER WITH DIELECTRIC OVERLAY IN PLACE.

D-12130

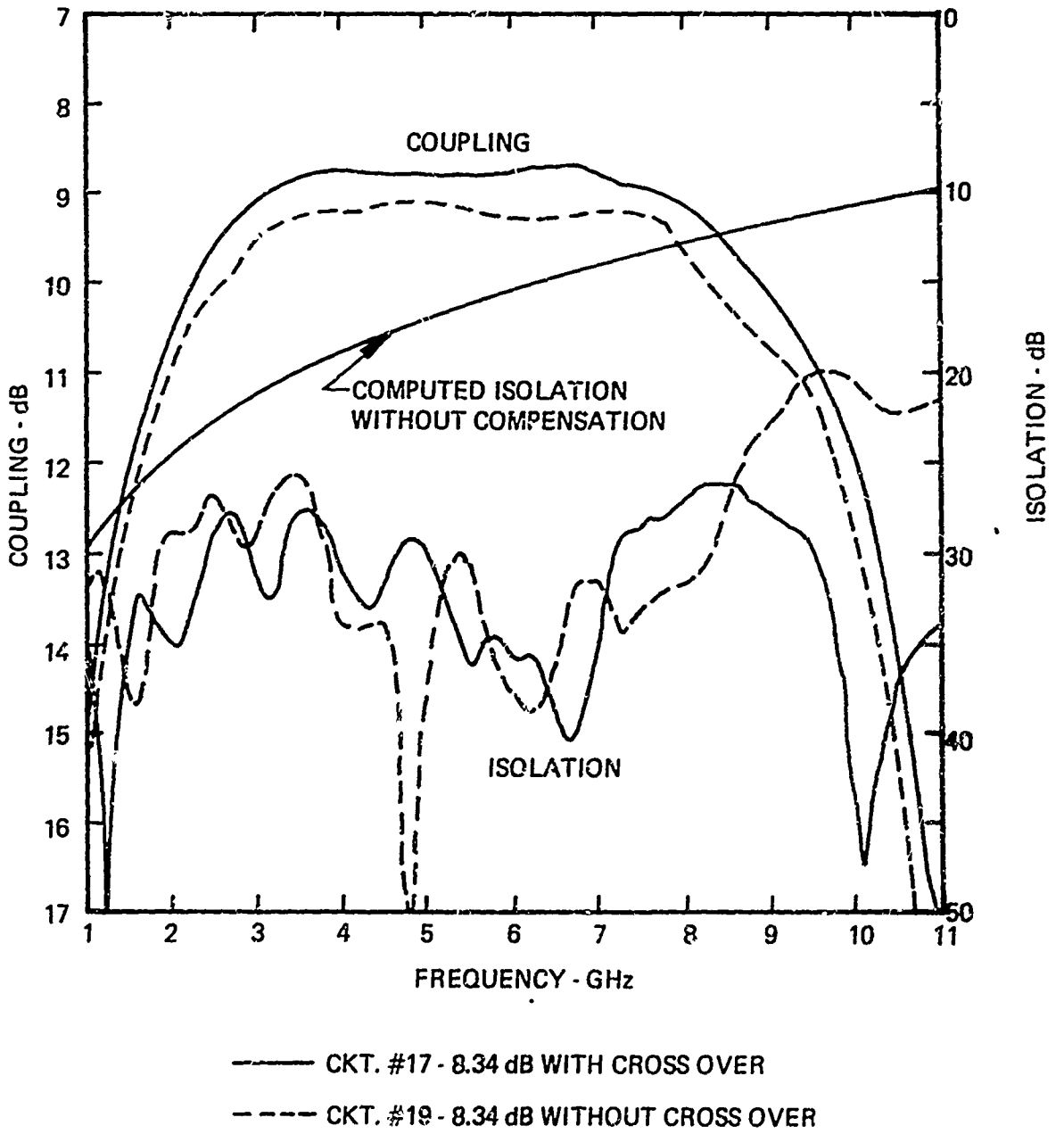

FIGURE 61 COUPLING AND ISOLATION RESPONSES OF 3-SECTION 8.34 dB COUPLERS. #17 & #19.

D-12109

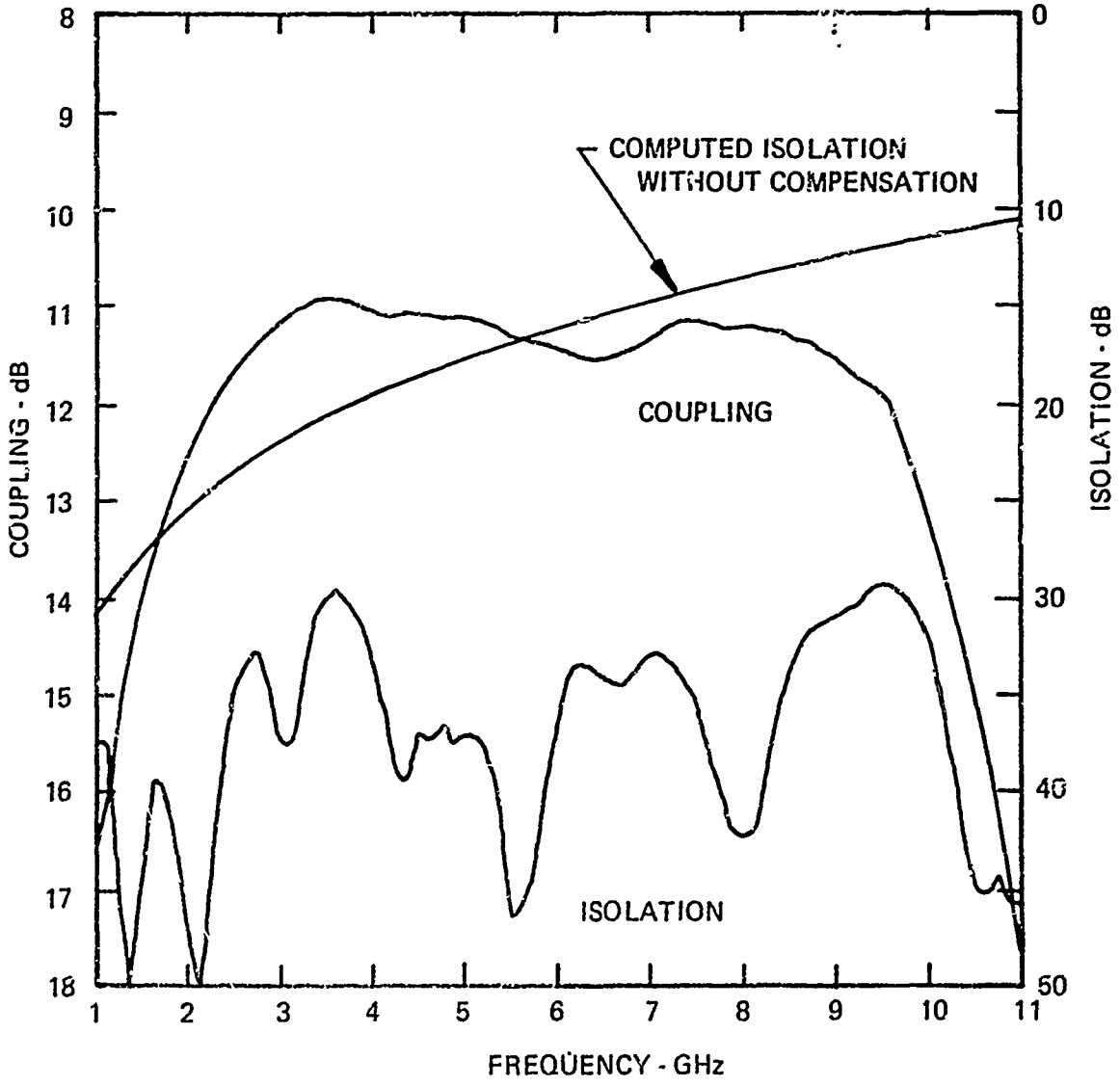

FIGURE 62 COUPLING AND ISOLATION RESPONSES OF 3-SECTION 10 dB COUPLER #20.

D-12110

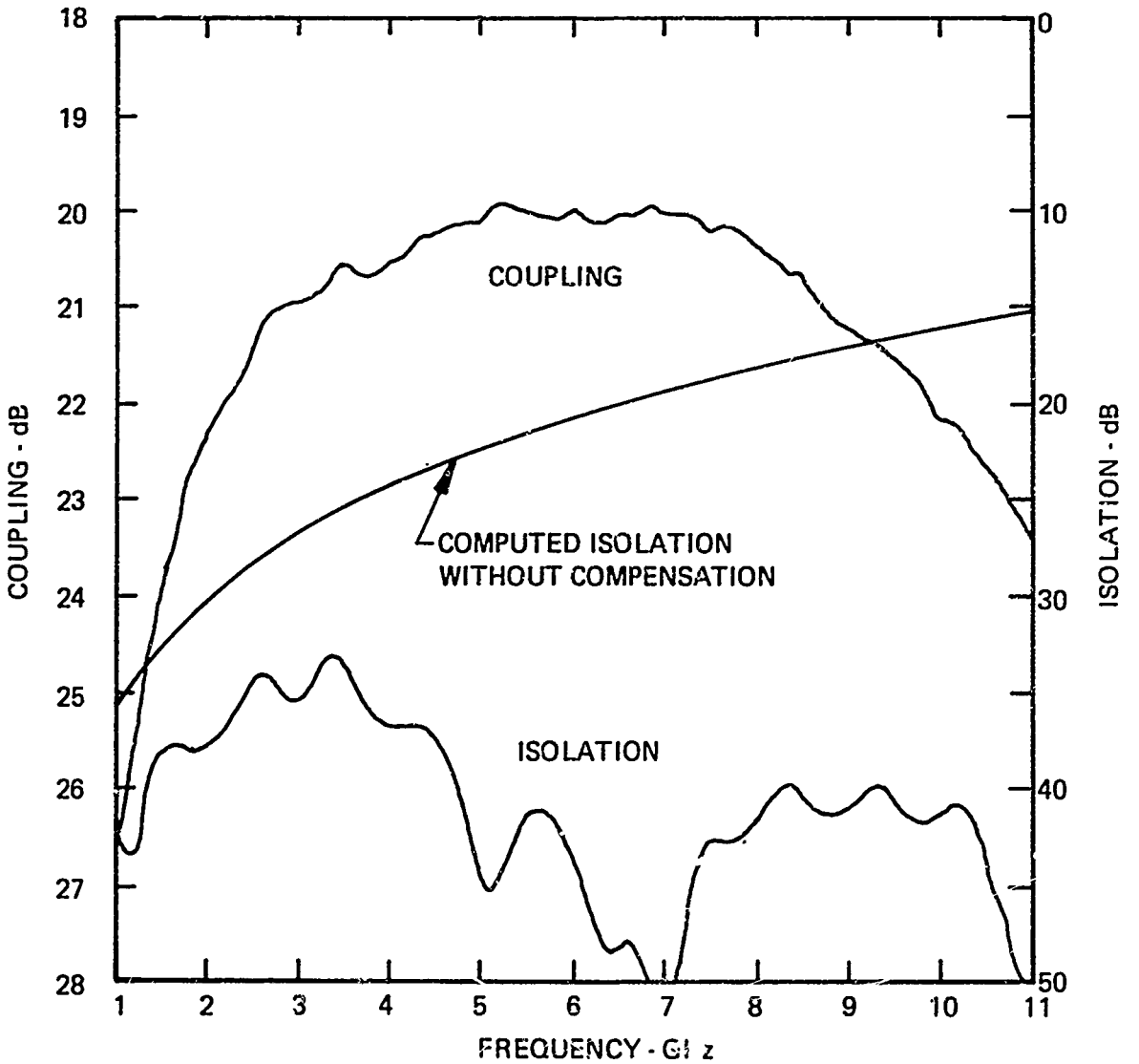

FIGURE 63 COUPLING AND ISOLATION RESPONSES OF 3-SECTION 20 dB COUPLER #21.

D-12111

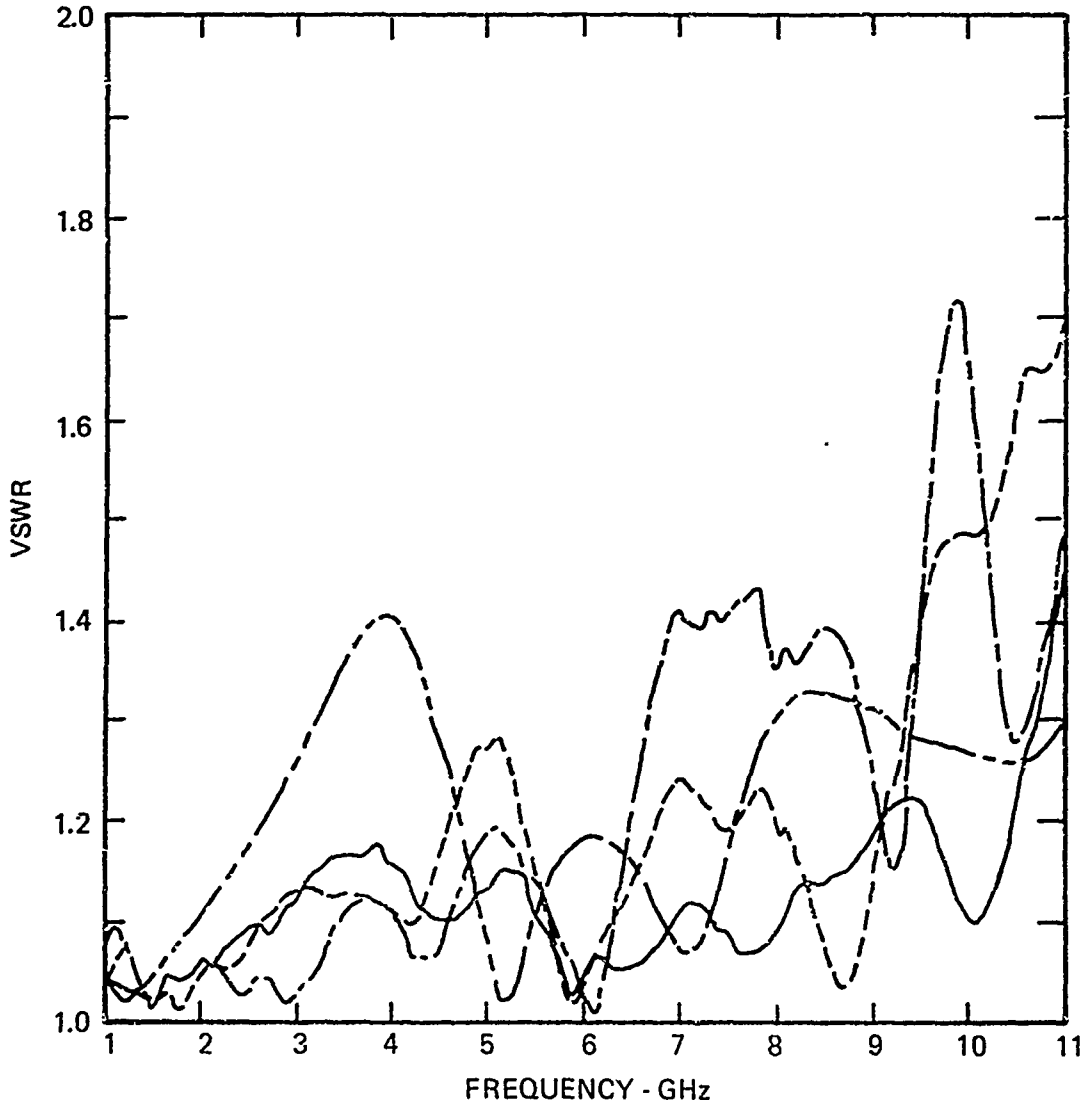

FIGURE 64 VSWR RESPONSES OF 3-SECTION 8.34, 10, AND 20 dB COUPLERS.

D-12112

The tuning procedure for these couplers entailed several tasks. First dielectric blocks were selected by trial and error to yield the flattest coupling response and highest average directivity possible. This combination was then checked on a time domain reflectometer to observe the general impedance levels of the couplers and to evaluate the mismatches, particularly at the intercoupler transitions. The transitions were then tuned up with indium foil for best TDR match. This cycle was then repeated until the best coupling and directivity responses were obtained, and then the blocks were glued in place.

We found that varying the lengths of the blocks and then positioning of the indium foil in the transitions could be used to control the coupler lengths and thereby adjust the coupling flatness. The size and position of the center coupler block seemed most critical with respect to directivity, while the end coupler blocks appeared to have a larger effect on flatness. Generally, the cement had to be kept out of the center coupler gap, as it would degrade the directivity obtained with the blocks simply resting in position.

In Figs. 61-63 note the substantial improvement in directivity from that theoretically expected for non-compensated couplers. It ranges from 5 dB at the low end of the 8.34 dB to over 25 dB near midband on the 20 dB coupler, counting just the peaks. Much of the residual directivity we attribute to small launcher and coupler mismatches and variations of $\pm$ 1 Ω in coupler impedance rather than velocity inequalities. Although the minimum directivities were not 20 dB across the entire potential bandwidths of the couplers, they were better than 18, 21 and 16 dB for the 8.34, 10 and 20 dB couplers, respectively, over the 4 to 8 GHz band. The directivity was better than 20 dB over substantial bandwidths on all couplers.

No attempt was made to tune for low VSWR; we aimed rather at high directivity. In general the VSWR $\lesssim$ 1.3 up to 9 GHz. Mismatches up to 1.45 on the 20 dB coupler suggests that some improvement in directivity is also possible here.

Note that the coupling bandwidths of the three couplers are somewhat narrower than the calculated curves. This is due to the finite length of the transition zones. Cf. Fig. 41 and discussion thereon, Section IV-A. Also, the coupling of the 10 dB coupler has a slight downward slope, because the end couplers are still a shade too short relative to the center.

The coupling and isolation responses are taken with respect to the input and output connectors and therefore include the connector and feed-line losses. By adding up the transmitted and reflected powers and subtracting from the incident power, we can estimate the dissipative losses. On the average we estimated that the dissipative losses varied from 0.5 dB to 0.9 dB from 3 to 9 GHz with $\sim$0.8 dB at 6 GHz. No attempt was made to apportion this loss among the connectors, feed lines, and couplers; the hermetic connectors tend to run from 0.1 to 0.5 dB per pair over the same band.

If we add about 0.8 dB to the coupling of these couplers to account for the loss, we see that they are indeed quite close to the design values, except that the 20 dB coupler lacks any ripple; it is not quite maximally falt. Before making a more detailed comparison of the results with the design data, consider the characteristics of the three couplers shown in Figs. 65, 66, and 67. These couplers were early models of the 8.34, 10 and 20 dB couplers designed in accordance with an earlier version of Figs. 29 and 30. All three couplers have very well-behaved

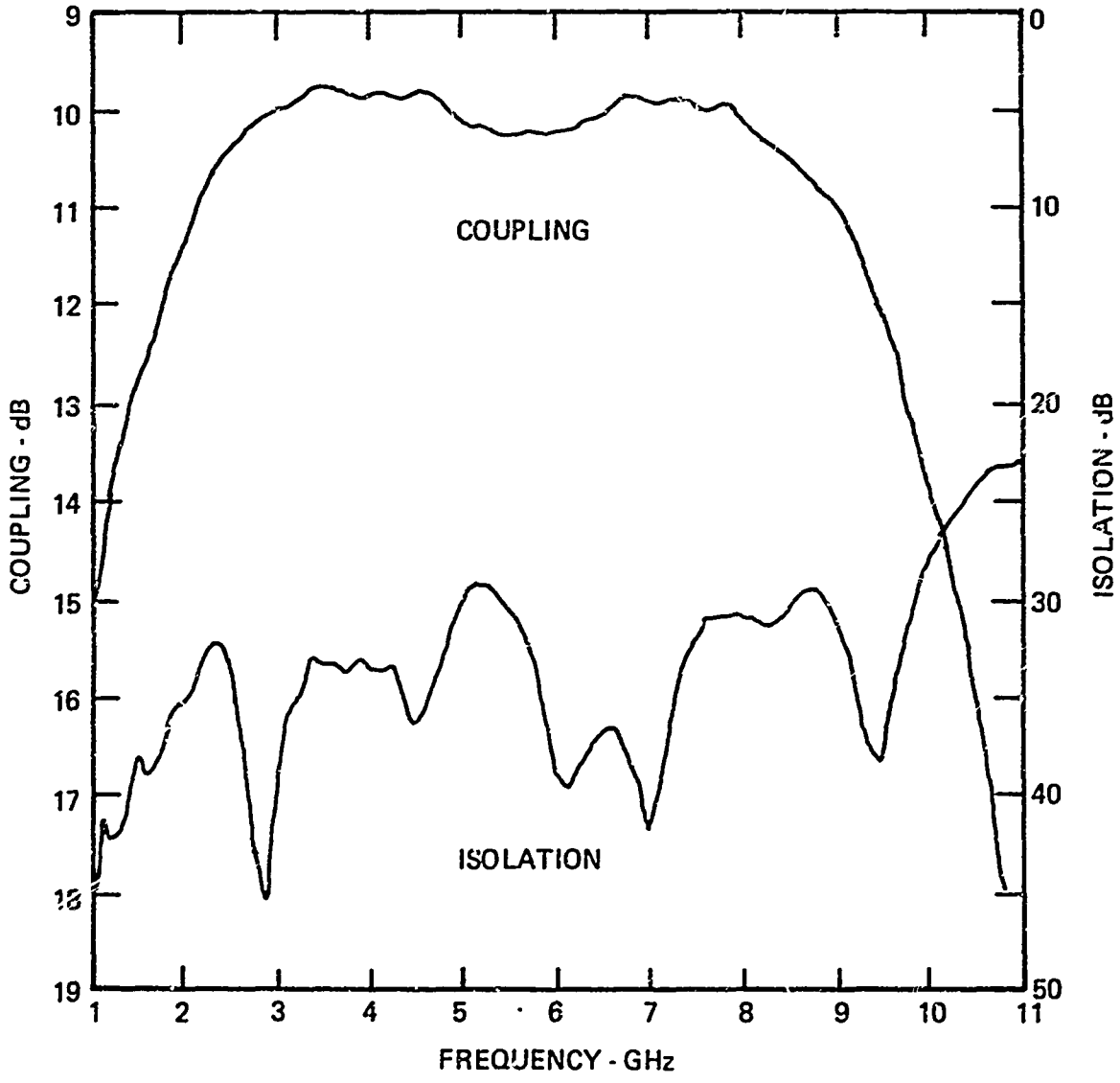

FIGURE 65 COUPLING & ISOLATION RESPONSES OF 3-SECTION 8.34 dB COUPLER #976.

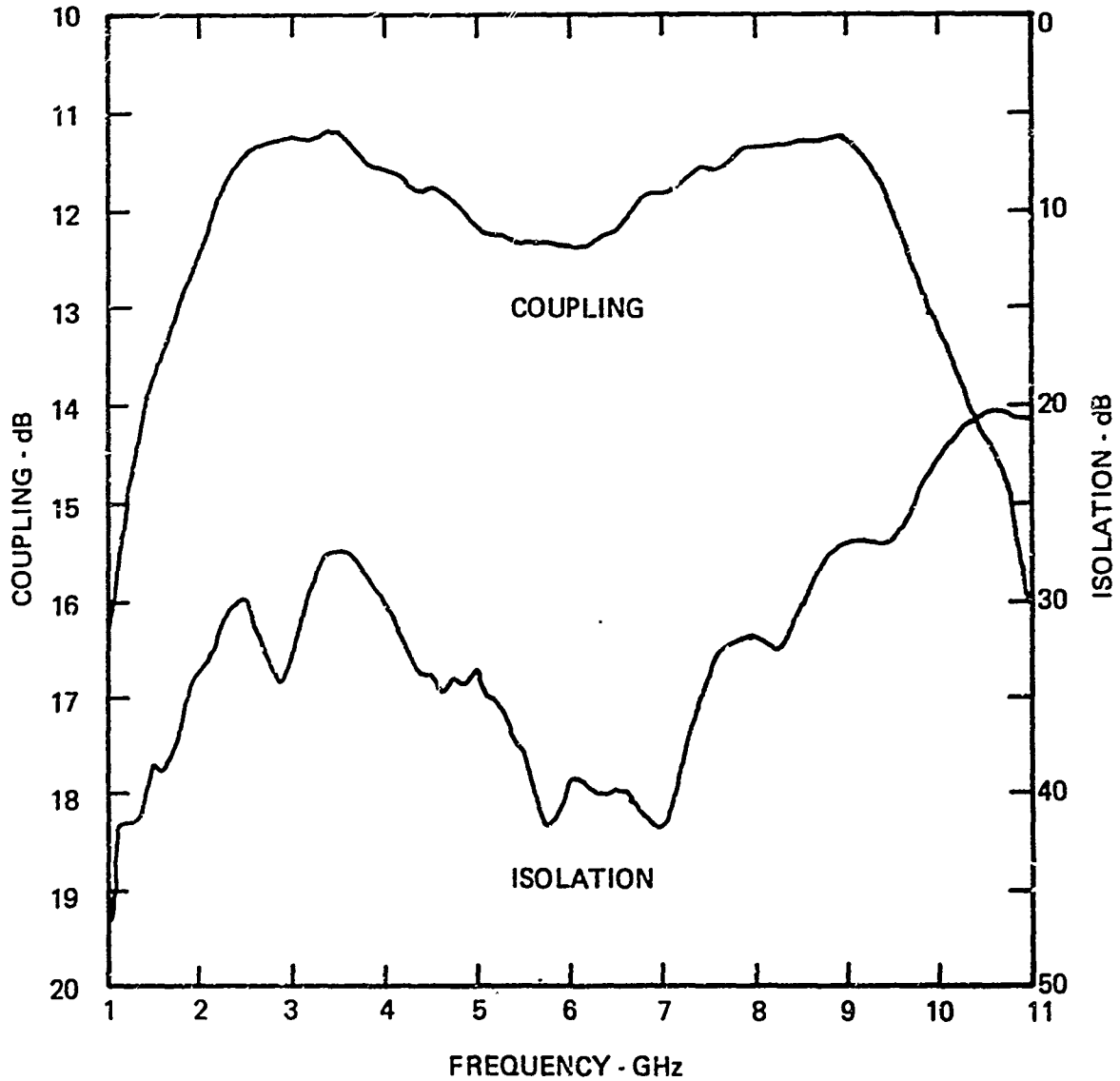

FIGURE 66 COUPLING & ISOLATION RESPONSES OF 3-SECTION 10 dB COUPLER #977.

D-12114

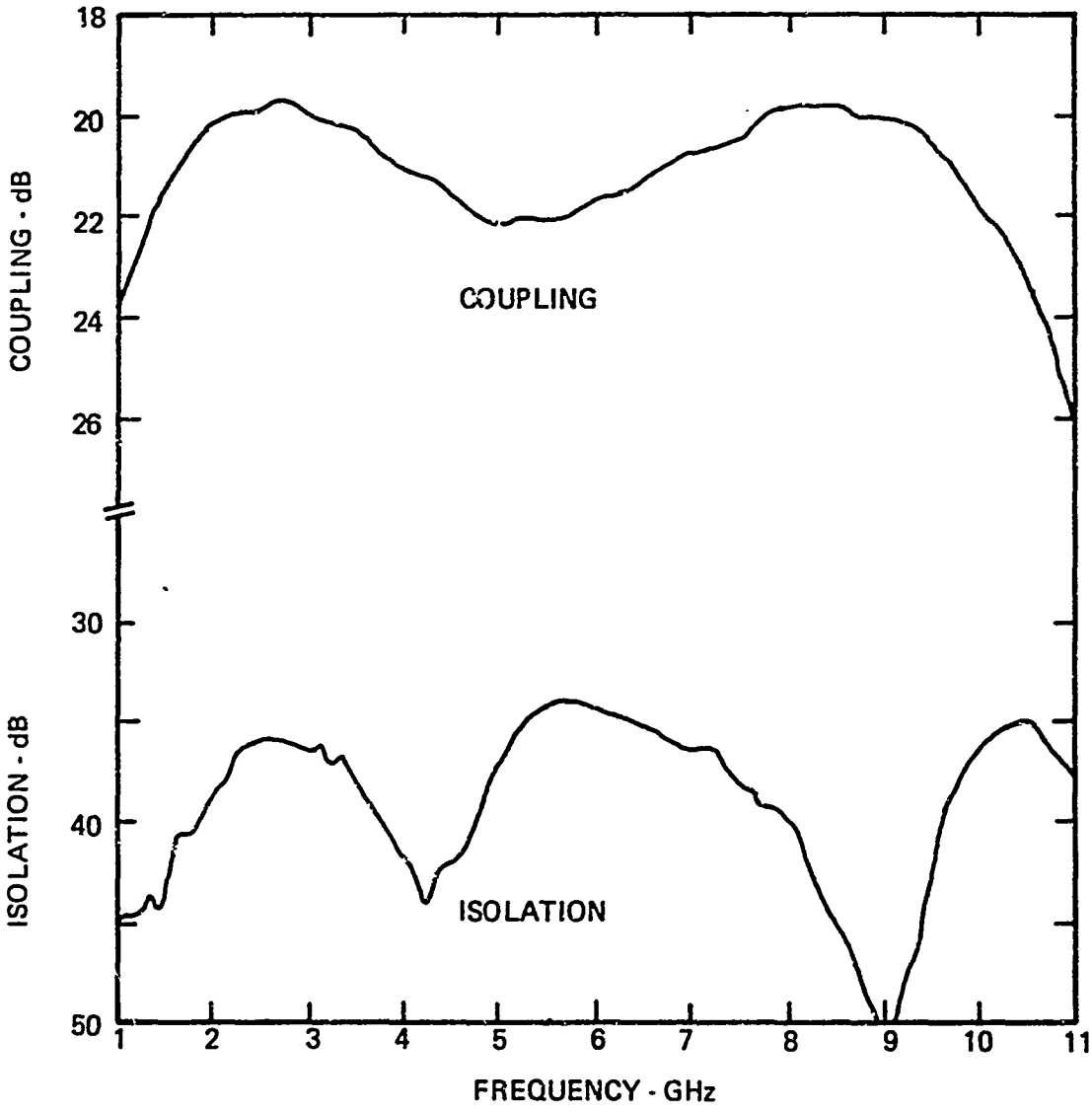

FIGURE 67 COUPLING & ISOLATION RESPONSE OF 3-SECTION 20 dB COUPLER #978.

coupling curves--in fact, the "8.34 dB" has exactly the curve we desired for the 10 dB, discounting losses--and the directivities are over 20 dB except for two small spots on the "8.34 dB" coupler. All three couplers, however, are too weakly coupled and have too much ripple. This is because the gap widths, which control the coupling, were incorrect. Nevertheless, the actual gap widths used imply certain "design" values for the couplers per Fig. 30. (The line widths used imply coupler impedances, estimated from Figs. 29 and 26, within a half-ohm of 50 ohm and can be safely ignored.) These coupling values, in turn, imply certain mean couplings and ripples, per Fig. 39, which may then be compared with experiment. Table I lists the "design" values of all the couplers in the seven 3-section units with their normalized gap widths. Under measured data it lists the dissipative losses at midband and the estimated mean coupling, and ripple corrected for loss by subtracting all of the loss from the mean coupling. Finally Fig. 39 was used to estimate the actual couplings of each coupler. In Fig. 68, a copy of the gap width design chart, these estimated coupling values are plotted against the actual normalized gap widths. The agreement is quite good except for very loosely coupled couplers, say less than 25 dB, which come out more lightly coupled than the curve predicts. Over the rest of the range, the couplings were within 6-7 %, in dB, of the design values, which is within the experimental accuracy.

TABLE I

DESIGN AND MEASURED COUPLINGS OF

3-SECTION SYMMETRICAL COUPLERS

	DESIGN					MEASURED				
Ckt. #	Cplg. & Ripple	Ctr. Cplg.	Cplr. s/h	End Cplg.	Cplr. s/h	Loss @ 6 GHz	Cplg. & Ripple	Ctr. Cplg.	End Cplg.	
17	8.34± .05	6.3	.112*	23.8	2.6	.73	8.1 ± .05	6.0	23.5	
19	8.34± .05	6.3	.112*	23.8	2.6	.87	8.3 ± .05	6.3	23.8	
20	10.0± .2	7.4	.19	23.5	2.55	.90	10.5 ± .3	7.5	23.0	
21	20.0 ± .2	17.2	1.40	33.8	4.9	.70	19.3± 0	17.5	37.5	
976	8.7± .15	6.4	.12	22.8	2.4	.8**	9.3 ± .2	6.6	22.6	
977	10.0±.5	6.9	.20	21.0	2.1	.8**	11.0±.6	7.9	21.8	
978	20.5± >1	16.6	1.30	26.4	3.2	.57	20.3 ± 1.2	16.3	29.0	

* ~ .118 as etched

** estimated; not measured

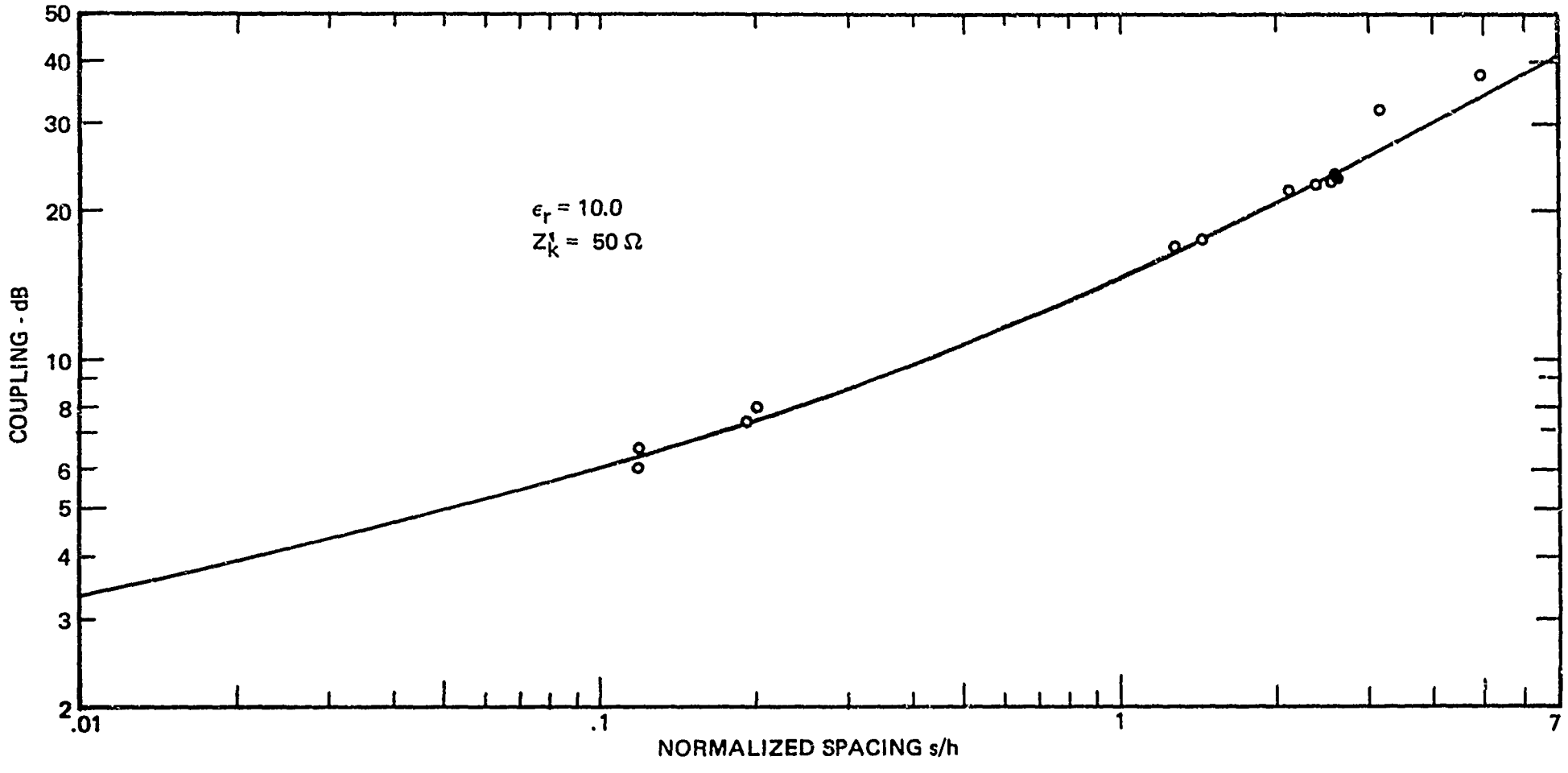

FIGURE 68 COMPARISON OF EXPERIMENTAL COUPLER RESULTS WITH OVERLAY COUPLER DESIGN CURVE.

D-12116

D. 3-dB Tandem Couplers

Figures 69 and 70 show a C-band tandem 8.34 dB quadrature 3 dB coupler with and without its dielectric overlays. Its transmission characteristics are given in Fig. 71 over the 1 -11 GHz band.

The difference between 3-dB and the straight line through the crossover points of the direct and coupled power curves represents the dissipative loss of the coupler, since the isolation and reflection contributions are negligible. (The VSWR $\lesssim$ 1.1 up to 7.5 GHz, has a peak of 1.4 at 8.8 GHz; between 9.5 and 11 GHz it climbs from 1.15 to 2). The dissipative loss of the tandem pair is comparable to that of a single section, in fact, within experimental error it is the same. The straight through path length on the tandem coupler is approximately 25% greater than that of the 8.34 dB, with its longer feed lines, and thus we should expect a proportionate increase in the loss. This suggests that the coupler losses are indeed modest compared to the connector losses.

From the transmission data in Figure 71, we estimate that the coupler is approximately 3.1 dB with 0.2 dB of ripple. Again this is within a few percent of the design target--with six couplers covered with dielectric!

The isolation is 25 dB up to 8.5 GHz, where it degrades slightly along with the increasing VSWR.

The phase quadrature property of the coupler is demonstrated in Fig. 72. The phase difference between the direct and coupled arms oscillates by less than 2^{o} about a line of constant slope, representing a differential line length of .026", in air, from 1 to 11 GHz.

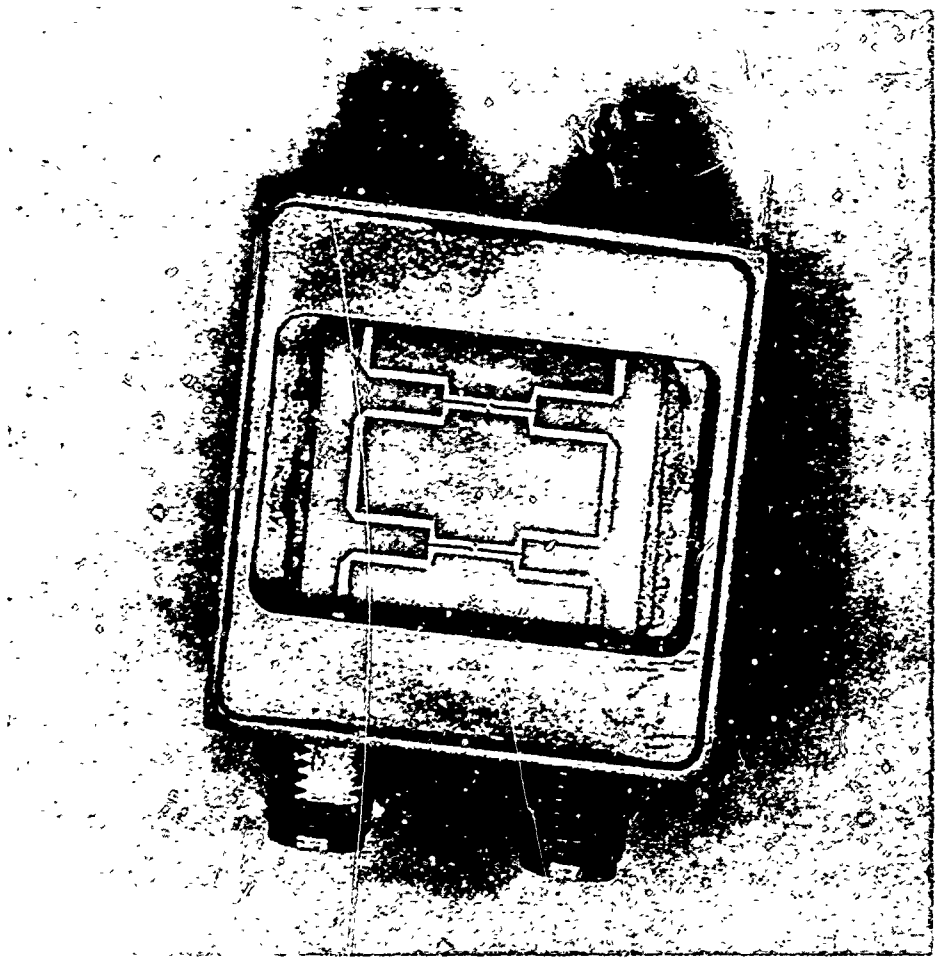

FIGURE 69 3 dB TANDEM 8.34 dB COUPLER AT 6 GHz WITHOUT DIELECTRIC

D-12131

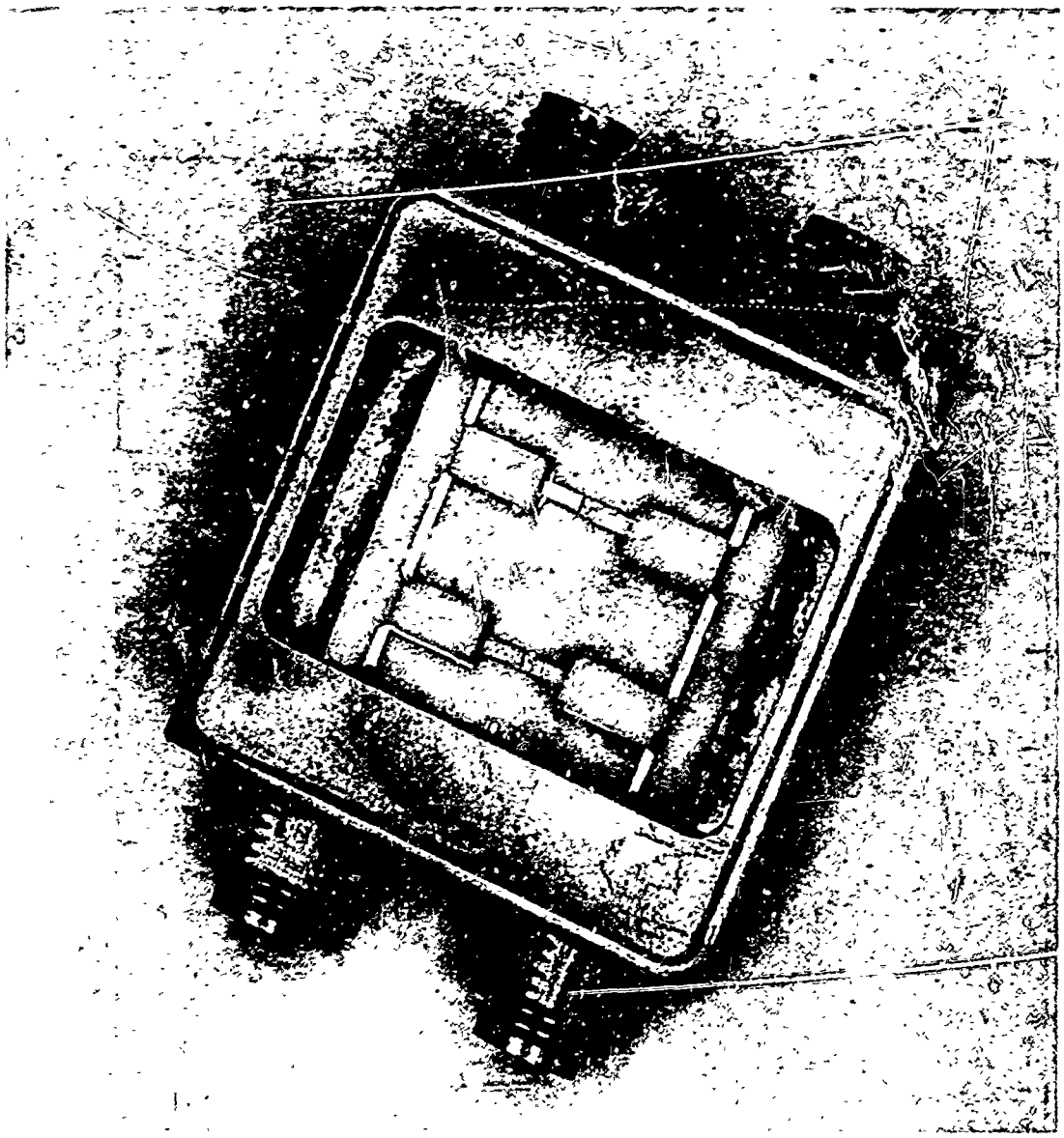

FIGURE 70 3 dB TANDEM 8.34 dB COUPLER AT 6 GHz WITH DIELECTRIC OVERLAYS IN PLACE.

D-12132

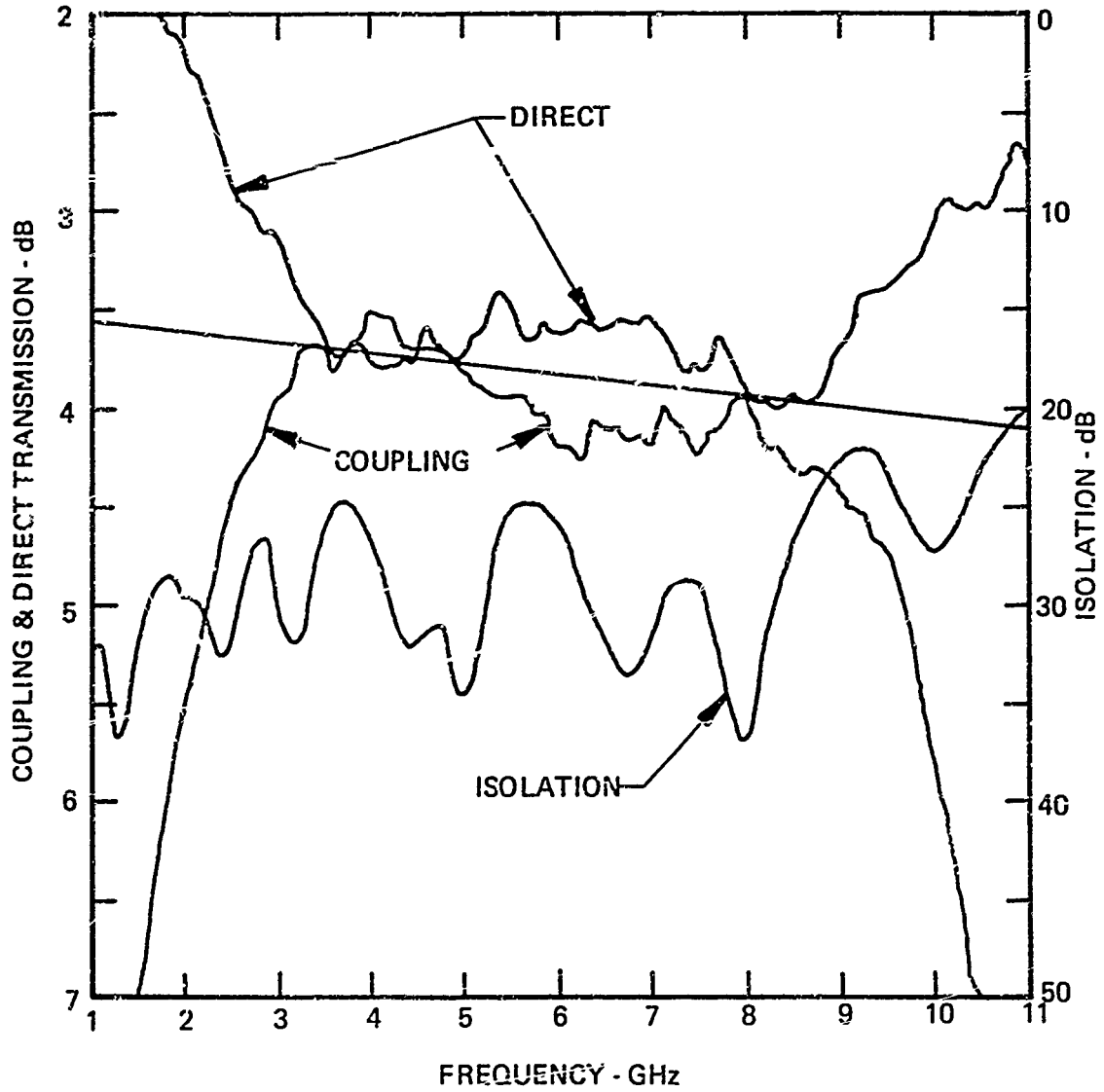

FIGURE 71 TRANSMISSION RESPONSES OF 3-dB, TANDEM 8.34 COUPLER, CENTERED AT 6 GHz, CKT #18.

D-12117

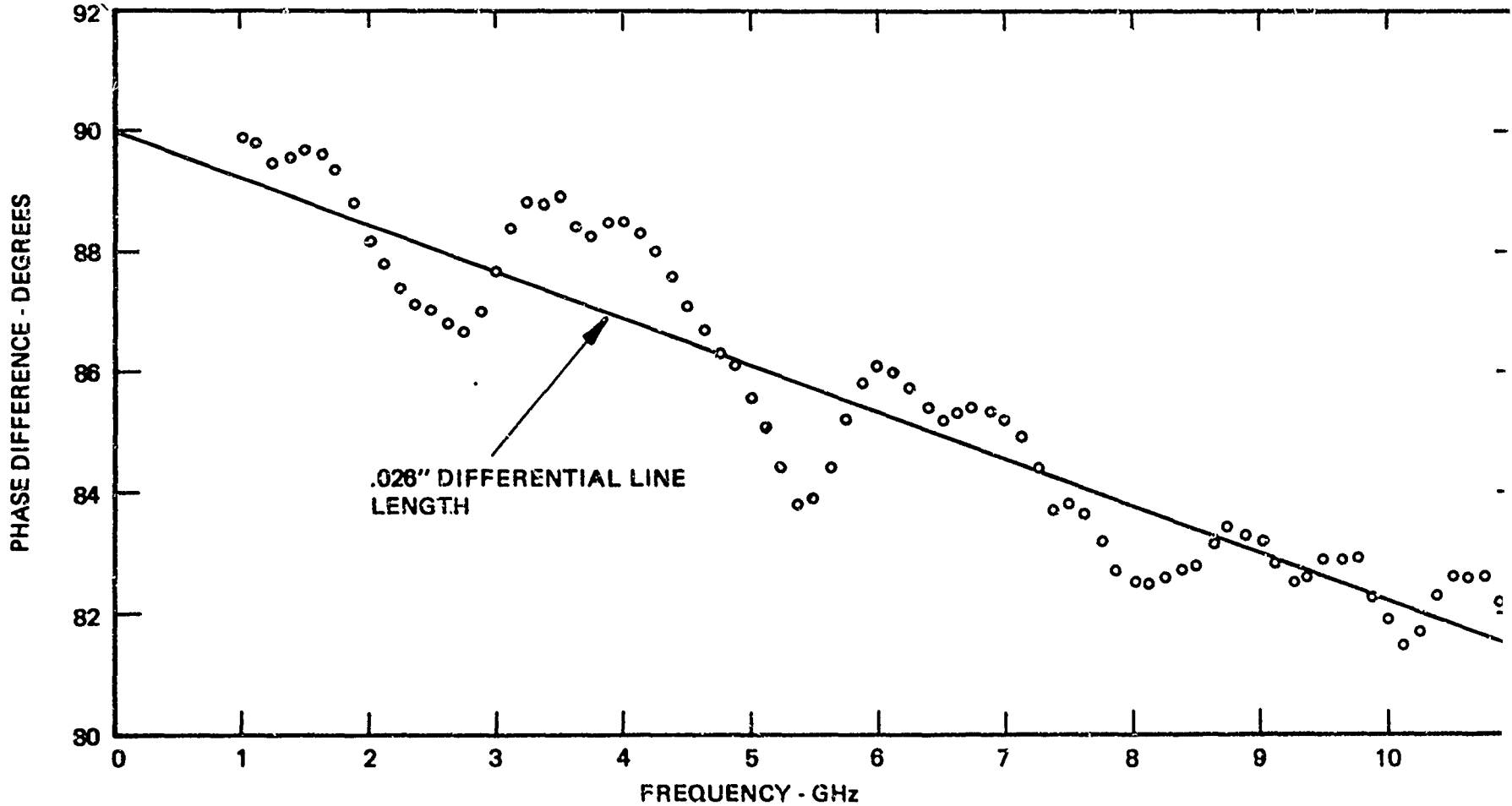

FIGURE 72 TRANSMISSION PHASE DIFFERENCE BETWEEN DIRECT AND COUPLED ARMS OF TANDEM 8.3 dB COUPLER, #18

Finally Figs. 73 and 74 give the transmission characteristics of couplers centered at 4.5 and 3.0 GHz. These couplers are exactly the same design as circuit #18 except the lengths of the coupled regions are 1.33 and 2.0 times as long, respectively. The dissipative losses of the couplers are greater for the lower frequency couplers, which we should expect since transmission line loss per wavelength increasing as the square root of wavelength. The directivity performance of these couplers is not quite as good as on the C-band unit. However the same amount of care was not taken to optimize the performance, and this represents what can be expected with relatively little tuning effort.

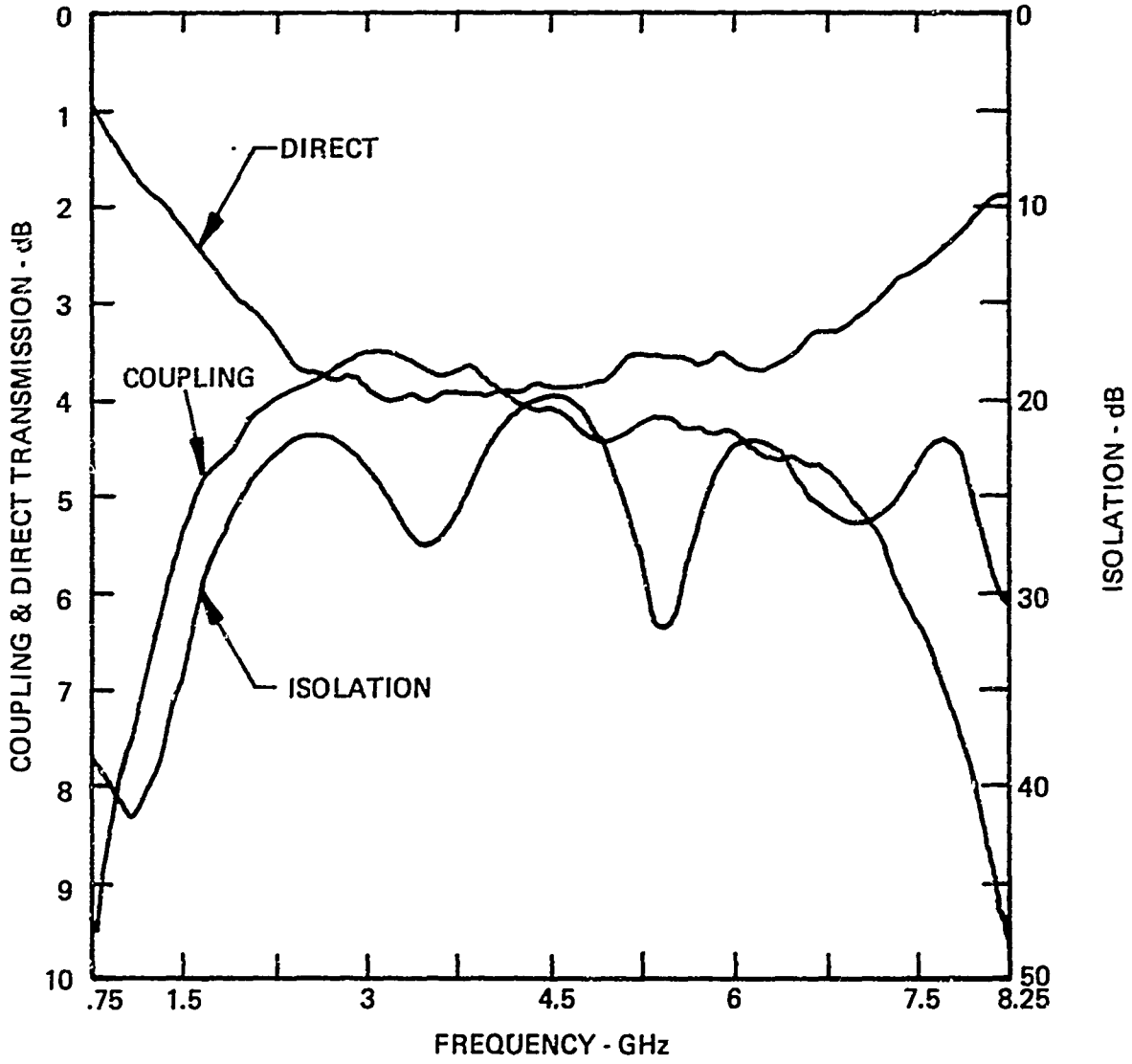

FIGURE 73 TRANSMISSION RESPONSES OF 3 dB TANDEM 8.34 dB COUPLER CENTERED AT 4.5 GHz, CKT #23.

D-12119

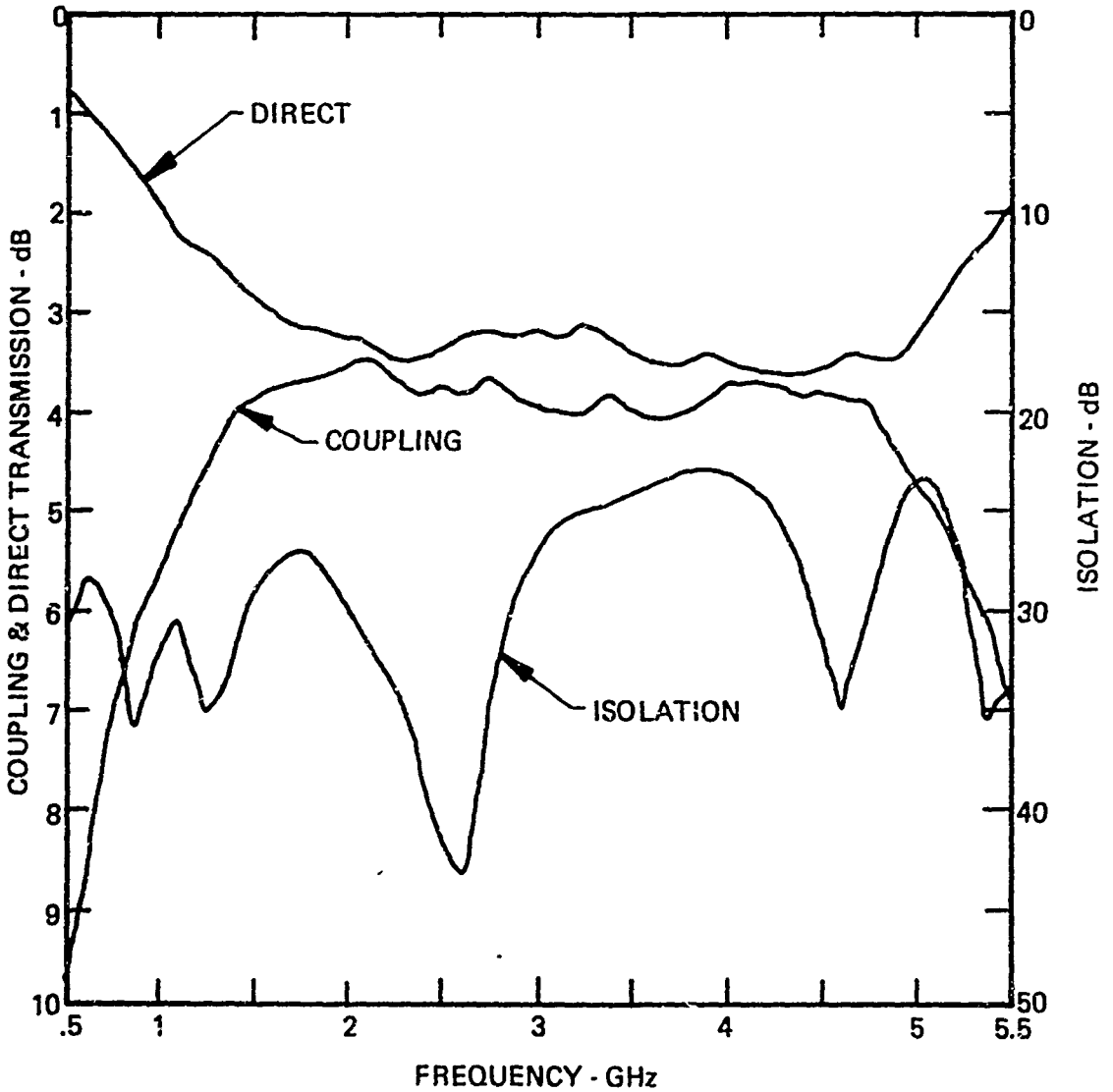

FIGURE 74 TRANSMISSION RESPONSES OF 3-dB TANDEM 8.34 dB COUPLER CENTERED AT 3 GHz, CKT. #22.

D-12120

E. Interdigitated Couplers

A 3-section 3-dB, .05 dB ripple coupler requires 1.75 dB center and 17.2 dB end sections. It appeared that it should be possible to make an interdigitated 1.75 dB coupler on a .050" substrate. Since little design data is available, we had to guess at the line dimensions based on our experience with 3-dB couplers and on Lange's figures for a 1.47 dB coupler.

We made a single center section and a 3-section coupler in which ends were designed to be 17.2 dB without an overlay. The "reversed" Lange geometry, Fig. 44(a) was used. The lines were .003" wide (w/h = .06) and the gaps .0014" (s/h = .028).

The single section came out 2.2 dB at 57Ω, with 0.5 dB of loss at mid band. The lines would have to be wider, the gaps narrower to bring it in, but it looks reasonable. However, the isolation of the single section was only 16 dB at mid band--a less than could be attributed to the 57 Ωimpedance. The approach did not appear too promising.

The 3-section coupler, however, had better than 20 dB of isolation up to 8 GHz. The overall coupling was approximately 3.5 dB with little or no ripple. Since the center was low in coupling and high in impedance, and since dielectric overlays were working so well on conventional couplers, it was logical to try this technique on the interdigital structure.

The transmission characteristics of the overlay--interdigital coupler are shown in Fig. 75. It is a nominal 3.2 dB coupler, centered at 6.5 GHz; it is almost flat, with a slight positive coupling slope. The directivity is >23 dB up to 7.5 GHz and about 16 dB above that. There was no dielectric on the end couplers.

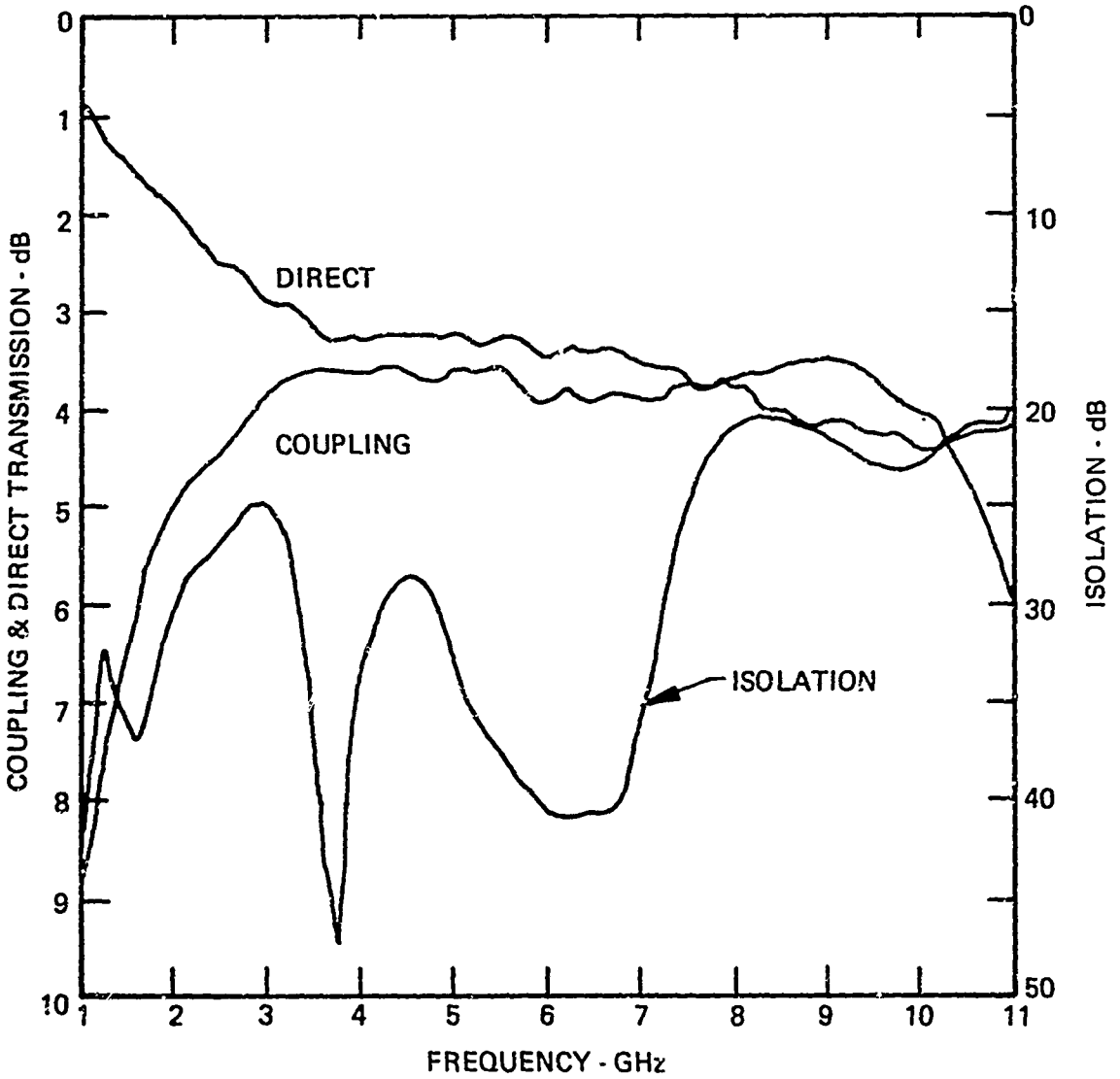

FIGURE 75 TRANSMISSION RESPONSE OF 3-SECTION 3-dB COUPLER WITH INTERDIGITATED CENTER SECTION. DIELECTRIC OVERLAY ON CENTER SECTION.

D-12121

We did not pursue the interdigitated coupler, but it is obvious that it could be made to perform as well as the tandem 8.34 dB units. Its disadvantages are that it needs a thicker substrate than we normally like to use above L-band, and the design, right now, is strictly empirical.

F. Sawtooth Couplers

In the early part of the program we experimented with sawtooth, or wiggly-line, couplers as proposed by Podell[8], as a convenient means of velocity compensation. The technique is very appealing since coupler fabrication is simple and they should not require tuning adjustments once the design is fixed.

We made 3-section 10 and 20 dB, couplers, in C-band, using various prescriptions to fix the angles, depths, and numbers of teeth in the gaps. Our results can be summarized by reference to the data for 10-dB couplers with varying sawtooth angles shown in Figure 76. The tooth angles in the center, 7.4 dB, coupler were 30^{o}, 35^{o}, and 40^{o}, corresponding to corrections for velocity ratios of 1.16, 1.22 and 1.30. These corrections are considerably larger than the expected ratio of 1.11, but smaller angles did not work, and we were attempting to allow for the possibility that the odd mode wave does not follow the center of the gap, but "cuts the corners" somewhat. The angles in the end couplers was 30^{o} in all cases. Here the gaps are so wide that the teeth do not reach the centerline, so the effective length of the gap is impossible to estimate.

The coupling responses of all the couplers has a very pronounced high-frequency roll-off. These couplers were designed before we recognized the effects of the relative coupler lengths and the transitions on the coupling characteristics, and the transition lengths were included as part of the end couplers.

Comparing the isolation responses with the computed, uncompensated, curve from Fig. 54, we see that the sawteeth have effected little, if any, improvement. Similarly, the measured isolation for the 20 dB couplers fall right on the calculated curve.

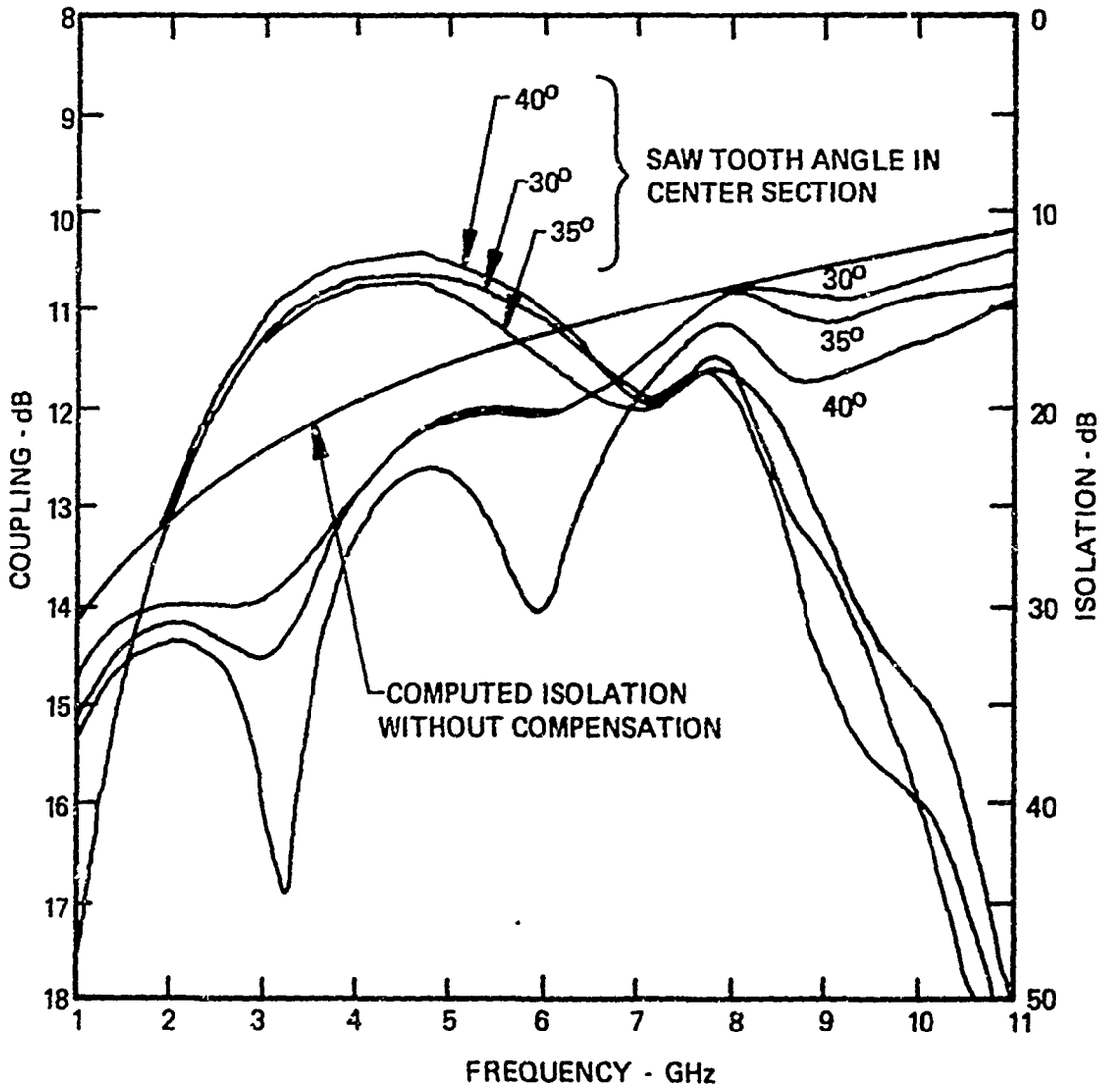

FIGURE 76 COUPLING & ISOLATION RESPONSES OF 3-SECTION 10 dB WIGGLY-LINE COUPLER.

D-12122

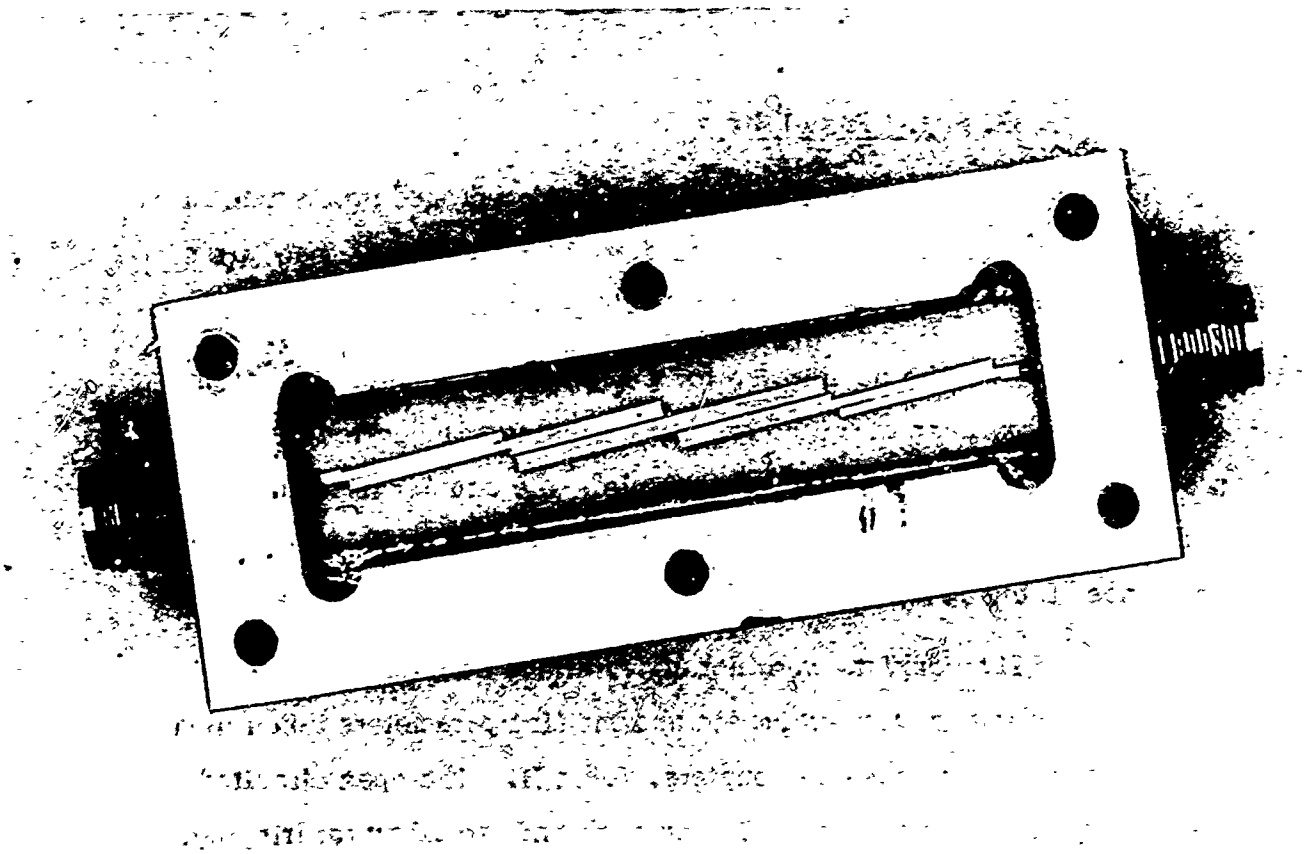

FIGURE 77 COUPLED-LINE, HALF-WAVE RESONATOR BAND PASS FILTER.

D-12133

We concluded, reluctantly, that the sawtooth velocity compensation technique does not work at C-band, and turned our attention to the dielectric overlay method.

G. Band Pass Filters

In order to exercise the design procedure on a different configuration, we applied it to the design of a half-octave, band pass filter, such as might be used in a multiplexer application.

The design was for a 4-coupler, coupled-line filter with half-wave, open circuited resonators; using a 3-section low-pass prototype* for an 0.2 dB Chebyshev ripple. The coupler impedances and coupling were determined from the equations given by Matthaei, Young, and Jones (Table 10.02-1, p 590).[29]

The couplers were not 50 Ω, so the coupler parameters without the overlays were estimated and the line parameters taken from the charts for uncompensated couplers, Table II. The open circuited resonators were shortened by .010" on each end to allow for fringing. Two filters were made, one centered at 3 GHz, one at 6 GHz, the only difference was in the coupler lengths. The S-band unit is shown, without dielectrics, in Fig. 77.

The transmission responses for three cases were computed and are plotted in Fig. 78. The dotted line shows the attenuation of the ideal filter; the solid line shows the case when the velocities are unequal (ratios of 1.12 and 1.14 in the ends and center, repectively), but the couplings and impedances have their design values. The dashed curve corresponds to the filter designed for overlays but with the dielectrics removed. The effect of the incorrect couplers is simply to

---

* A 3-section prototype has three $\lambda/2$ resonators, but four couplers.

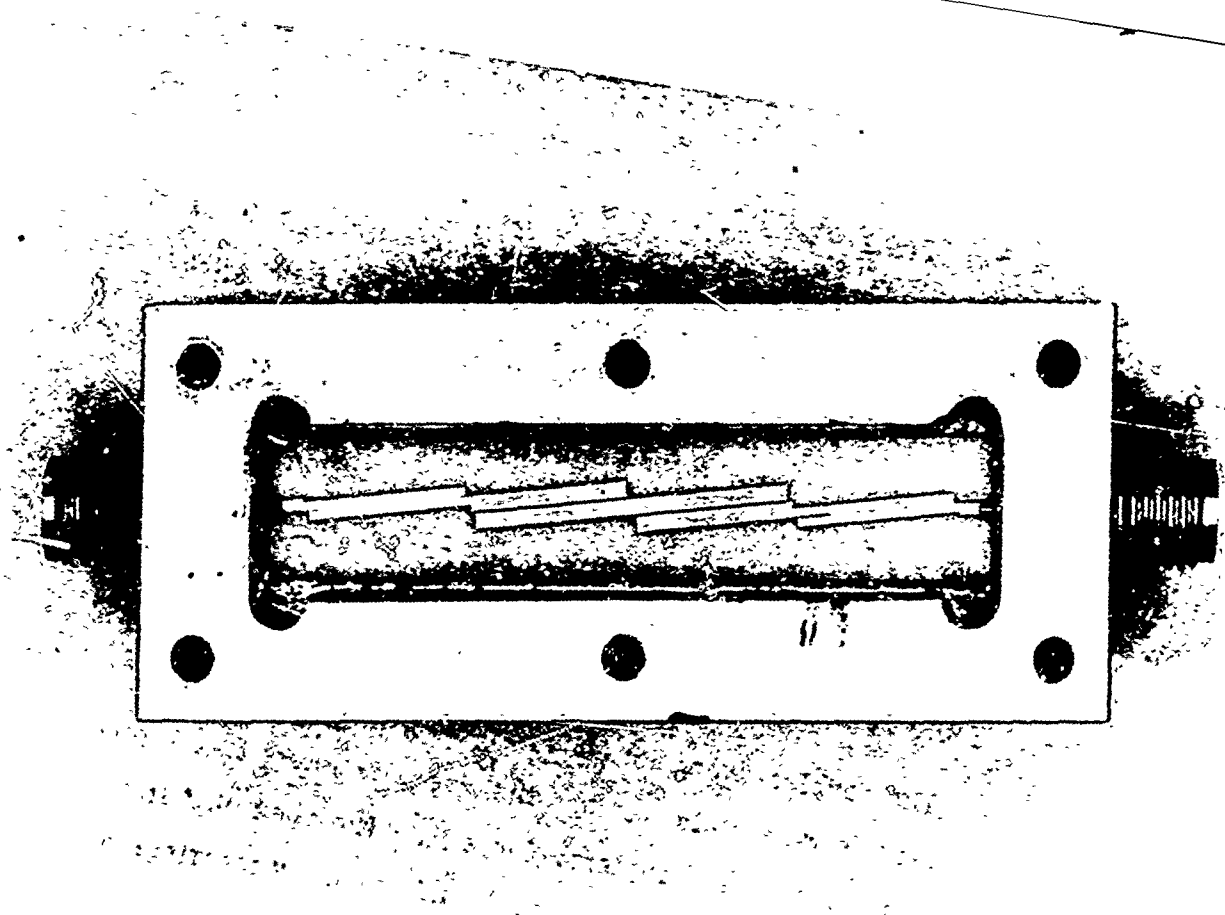

FIGURE 77 COUPLED-LINE, HALF-WAVE RESONATOR BAND PASS FILTER.

D-12133

TABLE II

FOUR-COUPLER BAND PASS FILTER PARAMETERS

33.3% Bandwidth

0.2 dB Ripple

Couplers	Design		Without Dielectric				On .025" Substrate			Length @	
	k_p	Z_k	k_p	Z_k	w/h	s/h	w	s	ϵ_{eff}	3 GHz	6 GHz
1,4 Ends	5.17	41.7	5.77	44.1	.76	.038	.019"	.0095"	7.0	.372"	.186"
2,3 Ctr.	7.73	34.8	8.90	37.3	1.33	.124	.033"	.0031"	7.5	.358"	.179"

narrow the bandwidth by a few percent. The effect of the velocity inequality, however, is to degrade the band rejection on the high frequency side to about 25 dB. The pass band ripple is almost the same in all three cases. (The upward velocity shift of the unequal velocity curves is due to the choice of $\theta_e = 90^o$, rather than $(\theta_e + \theta_o)/2 = 90^o$ in the calculations.)

Figures 79 and 80 show the measured transmission characteristics of the C- and S-band filters. The bandpass insertion losses are approximately 1.3 and 0.8 dB; these are primarily dissipative losses since the peak VSWRs are less approximately 1.5 within the bands, except for the high end of the S-band filter, where it is 2.1. The peak rejection on the high side of the uncompensated coupler is $\sim$24 dB, which is close to the calculated 26 dB. The addition of the dielectrics improved the rejection by about 5 dB; however, here again, we did not take painstaking care to optimize the performance. More work is clearly called for in the area of velocity compensating coupled-line filters.

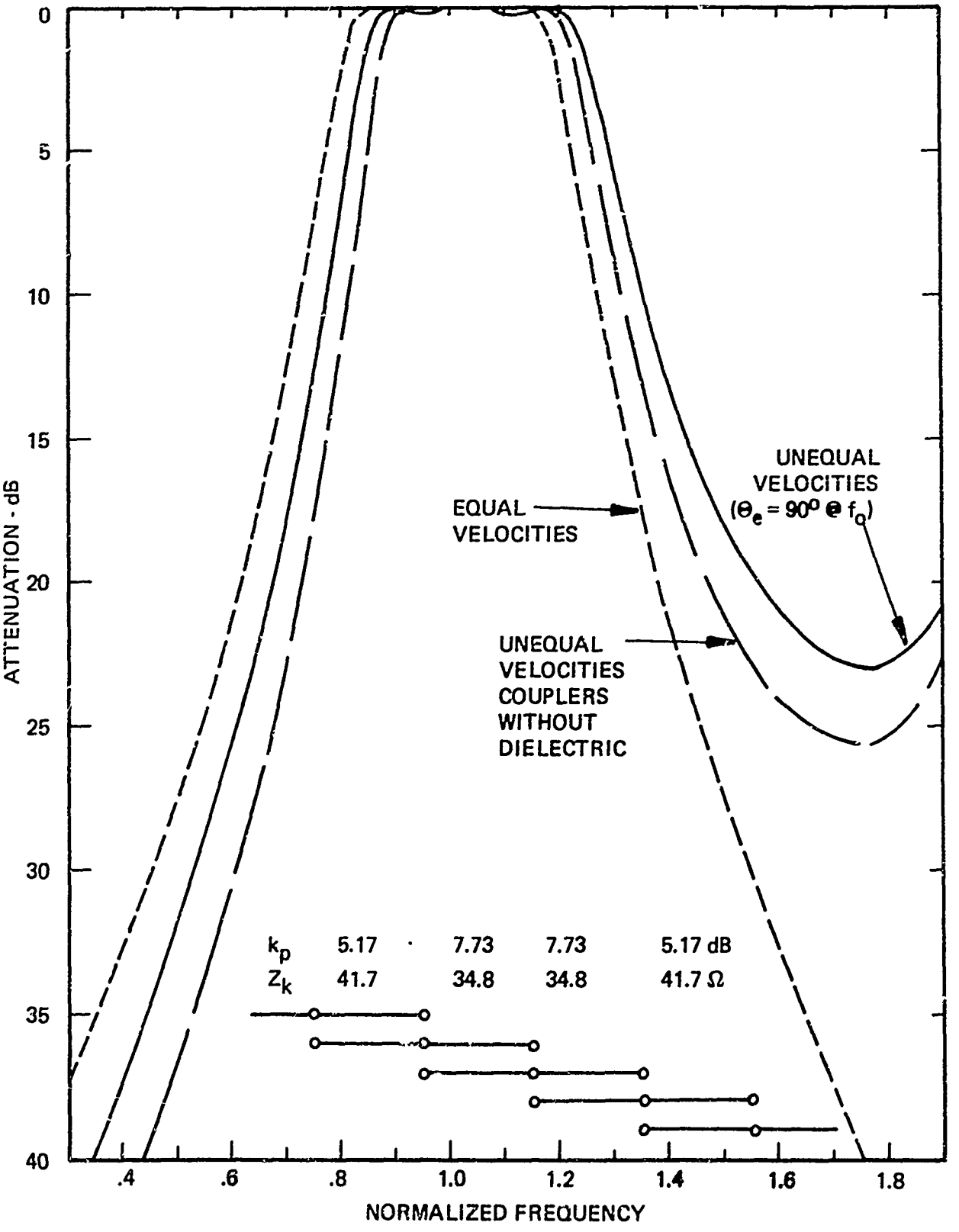

FIGURE 78 COMPUTED RESPONSE OF4-COUPLER, HALF OCTAVE, 0.2 dB RIPPLE BAND PASS FILTER.

D-12123

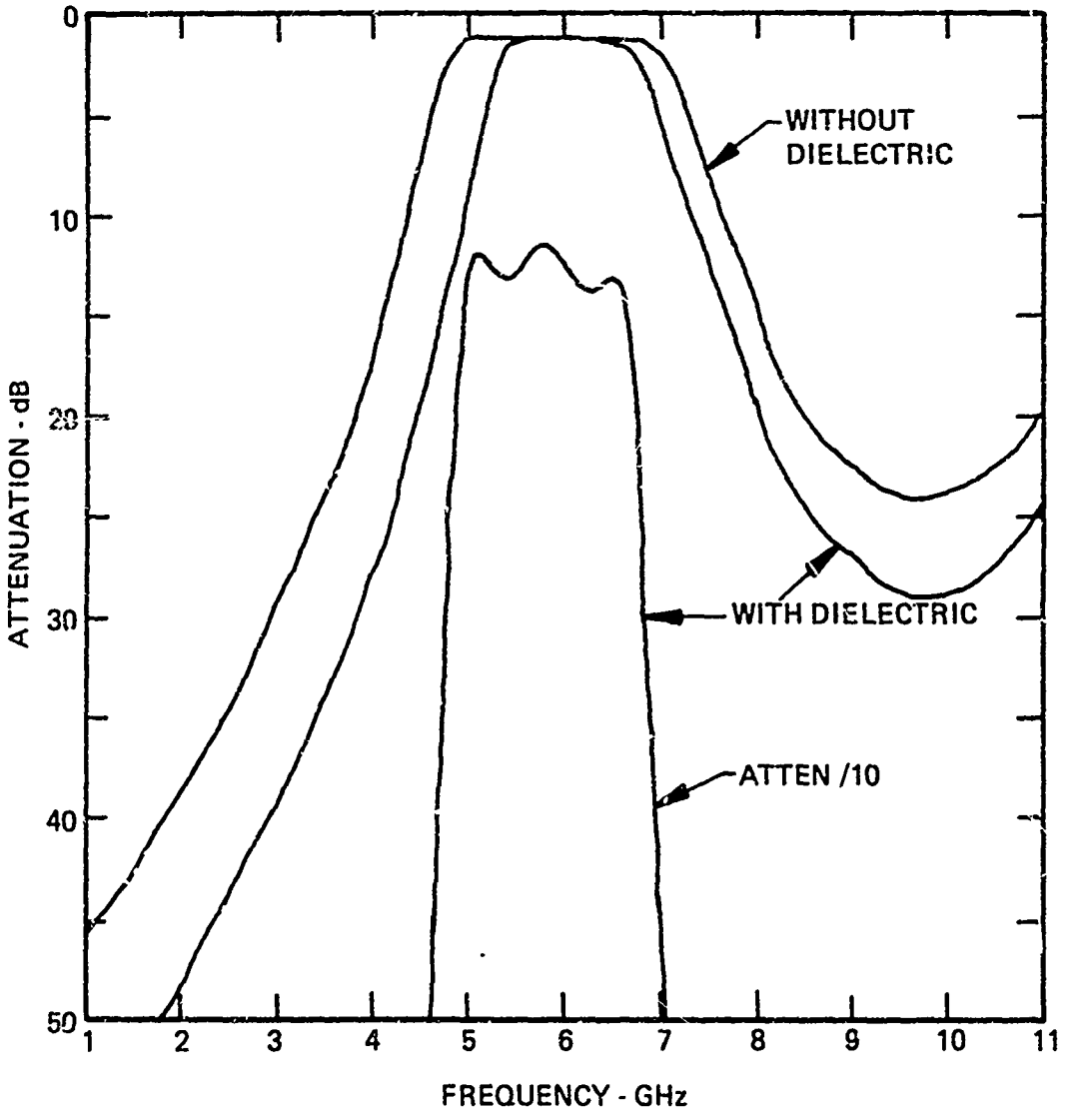

FIGURE 79 TRANSMISSION RESPONSE OF C-BAND BAND PASS FILTER WITH AND WITHOUT DIELECTRIC OVERLAY.

D-12124

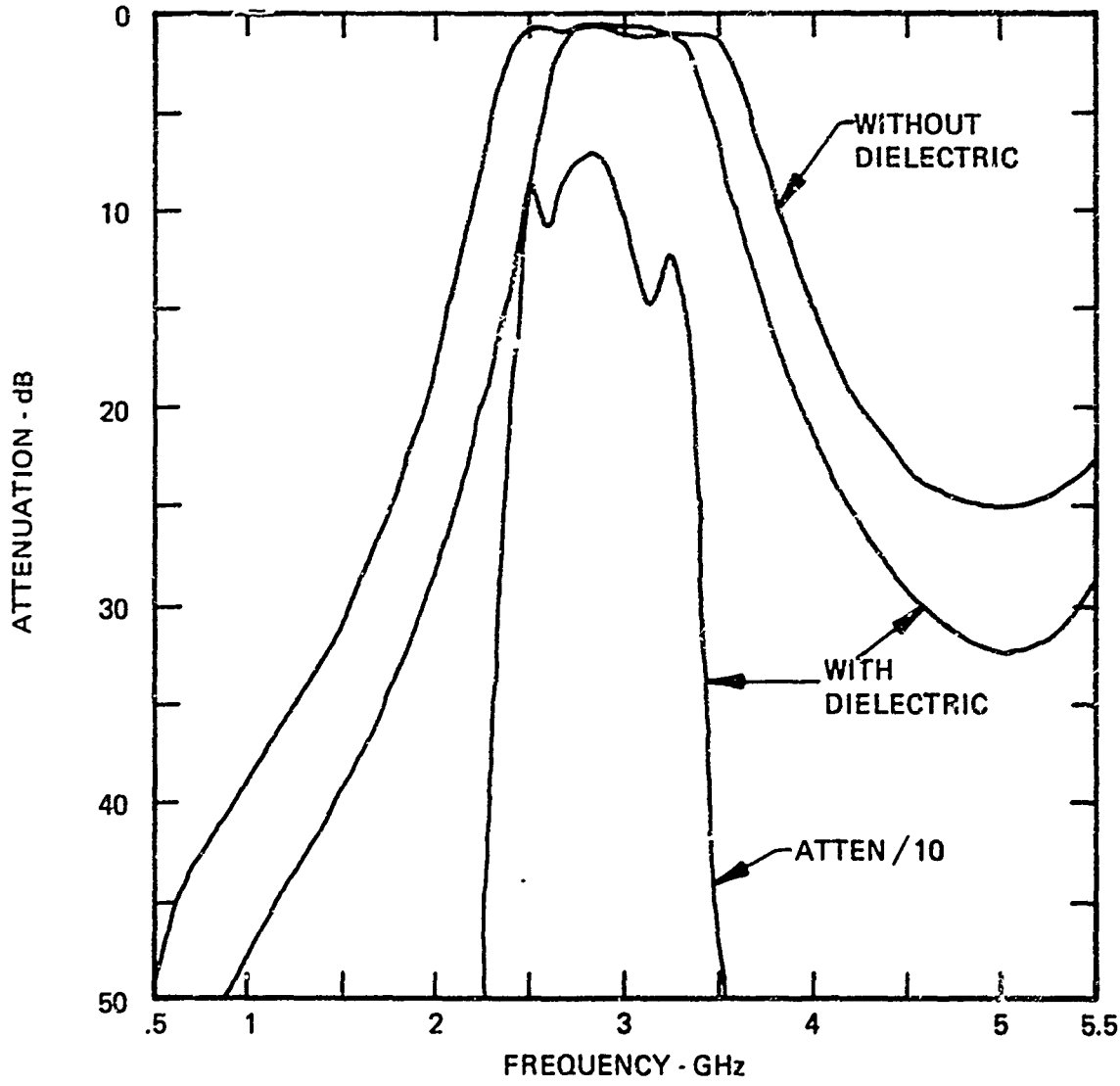

FIGURE 80 TRANSMISSION RESPONSE OF S-BAND BAND PASS FILTER WITH AND WITHOUT DIELECTRIC OVERLAY.

D-12125

VI. CONCLUSIONS AND RECOMMENDATIONS

Our principal conclusion drawn from this work is that the dielectric overlay technique described is an excellent method for making high-directivity directional couplers in conventional microstrip. As a corrollary, the design curves derived permit the semi-empirical design of compensated single-section couplers from 5 to 25 dB, generally within 5% in coupling.

We have also concluded that the sawtooth scheme of velocity compensation does not work at frequencies as high as C-band.

Finally, although we obtained only a modest improvement in coupled-line filter performance with dielectric overlays, we believe that significant improvement is possible with a commensurate improvement in tuning technique.

There are many areas in which we would recommend further study and experimentation. We shall just highlight a few here.

Foremost is the matter of loss. Our entire design treatment here has been for the lossless coupler. But the experimental couplers were indeed lossy--the high connector losses not withstanding--and it would be nice to be able to predict the dissipative losses reliably. A number of theoretical works are extant, but nothing of a simple-to-use, practical nature has appeared.

Another area is that of coupled line filters. When are they practical? For instance, we found that a half-octave, 4-coupler band-pass filter was, but a half-octave band stop and a full-octave band pass filters required impractically close coupling. Also, design procedures

exploiting unequal line widths should be developed. This may extend the practical range appreciably.

Third, Bryant and Weiss' program should be expanded and coupler parameters generated for the unequal strip and the interdigitated coupler cases.

Finally, the empirical part of our design procedure set forth here should be removed, and set on sounder theoretical footing. The size and placement of the overlay, and its quantitative effect on the effective dielectric constant and coupler impedance should be determined analytically.

APPENDIX A

DERIVATION OF THE SYMMETRICAL COUPLER SCATTERING MATRIX

The response of a coupled-line coupler terminated in resistive loads Z_o and excited at one port, as diagrammed in Fig. A-1 (a), may be obtained from the superposition of the responses to even and odd mode excitations shown in Fig. A-1(b) and (c)

Under even mode excitation, no current crosses the plane of symmetry, so that the following relations hold

$$V_{2e} = V_{1e} \qquad I_{2e} = I_{1e}$$
$$V_{3e} = V_{4e} \qquad I_{3e} = I_{4e}, \tag{A-1}$$

and the even mode response may be determined from two-port equivalent circuit in Fig. A-2(a). Similarly,under odd mode excitation, the voltage on the plane of symmetry is zero, so that we have

$$V_{2o} = -V_{1o} \qquad I_{2o} = -I_{1o}$$
$$V_{3o} = -V_{4o} \qquad I_{3o} = -I_{4o}, \tag{A-2}$$

and the response is determined by the two-port equivalent circuit in Fig. A-2 (b).

The input impedance, normalized to Z_o, of each of these circuits is

$$\mathcal{Z}_{1x} = \frac{Z_{1x}}{Z_o} = \mathcal{Z}_x \left[\frac{1 + j\mathcal{Z}_x \tan\theta}{\mathcal{Z}_x + j \tan\theta} \right], \tag{A-3}$$

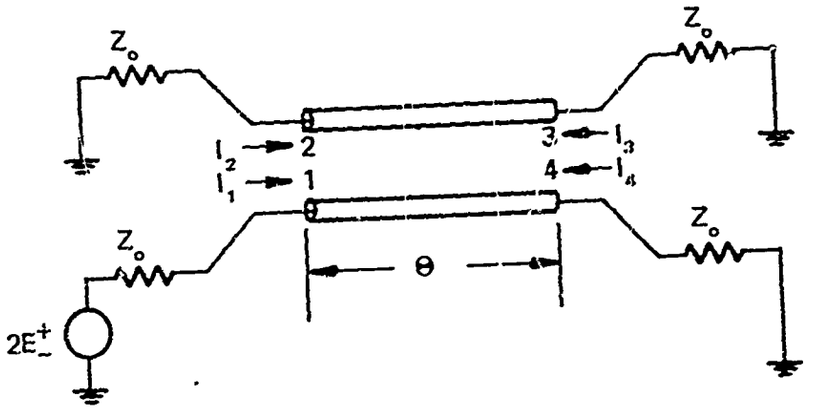

FIGURE A-1 COUPLED STRIP DIRECTIONAL COUPLER EQUIVALENT CIRCUIT

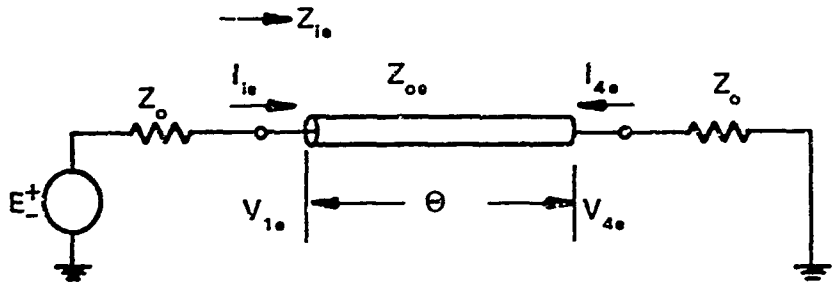

a) EVEN MODE EQUIVALENT CIRCUIT

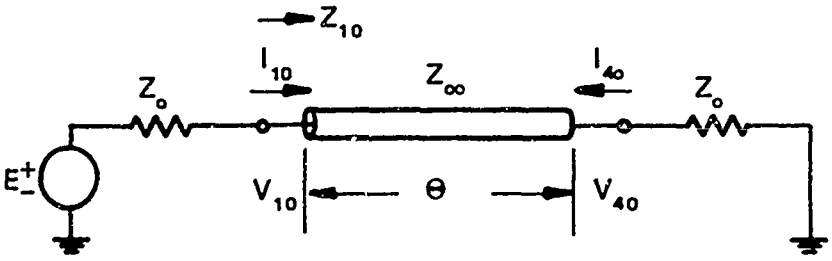

b) ODD MODE EQUIVALENT CIRCUIT

FIGURE A-2 TWO-PORT EQUIVALENT CIRCUITS FOR EVEN AND ODD MODE COUPLER EXCITATIONS

where x is e or o for the even and odd modes respectively. In terms of $\mathcal{Z}_{1x}$, the voltages at the input and output are given by

$$\frac{V_{1x}}{E} = \frac{\mathcal{Z}_{1x}}{1+\mathcal{Z}_{1x}} ; \quad \frac{I_{1x} Z_o}{E} = \frac{1}{1+\mathcal{Z}_{1x}} \tag{A-4}$$

$$\frac{V_{4x}}{E} = \frac{\mathcal{Z}_{1x}}{1+\mathcal{Z}_{1x}} \cdot \frac{1}{\cos\theta + j z_x \sin\theta} = \frac{I_{4x} Z_o}{E} \tag{A-5}$$

Superposing, we have at port 1

$$v_1 = \frac{V_1}{E} = \frac{V_{1e} + V_{1o}}{E} = \frac{\mathcal{Z}_{1e}}{1+\mathcal{Z}_{1e}} + \frac{\mathcal{Z}_{1o}}{1+\mathcal{Z}_{1o}} = a_1 + b_1 \tag{A-6}$$

$$i_1 = \frac{I_1 Z_o}{E} = \frac{I_{1e} + I_{1o}}{E} = \frac{1}{1+\mathcal{Z}_{1e}} + \frac{1}{1+\mathcal{Z}_{1o}} = a_1 - b_1 \tag{A-7}$$

where a_1 and b_1 are the normalized amplitudes of the incident and emerging waves. Solving for a_1 and b_1, we find $a_1 = 1$ and

$$b_1 = S_{11} = \frac{1}{2}\left[\frac{\mathcal{Z}_{1e} - 1}{\mathcal{Z}_{1e} + 1} + \frac{\mathcal{Z}_{1o} - 1}{\mathcal{Z}_{1o} + 1}\right]. \tag{A-8}$$

Similarly, superposing the even and odd modes at each port and solving for the wave amplitudes a_i, b_i we find $a_2 = a_3 = a_4 = 0$, and

$$b_2 = S_{12} = \frac{1}{2}\left[\frac{\mathcal{Z}_{1e} - 1}{\mathcal{Z}_{1e} + 1} - \frac{\mathcal{Z}_{1o} - 1}{\mathcal{Z}_{1o} + 1}\right] \tag{A-9}$$

$$b_3 = S_{13} = \frac{z_{1e}}{(1+z_{1e})(\cos\theta + j z_e \sin\theta)} - \frac{z_{1o}}{(1+z_{1o})(\cos\theta + j z_o \sin\theta)} \qquad \text{(A-10)}$$

$$b_4 = S_{14} = \frac{z_{1e}}{(1+z_{1e})(\cos\theta + j z_e \sin\theta)} + \frac{z_{1o}}{(1+z_{1o})(\cos\theta + j z_o \sin\theta)} \; . \qquad \text{(A-11)}$$

Since the coupler is reciprocal and symmetrical, there are only four distinct scattering coefficients. The remainder are given by

$$\begin{aligned} S_{11} &= S_{22} = S_{33} = S_{44} \\ S_{12} &= S_{21} = S_{34} = S_{43} \\ S_{13} &= S_{31} = S_{24} = S_{42} \\ S_{14} &= S_{41} = S_{23} = S_{32} \; . \end{aligned} \qquad \text{(A-12)}$$

If we next substitute Eq. (A-3) into Eqs. (A-8) thru (A-11) and eliminate z_e and z_o in favor of z_k, k and k_1, defined by

$z_k = \sqrt{z_e z_o}$ = coupler impedance,

$k = \dfrac{z_e - z_o}{z_e + z_o}$ = coupling coefficient (voltage),

$k_1 = \sqrt{1-k^2}$,

the scattering coefficients may be reduced to the following explicit forms:

$$S_{1m} = \frac{j \sin\theta}{2} \left\{ \frac{(z_k^2 - 1) + k(z_k^2 + 1)}{2z_k k_1 \cos\theta + j \sin\theta \left[(z_k^2 + 1) + k(z_k^2 - 1)\right]} \right.$$

$$\left. \pm \frac{(z_k^2 - 1) - k(z_k^2 + 1)}{2z_k k_1 \cos\theta + j \sin\theta \left[(z_k^2 + 1) - k(z_k^2 - 1)\right]} \right\} \tag{A-13}$$

where m = 1, 2 and the plus sign applies to S_{11}, the minus sign to S_{12},

$$S_{1n} = z_k k_1 \left\{ \frac{1}{2z_k k_1 \cos\theta + j \sin\theta \left[(z_k^2 + 1) + k(z_k^2 - 1)\right]} \right.$$

$$\left. \pm \frac{1}{2z_k k_1 \cos\theta + j \sin\theta \left[(z_k^2 + 1) - k(z_k^2 - 1)\right]} \right\} \tag{A-14}$$

where n = 3, 4 and the minus sign applies to S_{13}, the plus sign to S_{14}.

In the special case when $z_k = 1$, the coefficients reduce to:

$$S_{11} = 0$$

$$S_{12} = \frac{j k \sin\theta}{k_1 \cos\theta + j \sin\theta}$$

$$S_{13} = 0$$

$$S_{14} = \frac{k_1}{k_1 \cos\theta + j \sin\theta}, \tag{A-15}$$

which are the elements of the scattering matrix of an ideal directional coupler, i.e. perfectly matched and infinite directivity.

APPENDIX B

EVEN AND ODD MODES ON THE NON-SYMMETRICAL COUPLED-LINE COUPLER

In analogy to the symmetric coupled pair, we could define the even and odd mode waves on the non-symmetric pair as the modes present with equal currents flowing in the same and opposite directions on the A and B lines. (Refer to Figs. 6 and 7 of the text.) In this case the voltages of the two lines with respect to the ground plane will not be equal and we can define even and odd mode impedances with respect to each line; Z_{oe}^{a}, Z_{oo}^{a}, Z_{oe}^{b}, Z_{oo}^{b}.

Alternatively, we can define the even and odd modes as those modes existing with equal and opposite voltages on each line, with respect to ground. Then the currents on the two lines will not be equal, and we can define even and odd mode admittances with respect to each line: Y_{oe}^{a}, Y_{oo}^{a}, Y_{oe}^{b}, Y_{oo}^{b}.

These admittances are not, in general, equal to the reciprocals at the corresponding impedances. Furthermore, since there are just two independent waves on a 3-conductor line, there can be just two independent characteristic admittances or impedances, regardless of how the independent modes are chosen, and not four. The relationships among the admittance and impedances can best be understood by considering a non-symmetrical coupled pair extending to infinity from the terminals at ports 1 and 2 in lines A and B, respectively, Fig. 6. Then no reflected waves occur beyond the terminals and we have a simple two-port which may be described by an impedance matrix:

$$\begin{bmatrix} V_1 \\ V_2 \end{bmatrix} = \begin{bmatrix} Z_{oa} & Z_t \\ Z_t & Z_{ob} \end{bmatrix} \begin{bmatrix} I_1 \\ I_2 \end{bmatrix}, \qquad \text{(B-1)}$$

or an admittance matrix:

$$\begin{bmatrix} I_1 \\ I_2 \end{bmatrix} = \begin{bmatrix} Y_{oa} & Y_t \\ Y_t & Y_{ob} \end{bmatrix} \begin{bmatrix} V_1 \\ V_2 \end{bmatrix} . \tag{B-2}$$

It is clear from Eqs. (B-1) that Z_{oa} and Z_{ob} are the characteristic impedances of the modes on each line when the input to the other line is open circuited, so that I_2 and I_1, in turn, equal zero. Similarly Y_{oa} and Y_{ob} are the characteristic admittances of the modes on each line when the input to the other line is grounded, so that V_2 and V_1, in turn, equal zero. Z_t and Y_t are the transfer impedance and admittance, respectively, and describe the coupling between the lines under open and short circuit conditions. They are not the characteristic impedance and admittance of any mode of propagation. Thus, the two-mode structure is described by three immittances, two characteristic wave immittances and a transfer immittance. Note that for this selection of modes, which we might call the open or short circuit modes, the admittances are not the reciprocals of the corresponding impedances. However the admittance matrix is the reciprocal of the impedance matrix, so we have

$$Y_{oa} = \frac{Z_{ob}}{Z_{oa} Z_{ob} - Z_t^2} \tag{B-3}$$

$$Y_t = \frac{-Z_t}{Z_{oa} Z_{ob} - Z_t^2} \tag{B-4}$$

$$Y_{ob} = \frac{Z_{oa}}{Z_{oa} Z_{ob} - Z_t^2} . \tag{B-5}$$

Now, we can define the even and odd modes in two ways. First we have the modes withequal and opposite currents;this is a superposition of the open circuit modes. By defining the even and odd mode currents by $I_e = \frac{1}{2}(I_1+I_2)$ and $I_o = \frac{1}{2}(I_1-I_2)$, Eq. (B-1) can be written as

$$\begin{bmatrix} V_1 \\ V_2 \end{bmatrix} = \begin{bmatrix} (Z_{oa}+Z_t) & (Z_{oa}-Z_t) \\ (Z_{ob}+Z_t) & (Z_{ob}-Z_t) \end{bmatrix} \begin{bmatrix} I_e \\ I_o \end{bmatrix}$$

$$= \begin{bmatrix} Z_{oe}^{a} & Z_{oo}^{a} \\ Z_{oe}^{b} & Z_{oo}^{b} \end{bmatrix} \begin{bmatrix} I_e \\ I_o \end{bmatrix} \qquad \text{(B-6)}$$

In Eq. (B-6)

$$Z_{oe}^{a} = \left.\frac{V_1}{I_e}\right|_{I_o = 0} = \left.\frac{V_1}{I_1}\right|_{I_1 = I_2} \qquad \text{(B-7)}$$

is clearly the characteristic impedance of line A in the "equal current" even mode, i.e. when $I_1 = I_2$. Similar definitions hold for the remaining Z's. Second, we have the modes with equal and opposite voltages; this is a superposition of the short circuit modes. Letting $V_e = \frac{1}{2}(V_1+V_2)$ and $V_o = \frac{1}{2}(V_1-V_2)$, Eq. (B-2) becomes

$$\begin{bmatrix} I_1 \\ I_2 \end{bmatrix} = \begin{bmatrix} (Y_{oa}+Y_t) & (Y_{oa}-Y_t) \\ (Y_{ob}+Y_t) & (Y_{ob}-Y_t) \end{bmatrix} \begin{bmatrix} V_e \\ V_o \end{bmatrix}$$

$$= \begin{bmatrix} Y_{oe}^{a} & Y_{oo}^{a} \\ Y_{oe}^{b} & Y_{oo}^{b} \end{bmatrix} \begin{bmatrix} V_e \\ V_o \end{bmatrix} \qquad \text{(B-8)}$$

In Eq. (B-7)

$$Y_{oe}^{a} = \left.\frac{I_1}{V_e}\right|_{V_o = 0} = \left.\frac{I_1}{V_1}\right|_{V_1 = V_2} \qquad \text{(B-9)}$$

is the characteristic admittance of line A in the "equal voltage" even mode, i.e. when $V_1 = V_2$. And again, similar definitions hold for the other Y's.

It is evident from Eqs. (B-7) and (B-9) that $Z_{oe}^{a} \neq 1/Y_{oe}^{a}$. This is to be expected since Z_{oe}^{a} and Y_{oe}^{a} refer to fundamentally differently defined even modes.

In the text, we have chosen to work with the admittance formulation, or the "equal voltage" even and odd modes. This was done because it seems the more "natural" definition of even and odd modes. First it is conceptually easier to visualize the modes defined that way, and second, any calculation of the line parameters is bound to be based on line voltages rather than currents.

Finally, the admittance matrix for the lossless four-port coupler of electrical length θ is given by:

$$\bar{\bar{Y}} = -j \begin{bmatrix} Y_{oa} \operatorname{ctn}\theta & Y_t \operatorname{ctn}\theta & -Y_t \csc\theta & -Y_{oa} \csc\theta \\ Y_t \operatorname{ctn}\theta & Y_{ob} \operatorname{ctn}\theta & -Y_{ob} \csc\theta & -Y_t \csc\theta \\ -Y_t \csc\theta & -Y_{ob} \csc\theta & Y_{ob} \operatorname{ctn}\theta & Y_t \operatorname{ctn}\theta \\ -Y_{oa} \csc\theta & -Y_t \csc\theta & Y_t \operatorname{ctn}\theta & Y_{oa} \operatorname{ctn}\theta \end{bmatrix}. \qquad \text{(B-10)}$$

The scattering matrix for the matched coupler is the same as that for the symmetrical coupler, Eq. (A-15); recall, however that the wave amplitudes must be normalized to the matching resistances Z_a and Z_b, instead of Z_o. The scattering matrix for the general case is quite complicated, and has not yet appeared in print.

APPENDIX C

SCATTERING MATRIX OF THE MICROSTRIP COUPLER

The scattering matrix of the coupled-line coupler with unequal even and odd mode lengths, can be derived by superposing the even and odd modes at the coupler terminals, exactly as in Appendix A. Simply add the even and odd mode subscripts to θ in Eq. (A-3) and carry this throughout the derivation. This method is simple and straightforward, however some additional insight can be gained from the coupling-of-modes derivation, following the pattern of Krage and Haddad.[16]

The transmission line equations of the coupled lines for waves with time dependence $e^{+j\omega t}$ are:

$$\frac{\partial E_1}{\partial z} + j\omega L_1 I_1 + j\omega L_m I_2 = 0 \qquad \text{(C-1)}$$

$$\frac{\partial E_2}{\partial z} + j\omega L_2 I_2 + j\omega L_m I_1 = 0 \qquad \text{(C-2)}$$

$$\frac{\partial I_1}{\partial z} + j\omega C_1 E_1 - j\omega C_m E_2 = 0 \qquad \text{(C-3)}$$

$$\frac{\partial I_2}{\partial z} + j\omega C_2 E_2 - j\omega C_m E_1 = 0 \qquad \text{(C-4)}$$

where the variables are defined in Fig. C-1, and the two lines need not be identical. The variables are not normalized.

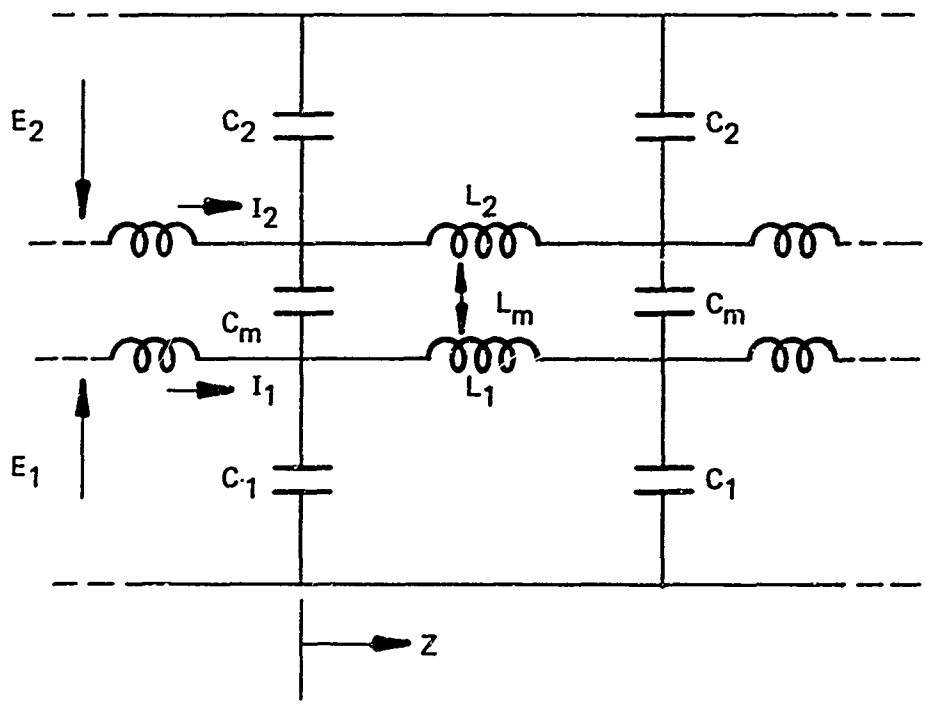

FIGURE C-1 COUPLED LINE NOTATION FOR COUPLED MODE ANALYSIS

D-12145

Define $\beta_i = \omega\sqrt{L_i C_i}$

$Z_i = 1/Y_i = \sqrt{L_i / C_i}$, for i - 1, 2, m, and introduce the even and odd mode voltages and currents:

$$E_e = \frac{1}{2}(E_1+E_2)\ ,\ E_o = \frac{1}{2}(E_1-E_2)$$

$$I_e = \frac{1}{2}(I_1+I_2)\ ,\ I_o = \frac{1}{2}(I_1-I_2). \qquad \text{(C-5)}$$

The transmission line equations for the even and odd modes then become:

$$\frac{\partial E_e}{\partial z} + \frac{1}{2} j(\beta_1 Z_1+\beta_2 Z_2+2\beta_m Z_m) I_e + \frac{1}{2} j(\beta_1 Z_1-\beta_2 Z_2) I_o = 0 \qquad \text{(C-6)}$$

$$\frac{\partial E_e}{\partial z} + \frac{1}{2} j(\beta_1 Z_1+\beta_2 Z_2-2\beta_m Z_m) I_o + \frac{1}{2} j(\beta_1 Z_1-\beta_2 Z_2) I_e = 0 \qquad \text{(C-7)}$$

$$\frac{\partial I_e}{\partial z} + \frac{1}{2} j(\beta_1 Y_1+\beta_2 Y_2-2\beta_m Y_m) E_e + \frac{1}{2} j(\beta_1 Y_1-\beta_2 Y_2) E_o = 0 \qquad \text{(C-8)}$$

$$\frac{\partial I_o}{\partial z} + \frac{1}{2} j(\beta_1 Y_1+\beta_2 Y_2+2\beta_m Y_m) E_o + \frac{1}{2} j(\beta_1 Y_1-\beta_2 Y_2) E_e = 0 \qquad \text{(C-9)}$$

At this point we introduce the symmetry of the coupler, letting $\beta_1 = \beta_2$ and $Z_1 = Z_2 = 1/Y_o$. Eqs. (C-6) - (C-9) then reduce to:

$$\frac{\partial E_e}{\partial z} = -j\beta_e Z_{oe} I_e \qquad \text{(C-10)}$$

$$\frac{\partial E_o}{\partial z} = -j\beta_o Z_{oo} I_o \qquad \text{(C-11)}$$

$$\frac{\partial I_e}{\partial z} = -j\beta_e Y_{oe} E_e \qquad \text{(C-12)}$$

$$\frac{\partial I_o}{\partial z} = -j\beta_o Y_{oo} E_o , \qquad \text{(C-13)}$$

where $\beta_e Z_{oe} = \beta_1 Z_1 + \beta_m Z_m$

$$\beta_o Z_{oo} = \beta_1 Z_1 - \beta_m Z_m$$

$$\beta_e Y_{oe} = \beta_1 Y_1 - \beta_m Y_m$$

$$\beta_o Y_{oo} = \beta_1 Y_1 + \beta_m Y_m \qquad \text{(C-14)}$$

are the even and odd mode impedances and admittance in terms of the basic line parameters, i.e. the inductances and capacitances. Note that for the symmetric line the even and odd modes, as defined by Eq. (C-5), are completely decoupled, regardless of the z-dependence, thus, regardless of the propagation constants or velocities of propagation.

It is also possible to define the even and odd modes for a non-symmetrical coupled line such that the modes are completely decoupled if $\beta_1 = \beta_2$, or $L_1 C_1 = L_2 C_2$. This condition will always hold for a homogeneous dielectric medium; it need not, and generally will not, hold for non-symmetric microstrip coupled pairs. When the condition holds, the decoupled even and odd modes are defined by $E_{e,o} = E_1 \pm \alpha E_2$, $I_{e,o} = I_1 \pm I_2 / \alpha$, where $\alpha^2 = Z_1 / Z_2 = \sqrt{L_1 C_2 / L_2 C_1}$. These are not the same even and odd modes defined in Appendix B on either the impedance or admittance basis.

From Eqs. (C-10) - (C-13), it is clear that the propagation constants of the even and odd modes are β_e and β_o, respectively. In microstrip ($\beta_e \neq \beta_o$, each being determined by the dielectric constant or phase velocity of the mode:

$$\beta_e = \frac{\omega}{v_e} = \frac{\omega}{c}\sqrt{\epsilon_{e\text{-}eff}}$$

and

$$\beta_o = \frac{\omega}{v_o} = \frac{\omega}{c}\sqrt{\epsilon_{o\text{-}eff}}\,.$$

Eqs. (C-5) and the symmetry require that

$$Z_{oe} = 1/Y_{oe}$$

and

$$Z_{oo} = 1/Y_{oo}\,.$$

Applying these conditions to Eqs. (C-14), with a little algebra we find that

$$Z_k^2 = Z_{oe}\,Z_{oo} = Z_1^2\sqrt{\frac{1-(L_m/L_1)^2}{1-(C_m/C_1)^2}}\,,$$

which relates the coupler impedance to the basic coupler parameters. It is interesting to note that $Z_1 = \sqrt{L_1/C_1}$, the impedance of one line when the other is removed, i.e. L_m, $C_m \rightarrow 0$, is not equal to Z_o, the impedance which matches the ideal coupler.

Return now to the decoupled transmission line Eqs. (C-10) - (C-13). The solutions for the even and odd mode voltage and currents are

$$e_e = a_e e^{-j\beta_e z} + b_e e^{j\beta_e z}$$

$$i_e = a_e e^{-j\beta_e z} - b_e e^{j\beta_e z}$$

$$e_o = a_o e^{-j\beta_o z} + b_o e^{j\beta_o z}$$

$$i_o = a_o e^{-j\beta_o z} - b_o e^{j\beta_o z} \qquad \text{(C-15)}$$

where the e's and i's are the normalized voltages and currents and the a's and b's are the normalized forward and reverse wave amplitudes: $e_e = E_e / \sqrt{Z_{oe}}$, $i_e = I_e \sqrt{Z_{oe}}$, etc.

Next, un-normalize Eqs. (C-15), add and subtract each pair to get E_1, I_1, E_2, I_2, re-normalize to Z_o - an arbitrary terminating impedance--and split into forward and reverse waves on each line $a_1(z)$, $b_1,(z)$, $a_2(z)$, $b_2(z)$. Turning the crank on this process yields

$$a_i(z) = a_e \left(\sqrt{\mathcal{Z}_e} + \sqrt{y_e}\right) e^{-j\beta_e z} + b_e \left(\sqrt{\mathcal{Z}_e} - \sqrt{y_e}\right) e^{j\beta_e z}$$

$$\pm a_o \left(\sqrt{\mathcal{Z}_o} + \sqrt{y_o}\right) e^{-j\beta_o z} \pm b_o \left(\sqrt{\mathcal{Z}_o} - \sqrt{y_o}\right) e^{j\beta_o z}$$

$$b_i(z) = a_e \left(\sqrt{\mathcal{Z}_e} - \sqrt{y_e}\right) e^{-j\beta_e z} + b_e \left(\sqrt{\mathcal{Z}_e} + \sqrt{y_e}\right) e^{j\beta_e z}$$

$$\pm a_o \left(\sqrt{\mathcal{Z}_o} - \sqrt{y_o}\right) e^{-j\beta_o z} \pm b_o \left(\sqrt{\mathcal{Z}_o} + \sqrt{y_o}\right) e^{j\beta_o z}, \qquad \text{(C-16)}$$

where $i = 1, 2$ and the upper sign applies when $i = 1$, the lower when $i = 2$. Eq. (C-16) is an explicit expression of Eq. (16) of Ref. 16, in our notation.

The constants a_e, b_e, a_o, b_o are determined by the boundary conditions. Assume a wave of unit amplitude incident at port one only, and all ports terminated in Z_o, the normalizing impedance. Ports 1 and 2 are at $z = 0$, 3 and 4 are at $z = \ell$ and let $\theta_e = \beta_e \ell$, $\theta_o = \beta_o \ell$. The boundary conditions are:

$$a_1(0) = 1 \quad .$$

$$a_2(0) = b_1(\ell) = b_2(\ell) = 0,$$

which, with four of Eqs. (C-16), evaluated at $z = 0$ and ℓ, determine the constants. The remaining four may be solved for the scattering matrix, yielding:

$$S_{1m} = \frac{j\,(z_e^2-1)\sin\theta_e}{4z_e\cos\theta_e + 2j\,(z_e^2+1)\sin\theta_e} \pm \frac{j\,(z_o^2-1)\sin\theta_o}{4z_o\cos\theta_o + 2j\,(z_o^2+1)\sin\theta_o} \tag{C-17}$$

$$S_{1n} = \frac{z_e}{2z_e\cos\theta_e + 2j\,(z_e^2+1)\sin\theta_e} \pm \frac{z_o}{4z_o\cos\theta_o + 2j\,(z_o^2+1)\sin\theta_o} \tag{C-18}$$

where m = 1, 2 and n = 3, 4. The upper signs apply for m = 1, n = 3. The remaining coefficients are determined from Eqs. (A-12)

Finally, substituting

$$z_k = \sqrt{z_e z_o}$$

$$k = \frac{z_e - z_o}{z_e + z_o}$$

$$k_1 = \sqrt{1-k^2}$$

The scattering coefficients become

$$S_{1m} = \frac{j}{2}\left\{\frac{(\mathcal{Z}_k^2-1) + k\,(\mathcal{Z}_k^2+1)\,\sin\theta_e}{2\mathcal{Z}_k k_1 \cos\theta_e + j\left[(\mathcal{Z}_k^2+1) + k\,(\mathcal{Z}_k^2-1)\right]\sin\theta_e} \pm \frac{(\mathcal{Z}_k^2-1) - k\,(\mathcal{Z}_k^2+1)\,\sin\theta_o}{2\mathcal{Z}_k k_1 \cos\theta_o + j\left[(\mathcal{Z}_k^2+1) + k\,(\mathcal{Z}_k^2-1)\right]\sin\theta_e}\right\}, \tag{C-17}$$

$$S_{1n} = \mathcal{Z}_k k_1\left\{\frac{1}{2\mathcal{Z}_k k_1 \cos\theta_e + j\left[(\mathcal{Z}_k^2+1) + k\,(\mathcal{Z}_k^2-1)\right]\sin\theta_e} \pm \frac{1}{2\mathcal{Z}_k k_1 \cos\theta_o + j\left[(\mathcal{Z}_k^2+1) + k\,(\mathcal{Z}_k^2-1)\right]\sin\theta_o}\right\} \tag{C-18}$$

Again m = 1, 2, n = 3, 4 and the upper signs apply to m = 1 and n = 3. Note that Eqs. (C-17) and (C-18) are exactly the same as Eqs. (A-13) and (A-14) for the ideal coupler except for the subscripting of the angles. We should also point out that these scattering coefficients are more general than those given by Eqs. (32) - (35) in Ref. 16, as the latter are for so-called "matched terminations", which apparently means for the special case when $Z_o = Z_1 = Z_2$. Our Eqs. (C-17) and (C-18) are valid for an arbitrary Z_o termination.

APPENDIX D

CASCADE - A COMPUTER PROGRAM TO CALCULATE THE RESPONSE OF CASCADED FOUR-PORT DIRECTIONAL COUPLERS

A. General

CASCADE computes the reflection and transmission response of cascaded four-port directional couplers. Up to 15 couplers may be cascaded. The couplers are parallel-coupled-line couplers of a very general type; that is the matching impedances of each line need not be equal (i.e. unequal line widths in microstrip or stripline), and the phase velocities of the even and odd mode waves may differ. The interconnection of ports in the cascade is quite arbitrary as long as the interconnection is a true cascade, i.e. each coupler is connected only to its immediate neighbors. Lengths of transmission line may be inserted between couplers. The free ports may be terminated by resistors or open-circuited or short-circuited stubs.

As a design aid, CASCADE is useful in studying the responses of several broad classes of coupled-line coupler networks, such as the stepped quarter wave couplers described by Cristal and Young[12], and by Levy[20], and all of the filter types described by Jones and Bolljahn[13]. Continuously tapered couplers can be approximated by cascading numerous short, untapered couplers. By making use of the various program features, such as unequal line impedances, unequal mode velocities, interconnecting lines, and different terminations, the performance of practical couplers can be modeled, so that the program is also very useful in analyzing and understanding the measured performance of actual coupler networks.

The program is written in Fortran IV for use in the time-sharing mode on a teletype terminal. It runs on a Digital Equipment Corporation PDP-10; minor alterations may be required to run it on other machines.

B. Coupler and Network Specifications

The sketch below represents a coupled-line directional coupler, terminated at each of its four ports in a matched load. If port 1 is considered the input port, ports 2, 3 and 4 are the coupled, isolated, and direct ports respectively.

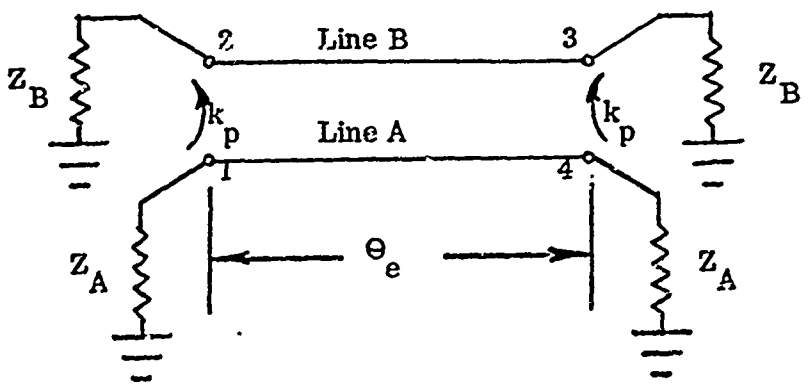

In CASCADE each coupler is specified by seven parameters as follows:

Z_A = impedance in ohms which matches ports 1 and 4, the ends of line A.

Z_B = impedance which matches ports 2 and 3, the ends of line B.

k_p = power coupling ratio, in dB, between ports 1 and 2 or 3 and 4.

θ = electrical length, in degrees, of the coupler for the even mode wave.

v_o/v_e = ratio of odd to even mode wave velocities.

α_e = loss, in dB per wavelength, of the even mode wave.

α_o = loss, in dB per wavelength of the odd mode wave.

If $Z_A \neq Z_B$, ports 1 and 4 must be on line A, 2 and 3 on line B. If $Z_A = Z_B$ any port may be labelled #1. In either case ports 2, 3 and 4 must be the coupled, isolated, and direct ports, respectively, with respect to the selected port #1.

The couplers may be joined and terminated in a variety of ways. Several examples will be illustrate the basic configurations which can be treated.

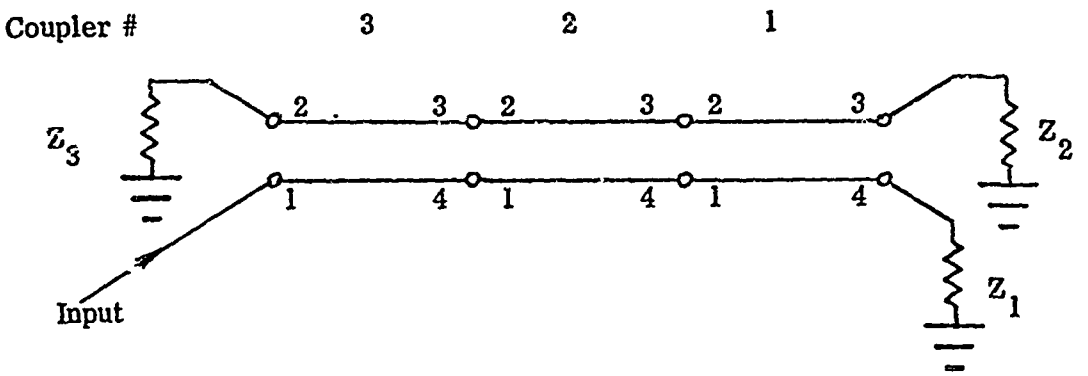

The preceding sketch shows a simple 3-section cascaded coupler with all free ports resistively terminated. Note that the couplers are sequentially numbered from output to input. There must always be one free input port and at least one resistive termination. The insertion loss, or more precisely, the transducer loss (ratio of power dissipated in load to power incident at input) is calculated for each resistive termination.

The sketch below illustrates a typical bandpass filter interconnection, with simple open circuits on the free ports.

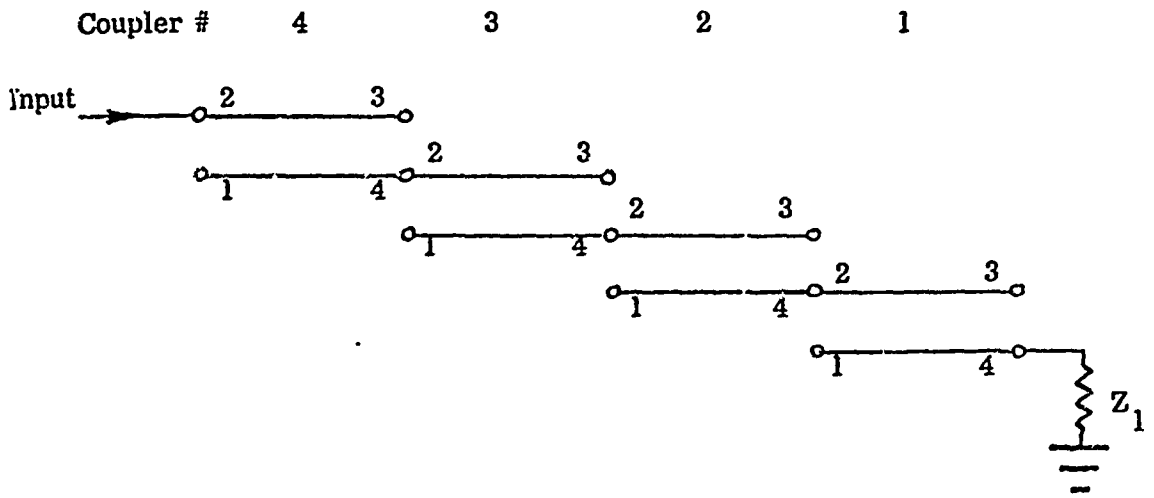

Some filter designs of this type require unequal line widths, $Z_A \neq Z_B$.

The bandstop filter structure below illustrates the use of an interconnecting line of impedance Z_I and length θ_I and, in section 2, an open stub of admittance Y_s and length $\theta_s = 90^o$, to simulate a shorted port.

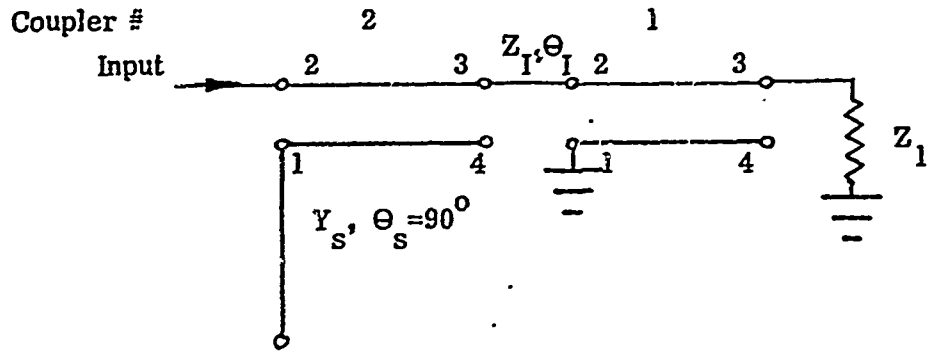

Finally, this all-pass structure:

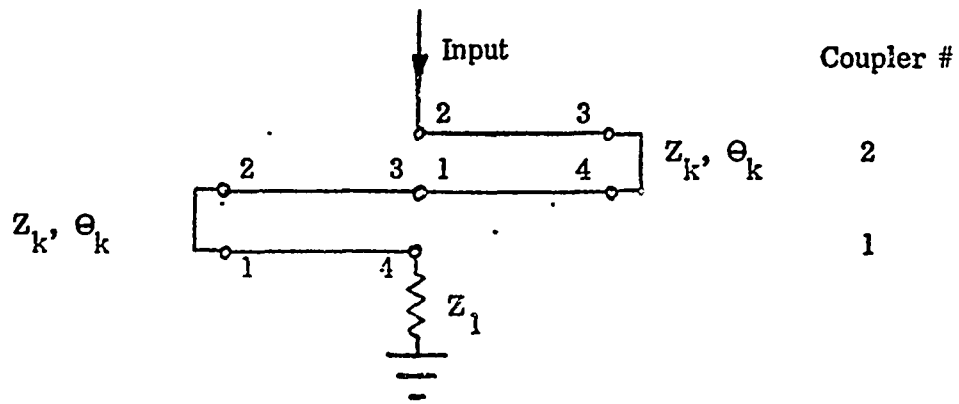

shows the case where two ports of a single coupler are connected together by a line of impedance Z_k of length θ_k.

The network sketched below shows the two interconnections which cannot be handled by CASCADE: namely coupler #3 can only be connected

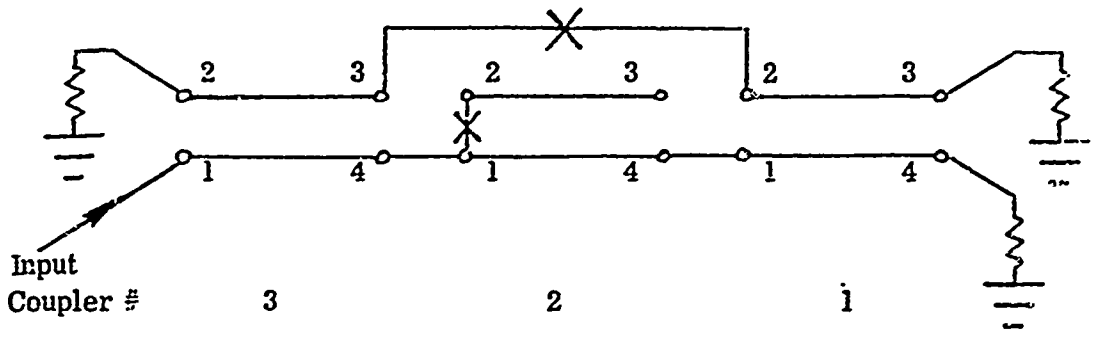

to coupler #2 or #1, but not both, and port #1 of coupler #2 can have only one connection- in this case to port #4, coupler #3. Note, also that we cannot disconnect port #4, coupler #3 from port #1, coupler #2 and leave the other connections in place, as this is no longer a cascade, but rather a tree network.

C. Data Input and Output

The use of CASCADE, and the entry of the data at the time-sharing terminal is best explained by going through a typical run. The next two pages show the typescript for a 3-section 20 dB coupler design. The underlined entries are made by the user. Carriage returns are indicated by the arrows.

The program begins by typing the date and asking for a title. It proceeds by asking for four frequencies, FO, FL, FU, FDEL, the center frequency, lower and upper limits and increment all in the same units, e.g. GHz. It will next request NS, ZO, the number of couplers in the cascade and the generator impedance in ohms. (If an input error is made up to this point, it is best to abort and start over.)

```
 9-APR-73  TITLE: 3 SECTION 20 DB COUPLER  .2 DB RIPPLE  UNEQUAL VEL

FØ,FL,FU,FDEL=
6 1 11 .25

NS,ZØ=
3 50

SEC #,ZIN-A,ZIN-B,KP(DB),THETA,VØDD,ALPHA-E,ALPHA-Ø=
   1   50 50 33.8 90 1.01

 #  1/YØE  1/YØØ  1/YØE  1/YØØ   Z-A    Z-B   K(DB)  LØSS-E,Ø(N/WL)
 1   51.0   49.0   51.0   49.0   50.0   50.0  33.80 1.0E-06 1.0E-06


PØRT # 1 TYPE,Z,TH=F 3
PØRT # 2 TYPE,Z,TH=F 4
PØRT # 3 TYPE,Z,TH=Z 50
PØRT # 4 TYPE,Z,TH=Z 50

ØK?

SEC #,ZIN-A,ZIN-B,KP(DB),THETA,VØDD,ALPHA-E,ALPHA-Ø=
   2   50 50 17.2 90 1.11

 #  1/YØE  1/YØØ  1/YØE  1/YØØ   Z-A    Z-B   K(DB)  LØSS-E,Ø(N/WL)
 2   57.5   43.5   57.5   43.5   50.0   50.0  17.20 1.0E-06 1.0E-06


PØRT # 1 TYPE,Z,TH=F 3
PØRT # 2 TYPE,Z,TH=F 4
PØRT # 3 TYPE,Z,TH=T 1
PØRT # 4 TYPE,Z,TH=T 2

ØK?

SEC #,ZIN-A,ZIN-B,KP(DB),THETA,VØDD,ALPHA-E,ALPHA-Ø=
   3   50 50 33.8 90 1.01

 #  1/YØE  1/YØØ  1/YØE  1/YØØ   Z-A    Z-B   K(DB)  LØSS-E,Ø(N/WL)
 3  51.0   49.0   51.0   49.0   50.0   50.0  33.80 1.0E-06 1.0E-06


PØRT # 1 TYPE,Z,TH=F 3
PØRT # 2 TYPE,Z,TH=Z 50
PØRT # 3 TYPE,Z,TH=T 1
PØRT # 4 TYPE,Z,TH=T 2

ØK?

                  REFL     ØUTPUT # 1          2                3
  FREØ     VSWR    ANG      LØSS     ANG      LØSS     ANG     LØSS     ANG
   GHZ             DEG        DB     DEG        DB     DEG       DB     DEG

 1.000     1.00    24.2     36.11  -134.5     0.01   -44.2    27.24    45.7
 1.250     1.00     7.9     34.19  -145.6     0.01   -55.3    25.51    34.7
 1.500     1.01    -8.2     32.62  -156.7     0.02   -66.3    24.17    23.6
 1.750     1.01   -24.2     31.29  -167.7     0.02   -77.4    23.12    12.6
 2.000     1.01   -40.0     30.15  -178.8     0.03   -88.4    22.29     1.6
 2.250     1.01   -55.6     29.14   170.2     0.04   -99.4    21.63    -9.5
 2.500     1.01   -70.9     28.24   159.2     0.04  -110.4    21.12   -20.5
 2.750     1.01   -86.1     27.42   148.2     0.04  -121.4    20.72   -31.5
 3.000     1.01  -101.0     26.67   137.2     0.05  -132.5    20.43   -42.5
```

3.750	1.01	-144.4	24.75	104.3	0.06	-165.5	20.02	-75.6
4.000	1.01	-156.3	24.20	93.3	0.06	-176.5	20.00	-86.6
4.250	1.01	-171.9	23.67	82.3	0.06	172.5	20.01	-97.6
4.500	1.01	174.7	23.17	71.3	0.06	161.5	20.05	-108.6
4.750	1.01	161.6	22.71	60.3	0.07	150.5	20.10	-119.6
5.000	1.02	148.7	22.26	49.3	0.07	139.4	20.16	-130.6
5.250	1.02	136.0	21.84	38.3	0.07	128.4	20.22	-141.6
5.500	1.02	123.4	21.43	27.3	0.07	117.4	20.26	-152.7
5.750	1.02	111.0	21.05	16.3	0.08	106.4	20.28	-163.7
6.000	1.02	98.7	20.68	5.3	0.08	95.3	20.28	-174.7
6.250	102	86.4	20.33	-5.7	0.08	84.3	20.25	174.3
6.500	1.02	74.0	19.99	-16.7	0.09	73.3	20.20	163.3
6.750	1.02	61.6	19.66	-27.7	0.09	62.3	20.13	152.3
7.000	1.02	49.0	19.35	-38.7	0.10	51.2	20.04	141.3
7.250	1.02	36.2	19.05	-49.8	0.10	40.2	19.94	130.3
7.500	1.02	23.2	18.76	-60.7	0.10	29.2	19.84	119.3
7.750	1.03	10.0	18.48	-71.7	0.11	18.2	19.74	108.3
8.000	1.03	-3.5	18.20	-82.7	0.11	7.2	19.66	97.3
8.250	1.03	-17.2	17.94	-93.7	0.12	-3.9	19.61	86.4
8.500	1.03	-31.2	17.68	-104.7	0.12	-14.9	19.60	75.4
8.750	1.03	-45.4	17.43	-115.6	0.13	-25.9	19.64	64.5
9.000	1.03	-59.8	17.18	-126.6	0.13	-36.9	19.73	53.6
9.250	1.03	-74.5	16.94	-137.6	0.14	-47.9	19.89	42.7
9.500	1.03	-89.4	16.70	-148.6	0.14	-58.9	20.13	31.9
9.750	1.04	-104.5	16.46	-159.5	0.14	-69.9	20.47	21.0
10.000	1.04	-119.9	16.23	-170.5	0.14	-80.9	20.91	10.2
10.250	1.04	-135.4	16.01	178.5	0.14	-91.9	21.47	-0.5
10.500	1.04	-151.1	15.78	167.4	0.14	-103.0	22.18	-11.2
10.750	1.04	-167.0	15.57	156.4	0.15	-114.0	23.07	-21.8
11.000	1.04	176.9	15.35	145.3	0.15	-125.0	24.18	-32.2

CHANGE ALL?Y)

The program will now step through each coupler, from output to input asking for each coupler's specifications and interconnections. It first requests the 7 coupler parameters, Z_A, Z_B in ohms, k_p in dB, θ_e in degrees at FO, v_o/v_e as a ratio, and α_e and α_o in dB per wavelength. The even and odd mode impedances for lines A and B are computed and typed out; Z_A, Z_B, k_p are repeated to help insure that they were correctly received, and α_e and α_o are converted to nepers per wavelength and typed. If zero losses are entered, they are set to a minimum, negligible, value of 10^{-6} nepers per wavelength.

If the two lines are of unequal width, such that $Z_A \neq Z_B$, the even and odd mode impedances of each line do not equal the reciprocals of the even and odd mode admittances, CASCADE computes the admittances and prints the reciprocals, hence the 1/YOE, 1/YOO labeling of the columns.

Next the interconnection specifications are requested for each port. This is the tricky part, and can be confusing at first. Up to 3 entries are required for each port, a type code letter and one or two numbers whose meaning depends on the code. The allowable type codes and the meanings of the numbers are given in Table D-I. If port assignments are made that cannot be interpreted, a diagnostic will be typed and the program will ask for a new assignment.

TABLE D-I

Coupler Port Assignment Codes for CASCADE

Code Letter	Meaning	First Number	Second Number
L	Line – input port with connecting line	Z_I = impedance of line in Ω	θ_I = length of line in degrees at fo
F	From input port (equivalent to L with $\theta_I = 0$)	Number of connecting output port (this data not required by program)	None
T	To – output port	Number of connecting input port	None
K	Interconnected port	Z_k = impedance of line connecting ports (Z_k, θ_k must be specified on lower number port; these data on higher number port are ignored)	θ_k = length (deg @ fo) of line connecting ports
Z	Resistive termination; Load	Resistance of load in Ω	None
Y	Resistive termination; Load	Conductance of load in mhos	None
S	Shorted stub termination	Y_s = stub impedance in Ω	θ_s = stub length in degrees @ fo
O	Open stub termination	Y_s = stub admittance in mhos	θ_s = stub length in degrees @ fo

At the end of the data entry for each coupler, the computer will ask "OK?". Typing an N (for NO) at this point will return to the beginning of the entries for that particular coupler. Any other response allows the program to proceed.

Although the tabular data of the network response is straightforward and relatively self-explanatory, several comments are in order. First, the reflection angle is meaningless if the VSWR equals unity. Second, although the transducer loss is computed and printed for each resistive load, they do not necessarily appear in the order they were entered. The order of the outputs does proceed from section 1 through section NS, but the ordering of the loads on any coupler depends on the assignment of the ports. Which loss goes with which load can readily be determined by inspection. Third, insertion loss values over approximately 100 dB are unreliable due to round-off error and machine precision limits. Fourth, since the admittance matrix of a coupler with equal mode velocities is singular at 2 fo, i.e. when it is 180° long, the calculated responses at and very close to this frequency are also not reliable.

After the resonse data table is completed, the computer will ask "Change All?" A positive response (anything except "N") starts the program from the top. An "N" response elicits "Change Cplrs?" After a positive response the program will ask for everything following the generator impedance. An "N" elicits "Change Ports?" A positive response to this allows the user to change the port assignments, loads, etc. of all the couplers, leaving the rest of the data intact. An "N" brings up "Stop or Go", to which any reply but an "S" (for Stop) will return to the beginning of the program. An "S" terminates the program operation.

D. Program Listing and Summary of Logic

The complete Fortran listing of CASCADE appears on the following pages. Very briefly, the program works as follows:

The input coupler specification data for each coupler is transformed to even and odd mode parameters and stored. Subroutine ASSIGN takes the port assignment for each coupler and classifies the coupler according to its interconnections, constructs a matrix to reassign the ports to standard positions, and sets up matrices describing the terminations and interconnections.

After all the couplers have been read in and the assignments made, the frequency scan starts. At each frequency the admittance matrix of the first coupler is calculated in a standard form in ADMIT. Then the rows and columns are interchanged according to the assignments made by ASSIGN. The resulting admittance matrix is then transformed to a four-port ABCD matrix in INTCHG. This ABCD matrix is then manipulated in various ways, depending on the interconnections. When possible it is reduced to a two-port ABCD matrix, which is stored; when not, the four-port matrix is stored.

Next the second coupler is taken through the same route. When its two or four-port ABCD is found, it is cascaded with that for the first coupler and reduced to a two-port if possible. This process repeats until all couplers have been cascaded.

Reduction to a two-port occurs whenever there is one input port and one output port. If there are loads, a separate 2-port matrix is determined between the input and each load in turn. Thus, at the end, there will be a two-port ABCD matrix stored for each resistive termination. These ABCD matrices are then used to compute the reflection and transmission response at that frequency; the frequency is incremented and the process repeated.

```
C              CASCADE - PROGRAM TO COMPUTE THE TRANSMISSION
C                        AND REFLECTION PROPERTIES OF CASCADED
C                        FOUR-PORT DIRECTIONAL COUPLERS
C
      INTEGER STAR,TAG,CHGPT
      REAL KP,KV2,KV1,LOS,LOSDB(30),MINUS(2,2),JUGL(4,4)
      DIMENSION THETA(15),V0DD(15),Y0EA(15),Y00A(15),Y0EB(15),
     1Y00B(15),CODE(4),RESIST(4),REACT(4),SGN(2,2),FLIP(4,4),R0W(16),
     2KLAS(15),RW(4,4),PSI(30),DTE(2),ALPE(15),ALP0(15),NR0W(15)
      COMPLEX ZL(4,15),RL(2,2),Y(4,4),Y11(2,2),Y12(2,2),Y21(2,2),Y22(2,2
     1),A(4,4),A11(2,2),A12(2,2),A21(2,2),A22(2,2),B(4,4),B11(2,2),B12(2
     2,2),B21(2,2),B22(2,2),X(4,4),X1(2,2),X2(2,2),U(2,2),UI(2,2, 30),AA
     3(4,4),AI(4,4,30),R(30),R4,YL,G1,G2,GAM,TRAN,Z2PT(2,2),0NE(2,2),
     4UL(2,2,2),UL1(2,2),UL2(2,2),X3(2,2),X11(2,2),X12(2,2),X21(2,2),X22
     5(2,2)
      COMMON /COUP/Y0EA,Y00A,Y0EB,Y00B,THETA,V0DD,ALPE,ALP0/PORT/CODE,RE
     1SIST,REACT,ZL/UNIT/0NE,MINUS,SGN,JUGL,FLIP
      DATA CS/'S'/,CN/'N'/,CNEP/54.575052/,ALPMIN/1.E-6/,FACTOR/.9994/
      EQUIVALENCE (RW(1,1),R0W(1)),(UL(1,1,1),UL1(1,1)),(UL(1,1,2),
     1UL2(1,1))
    1 CALL DATE (DTE)
      WRITE (5,981) DTE
      WRITE (5,920)
      READ (5,990,ERR=1)
    2 WRITE (5,922)
      READ (5,992,ERR=2) FO,FL,FU,FDEL
    3 WRITE (5,924)
      READ (5,992,ERR=3) CNS,ZO
      NS=CNS
      NF=(FU-FL)/FDEL+1
    5 LIN=0
      DO 1000 IS=1,NS
      IF (CHGPT.EQ.0) GO TO 6
      WRITE (5,927) IS
      GO TO 7
    6 WRITE (5,926) IS
      READ (5,992,ERR=6) ZA,ZB,KP,THETA(IS),V0DD(IS),ALPE(IS),ALP0(IS)
      KV2=10.**(-KP/10.)
      KV1=SQRT(1.-KV2)
      YA=1./(ZA*KV1)
      YB=1./(ZB*KV1)
      YD=SQRT(YA*YB*KV2)
      Y0EA(IS)=(YA-YD)
      Y00A(IS)=(YA+YD)
      Y0EB(IS)=(YB-YD)
      Y00B(IS)=(YB+YD)
      Z0EA=1./Y0EA(IS)
      Z00A=1./Y00A(IS)
      Z0EB=1./Y0EB(IS)
      Z00B=1./Y00B(IS)
      ALPE(IS)=ALPE(IS)/CNEP+ALPMIN
      ALP0(IS)=ALP0(IS)/CNEP+ALPMIN
      WRITE (5,910)
      WRITE (5,994) IS,Z0EA,Z00A,Z0EB,Z00B,ZA,ZB,KP,ALPE(IS),ALP0(IS)
    7 WRITE (5,998)
      DO 1100 IP=1,4
      WRITE (5,928) IP
      READ (5,993,ERR=7) CODE(IP),RESIST(IP),REACT(IP)
      IF (CODE(IP).EQ.0)GO TO 7
 1100 CONTINUE
C ASSIGN PORTS TO STANDARD POSITIONS & CLASSIFY CKT
      LOWIN=LIN
      CALL ASSIGN(IS,NRW,LIN,LTO,KLAS)
      IF (KLAS(IS).NE.10) GO TO 8
      WRITE (5,940)
      GO TO 7
```

```
    8 IF (LTO.NE.LOWIN) KLAS(IS)=-KLAS(IS)
      WRITE (5,935)
      READ (5,980) STP
      IF (STP.EQ.CN) GO TO 6
      NROW(IS)=NRW
 1000 CONTINUE
      CHGPT=0
      WRITE (5,915)
      DO 2000 IF=1,NF
      NERR=0
      STAR=0
      F=FL+(IF-1)*FDEL
      GO TO 12
   10 F=F*FACTOR
      STAR=STAR+1
      IF (STAR.GT.10) GO TO 2000
   12 FFO=F/FO
      NL=0
      N2=0
      N4=0
      DO 2100 IS=1,NS
      DO 2110 I=1,2
      DO 2110 J=1,2
 2110 RL(I,J)=(0.,0.)
      CALL ADMIT(IS,FFO,Y)
      NRW=NROW(IS)
      I=32768
      DO 2115 K=16,1,-1
      J=NRW/I
      ROW(K)=FLOAT(J)
      NRW=NRW-J*I
 2115 I=I/2
      CALL MATMCR(Y,RW,AA,4)
      DO 2120 I=1,4
      DO 2120 J=1,4
      Y(I,J)=(0.,0.)
      DO 2120 K=1,4
      Y(I,J)=Y(I,J)+RW(K,I)*AA(K,J)
 2120 CONTINUE
      IX=0
      IY=0
      CALL SUBMAT(Y,Y11,Y12,Y21,Y22)
      CALL INTCHG(Y11,Y12,Y21,Y22,A11,A12,A21,A22,1,NERR)
      IF (NERR.EQ.1) GO TO 13
      GO TO 14
   13 CALL MATMCR(Y,JUGL,X,4)
      CALL MATMRC(JUGL,X,Y,4)
      CALL SUBMAT(Y,Y11,Y12,Y21,Y22)
      CALL INTCHG(Y11,Y12,Y21,Y22,A11,A12,A21,A22,1,NERR)
      IF (NERR.EQ.1) GO TO 10
      IX=1
   14 CALL SPRMAT(A11,A12,A21,A22,A)
      CALL MATMCP(A,JUGL,X,4)
      CALL MATMRC(JUGL,X,A,4)
   15 KLASS=IABS(KLAS(IS))
      DO 2130 I=1,4
      IF (I.EQ.3) GO TO 2130
      RH=REAL(ZL(I,IS))
      TH=AIMAG(ZL(I,IS))*FFO
      IF (I.EQ.2.AND.KLASS.LT.4) GO TO 17
      IF (I.EQ.4) GO TO 16
      UL(1,1,I)=CMPLX(COS(TH),0.)
      UL(1,2,I)=CMPLX(0.,RH*SIN(TH))
      UL(2,1,I)=CMPLX(0.,SIN(TH)/(RH+1.E-9))
      UL(2,2,I)=UL(1,1,I)
      GO TO 2130
```

```
   16 IF (KLASS.EQ.6) GO TO 22
      IF (KLASS.EQ.5) GO TO 60
   17 J=I/2
      IF (TH.EQ.0.) GO TO 18
      IF (RH.GE.0.) TH=SIN(TH)/(COS(TH)+1.E-9)
      IF (RH.LT.0.) TH=COS(TH)/(SIN(TH)+1.E-9)
      RL(J,J)=CMPLX(0.,RH*TH)
      GO TO 2130
   18 RL(J,J)=CMPLX(RH,0.)
 2130 CONTINUE
      GO TO (30,30,40,50) KLASS
   22 CALL MATMCR(UL2,SGN,X1,2)
      IF (IX.EQ.0) GO TO 23
      CALL REDUCE(A,X1,Z2PT,IY,NERR)
      CALL MATMCR(Z2PT,SGN,U,2)
      GO TO 24
   23 CALL MATMRC(SGN,X1,UL2,2)
      CALL SUBMAT(A,A11,A12,A21,A22)
      CALL MATADD(UL2,-1.,A22,X1,2)
      CALL MATINV(X1,X2,NERR)
      CALL MATMCC(X2,A21,X1,2)
      CALL MATMCC(A12,X1,X2,2)
      CALL MATADD(A11,1.,X2,U,2)
   24 CALL MATMCC(UL1,U,X1,2)
      IF (IS.GT.1) GO TO 26
      R(1)=ZL(3,1)
      CALL ADSBCX(X1,UI,1,2)
      NL=1
      N2=1
      GO TO 2100
   26 DO 2140 IL=1,NL
      CALL DPSBCX(UI,X2,IL,2)
      CALL MATMCC(X1,X2,U,2)
      CALL ADSBCX(U,UI,IL,2)
 2140 CONTINUE
      GO TO 2100
   30 CALL SUBMAT(A,A11,A12,A21,A22)
      IF (IS.GT.1) GO TO 31
      NL=1
      CALL ADSBCX(ONE,UI,1,2)
      R(1)=ZL(3,1)
   31 NN=NL+2
      DO 2150 IL=1,NN
      IY=0
      IF (IL-NN+1) 36,34,32
   32 IF(REAL(RL(1,1)).EQ.0.) GO TO 2150
      IF (IX.EQ.1) CALL INTCHG(B11,B12,B21,B22,A12,X1,A22,X2,0,NERR)
      CALL SPRMAT(A12,X1,A22,X2,B)
      R(IL)=RL(1,1)
      RL(1,1)=R(IL-1)
      NL=IL
      GO TO 39
   34 IF (REAL(RL(2,2)).EQ.0.) GO TO 2151
      IF (IX.EQ.1) GO TO 341
      CALL INTCHG(A12,X1,A22,X2,B11,B12,B21,B22,0,NERR)
      IF (NERR.EQ.0) GO TO 35
      CALL INTCHG(X1,A12,X2,A22,X11,X12,X21,X22,0,NERR)
      IF (NERR.EQ.1) GO TO 10
      CALL INTCHG(X12,X11,X22,X21,B12,B11,B22,B21,0,NERR)
      IF (NERR.EQ.1) GO TO 10
      GO TO 35
  341 CALL INTCHG(A12,A11,X2,X1,B12,B11,B22,B21,0,NERR)
      IF (NERR.EQ.0) GO TO 35
      CALL INTCHG(A11,A12,X1,X2,X12,X11,X22,X21,0,NERR)
      IF (NERR.EQ.1) GO TO 10
      CALL INTCHG(X12,X11,X22,X21,B11,B12,B21,B22,0,NERR)
```

```
      IF (NERR.EQ.1) GO TO 10
   35 R(IL)=RL(2,2)
      RL(2,2)=R(IL-1)
      NL=IL
      GO TO 38
   36 CALL DPSBCX(UI,U,IL,2)
      IF(IX.EQ.0) GO TO 37
      CALL MATINV(U,X1,NERR)
      IF (NERR.EQ.1) GO TO 10
      CALL MATMCR(X1,SGN,X2,2)
      CALL MATMRC(SGN,X2,U,2)
      CALL MATMCC(U,A21,X1,2)
      CALL MATMCC(U,A22,X2,2)
      CALL SPRMAT(A11,A12,X1,X2,B)
      GO TO 39
   37 CALL MATMCC(A11,U,X1,2)
      CALL MATMCC(A21,U,X2,2)
      CALL INTCHG(X1,A12,X2,A22,B11,B12,B21,B22,0,NERR)
      IF (NERR.EQ.0) GO TO 38
      CALL SPRMAT(X1,A12,X2,A22,AA)
      CALL MATMCR(AA,JUGL,X,4)
      CALL MATMRC(JUGL,X,AA,4)
      CALL SUBMAT(AA,X11,X12,X21,X22)
      CALL INTCHG(X11,X12,X21,X22,B11,B12,B21,B22,0,NERR)
      IF (NERR.EQ.1) GO TO 10
      IY=1
   38 CALL SPRMAT(B11,B12,B21,B22,B)
   39 CALL MATMCR(B,JUGL,X,4)
      CALL MATMRC(JUGL,X,B,4)
      CALL REDUCE(B-RL,Z2PT,IY,NERR)
      IF (NERR.EQ.1) GO TO 10
      CALL ZUC0N(Z2PT,U)
      CALL MATMCC(UL1,U,X3,2)
      CALL ADS8CX(X3,UI,IL,2)
 2150 CONTINUE
 2151 N2=NL
      GO TO 2100
   40 IF (IX.EQ.0) GO TO 41
      CALL INTCHG(A11,A12,A21,A22,B11,B12,B21,B22,0,NERR)
      IF (NERR.EQ.1) GO TO 90
      CALL SPRMAT(B11,B12,B21,B22,A)
   41 IF (KLAS(IS).GT.0) GO TO 42
      CALL MATMCR(A,FLIP,X,4)
      CALL MATEQ(X,A,4)
   42 IF(TAG.EQ.0) RL(2,2)=R4
      IF (TAG.EQ.1) RL(2,2)=R(NL)
      NN=N4+1+TAG
      DO 2160 IL=1,NN
      IF (IL.LE.N4) GO TO 44
      IF (TAG.EQ.0) GO TO 43
      CALL MATMCR(AA,FLIP,X,4)
      CALL MATEQ(X,AA,4)
      RL(2,2)=R(NL-1)
      TAG=0
      GO TO 46
   43 IF (REAL(RL(1,1)).EQ.0.) GO TO 2160
      CALL MATEQ(AA,B,4)
      R(NL+1)=RL(1,1)
      RL(1,1)=R(NL)
      NL=NL+1
      GO TO 48
   44 CALL DPSBCX(AI,X,IL,4)
      CALL MATMCC(A,X,AA,4)
   46 CALL SUBMAT(AA,A11,A12,A21,A22)
      CALL INTCHG(A11,A12,A21,A22,B11,B12,B21,B22,0,NERR)
      IF (NERR.EQ.1) GO TO 10
```

```
      CALL SPRMAT(B11,B12,B21,B22,B)
   48 CALL MATMCR(B,JUGL,X,4)
      CALL MATMRC(JUGL,X,B,4)
      CALL REDUCE(B,RL,Z2PT,IY,NERR)
      IF (NERR.EQ.1) GO TO 10
      CALL ZUCON(Z2PT,U)
      CALL MATMCC(UL1,U,X1,2)
      CALL ADSBCX(X1,UI,IL,2)
 2160 CONTINUE
      N4=0
      N2=NL
      GO TO 2100
   50 IF (IS.GT.1) GO TO 51
      NL=1
      R(1)=ZL(3,1)
      CALL ADSBCX(ONE,UI,1,2)
   51 IF (IX.EQ.0) GO TO 52
      CALL INTCHG(A11,A12,A21,A22,B11,B12,B21,B22,0,NERR)
      IF (NERR.EQ.1) GO TO 90
      GO TO 53
   52 CALL SUBMAT(A,B11,B12,B21,B22)
   53 CALL MATMCC(UL1,B11,A11,2)
      CALL MATMCC(UL1,B12,A12,2)
      CALL MATMCC(UL2,B21,A21,2)
      CALL MATMCC(UL2,B22,A22,2)
      DO 2170 IL=1,NL
      CALL DPSBCX(UI,U,IL,2)
      CALL MATMCC(A11,U,X1,2)
      CALL MATMCC(A21,U,X2,2)
      CALL SPRMAT(X1,A12,X2,A22,A)
 2170 CALL ADSBCX(A,AI,IL,4)
      N4=NL
      N2=0
      TAG=0
      IF (REAL(RL(2,2)).EQ.0.) GO TO 54
      TAG=1
      NL=NL+1
      R(NL)=RL(2,2)
      GO TO 2100
   54 R4=RL(2,2)
      GO TO 2100
   60 IF (IX.EQ.0) GO TO 61
      CALL SUBMAT(A,A11,A12,A21,A22)
      CALL INTCHG(A11,A12,A21,A22,B11,B12,B21,B22,0,NERR)
      IF (NERR.EQ.1) GO TO 90
      CALL SPRMAT(B11,B12,B21,B22,A)
   61 IF (KLAS(IS).GT.0) GO TO 62
      CALL MATMCR(A,FLIP,X,4)
      CALL SUBMAT(X,B11,B12,B21,B22)
      GO TO 63
   62 CALL SUBMAT(A,B11,B12,B21,B22)
   63 CALL MATMCC(UL1,B11,A11,2)
      CALL MATMCC(UL1,B12,A12,2)
      CALL MATMCC(UL2,B21,A21,2)
      CALL MATMCC(UL2,B22,A22,2)
      CALL SPRMAT(A11,A12,A21,A22,A)
      DO 2180 I=1,N4
      CALL DPSBCX(AI,X,I,4)
      CALL MATMCC(A,X,AA,4)
 2180 CALL ADSBCX(AA,AI,I,4)
 2100 CONTINUE
      DO 2200 IL=1,NL
      YL=ZO/R(IL)
      G1=UI(1,1,IL)+UI(1,2,IL)*YL/ZO
      G2=UI(2,1,IL)*ZO+UI(2,2,IL)*YL
      IF (IL.EQ.1) GAM=(G1-G2)/(G1+G2)
C     COMPUTE TRANSDUCER LOSS=PWR TO LOAD/INCIDENT PWR
      G12=REAL((G1+G2)*CONJG(G1+G2))
```

```
      LØS=4.*REAL(YL)/G12
      LØSDB(IL)=-10.*ALOG10(LØS)
      TRAN=(1.+YL)/(G1+G2)
 2300 PSI(IL)=ATAN2(AIMAG(TRAN),REAL(TRAN))/1.7453293E-2
      GM=CABS(GAM)
      IF(GM.GT.0.999999) GM=0.999999
      VSWR=(1.+GM)/(1.-GM)
      PHI=ATAN2(AIMAG(GAM),REAL(GAM))/1.7453293E-2
      NMIN=1
   80 NMAX=NMIN+2
      NM=NMAX
      IF(NL.LT.NMAX) NM=NL
      IF (NMIN.EQ.1) WRITE(5,995) F,VSWR,PHI,(LØSDB(I),PSI(I),I=1,NM)
      IF (NMIN.NE.1) WRITE (5,996) (LØSDB(I),PSI(I),I=NMIN,NM)
      NMIN=NMAX+1
      IF (NL.GT.NMAX) GØ TØ 80
      IF (STAR.NE.0) WRITE (5,936) F,STAR
      IF (STAR.LE.0) GØ TØ 2000
      F=F/FACTØR**(STAR+2)
      STAR=-STAR
      GØ TØ 12
   90 WRITE (5,942) IS
 2000 CØNTINUE
      WRITE (5,999)
      WRITE (5,932)
      READ (5,980) CHG
      IF (CHG.NE.CN) GØ TØ 1
      WRITE (5,933)
      READ (5,980) CHG
      IF (CHG.NE.CN) GØ TØ 5
      WRITE (5,934)
      READ (5,980) CHG
      IF (CHG.EQ.CN) GØ TØ 100
      CHGPT=1
      GØ TØ 5
  100 WRITE (5,930)
      READ (5,980) CHG
      IF (CHG.NE.CS) GØ TØ 1
      CALL EXIT
  905 FØRMAT (' CENTER FREQUENCY =',F8.2,' GHZ',/' GEN IMPEDANCE    =',F
     18.2,' ØHMS',/' NUMBER SECTIØNS  =',I8,/)
  910 FØRMAT ('  #   1/YØE   1/YØØ   1/YØE   1/YØØ    Z-A     Z-B    K(DB)  L S
     1S-E,Ø(N/WL)')
  911 FØRMAT (T10,' PØRT INTERCØNNECTIØNS + TERMINATIØNS',//,7X,'1',14X,
     1'2',14X,'3',14X,'4',//)
  915 FØRMAT ( T2Ø,'REFL     ØUTPUT # 1',1ØX,'2',15X,'3',//,'    FREQ      V
     1SWR     ANG     LØSS     ANG     LØSS     ANG     LØSS     ANG',//,'     GH
     2Z              DEG       DB     DEG       DB     DEG       DB     DEG',/)
  920 FØRMAT ('+TITLE:  ',$)
  922 FØRMAT (' FØ,FL,FU,FDEL=',/)
  924 FØRMAT (' NS,ZØ=',/)
  926 FØRMAT (' SEC #,ZIN-A,ZIN-B,KP(DB),THETA,VØDD,ALPHA-E,ALPHA-Ø=',/
     1,I5,3X,$)
  927 FØRMAT (' SEC #',I4)
  928 FØRMAT ('+PØRT #',I2,' TYPE,Z,TH=',$)
  930 FØRMAT (' STØP ØR GØ?',$)
  932 FØRMAT (' CHANGE ALL?',$)
  933 FØRMAT (' CHANGE CPLRS?',$)
  934 FØRMAT (' CHANGE PØRTS?',$)
  936 FØRMAT (' * * * FREQ CHGD TØ ',F10.6,' TØ AVØID DIV BY ZERØ',3X,I4
     1,' * * *')
  938 FØRMAT (' ØK?',$)
  940 FØRMAT (' PØRTS INCØRRECILY ASSIGNED',/)
  942 FØRMAT ('  * * *  WILL NØT CØMPUTE - - - TRY ALTERNATE PØRT
     1 ARRANGEMENT IN SEC #',I4,/)
  980 FØRMAT (A1)
```

```
  981 FORMAT (1X,2A5,2X,5)
  990 FORMAT (1H+,50H                                                    )
  991 FORMAT (6G)
  992 FORMAT (8F)
  993 FORMAT (A1,2F)
  994 FORMAT (I3,2F7.1,F8.1,2F7.1,F6.1,1X,F6.2,1P2E8.1,/)
  995 FORMAT (F8.3,1X,F7.2,F7.1,3(F8.2,F7.1))
  996 FORMAT (23X,3(F8.2,F7.1))
  997 FORMAT (1H+)
  998 FORMAT (1H0)
  999 FORMAT (1H1)
      END
      BLOCK DATA
      COMMON /PORT/CODE,RESIST,REACT,ZL/UNIT/ONE,MINUS,SGN,JUGL,FLIP
      DIMENSION CODE(4),RESIST(4),REACT(4)
      REAL MINUS(2,2),SGN(2,2),JUGL(4,4),FLIP(4,4)
      DATA MINUS/-1.,2*0.,-1./,SGN/1.,2*0.,-1./,JUGL/1.,5
     1*0.,1.,2*0.,1.,5*0.,1./,FLIP/2*0.,1.,4*0.,2*1.,4*0.,1.,2*0./
      COMPLEX ZL(4,15),ONE(2,2)
      DATA ZL/ 60*(0.,0.)/,ONE/(1.,0.),2*(0.,0.),(1.,0.)/
      END
      SUBROUTINE ASSIGN(IS,NRW,LIN,LTO,KLAS)
      DIMENSION CODE(4),RESIST(4),REACT(4),KLAS(15)
      COMPLEX ZL(4,15)
      COMMON /PORT/CODE,RESIST,REACT,ZL
      DATA CF/'F'/,CT/'T'/,CK/'K'/,CZ/'Z'/,CY/'Y'/,CS/'S'/,C0/'0'/,CL/'L
     1'/
      ROW(I,J)=2**(I-1+4*(J-1))
      JI=0
      J0=0
      JX=0
      JK=0
      JL=0
      JT=0
      NRW=0
      KLAS(IS)=2
      DO 1000 I=1,4
 1000 ZL(I,IS)=(0.,0.)
C  ASSIGN INPUT AND OUTPUT PORTS
      DO 2000 IP=1,4
      IF (CODE(IP).NE.CL) GO TO 210
      JI=JI+1
      TH=REACT(IP)*1.7453293E-2
      ZL(JI,IS)=CMPLX(RESIST(IP),TH)
      GO TO 220
  210 IF (CODE(IP).NE.CF) GO TO 230
      JI=JI+1
  220 NRW=NRW+ROW(IP,JI)
      IF (JI.EQ.1) LIN=IP
      IF (JI.EQ.2) KLAS(IS)=4
      GO TO 2000
  230 IF (CODE(IP).NE.CT) GO TO 2000
      J0=J0+1
      NRW=NRW+ROW(IP,J0+2)
      IF (J0.EQ.1) LTO=RESIST(IP)+REACT(IP)+0.1
      IF (J0.EQ.2) KLAS(IS)=3
 2000 CONTINUE
      JT=JI+J0
      IF (JT.EQ.4) KLAS(IS)=5
      IF (JT.EQ.4) RETURN
C  ASSIGN JOINED PORTS
      DO 4000 IP=1,4

      IF (CODE(IP).NE.CK) GO TO 4000
      JK=JK+1
      JT=JT+1
      IF (JK.EQ.2) GO TO 12
      TH=REACT(IP)*1.7453293E-2
```

```
      ZL(2,IS)=CMPLX(RESIST(IP),TH)
      KLAS(IS)=6
   12 NRW=NRW+ROW(IP,2*JK)
 4000 CONTINUE
      IF (JT.EQ.4) RETURN
C ASSIGN TERMINATED PORTS
      DO 5000 IP=1,4
      IF (CODE(IP).NE.CZ) GO TO 510
      IF (ABS(RESIST(IP)).LT.1.E-9) GO TO 550
      GO TO 515
  510 IF (CODE(IP).NE.CY) GO TO 520
      IF (ABS(RESIST(IP)).LT.1.E-9) GO TO 540
      RESIST(IP)=1./RESIST(IP)
  515 JL=JL+1
      IF (NRW.LE.4095) JP=4
      IF (NRW.GT.4095) JP=2
      IF (IS.EQ.1.AND.JL.EQ.1) JP=3
      ZL(JP,IS)=CMPLX(RESIST(IP),0.)
      GO TO 560
  520 IF (CODE(IP).NE.CS) GO TO 530
      GO TO 550
  530 IF (CODE(IP).NE.CO) GO TO 5000
  540 RESIST(IP)=-1./(RESIST(IP)+1.E-9)
  550 JX=JX+1
      JP=2*JX+JI
      TH=REACT(IP)*1.7453293E-2+1.E-10
      ZL(JP,IS)=CMPLX(RESIST(IP),TH)
  560 NRW=NRW+ROW(IP,JP)
 5000 CONTINUE
      JT=JT+JX+JL
      IF (JX.EQ.2) KLAS(IS)=1
      IF (JT.NE.4) KLAS(IS)=10
      RETURN
      END
      SUBROUTINE ADMIT(IS,FFO,Y)
      DOUBLE PRECISION THE,TH0,RAD,THETAD,V0DDD,FFOD
      COMPLEX Y(4,4),SINHE,SINH0,COTHE,COTH0,CSCHE,CSCH0
      COMMON /COUP/Y0EA(15),Y00A(15),Y0EB(15),Y00B(15),THETA(15),V0DD(15
     1),ALPE(15),ALP0(15)
      RAD=.17453292519943300-1
      YEA=Y0EA(IS)
      Y0A=Y00A(IS)
      YEB=Y0EB(IS)
      Y0B=Y00B(IS)
      THETAD=DBLE(THETA(IS))
      V0DDD=DBLE(V0DD(IS))
      FFOD=DBLE(FFO)
      THE=THETAD*FFOD*RAD
      TH0=THE/V0DDD
      SINE=SNGL(DSIN(THE))
      SIN0=SNGL(DSIN(TH0))
      COSE=SNGL(DCOS(THE))
      COS0=SNGL(DCOS(TH0))
      ALE=ALPE(IS)*THE
      AL0=ALP0(IS)*TH0
      IF (ALE.LT.1.E-4) GO TO 1
      TNE=TANH(ALE)
      CHE=COSH(ALE)
      GO TO 2
    1 TNE=ALE
      CHE=1.
    2 IF (AL0.LT.1.E-4) GO TO 3
      TN0=TANH(AL0)
      CH0=COSH(AL0)
      GO TO 4
```

```
    3 TN0=AL0
      CH0=1.
    4 SINHE=CMPLX(SINE,-TNE*C0SE)
      SINH0=CMPLX(SIN0,-TN0*C0S0)
      C0THE=CMPLX(TNE*SINE,-C0SE)/SINHE
      C0TH0=CMPLX(TN0*SIN0,-C0S0)/SINH0
      CSCHE=CMPLX(0.,-1./CHE)/SINHE
      CSCH0=CMPLX(0.,-1./CH0)/SINH0
      Y(1,1)=( YEA*C0THE+Y0A*C0TH2)/2.
      Y(1,2)=( YEA*C0THE-Y0A*C0TH0)/2.
      Y(2,1)=( YEB*C0THE-Y0B*C0TH0)/2.
      Y(2,2)=( YEB*C0THE+Y0B*C0TH0)/2.
      Y(1,3)=(-YEA*CSCHE+Y0A*CSCH0)/2.
      Y(1,4)=(-YEA*CSCHE-Y0A*CSCH0)/2.
      Y(2,3)=(-YEB*CSCHE-Y0B*CSCH0)/2.
      Y(2,4)=(-YEB*CSCHE+Y0B*CSCH0)/2.
      D0 1000 I=3,4
      D0 1000 J=1,4
 1000 Y(I,J)=Y(5-I,5-J)
      RETURN
      END
      SUBR0UTINE INTCHG(A11,A12,A21,A22,B11,B12,B21,B22,INDEX,NERR)
      REAL MINUS(2,2),JUGL(4,4)
      C0MPLEX A11(2,2),A12(2,2),A21(2,2),A22(2,2),B11(2,2),B12(2,2),B21(
     12,2),B22(2,2),DM1(2,2),DM2(2,2),0NE(2,2)
      C0MM0N /UNIT/0NE,MINUS,SGN(2,2),JUGL,FLIP(4,4)
C     IF INDEX=1 C0NVERTS Y T0 A; IF INDEX=0 C0NVERTS A' T0 B'
      CALL MATINV(A21,B21,NERR)
      IF (NERR.E0.1)G0 T0 15
      CALL MATMCC(B21,A22,DM1,2)
      CALL MATMRC(MINUS,DM1,B11,2)
      IF (INDEX.E0.0) CALL MATMRC (SGN,B11,B22,2)
      CALL MATMCC(A11,B21,DM1,2)
      IF (INDEX.E0.1) CALL MATMRC(MINUS,DM1,B22,2)
      IF (INDEX.E0.0) CALL MATMCR(DM1,SGN,B11,2)
      CALL MATMCC(DM1,A22,DM2,2)
      CALL MATADD(A12,-1.,DM2,B12,2)
      IF (INDEX.E0.1) G0 T0 10
      CALL MATMCR(B21,SGN,DM1,2)
      CALL MATMRC(SGN,DM1,B21,2)
      RETURN
   10 CALL MATMRC(MINUS,B21,DM1,2)
      CALL MATEQ(B12,B21,2)
      CALL MATEQ(DM1,B12,2)
   15 RETURN
      END
      SUBR0UTINE REDUCE(B,RL,Z,IY,NERR)
      REAL MINUS(2,2),JUGL(4,4)
      C0MPLEX B(4,4),B11(2,2),B12(2,2),B21(2,2),B22(2,2),RL(2,2),Z(2,2)
     1,0NE(2,2)
      C0MM0N /UNIT/0NE,MINUS,SGN(2,2),JUGL,FLIP(4,4)
      CALL SUBMAT(B,B11,B12,B21,B22)
      IF (IY.E0.1) G0 T0 10
      CALL MATMCC(B21,RL,Z,2)
      CALL MATADD(Z,1.,B22,B21,2)
      CALL MATINV(B21,B22,NERR)
      IF (NERR.E0.1) RETURN
      CALL MATMCC(B11,RL,Z,2)
      CALL MATADD(Z,1.,B12,B11,2)
      CALL MATMCC(B11,B22,Z,2)
      RETURN
   10 CALL MATMRC(SGN,B22,Z,2)
      CALL MATADD(Z,-1.,RL,B22,2)
      CALL MATINV(B22,Z,NERR)
      IF (NERR.E0.1) RETURN
      CALL MATMCC(B12,Z,B22,2)
      CALL MATMCR(B22,SGN,B12,2)
      CALL MATMCC(B12,B21,B22,2)
```

```
      CALL MATADD(B11,-1.,B22,B12,2)
      CALL MATMCR(B12,SGN,Z,2)
      RETURN
      END
      SUBROUTINE ZUCON(Z,U)
      COMPLEX Z(2,2),U(2,2),Z21
      CX=2.E-13
      Z21=Z(2,1)
      Z11=CABS(Z(1,1))
      IF (CABS(Z21).LT.2.E-10) Z21=CMPLX(0.,Z11*CX)
      U(1,1)=Z(1,1)/Z21
      U(1,2)=(Z(1,1)*Z(2,2)-Z(1,2)*Z(2,1))/Z21
      U(2,1)=1./Z21
      U(2,2)=Z(2,2)/Z21
      RETURN
      END
      SUBROUTINE MATEQ(A,B,N)
      COMPLEX A(N,N),B(N,N)
      DO 1000 I=1,N
      DO 1000 J=1,N
 1000 B(I,J)=A(I,J)
      RETURN
      END
      SUBROUTINE MATADD(A,SUB,B,C,N)
      COMPLEX A(N,N),B(N,N),C(N,N)
      DO 1000 I=1,N
      DO 1000 J=1,N
 1000 C(I,J)=A(I,J)+SUB*B(I,J)
      RETURN
      END
      SUBROUTINE MATMCC(A,B,C,N)
      COMPLEX A(N,N),B(N,N),C(N,N)
      DO 1000 I=1,N
      DO 1000 J=1,N
      C(I,J)=(0.,0.)
      DO 1000 K=1,N
 1000 C(I,J)=C(I,J)+A(I,K)*B(K,J)
      RETURN
      END
      SUBROUTINE MATMRC(A,B,C,N)
      DIMENSION A(N,N)
      COMPLEX B(N,N),C(N,N)
      DO 1000 I=1,N
      DO 1000 J=1,N
      C(I,J)=(0.,0.)
      DO 1000 K=1,N
 1000 C(I,J)=C(I,J)+A(I,K)*B(K,J)
      RETURN
      END
      SUBROUTINE MATMCR (A,B,C,N)
      DIMENSION B(N,N)
      COMPLEX A(N,N),C(N,N)
      DO 1000 I=1,N
      DO 1000 J=1,N
      C(I,J)=(0.,0.)
      DO 1000 K=1,N
 1000 C(I,J)=C(I,J)+A(I,K)*B(K,J)
      RETURN
      END
      SUBROUTINE MATINV(A,B,NERR)
      COMPLEX A(2,2),B(2,2),DET,R,S,SUM
      NERR=0
      R=A(1,1)*A(2,2)
      S=A(1,2)*A(2,1)
```

```
      DET=R-S
      SUM=R+S
      ADET=CABS(DET)
      ASUM=CABS(SUM)
      IF (ADET.EQ.0.) GO TO 20
      IF (ASUM.EQ.0.) GO TO 10
      ASUM=ADET/ASUM*1.E7
      IF (ASUM.LT.50.) GO TO 20
   10 B(1,1)=A(2,2)/DET
      B(1,2)=-A(1,2)/DET
      B(2,1)=-A(2,1)/DET
      B(2,2)= A(1,1)/DET
      RETURN
   20 NERR=1
      RETURN
      END
      SUBROUTINE ADSBCX(A,B,IS,N)
      COMPLEX A(N,N),B(N,N,100)
      DO 1000 I=1,N
      DO 1000 J=1,N
 1000 B(I,J,IS)=A(I,J)
      RETURN
      END
      SUBROUTINE DPSBCX(A,B,IS,N)
      COMPLEX A(N,N,100),B(N,N)
      DO 1000 I=1,N
      DO 1000 J=1,N
 1000 B(I,J)=A(I,J,IS)
      RETURN
      END
      SUBROUTINE SUBMAT(A,A11,A12,A21,A22)
      COMPLEX A(4,4),A11(2,2),A12(2,2),A21(2,2),A22(2,2)
      DO 1000 I=1,2
      DO 1000 J=1,2
      A11(I,J)=A(I,J)
      A12(I,J)=A(I,J+2)
      A21(I,J)=A(I+2,J)
 1000 A22(I,J)=A(I+2,J+2)
      RETURN
      END
      SUBROUTINE SPRMAT(A11,A12,A21,A22,A)
      COMPLEX A11(2,2),A12(2,2),A21(2,2),A22(2,2),A(4,4)
      DO 1000 I=1,2
      DO 1000 J=1,2
      A(I,J  )  =A11(I,J)
      A(I,J+2)  =A12(I,J)
      A(I+2,J)  =A21(I,J)
 1000 A(I+2,J+2)=A22(I,J)
      RETURN
      END
```

LIST OF REFERENCES

(Note: References denoted by an asterisk are included in the reprint volume, Ref. 1)

1. L. Young, ed., "Parallel Coupled Lines and Directional Couplers", Artech House, Inc., Dedham, Ma., 1972.

2. L. Young, ed., "Microwave Filters Using Parallel Coupled Lines", Artech House, Inc., Dedham, Ma., 1972.

3.* T. G. Bryant and J. A. Weiss, "Parameters of Microstrip Transmission Lines and of Coupled Pairs of Microstrip Lines, " IEEE Trans on Microwave Theory and Tech., MTT-16,p102, Dec. 1968.

4. W. J. Getsinger, " Dispersion of Parallel-Coupled Microstrip," IEEE Trans on Microwave Theory and Tech., MTT-21,p144, Mar. '73; and W. J. Getsinger, "Microstrip Dispersion Model", IEEE Trans on Microwave Theory and Tech., MTT-21,p34, Jan.'73.

5. M. K. Krage and G. I. Haddad, "Frequency Dependent Characteristics of Microstrip Transmission Lines", IEEE Trans on Microwave Theory and Tech., MTT-20,p678, Oct. '72.

6. E. J. Denlinger, "Frequency Dependence of a Coupled Pair of Microstrip Lines", IEEE Trans on Microwave Theory and Tech., MTT-18,p731, Oct. '70.

7. D. Gelder, "Numerical Determination of Microstrip Properties Using the Transverse Components", Proc. IEE, Vol. 117,p699 Apr. '70.

8.* A. Podell, "A High Directivity Microstrip Coupler Technique", IEEE 1970 G-MTT Symposium Digest, p 33.

9. J. Lange, "Interdigitated Stripline Quadrature Hybrid", IEEE Trans on Microwave Theory and Tech., MTT-17,p 1150, Dec 1969

10. K. C. Walters, P. L. Clar and C. W. Stiles, "Analysis and Experimental Evaluation of Distributed Overlay Structures in Microwave Integrated Circuits", IEEE 1968 G-MTT Symposium Digest

11. B. Spielman, "The Development of a 20 dB Multi-octave Directional Coupler for MIC Applications", Late Paper Presented at IEEE-GMTT International Microwave Symposium.

12. E. G. Cristal and L. Young, 'Theory and Tables of Optimum Symmetrical TEM-Mode Coupled-Transmission-Line Directional Couplers", IEEE Trans on Microwave Theory and Techniques, MTT-13, p 544, Sept 1965.

13. E.M. T. Jones and J. T. Bolljahn, "Coupled-Strip-Transmission Line Filters and Directional Couplers", IRE Trans on Microwave Theory , MTT-4, p 75 April 1956

14.* E. G. Cristal, "Coupled-Transmission-Line Directional Couplers with Coupled Lines of Unequal Characteristic Impedances", IEEE Trans on Microwave Theory and Tech. MTT-14, p 337, July 1966.

15. G. I. Zysman and A. K. Johnson, "Coupled Transmission Line Networks in an Inhomogeneous Dielectric Medius, IEEE Trans on Microwave Tehory and Tech., METT-17, p 753, Oct 1969

16. M. K. Krage and G. I. Haddad, "Characteristics of Coupled Microstrip Transmission Lines - I: Coupled Mode Formulation of Inhomogenecus Lines", IEEE Trans on Microwave Theory and Tech.,MTT-18, p 217, April 1970

17. T. S. Saad, ed. "Microwave Engineers' Handbook", Artech House, Dedham, Ma., 1971; Vol I, pp 132,133.

18. M. Caulton, J. J. Hughes, and H. Sobel, "Measurements on the Properties of Microstrip Transmission Lines for Microwave Intergrated Circuits", RCA Review, Vol 27, p377, Sept 1966.

19. M. Krage, and G. I. Haddad, "Frequency-Dependent Characteristics of Microstrip Transmission Lines", IEEE Trans on Microwave Theory and Tech., MTT-20, p678, Oct 1972.

20.* R. Levy, "General Synthesis of Asymmetric Multi-Element Coupled-Transmission-Line Directional Couplers", IEEE Trans on Microwave Theory and Tech., MTT-11, p226, July 1963.

21.* R. Levy, "Tables for Asymmetric Multi-Element Coupled-Transmission-Line Directional Couplers," IEEE Trans on Microwave Theory and Tech., MTT-12, p 275, May 1964.

22.* E. G. Cristal and L. Young, "Theory and Tables of Optimum Symmetrical TEM-Mode Coupled-Transmission-Line Directional Couplers", IEEE Trans on Microwave Theory and Tech., MTT-13, p 544, Sept. 1965.

23. F. Arndt, "Tables of Asymmetric Chebyshev High-Pass TEM-Mo Directional Couplers", IEEE Trans on Microwave Theory and Tech., MTT-18, p 633, Sept. 1970.

24.* R. DuHamel and M. Armstrong, "The Tapered-Line Magic-T", Abstracts of the Fifteenth Annual Symposium on the USAF Antenn Research and Development Program, Monticello, Illinois, Oct. 1965.

25.* C. Tresselt, "The Design and Construction of Broadband, High-Directivity, 90-Degree Couplers Using Nonuniform Line Techniques", IEEE Trans on Microwave Theory and Tech., MTT-14, p 647, Dec 1966.

26. D. Kammler, "The Design of Discrete N-Section and Continuou Tapered Symmetrical Microwave TEM Directional Coupler", IEEE Trans on Microwave Theory and Tech., MTT-17, p577, Aug. 1969.

27. J. Lange, "Interdigitated Stripline Quadrature Hybrid", IEEE Trans on Microwave Theory and Tech., MTT-17, p 1150, Dec. 1969

28. J. Wasad, J. Lange, J. Horton, "Intergrated Low Noise Broad-Band Microwave Amplifier", Quarterly Report, ECOM-0283-2, June 1970.

29. G. Matthaei, L. Young, E.M.T. Jones, "Microwave Filters, Impedance Matching Networks, and Coupling Structures", McGraw Hill, New York, 1964.